UNCLASSIFIED

CENTRAL RESEARCH LIBRARY
DOCUMENT COLLECTION

MARTIN MARIETTA ENERGY SYSTEMS LIBRARIES
3 4456 0049744 2

ORNL-2222
Progress Cy. 7

HOMOGENEOUS REACTOR PROJECT

QUARTERLY PROGRESS REPORT

FOR PERIOD ENDING OCTOBER 31, 1956

CENTRAL RESEARCH LIBRARY
DOCUMENT COLLECTION

LIBRARY LOAN COPY

DO NOT TRANSFER TO ANOTHER PERSON

If you wish someone else to see this document, send in name with document and the library will arrange a loan.

OAK RIDGE NATIONAL LABORATORY
OPERATED BY
UNION CARBIDE NUCLEAR COMPANY
A Division of Union Carbide and Carbon Corporation
UCC
POST OFFICE BOX X · OAK RIDGE, TENNESSEE

UNCLASSIFIED

Printed in USA. Price 1.00 cents. Available from the

Office of Technical Services
U. S. Department of Commerce
Washington 25, D. C.

LEGAL NOTICE

This report was prepared as an account of Government sponsored work. Neither the United States, nor the Commission, nor any person acting on behalf of the Commission:

A. Makes any warranty or representation, express or implied, with respect to the accuracy, completeness, or usefulness of the information contained in this report, or that the use of any information, apparatus, method, or process disclosed in this report may not infringe privately owned rights; or

B. Assumes any liabilities with respect to the use of, or for damages resulting from the use of any information, apparatus, method, or process disclosed in this report.

As used in the above, "person acting on behalf of the Commission" includes any employee or contractor of the Commission to the extent that such employee or contractor prepares, handles or distributes, or provides access to, any information pursuant to his employment or contract with the Commission.

UNCLASSIFIED

ORNL-2222

Contract No. W-7405-eng-26

HOMOGENEOUS REACTOR PROJECT

QUARTERLY PROGRESS REPORT

For Period Ending October 31, 1956

Project Director – R. B. Briggs
Associate Director – C. E. Winters

Homogeneous Reactor Test – S. E. Beall
Reactor Design and Analysis – J. A. Lane
Engineering Development – J. A. Lane
Corrosion and Materials – E. G. Bohlmann
Chemical Engineering Development – F. R. Bruce
Supporting Chemical Research – E. H. Taylor

DATE ISSUED

FEB 5 1957

OAK RIDGE NATIONAL LABORATORY
Operated by
UNION CARBIDE NUCLEAR COMPANY
A Division of Union Carbide and Carbon Corporation
Post Office Box X
Oak Ridge, Tennessee

UNCLASSIFIED

SYSTEMS LIBRARIES

3 4456 0049744 2

ORNL-2222
Progress

INTERNAL DISTRIBUTION

1. C. E. Center
2. Biology Library
3. Health Physics Library
4. Metallurgy Library
5–6. Reactor Experimental Engineering Library
7–9. Central Research Library
10–14. Laboratory Records Department
15. Laboratory Records, ORNL R.C.
16. G. M. Adamson
17. J. E. Baker
18. S. E. Beall
19. A. M. Billings
20. D. S. Billington
21. E. P. Blizard
22. E. G. Bohlmann
23. C. J. Borkowski
24. G. E. Boyd
25. J. C. Bresee
26. F. R. Bruce
27. A. D. Callihan
28. D. W. Cardwell
29. W. L. Carter
30. G. H. Cartledge
31. R. A. Charpie
32. H. C. Claiborne
33. W. E. Clark
34. T. E. Cole
35. E. L. Compere
36. D. D. Cowen
37. S. Cromer
38. F. L. Culler
39. J. S. Culver
40. J. S. Drury
41. W. K. Eister
42. L. B. Emlet (K-25)
43. D. E. Ferguson
44. J. H. Frye, Jr.
45. J. L. Gabbard
46. W. R. Gall
47. H. E. Goeller
48. J. C. Griess
49. E. Guth
50. P. N. Haubenreich
51. J. W. Hill
52. C. J. Hochanadel
53. A. Hollaender
54. A. S. Householder
55. G. H. Jenks
56. W. H. Jordan
57. P. R. Kasten
58. C. P. Keim
59. M. T. Kelley
60. R. B. Korsmeyer
61. A. S. Kitzes
62. K. A. Kraus
63. J. A. Lane
64. W. J. Leonard
65. R. E. Leuze
66. S. C. Lind
67. R. B. Lindauer
68. R. S. Livingston
69. M. I. Lundin
70. R. N. Lyon
71. J. L. Marsh (C&CCC, South Charleston)
72. H. F. McDuffie
73. J. P. McBride
74. R. A. McNees
75. J. R. McWherter
76. O. Menis
77. E. C. Miller
78. K. Z. Morgan
79. E. J. Murphy
80. M. L. Nelson
81. E. O. Nurmi
82. J. P. Murray (Y-12)
83. L. F. Parsly
84. M. L. Picklesimer
85. L. R. Quarles
86. W. D. Reel
87. P. M. Reyling
88. A. M. Rom
89. M. W. Rosenthal
90. W. L. Ross
91. H. C. Savage
92. C. H. Secoy
93. C. L. Segaser
94. E. D. Shipley
95. M. J. Skinner
96. R. W. Stoughton
97. A. H. Snell
98. I. Spiewak
99. C. D. Susano
100. J. A. Swartout

101. E. H. Taylor
102. D. G. Thomas
103. P. F. Thomason
104. M. Tobias
105. D. S. Toomb
106. W. E. Unger
107. R. Van Winkle
108. B. Weaver
109. A. M. Weinberg
110. E. P. Wigner (consultant)
111. G. C. Williams
112. J. C. Wilson
113. C. E. Winters
114. F. C. Zapp
115. ORNL – Y-12 Technical Library Document Reference Section
116. HRP Director's Office, Y-12

EXTERNAL DISTRIBUTION

117. Houdry Corporation (Attn: G. A. Mills)
118. Division of Research and Development, AEC, ORO
119-128. TISE for P.A.R.P.
129-704. Given distribution as shown in TID-4500 (12th ed.) under Engineering category (200 copies – OTS)

Reports previously issued in this series are as follows:

ORNL-527	Date Issued, December 28, 1949
ORNL-630	Period Ending February 28, 1950
ORNL-730	Feasibility Report – Date Issued, July 6, 1950
ORNL-826	Period Ending August 31, 1950
ORNL-925	Period Ending November 30, 1950
ORNL-990	Period Ending February 28, 1951
ORNL-1057	Period Ending May 15, 1951
ORNL-1121	Period Ending August 15, 1951
ORNL-1221	Period Ending November 15, 1951
ORNL-1280	Period Ending March 15, 1952
ORNL-1318	Period Ending July 1, 1952
ORNL-1424	Period Ending October 1, 1952
ORNL-1478	Period Ending January 1, 1953
ORNL-1554	Period Ending March 31, 1953
ORNL-1605	Period Ending July 31, 1953
ORNL-1658	Period Ending October 31, 1953
ORNL-1678	Period Ending January 31, 1954
ORNL-1753	Period Ending April 30, 1954
ORNL-1772	Period Ending July 31, 1954
ORNL-1813	Period Ending October 31, 1954
ORNL-1853	Period Ending January 31, 1955
ORNL-1895	Period Ending April 30, 1955
ORNL-1943	Period Ending July 31, 1955
ORNL-2004	Period Ending October 31, 1955
ORNL-2057	Period Ending January 31, 1956
ORNL-2096	Period Ending April 30, 1956
ORNL-2148	Period Ending July 31, 1956

HRP QUARTERLY PROGRESS REPORT

SUMMARY

PART I. HOMOGENEOUS REACTOR TEST

1. HRT Operations

The reactor operations were suspended for the first two months of the quarter while chloride contaminant was being flushed from the flange leak-detector system and new ring gaskets and better bolting materials were being installed.

During October the reactor testing proceeded satisfactorily at temperatures up to 293°C and pressures as high as 2000 psig.

The following information was obtained from the tests:

1. The pressurizer vent valves were adjudged to be too small. Other features of the dumping system were found to be satisfactory in the absence of the rupture-disk assembly.
2. The full output of the 300-kw package boiler was required in heating the system to 293°C. The cell air coolers were used and maintained the cell temperature in the satisfactory range of 50 to 60°C.
3. The gas-pressurized leak-detector system was adequate and indicated leaking flanges, but it cannot be properly evaluated until the bar-stock valves are replaced with new bellows-sealed Hoke valves.
4. During operation without the rupture-disk assembly which separates the fuel and blanket systems, it was possible to control the transfer of liquid between systems to a satisfactorily low rate.
5. During the dump test the low-pressure systems handled all the liquid from the high-pressure systems with ease and maintained pressures below 140 psig in the fuel tanks and 225 psig in the blanket tanks.

Difficulties experienced were as follows:

1. Pressurizer condensate-level instruments indicated erronously because of density differences in piping connections to the pressurizers. Some changes in piping will be necessary.
2. Rupture disks between pressurizers failed because of cyclic flexing, which resulted from pressure variations. Work is proceeding on improvement of the rupture disks, but it may be both practical and desirable to operate with an open pipe between the pressurizers.
3. Purge-pump performance was erratic. The difficulties were corrected by installing vents in the suction lines and modifying the phasing systems.
4. Many flanges were found to leak after thermal cycling and had to be retightened. Sealing of flanges with a minimum bolt loading is still being attempted.

Operations were interrupted when a leak developed from a crack which formed at a seal weld in a length of ¼-in. sched-80 pipe carrying condensate to the blanket pressurizer. The cause of the crack is not known at this time.

2. HRT Design

Extensive redesign of the HRT cooling-water system was undertaken because of the possibility that chloride-induced stress corrosion in stainless steel reactor components would occur if water from the cooling tower were circulated to those components as originally planned. The design of fuel and blanket corrosion specimen holders and handling facilities for their removal following operation of the HRT was completed. Shielded handling facilities for the HRT neutron source and the rupture-disk holder were also designed.

Design of the HRT pressure-balancing valve was completed and a contract let for its fabrication. Although design of tools and facilities for underwater maintenance on the HRT continues, the possibilities of dry maintenance are being explored. It was recommended that all high-pressure flange bolts in the HRT be replaced with longer bolts and ferrules to increase the elasticity of the bolting in order to provide more reliable flange sealing under the thermal cycling which will be experienced in the HRT.

3. HRT Component Development

The 400A-1 and 300A-1 circulating pumps have operated satisfactorily for 4278 and 4983 hr, respectively, since the thermal barriers were seal

welded to the stator flanges. The 400A-2 pump is being used to develop a suitable mechanically sealed thermal barrier, but a satisfactory bolting material has not yet been found. The spare reactor fuel pump suffered a thrust-bearing failure after 1300 hr of operation with UO_2SO_4.

The contract for fabrication of a 5-Mw spare heat exchanger for the HRT has been awarded to Babcock & Wilcox Co.

The deflection of feed-pump diaphragms was determined at various operating conditions. Operating characteristics of 0.031-in.-thick diaphragms appear to be better than those of the 0.019-in.-thick diaphragms now in use. A subcontract for a study of the corrosion fatigue of diaphragm materials is being placed with Ohio State University.

Two-region dump tests were completed on a $\frac{1}{18}$-scale model of the HRT, and in these tests good pressure balance was obtained. Limit switches were found to work satisfactorily on the HRT sampler. It was found that water leaking at a rate of 11 cc/min from a 2000-psi, 300°C system could be frozen off in 20 min in a $\frac{1}{2}$-in. pipe. A natural-circulation recombiner of the type to be used above the HRT fuel storage tanks was constructed and was tested at 156% of design capacity.

The HRT mockup ran for 1628 hr during the quarter. Major components operated reliably, except for a valve-bellows failure. Investigation of fission- and corrosion-solids removal was continued.

4. HRT Reactor Analysis

A study of circumstances which could lead to excessive pressures within the HRT reactor cell has been made. Dangerous pressures (greater than ~45 psia) would be obtained if reaction of a large fraction of the Zircaloy-2 core tank with fuel solution were followed by rupture of the high-pressure system. Reaction of 10% of the Zircaloy-2 with D_2O without subsequent D_2 recombination would result in a maximum cell pressure of approximately 38 psia; no D_2-O_2 explosion hazard would exist if these gases were uniformly dispersed. If all the D_2 resulting from a 10% reaction were to accumulate as an explosive mixture and ignite, the maximum cell pressure would be near 50 psia, assuming adiabatic expansion. Although this would exceed the 45 psia static pressure at which the cell was tested, the probability that such a combination of events will rupture the cell is considered to be so small that no revisions in cell construction will be made.

The radiation level within the HRT cell following reactor shutdown will be controlled by the amount of fission products retained upon the equipment walls.

5. HRT Controls and Instrumentation

5.1 Component and System Testing. – The testing of the control systems is proceeding as part of the reactor startup program. The remote-radiation-monitoring system was tested at the Health Physics Division calibration facility and found to be very satisfactory. The optimization of the pressurizer-level control was furthered by a frequency-response analysis of the HRT-mockup pneumatic system. Temporary high-speed recorders were installed for the recording of transient conditions during the reactor dump tests.

5.2 Design. – The design of the instrumentation for the radioactive-waste disposal system was completed. Control-circuit drawings are being revised to delay the venting of the pressurizer at the start of a dump to allow time for recombination of the D_2 and O_2 dissolved in the fuel solution and to permit the addition of oxygen to the high-pressure system rather than to the feed-pump suction.

6. Fuel Processing Plant

The insoluble corrosion and fission products which accumulate in the reactor fuel are to be removed centrifugally with a hydroclone. The slurry discharged from the hydroclone will be dissolved periodically in sulfuric acid to permit representative sampling. The dissolution of the solids is essentially a metathesis, and digestion alternately in concentrated and dilute sulfuric acid is required for complete conversion of the oxides to the sulfates. The dissolver solution after sampling will be stored in decay tanks pending transfer to a solvent-extraction facility for uranium recovery. The 4 *M* sulfuric acid solution is corrosive if boiled; therefore the use of steam as an inert diluent for transporting radiolytic gases to a recombiner is not practical. Instead, an oxygen atmosphere will be used which will be continuously circulated through the recombiner by means of a convection loop.

Construction of the high-pressure equipment for the fuel processing system was completed and

hydrostatically tested and was checked out with oxygenated-water runs in which normal startup and shutdown operations were simulated. Some difficulties were experienced in freezing plugs in the high-pressure loop when it was at high temperature. Shop fabrication of the dissolver equipment is under way, and field installation will begin as completed units become available.

The hydroclone and the hydroclone retainer plug were removed remotely during shakedown operations with tools designed for this purpose. A lightweight right-angle starting wrench was designed to facilitate insertion and engagement of horizontal bolts. A thermocouple-lead cutter was designed to sever the stainless steel thermocouple leads on equipment to be removed.

Further tests with ½-in. flanges subjected to thermal cycling emphasized the need for increasing the extensibility of the bolts, either by using extension sleeves or Belleville spring washers. Belleville springs have been fabricated of Inconel for testing.

The continuous processing of the HRT natural-uranium blanket solution is based upon the centrifugal removal of insoluble plutonium and corrosion products and is, in this respect, similar to the core processing. Once plutonium is precipitated, temperature has little effect upon its apparent solubility, and the centrifugation may be carried out at room temperature. This will minimize problems introduced by the corrosiveness of the concentrated uranium blanket solution.

Two promising processes for the dissolution of plutonium and corrosion-product oxides are being investigated, one similar to the sulfuric acid system to be used in the core plant, the other employing concentrated phosphoric acid.

Procurement of materials and equipment items for the blanket processing plant that will require considerable time for delivery has been initiated in advance of the issuance of a detailed flowsheet or equipment design.

PART II. REACTOR DESIGN AND ANALYSIS

7. Reactor Analysis

Two-group, two-region studies were made for 10- and 12-ft-dia spherical reactors containing D_2O-ThO_2-$U^{233}O_2$ in both the core and the blanket regions. The following results were obtained for these reactors: the breeding ratio increased when the thorium concentration was increased in either the core or the blanket region; the core-wall power density decreased when the blanket thorium concentration was increased; decreasing the core size increased the breeding ratio but also increased the power density at the core wall; increasing the blanket U^{233} concentration slightly decreased the breeding ratio; the wall power density was relatively insensitive to changes in the blanket fuel concentration for specified thorium concentrations greater than 100 and 500 g/liter in the core and blanket, respectively.

The effect of neutron resonance absorption in fuel upon breeding ratio and critical mass has been investigated for single-region ThO_2-D_2O-$U^{233}O_2$ reactors. If the resonance-energy value of η^{23} relative to the thermal-energy value were 0.95 rather than 1.0, the breeding ratio would be decreased by 1.3% and the critical mass increased by 1.3% for a slurry containing 300 g of thorium per liter.

Calculations have been performed to determine the power level attainable in natural-circulation homogeneous reactor systems. The results obtained indicate that for comparable systems the power level achievable by a natural-circulation system is one-fifth to one-third that attainable by a forced-flow system.

Physical-property data for light and heavy water and their mixtures, UO_2SO_4 solutions, UO_2SO_4-Li_2SO_4 equimolal solutions, UO_2SO_4-$BeSO_4$ equimolal solutions, ThO_2 slurries, and uranium oxide slurries were compiled for use in nuclear calculations.

Oracle codes have been devised to calculate the time behavior of fuel concentrations in single-region reactors and the fraction of gamma rays originating from a shielded source which would escape through a hole in the shield as a result of air scattering and wall scattering.

PART III. ENGINEERING DEVELOPMENT

8. Development of Fuel-System Components

Exposure of titanium and zirconium materials in the high-pressure recombiner loop is being repeated to confirm the hydrogen-absorption data obtained in previous runs.

The 20-cfm canned-rotor blower was received from Allis-Chalmers after passing hydrostatic and performance tests. Two of the three ORNL pumps receiving life tests were introduced to UO_2SO_4 service.

The Byron Jackson 4000-gpm pump was inspected, and its Stellite wear rings were replaced with type 347 stainless steel.

A test to evaluate nickel plating and counterbored tube-sheet holes as methods of inhibiting stress corrosion in heat-exchanger tubes was started.

Permanent bolt deformation as a result of flange thermal cycling is reported. Leak rates in two ring-joint flanges remained very low after eight thermal cycles.

9. Development of Reactor Slurry Systems

Specifications were drawn up for an interim standard slurry for the purpose of providing a reproducible reference material for comparison of the work of the groups participating in the HRP slurry program. The slurry was prepared according to these specifications by circulating pure thorium oxide in distilled water in loop 200A. This resulted in the formation of small balls of thorium oxide about 8 to 30 μ in diameter which have a high settling rate, low yield stress, low coefficient of rigidity at room temperature, and a settled-bed density of at least 3000 g of thorium per kilogram of H_2O.

A highly fluid, silicated thorium oxide slurry was boiled and also circulated at 300°C in a 100-gpm loop for an extended period of time without adverse effect on either its viscosity or resuspendability. The slurry remained essentially Newtonian in its flow properties.

An equation relating the heat-transfer coefficient and the turbulent flow conditions for Bingham plastic slurries was developed on the basis of a momentum–heat-transfer analogy.

During the investigation of the effect of ThO_2 concentration on the behavior of slurries containing little or no sulfate, a hard cake was formed in loop 200A, necessitating complete shutdown and cleanout. During part of the run the flow was observed to be nonhomogeneous, based on a gamma-ray scan of a horizontal pipe with a Co^{60} source. Modifications to improve flow measurement and sampling will be made to the loop during the shutdown.

A comparative survey of Graphitar-radial-bearing life in 100A pumps for both solution and slurry service is presented.

The blanket test facility was operated for 127 hr on slurry, utilizing the high-pressure system. The heat exchanger plugged rapidly twice during the run and could not be operated. The main loop operated fairly well after some instrument failures were corrected. The facility was switched to the low-pressure system and shaken down for 300 hr with water. At the same time operating personnel were given training in system behavior with the blanket vessel in service. A number of shortcomings in instrument and equipment performance were corrected, and a nitrogen cylinder station was added to permit gas pressurization of the core vessel as an alternative to steam pressurization. With steam pressurization of the core the heat transfer from core to blanket was about 39 kw, with an over-all heat-transfer coefficient of 212 $Btu/hr \cdot ft^2 \cdot {}^\circ F$.

10. Instrument and Valve Development

Two special high-temperature-resistant and radiation-resistant linear differential transformers suitable for use as sensing elements on the HRT level transmitters have been ordered for test and evaluation.

Type 17-4 PH stainless steel, a hardenable alloy, has been shown to be similar in performance to type 347 stainless steel for dump-valve service. An all-metal actuator for small valves is being evaluated; however, the life in initial tests at operating conditions considerably more severe than those recommended by the manufacturer has been unsatisfactory.

PART IV. CORROSION AND MATERIALS

11. Solution Corrosion

The mockup of the expansion joint and Zircaloy-2–stainless steel transition joint used in the HRT reactor vessel was exposed to circulating HRT fuel solution for 1240 hr in a 100A corrosion test loop (loop F). Fifty thermal cycles between 100 and 300°C and 50 mechanical deflections of the bellows were imposed on the unit during this 1240-hr period. No leakage across the joint was observed.

Several types of corrosion specimens of a number of alloys were subjected to a daily thermal cycle between 100 and 300°C during the testing of the Zircaloy-2–stainless steel transition joint. None of the specimens showed unusually high corrosion rates as a result of the thermal cycling, although the generalized corrosion rate of the entire system

based on nickel analysis was somewhat higher than usual.

The 100A loop O, designed to circulate uranium solutions containing beryllium as an additive, is now in operation. One preliminary run with a solution of uranium trioxide in beryllium sulfate was made.

Loop runs were made at 200, 250, and 300°C with solutions containing 0.04 *m* UO_2SO_4, 0.005 *m* $CuSO_4$, and 0.02 *m* H_2SO_4. Each run lasted for approximately 2000 hr, and in each case the solution was completely stable. The critical velocities observed with type 347 stainless steel coupons were 15 to 20 fps at 200°C, 25 to 30 fps at 250°C, and 40 to 45 fps at 300°C.

Further testing directed at determining the effect of chromium(VI) on the corrosion of stainless steel by uranyl sulfate solutions was completed. At 275°C the effect of chromium(VI) additions was the same as at 250°C; that is, the film-free corrosion rate was increased and the amount of metal dissolved during the formation of a film was decreased.

An attempt was made to descale a 100A loop with a solution containing phosphorous acid and sodium hypophosphite. Very little scale was dissolved during the treatment, and further testing with this solution has been discontinued.

Additional testing of stressed type 347 stainless steel specimens showed that, at 100°C in boiling 0.04 *m* UO_2SO_4, stress-corrosion cracking was not observed in the absence of chloride ions. In the presence of chloride ions, new specimens developed pits and cracks in less than 500 hr, but when the specimens had been exposed to the boiling uranyl sulfate solution for long periods before the addition of chloride ions, no pitting or cracking was observed for periods in excess of 2000 hr.

A series of tests was completed in which different alloys and metals were exposed to 4.0 and 10.8 *M* H_2SO_4 solutions at their boiling points. In addition, the same materials were tested in the acid solutions to which had been added rather large amounts of ferric, chromic, and zirconium sulfates and lesser amounts of uranyl, copper, and ruthenium sulfates. In the 10.8 *M* solution containing the additives, only tantalum showed adequate corrosion resistance. In 4.0 *M* H_2SO_4 with the additives, tantalum, zirconium, and Zircaloy-2 had excellent corrosion resistance, and Carpenter 20-Cb and types 316 and 347 stainless steel corroded between 1 and 3 mpy. In the absence of the additives, types 316 and 347 stainless steel corroded at a rate of 2000 mpy and Carpenter 20-Cb at 30 mpy. In addition, Carpenter 20-Cb showed a strong tendency toward stress-corrosion cracking; in the presence of the additives, cracking was not observed.

12. Slurry Corrosion

12.1 Pump Loops. – Dynamic-corrosion data and operating observations are reported for five slurry runs made in 100A pump loops. Two runs, of 22- and 11-hr duration, which marked the first slurry operation for loop BS, were made at 250°C and with approximately 570 g of thorium per kilogram of water, with added oxygen. In each run, average particle size increased substantially, with spheroid formation, accompanied by deposition of cake in the pump and loop.

A test on loop CS employing previously circulated thorium oxide at 346 g of thorium per kilogram of water, at 300°C with added oxygen, for 266 hr, operated without incident. Corrosion observed on all materials was substantially lower than in a similar previous run in which raw slurry was circulated. A test in which "standard" slurry was circulated at 400 g of thorium per kilogram of water, at 300°C with added oxygen, was terminated after 26 hr because of caking in the pump. An 83-hr run at 300°C under a hydrogen atmosphere, at a concentration of 426 g of thorium per kilogram of water, was made with the same batch of slurry as was used in BS loop. Again spheroids were formed. A severe hard caking in the pump caused termination.

In short runs on the experimental in-pile slurry loop, slurry was added successfully while circulation proceeded at operating temperature and pressure. Concentration was not maintained as circulation continued.

12.2 Toroids. – Degradation of thoria slurry by circulation in toroids at 250°C and 26 fps for several hundred hours was shown to depend on the calcination temperature and the particle size of the oxide. Thus only those particles whose calcination temperature was below 1400 to 1600°C and whose original particle size was above 1.3 μ were observed to have been degraded. Studies are presented of the effects of $Na_4P_2O_7$ and Na_2SiO_3 as slurry additives, under oxygen or hydrogen

atmospheres, on corrosion by thoria slurries circulating in toroids. Physical examination of a toroid after 4909 hr of slurry-circulation service showed only slight attack, with greatest attack in the vicinity of protuberances such as weld beads or pins. Circulation of "standard" slurry in toroids at 200°C and 10 or 20 fps resulted in an increase in the particle size of the thoria spheroids from about 10 μ to over 20 μ, with some fracturing at 20 fps. Circulation at 20 fps at 300°C also caused growth, and possible fracturing, but circulation at 26 fps at 200 or 250°C caused degradation of the particles. Circulation of the raw slurry from which the standard slurry had been made under all these conditions resulted not in growth but in normal degradation of the particle size.

Corrosion attack rates for the standard slurry did not differ significantly in any of the above cases from rates for its raw-slurry precursor or for other slurries produced under the same conditions.

13. Radiation Corrosion

13.1 In-Pile Loops. – The fabrication and operational testing of in-pile loop L-2-15 were completed. Loops L-2-14 (titanium) and L-2-15 are ready for installation in beam hole HB-2 of the LITR. The construction of loop L-4-16 is under way. One of the Byron Jackson 5-gpm circulating pumps is now undergoing operational tests with a uranyl sulfate solution. Several leaks developed in the pump but were repaired, and operation was continued. Development of an in-pile loop for use in the ORR is continuing.

The seventh in-pile loop experiment, L-4-12, was completed. The loop operated under initial conditions similar to those of loops GG, L-4-8, and L-4-11 (0.17 *m* UO_2SO_4, 0.031 *m* $CuSO_4$, 0.04 *m* H_2SO_4). The main-stream and pressurizer temperatures were 250 and 280°C, respectively. Loop L-4-12 was the first in-pile experiment with a titanium core tank. One result was the absence of the high initial corrosion rate observed in previous loops with stainless steel core tanks. As a result of the low over-all corrosion rate (1.4 mpy initial, 1.0 mpy final), the excess acid remained high, between 0.03 and 0.04 *m*, for almost the entire run as compared with previous experiments in which the excess acid had decreased to about 0.02 *m* early in the run. The higher acid had little effect on the corrosion rates of titanium and zirconium alloys, which were in good agreement with rates observed in previous loops. However, the type 347 stainless steel coupons exposed at the highest power densities (3 to 4 w/ml) and at solution velocities of 12 to 17 fps apparently dissolved. This dissolution would require a minimum corrosion rate of 186 mpy during the time of exposure. Rates of 8 to 13 mpy were observed in loop L-4-8 at similar conditions. The stainless steel coupons in the lower-power-density end (1 to 2 w/ml) of the L-4-12 core showed very low corrosion rates, averaging around 0.1 mpy.

Exposure of in-pile loop L-2-10 in the HB-2 hole at the LITR has been completed. The main-stream operating temperature was 280°C, and the uranyl sulfate concentration was the same as that of HRT solution, 0.04 *m*, with 0.02 *m* excess H_2SO_4. The over-all stainless steel corrosion rates obtained from oxygen and nickel data were 0.4 mpy and 0.2 mpy, respectively.

In-pile loop L-4-13 is now inserted in the HB-4 hole at the LITR. Operating conditions are similar to those of experiment L-4-8, except that the initial excess acid is only 0.02 *m* and, for the first time, the solution has been made up by using heavy water.

13.2 In-Pile Autoclave Tests – LITR Tests. – Three previously unreported Zircaloy-2 experiments are discussed. Experiment Z-21, which received only 36 hr of exposure, indicated a reduction, by a factor of 2, in corrosion rate in a 0.17 *m* UO_2SO_4 solution to which had been added 0.17 *m* Li_2SO_4. Precipitation may have occurred in this experiment. In Z-24 a reduction of about 12% in corrosion rate was shown on pins etched to remove the machine-disturbed surface as compared with the as-machined surface usually tested. This effect may be due only to the reduction in microscopic surface area from the chemical polishing treatment. The 1 atm of air usually included in bomb experiments was carefully excluded from Z-24. The corrosion rate observed was significantly higher than had been predicted from previous experiments in which atmospheric nitrogen was included. However, other data render uncertain any conclusions as to whether nitrogen has an effect on corrosion. In a low-power-density exploratory experiment, Z-25, with a UO_2CO_3-Li_2CO_3 solution, the corrosion rate observed was

higher than that predicted for a UO_2SO_4 solution at a similar power density and temperature.

Recently available data from earlier experiments are tabulated. The recent power-density value, along with previously reported data for Z-20, which used D_2O as the solvent, indicates for D_2O about a 30% increase in corrosion rate over that anticipated for water solutions.

13.3 Correlation of Zircaloy-2 Data. – Further analysis of the available data for the radiation corrosion of Zircaloy-2 has revealed that the power-density–corrosion-rate relationship is not accurately represented by equations of the form $CR = K(PD)^{2/3}$, as suggested in the previous report. In this equation CR is the corrosion (mpy) based on radiation time, PD is the fission power density (w/ml) which prevails in solution during exposure, and K is a constant, the value of which depends upon temperature and solution composition. From the present analysis it is shown that the apparent value of the exponent is greater than $\frac{2}{3}$ at low corrosion rates and less than $\frac{2}{3}$ at high corrosion rates. The data over the full range of power densities and corrosion rates which have been studied can be represented by equations of the form $CR = A\ PD(1 - e^{-B/CR^{1.5}})$, where A and B are constants which depend upon temperature and solution composition. The meaning of the other symbols is as before. Conclusions as to the effect of variables other than power density on the corrosion of Zircaloy-2 within the conditions studied are not changed appreciably from those discussed in the previous report. A plot of the data is shown, together with equations for lines which are drawn through the various sets of data.

13.4 Supporting Research. – G values of 0.31 and 0.082 for the production of chlorine and fluorine, respectively, were obtained when a sample of Freon-11 (CCl_3F) was irradiated at –70°C with an electron beam from the Van de Graaff.

Zircaloy-2 foil specimens, contained in a thermal loop, were exposed for approximately 40 hr at 250°C to Van de Graaff electrons. At the metal, current densities as high as 90 $\mu a/cm^2$ were used, and the power density in the solution adjacent to the specimens was estimated to be 60 to 90 w/ml. Although the previously etched specimen surfaces are still being studied, it appears that ionizing radiation has little if any effect on the rate of corrosion of Zircaloy-2. The previous history of the surface appears to be a more important factor than either the composition of the solution or the amount of radiation energy under the conditions employed.

14. Metallurgy

Heat treatment of Zircaloy-2 in the low alpha-plus-beta field (higher than 810°C), followed by air cooling, results in an embrittlement as shown by an impact transition curve. Microstructural examination showed the appearance of beta phase in the grain boundaries and its decomposition on cooling into the intermetallics which are deposited in the grain boundaries, resulting in embrittlement. A microstructural examination of the impact specimens of in-pile loop GG showed that the specimens had undergone the same type of embrittling heat treatment, and thus it was concluded that the impact curve shown by those specimens was primarily a result of the heat treatment and not necessarily due to radiation damage.

Recent improvements in chemical polishes and etchants permitted microstructural examination of the Zr-Nb base alloys heat treated below 600°C. Time-temperature-transformation curves by both hardness and metallography indicated that increasing the niobium content decreases the rate of transformation, while the ternary additions of palladium, platinum, or iron increase the rate of transformation; the ternary addition of molybdenum, however, decreases the rate of transformation. Age hardening of the retained beta structure occurred at 300, 400, and 500°C. A soft transformation product occurred at 600°C. All transformations are quite sluggish.

On zirconium-niobium alloys it has been possible to obtain oxide films consisting entirely of the orthorhombic compound $6ZrO_2 \cdot Nb_2O_5$, which is the densely packed phase. This has been possible, however, only with niobium contents approaching the stoichiometric ratio and with high oxidation temperatures. The addition of other metals to this system permits lowering of the niobium concentration.

Impact, tensile, and corrosion specimens of A55 titanium were prepared in order to simulate the structures obtained in welding with essentially the same thermal cycle. These specimens will be used to determine the properties of the heat-affected zone of a welded material.

A procedure is being developed by which the drop-weight test for determining the brittle transition temperature in metals may be adapted to titanium and zirconium. Suitable crack-starter materials have been developed for both metals.

Welding procedures developed for tungsten-arc inert-gas welding of stainless steel, using preplaced inserts for the root metal, were modified to permit the use of round-wire inserts. These inserts are much cheaper than the Electric Boat mushroom-type inserts and are only slightly harder to use.

A metallurgical investigation conducted on two sets of titanium-alloy valve trim which had failed in tests in the HRP dump-valve loop revealed that the failures had resulted from rapid burning. Approximately 4 g of metal was consumed in each failure, both of which occurred, probably on opening the valve, during a single cycle of operation. These failures are believed to have resulted from special conditions in these tests and are not a general possibility.

The feasibility of roll-cladding titanium on steel by using copper combined with vanadium as a diffusion barrier was demonstrated on an experimental basis. The strength of the bond is now being determined.

Several experiments are being constructed or designed for use in irradiating metals in the MTR, ORR, ETR, and HRT. Two new impact testing machines are being modified for hot-cell operation.

Impact- and tensile-test results for a number of irradiated metals are summarized, and the results of irradiation tests on a carbon-steel weldment are presented.

PART V. CHEMICAL ENGINEERING DEVELOPMENT

15. Fuel Processing

The hydroclone circuit operating in conjunction with the HRT mockup loop has reduced the solids concentration of the fuel circulating in the loop system to about 1 mg/liter. At the same time solids concentration factors (g/liter in the underflow pot divided by g/liter in the loop) in excess of 1000 were obtained. The solids disappeared from the circulating stream with or without the hydroclone operating. This disappearance of solids from the circulating stream followed first-order kinetics. With the hydroclone operating, the half-time for solids removal was measured as 1.2 hr; without the clone operating, the half-time for solids disappearance was 2.5 hr.

Reactor solids may be dissolved without mechanical agitation by treating alternately with 10.8 and 4 *M* H_2SO_4. Two such cycles were adequate on a laboratory scale, and three were sufficient on a unit-operations scale.

Experiments showed that uranium can be satisfactorily recovered and partially decontaminated, by peroxide precipitation, from a UO_2SO_4 solution containing nickel and rare-earth sulfates. Recovery of 99.9% of the uranium was achieved by such a precipitation when proper pH control was maintained. Decontamination factors for uranium from nickel and neodymium ranged from about 10 to 50, and either H_2O_2 or Na_2O_2 was a satisfactory source of peroxide.

The valence distribution of iodine in simulated HRT fuel at 100°C was influenced by the radiation level and the gas-phase composition. Increasing the radiation intensity or mole fraction of H_2 in the gas phase above the simulated fuel solution increased the proportion of elemental iodine present in the liquid phase. In dynamic loop tests iodine was stripped from simulated fuel solution at 230°C and 1000 psi sufficiently fast to halve the initial concentration in 13 min. Iodate was rapidly reduced to free iodine at the same temperature; the half-time was measured as 0.1 min. At 100°C the distribution coefficient for elemental iodine between vapor and liquid phases was 0.005 for water at pH 4.15 and was 0.31 for fuel solutions, with some evidence that the presence of impurities such as ferric iron or ruthenium influences the distribution.

16. Plutonium-Producer Blanket Processing

A test loop for studies on processing of the plutonium-producer blanket has been fabricated and is being installed.

Further chemical studies in which plutonium was gradually added to 1.4 *m* UO_2SO_4 at 250°C in a pyrex-lined autoclave under 100 psi O_2 and 200 psi H_2 confirmed previous results. No PuO_2 precipitate was formed while the plutonium was gradually increased to 26 mg per kilogram of H_2O. After the next addition, which increased the plutonium to 28 mg per kilogram of H_2O, partial precipitation occurred, leaving 22 mg per kilogram of H_2O in

solution. Most of the plutonium remaining in solution was Pu(IV). Under the same conditions in a titanium-lined autoclave, no PuO_2 was precipitated when the plutonium concentration was gradually increased to 21.3 mg per kilogram of H_2O. Partial precipitation occurred at a plutonium concentration of 25.8 mg per kilogram of H_2O, leaving 22.8 mg of plutonium per kilogram of H_2O in solution. In a stainless steel container there was no precipitation at a plutonium concentration of 33.4 mg per kilogram of H_2O, but at 37.2 mg, PuO_2 precipitated, leaving only 7.5 mg of plutonium per kilogram of H_2O in solution. Further plutonium additions also caused precipitation, leaving 6 to 9 mg of plutonium per kilogram of H_2O in solution. After heating in type 347 stainless steel, all the plutonium in solution was Pu(VI).

In 1.4 *m* UO_2SO_4 at 25°C, Pu(IV) was stable; however, upon heating to 90°C about 30% of the plutonium disproportionated to Pu(III) and Pu(VI). It therefore seems unlikely that significant amounts of Pu(IV) can exist in solution in 1.4 *m* UO_2SO_4 at 250°C.

Simulated HRT blanket solids containing 70% Fe_2O_3, 18% Cr_2O_3, 9% NiO_2, 1.2% ZrO_2, 1% UO_3, and 0.8% PuO_2 were dissolved readily and completely in anhydrous H_3PO_4 at 230°C. Complete solution was also obtained by heating the solids in 10.8 *M* H_2SO_4 at 156°C followed by dilution to 4.5 *M* H_2SO_4 and refluxing. There was no indication of hydrolysis or reprecipitation.

17. Thorium Oxide Slurry Development

Investigation of the effect of reactor irradiation on thorium oxide slurries was continued with four more irradiations carried out at 300°C in the LITR – two with pure thorium oxide and two with thorium oxide containing 0.5 mole % enriched uranium. All slurries were at a concentration of 750 g of thorium per kilogram of H_2O. No difficulty was encountered in stirring any of the slurries, and no significant change in relative viscosity was noted under irradiation. The calculated power density under irradiation for the slurries containing the enriched uranium was approximately 5 kw/liter (the average power density expected in the TBR blanket).

In out-of-pile studies on the catalytic combination of hydrogen and oxygen in thorium-uranium oxide slurries containing MoO_3, molybdenum oxides prepared by several different methods showed comparable activities. With a slurry containing a thorium-uranium oxide prepared from the coprecipitated oxalates, combination rates greater than 30 moles of hydrogen per hour per liter of slurry were obtained at 225°C and a hydrogen partial pressure of 500 psi after addition of 0.05 *m* MoO_3 and activation with hydrogen at elevated temperatures. The addition of 1000 ppm of iron oxide to a slurry of thorium-uranium-molybdenum oxide significantly lowered its catalytic activity at 150°C. Satisfactory rates were obtained by increasing the reaction-rate temperature slightly. With 1500 ppm of iron oxide, combination rates were unsatisfactory for reactor use. Treatment of the slurry containing this level of iron oxide with hydrogen at elevated temperatures greatly increased its activity, but subsequent treatment with oxygen reduced its activity to the former value.

Laboratory evaluation of the standard slurry did not reveal any chemical or physical differences in this material, when compared with other pumped oxides, which could give an insight into the mechanism by which the microspheres, characteristic of this material, were formed. Sulfuric acid titration curves of the standard slurry and the original oxide showed no differences in specific surface activities, despite the almost twofold increase in surface area occasioned by the pumping. The microspheres were readily degraded by mild stirring in laboratory glassware at 98°C, during which a marked increase in slurry conductivity was observed.

In high-temperature sedimentation studies with the standard slurry, an abnormal change in the hindered-settling rate was observed in the temperature region 150 to 200°C upon the addition of 500 to 1000 ppm of sulfate and again at 5000 ppm of sulfate. Comparison with the sulfate titration curves showed the regions of temperature instability to bracket the break in the pH curve and that at pH 7 (in the presence of sulfate) relatively low settling rates and good temperature stability are obtained. With pure slurries the settling rate was found to be an exponential function of the concentration. A calculated Stokes' diameter for settling particles, which did not change with temperature, was obtained by extrapolating to zero concentration curves of settling rate vs slurry concentration obtained with the standard slurry for a series of temperatures.

Thoria sols with a thoria/nitrate weight ratio of 7.5/1 containing thoria micels 140 Å in size have

been prepared by ultrafiltration of thorium nitrate sols. Hexamethylenetetramine and ammonium acetate buffers were used to prepare thoria gels. Electrophoretic techniques for the study of thoria sols and slurries are under investigation.

18. Equipment Decontamination

A chromous sulfate solution for use in equipment decontamination was prepared by electrolytic reduction of a chromic acid solution in a two-chamber anion-exchange membrane cell. Amalgamated lead electrodes were used, with a current density of 0.1 amp/cm^2.

A 2% H_3PO_3–2% NaH_2PO_2 solution at 175°C for 24 hr was not satisfactory for defilming a Y-12 corrosion loop.

PART VI. SUPPORTING CHEMICAL RESEARCH

19. Aqueous Systems at Elevated Temperatures

By means of experiments carried out in sealed quartz tubes, the number and types of phases present in the CuO-UO_3-SO_3-H_2O system at 304°C are being ascertained. The work has been completed for solutions containing no excess H_2SO_4 and will continue with solutions containing various amounts of excess acid. Analysis of the data after completion of the experimental work should define the liquidus surface and identify the solid phases.

Experiments in titanium bombs have disclosed that at least 20 hr is required to establish equilibrium in the "green precipitate" region of the UO_2SO_4-$CuSO_4$-$NiSO_4$-H_2SO_4-H_2O system at about 200°C. Experiments with adequate equilibration time have disclosed that previously reported temperatures of initial precipitation are 20 to 50°C too high in this region. Better values based on the bomb experiments are given.

20. Effect of Uranyl Ion on Ferrous Oxidation

The ferric-ion yield from the gamma-ray oxidation of air-saturated ferrous sulfate solutions is reduced by the presence of uranyl ion. The reduction in yield is attributed to the reaction of uranyl ion with hydrogen atoms before they react with dissolved oxygen.

CONTENTS

SUMMARY v

PART I. HOMOGENEOUS REACTOR TEST

1. HRT OPERATIONS 3
   - 1.1 Reactor Operations 3
     - 1.1.1 Dump Tests 3
     - 1.1.2 Heatup to Operating Temperature 4
     - 1.1.3 Gas-Pressurized Leak-Detector System 5
     - 1.1.4 Transfer of Fluid Between Core and Blanket Systems 5
     - 1.1.5 Miscellaneous Tests 5
     - 1.1.6 Operating Difficulties 5

2. HRT DESIGN 7
   - 2.1 Cooling-Water System 7
   - 2.2 Corrosion Specimen Holders 7
   - 2.3 Source-Handling Facilities 10
   - 2.4 Pressure-Balancing System 11
   - 2.5 Flange Bolting 13
   - 2.6 Dry Maintenance 13
   - 2.7 Miscellaneous 13

3. HRT COMPONENT DEVELOPMENT 15
   - 3.1 Pump Development 15
     - 3.1.1 400A-1 Pump and Loop 15
     - 3.1.2 400A-2 Pump and Loop 15
     - 3.1.3 300A-1 Pump 15
     - 3.1.4 Spare Reactor Fuel Pump and 400A-2 Test Loop 15
   - 3.2 HRT Spare Heat Exchanger 16
   - 3.3 Diaphragm Pumps 16
     - 3.3.1 HRT Feed Pumps 16
     - 3.3.2 HRT Purge Pump 16
   - 3.4 HRT Dump Test 17
   - 3.5 HRT Sampler 17
   - 3.6 Freeze Jackets 17
   - 3.7 Natural-Circulation Recombiner 17
   - 3.8 HRT Mockup 18
     - 3.8.1 Operation 18
     - 3.8.2 Inspection 18
     - 3.8.3 Component Failures 18
     - 3.8.4 Special Tests 19

4. HRT REACTOR ANALYSIS 20
   - 4.1 Explosion Hazard in HRT Reactor Cell 20
     - 4.1.1 Zirconium-Water Reaction 20
     - 4.1.2 Explosion Hazards in Reactor Cell 20
     - 4.1.3 Pressure Rise from D_2-O_2 Explosions 21
   - 4.2 Radiation Level Within HRT Cell 21

5. HRT CONTROLS AND INSTRUMENTATION 22
5.1 Component and System Testing 22
5.1.1 Remote-Radiation-Monitoring System 22
5.1.2 Oxygen-Injection System 22
5.1.3 Pressurizer-Level Control System 22
5.1.4 Dump Tests 22
5.1.5 Disconnects for Valve-Actuator Air Lines 23
5.1.6 Heat-Balance Flowmeters 24
5.1.7 Sample Stations 24
5.1.8 Emergency Air System 24
5.1.9 Conduit Leakage Tests 24
5.2 Design 25
5.2.1 Waste Disposal System 25
5.2.2 Control Circuits 25

6. HRT PROCESSING PLANT 26
6.1 Core Fuel Processing – Flowsheet 26
6.2 Construction Status 26
6.3 Engineering Tests and Shakedown Operations 29
6.3.1 Refrigeration System 29
6.3.2 Hydrostatic Test 29
6.3.3 Trisodium Phosphate and Nitric Acid Rinses 29
6.3.4 Westinghouse Circulating Pump 31
6.3.5 D_2O-Storage-Tank Calibrations 31
6.3.6 Shakedown-Loop Operation 31
6.3.7 Oxygenated-Water Runs 31
6.3.8 Flange Leakage During Thermal Cycles 31
6.4 Remote-Maintenance Tools 31
6.5 Corrosion and Component Tests 33
6.5.1 Flange Tests 33
6.5.2 Hydroclone Tests 36
6.6 Blanket Processing – Flowsheet 36

PART II. REACTOR DESIGN AND ANALYSIS

7. REACTOR ANALYSIS 41
7.1 Two-Region Slurry Reactor Studies 41
7.2 Effect of U^{233} Resonance Absorption on Breeding Ratio and Critical Mass 43
7.3 Natural-Circulation Reactors 45
7.4 Physical-Property Data for Homogeneous Reactor Solutions and Slurries 46
7.5 HRP Mathematics and Computation 46

PART III. ENGINEERING DEVELOPMENT

8. DEVELOPMENT OF FUEL-SYSTEM COMPONENTS 51
8.1 High-Pressure Recombiner Loop 51
8.2 Small Reactor Components 51
8.2.1 20-cfm Canned-Rotor Blower 51
8.2.2 Small Circulating Pumps 51

8.3 4000-gpm Loop 51
8.4 Titanium Program 52
8.5 Heat-Exchanger Tube-Joint Test 52
8.6 High-Pressure Flange Test 53

9. DEVELOPMENT OF REACTOR SLURRY SYSTEMS 54

9.1 Interim Standard Slurry 54
9.1.1 Preparation 54
9.1.2 Physical Properties 54
9.1.3 Rheology 57
9.2 Heat-Transfer Measurements 59
9.3 Thermal Stability of a Deflocculated Slurry 60
9.4 Component Development 62
9.4.1 Effect of Sulfate and ThO_2 Concentration on Slurry Behavior 62
9.4.2 Modifications to Loop 200A 63
9.4.3 Venturi Flowmeters 65
9.4.4 Survey of Graphitar-Radial-Bearing Life in 100A Pumps 65
9.5 Blanket-System Development 68
9.5.1 High-Pressure-System Run 68
9.5.2 Low-Pressure-System Shakedown 68

10. INSTRUMENT AND VALVE DEVELOPMENT 71

10.1 Instrument Development 71
10.1.1 Liquid-Level Transmitters 71
10.2 Valve Development 71
10.2.1 Sealing Bellows 71
10.2.2 Valve Trim 71
10.2.3 Actuators 71

PART IV. CORROSION AND MATERIALS

11. SOLUTION CORROSION 75

11.1 Pump Loops 75
11.1.1 Loop Engineering 75
11.1.2 Loop Test Results 77
11.2 Laboratory Service Corrosion 79

12. SLURRY CORROSION 81

12.1 Pump Loops 81
12.1.1 100A Pump Loops 81
12.1.2 In-Pile Slurry Loop Development 88
12.2 Toroids 88
12.2.1 Particle-Size Degradation 89
12.2.2 Dispersing Additives 90
12.2.3 Toroid Examination 92
12.2.4 Circulation of "Standard" Slurry 93

13. RADIATION CORROSION 100

13.1 In-Pile Loops 100
13.1.1 Development and Construction 100
13.1.2 General Description of In-Pile Loop Experiment L-4-12 101
13.1.3 Qualitative Results of Inspection and Evaluation of Loop L-4-12 102

13.1.4 Quantitative Results of Inspection and Evaluation of Loop L-4-12 103
13.1.5 Discussion of Results from Loop L-4-12 105
13.1.6 In-Pile Loop L-2-10 106
13.1.7 In-Pile Loop L-4-13 106
13.2 In-Pile Autoclave Tests – LITR Tests 107
13.2.1 Experiment Z-21 107
13.2.2 Experiment Z-24 107
13.2.3 Experiment Z-25 109
13.2.4 Experiment Z-17 109
13.2.5 Experiment Z-20 109
13.3 Correlation of Zircaloy-2 Data 111
13.4 Supporting Research 112
13.4.1 Radiation Damage to Freon 112
13.4.2 Effects of Electron Irradiation on the Corrosion of Zircaloy-2 in a Thermal Loop 112

14. METALLURGY 114

14.1 Physical Metallurgy 114
14.1.1 Zirconium Alloy Development 114
14.1.2 Morphology of Zircaloy-2 116
14.1.3 Oxidation of Zirconium Alloys 118
14.1.4 Development of Simulated Weld and Heat-Affected Structures in Zirconium and Titanium 119
14.2 Mechanical Metallurgy 120
14.2.1 Embrittlement of Alpha Titanium by Hydrogen 120
14.2.2 Drop-Weight Testing 120
14.3 Welding Development 120
14.3.1 Stainless Steel Welding with Preplaced Inserts 120
14.4 Metallurgical Development and Service 121
14.4.1 Failure of Titanium Alloy Valve Trim 121
14.4.2 Roll-Cladding Titanium on Steel 121
14.5 Inspection Development 123
14.6 Effects of Radiation on Structural Metals and Alloys 123
14.6.1 Equipment and Facilities 123
14.6.2 Results of Irradiation Experiments 124

PART V. CHEMICAL ENGINEERING DEVELOPMENT

15. FUEL PROCESSING 135

15.1 Behavior of Solids in the HRT Mockup 135
15.2 Reactor Solids Dissolution 135
15.3 Reprocessing of UO_2SO_4 136
15.4 Iodine Chemistry 136
15.5 Volatility of Iodine Under Reactor Conditions 137

16. PLUTONIUM-PRODUCER BLANKET PROCESSING 140

16.1 Hydrolysis of Zirconium Sulfate in 0.17 *m* UO_2SO_4 140
16.2 Prototype-Pressurizer Tests 142

16.3 Plutonium Behavior in UO_2SO_4 Solution at 250°C 142
16.3.1 Pyrex Containers 142
16.3.2 Titanium Containers 143
16.3.3 Type 347 Stainless Steel Containers 143
16.4 Effect of Temperature on Plutonium Valence 143
16.5 Blanket Solids Dissolution 144

17. THORIUM OXIDE SLURRY DEVELOPMENT 145

17.1 Slurry Irradiation Studies 145
17.1.1 Slurry Irradiations in the LITR 145
17.1.2 Viscosity Measurements in the Irradiation Bomb 146
17.1.3 Corrosion-Erosion Data Obtained in Out-of-Pile Tests with the Dash-Pot Irradiation Bomb 146
17.1.4 Diagonal-Tube Irradiation Facility in the LITR 149
17.1.5 Bomb Dismantling Facility 149
17.2 Gas-Recombination Studies 149
17.2.1 Effect of Molybdenum Oxide Preparation Method 149
17.2.2 Studies with Slurries Containing Thorium-Uranium Oxide Prepared from the Coprecipitated Oxalates 150
17.3 Laboratory Evaluation of the "Standard" Slurry 151
17.4 Preparation and Characterization of Aqueous Thoria Sols and Suspensions 156

18. EQUIPMENT DECONTAMINATION 158

18.1 Electrolytic Preparation of Chromous Sulfate for Use in Decontamination 158
18.2 Descaling with H_3PO_3-NaH_2PO_2 158

PART VI. SUPPORTING CHEMICAL RESEARCH

19. AQUEOUS SYSTEMS AT ELEVATED TEMPERATURES 161

19.1 An Exploration of the System CuO-UO_3-SO_3-H_2O at 304°C 161
19.2 Dilute Solutions in the System UO_2SO_4-$CuSO_4$-$NiSO_4$-H_2SO_4-H_2O 161

20. EFFECT OF URANYL ION ON FERROUS OXIDATION 165

Part I

HOMOGENEOUS REACTOR TEST

S. E. Beall

1. HRT OPERATIONS

S. E. Beall

R. E. Brooksbank
W. D. Burch
J. S. Culver
N. W. Curtis[1]
J. R. Engel
J. D. Flynn
D. F. Frech
T. H. Gladney
J. L. Gory
B. H. Hamling[2]
P. N. Haubenreich
J. W. Hill, Jr.
D. M. Johnson[3]
R. W. Jurgensen[4]
S. I. Kaplan
J. O. Kolb
G. W. Rivenbark
H. K. Search[1]
R. Van Winkle
H. E. Williamson

1.1 REACTOR OPERATIONS

The first week in August was spent in tightening flanges and in preparing for operation at high temperature and pressure. On August 9, with the system ready for operation, chemical analysis of water removed from the leak-detector system revealed that water-soluble chloride was present in the leak-detector tubing at concentrations in the range 500 to 1000 ppm. Investigation revealed that the leak-detector tubing had not been cleaned prior to installation and that some of the tubing received from the manufacturer contained chloride-bearing material. Thus all the flanges in the system were broken, and water was flushed for 48 hr through each leak-detector line in an attempt to dissolve the chloride compounds from the tubes. After the flushing operation, water was allowed to remain stagnant in each line for at least 24 hr. The water was then analyzed, and, if the chloride content was 1 ppm or less, the line was adjudged to be clean. Later it was found that when water remained in the tubes for longer than 500 hr the concentration of chloride in some of the lines increased to as much as 10 ppm, which is sufficiently high to cause attack of the flange grooves; for this reason, the leak-detector system will be operated with high-pressure oxygen instead of with D_2O.

After the water flush of the leak-detector lines, the oval-ring gaskets were removed from all the flanges, and the grooves were inspected and cleaned. Some grooves had become pitted by exposure to the high-chloride water and required lapping to restore smooth surfaces. New oval rings were installed. New bolts (with reduced shanks and with ferrules to give extra length for added elasticity to reduce bolt stress upon thermal cycling) were installed in flanges that would be subjected to high temperature and pressure. By October 2, the system had been reassembled and was ready for operation. The balance of the month was spent in shakedown operations and in testing of various components. Generally, the performance of the reactor was satisfactory over the 350-hr period of operation at temperatures up to 293°C and pressures up to 2000 psig.

Tests made during the October period of operation are outlined in the following paragraphs.

1.1.1 Dump Tests

The reactor was dumped from high pressure a total of four times, but, because the rupture-disk assembly had been removed, there was no real test of the pressure-balancing control system, as had been planned earlier.

Perhaps the most significant fact gleaned from the dump tests was the inadequacy of the pressurizer vent valves in attaining the desired rate of pressure reduction during the first stage of a dump. Figure 1.1 shows pressure-time curves obtained while the pressurizers were being vented. Dump tests 1 and 2 were made under normal conditions (vent valves about half open), while the "fast" bleed was made with both valves wide open. Larger trim will be installed in the valves to increase their capacity.

Figure 1.2 shows the system pressure during the second dump test. This test was carried out by blocking the dump timers and manually initiating the second stage of the dump. Owing to the interconnection through the rupture-disk pot, the electric differential pressure cell connected directly between the core and the blanket did not register a

[1]On loan from Pennsylvania Power and Light Co.

[2]On loan from Union Carbide Nuclear Co., New York Office.

[3]On loan from The Glenn L. Martin Co.

[4]On loan from American Gas and Electric Company.

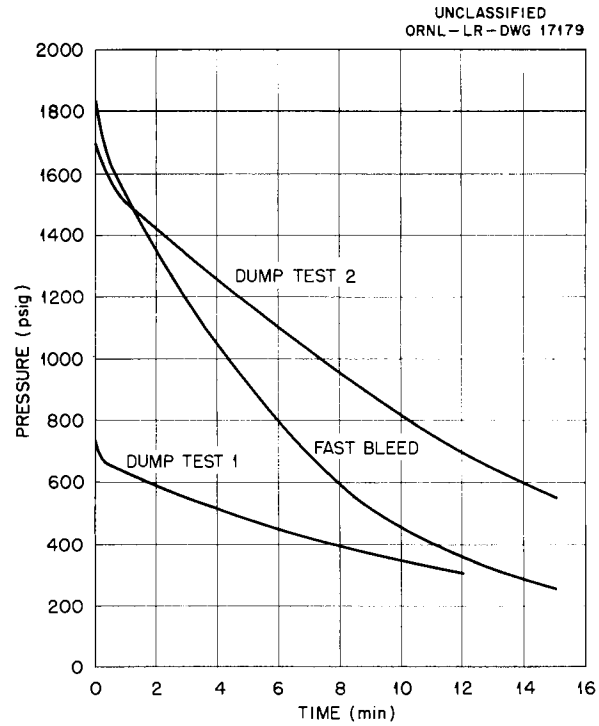

Fig. 1.1. Reduction in System Pressure by Venting Pressurizers.

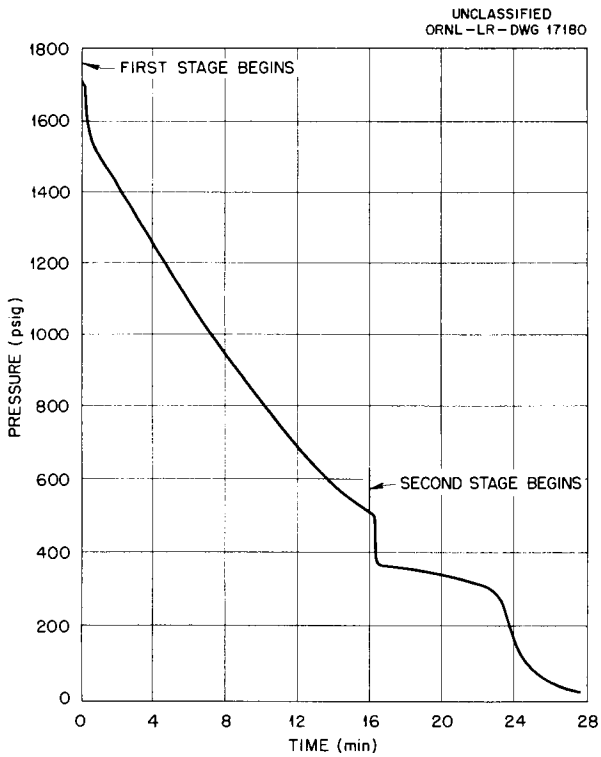

Fig. 1.2. System Pressure During Dump Test 2.

differential pressure greater than 2 psi at any time during this dump.

During the portion of the dumps in which saturated liquid was entering the dump lines, mass flow rates were around 7 lb/sec from the blanket and 2.5 lb/sec from the core with 400 psig in the high-pressure system. Figure 1.3 shows dump-tank weights during a dump test.

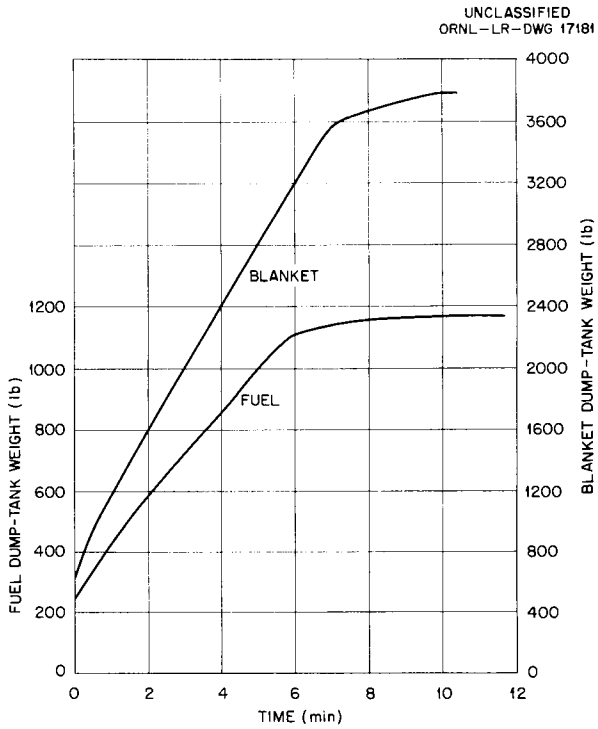

Fig. 1.3. Dump-Tank Weights During Dump Test 2. Time measured from dump-valve opening.

The cooling capacity in the recombiner condensers was found to be adequate to prevent excessive pressures in the dump tanks. In the most severe test the reactor was dumped while the fuel and blanket circulating systems were at 290°C. The maximum pressures reached in the dump tanks were 140 psig in the fuel tanks and 225 psig in the blanket tanks.

Because of uncertainties in inventory measurements the exact amount of transfer between systems during dumps could not be fixed. It appeared, however, that there was some transfer from the blanket to the fuel system, probably 50 lb or less.

1.1.2 Heatup to Operating Temperature

After some difficulty with leaking steam block valves, the system was heated to a temperature of

293°C by using the 300-kw package boiler to supply 1500-psig heating steam. A temperature of 280°C will be required to conduct the oxygenated water run. The cell air temperature was observed to be 60 to 70°C without the cell air coolers in operation (but with some leakage of heat from the cell through cracks between blocks and through other small openings). The cell air coolers were operated to bring the cell air temperature down to the range 50 to 60°C. Performance data on the space coolers will be taken at a later time.

1.1.3 Gas-Pressurized Leak-Detector System

The leak-detector system was operated with oxygen at pressures in the range 500 to 750 psi in the low-pressure leak-detector headers and 2200 to 2500 psi in the high-pressure system headers. It was found that the individual leaking flanges could be easily located. However, the barstock-type needle valves originally installed on the leak-detector system have been unsatisfactory and are being replaced by bellows-sealed, soft-seated Hoke valves. Until the new valves are installed, it will not be possible to properly evaluate the gas-filled leak-detector system.

1.1.4 Transfer of Fluid Between Core and Blanket Systems

Inventories of the water in the fuel and blanket systems taken at intervals during operation without rupture disks indicated a transfer from the fuel system to the blanket system. With both systems at approximately the same temperature (less than 5°C difference) and with both sets of pressurizer heaters operating on the same time cycle, the rate of transfer was about 5 lb/hr. Figure 1.4 is a plot of inventory readings for several days. On October 25 efforts were made to reduce the transfer by heating the fuel pressurizer at a rate lower than that for the blanket pressurizer. The effect can be seen on the curve in Fig. 1.4.

1.1.5 Miscellaneous Tests

The letdown heat exchangers were found to cool the letdown stream well below the specified 90°C (to protect the Stellite trim of the letdown valve). The thermal flowmeters (for measuring purge- and feed-pump flow rates) were tested and were found to be suitable for indicating flow. Off-gas flow (~2 liters/min) was directed through the charcoal adsorbers to observe the effect on dump-tank pressure control. It was found that the dump-tank pressure was very sluggish in following changes in flow through the charcoal.

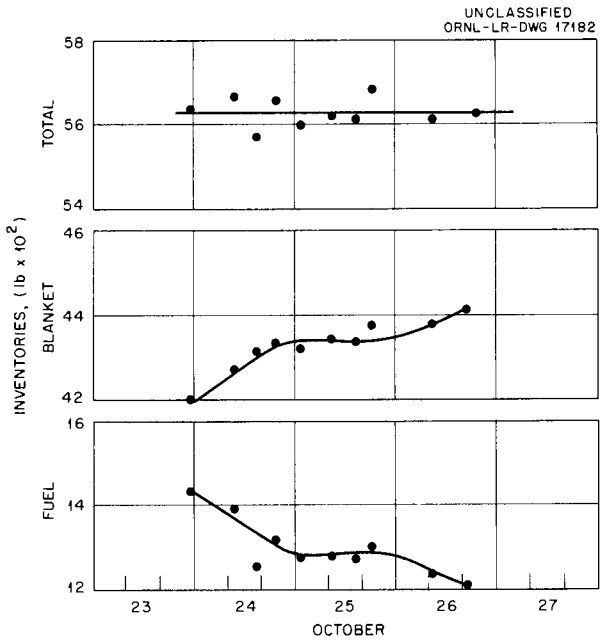

Fig. 1.4. Water Inventory During Operation with Rupture Disks Removed.

Operation during October was ended when a leak developed in line 211 (blanket-pressurizer purge-water feed line). A crack was formed at the base of a seal weld between the ¼-in. sched-80 pipe and the ½-in. stainless steel pipe which served as a sleeve penetrating the bulkhead between the reactor compartment and the blanket cell space. The cause of this cracking has not been determined.

1.1.6 Operating Difficulties

The following difficulties were encountered during the shakedown tests:

1. The pressurizer condensate-level indicators would not indicate liquid level when the system was hot, because there were density differences in the level-indicator piping.

2. The rupture disks and back-pressure supports did not fit together well enough to prevent flexing of the thin stainless steel rupture disk when the differential pressure across the disk fluctuated. During the initial operation, with pressures up to 1000 psi, a rupture disk was flexed to failure in a few hours. Although room-temperature tests had

indicated that the rupture disk might withstand 7000 or more flexes before failing, the fit in the HRT rupture-disk assembly was poorer than in the test assembly. A rupture disk and back-pressure support of different design are on order, but until they are delivered the reactor will be operated and subsequent tests performed without rupture disks separating the fuel and blanket pressurizers.

3. Great difficulty was encountered in keeping the purge pumps pumping; as a consequence, the flow of condensate purge to the pressurizers and circulating pumps was uncertain. It was concluded that the suction lines, having no gas vents, were permitting the pumping heads to become gas-bound. The system was shut down for three days so that the purge-pump suction lines could be modified and vents could be installed on those lines and so that the piping in the phasing system between the primary pulsators and the remote pumping heads could be modified. After these changes were made, the pumps operated satisfactorily.

4. A number of flanges in the system leaked (as evidenced by gas leaking from the leak-detector system) after each of the three thermal cycles. Each time they were retightened to torques intended to produce stresses of approximately 25,000 psi in the bolts. Stresses are being kept low purposely in an effort to minimize flange-groove deformation.

2. HRT DESIGN

W. R. Gall

R. E. Aven
C. A. Burchsted
R. H. Chapman
R. D. Cheverton
C. J. Claffey
H. N. Culver[1]
E. H. Gift
R. F. Hughes[2]
J. E. Kuster[3]
M. I. Lundin
H. A. McLain
C. Michelson[1]
R. C. Moren[4]
R. C. Robertson
J. N. Robinson
W. Robinson
C. L. Segaser
W. Terry
T. H. Thomas
F. C. Zapp

2.1 COOLING-WATER SYSTEM

Because of the possibility of chloride-induced stress corrosion in stainless steel components in contact with potable water or water from the cooling tower, the HRT cooling-water system was redesigned to incorporate a closed loop which will circulate distilled water (or service-steam condensate) as a primary coolant to equipment within the reactor cell.[5,6] In the original design, all process water for the HRT was to be taken from the cooling-tower basin; however, in view of the high chloride content of that water (as much as 20 ppm), its use as a primary coolant is inadvisable. Under the modified design, cooling-tower effluent will be circulated to a new heat exchanger (approximately 1000 ft^2 of heat-transfer area) to cool the distilled water which is circulated in the closed loop by a 300-gpm pump.

The cooling water which is circulated to the reactor cell may reach a maximum temperature of about 100°F, as compared with a design maximum temperature of cooling-tower effluent of 90°F. The refrigeration condenser, charcoal beds, and waste evaporator-condenser, which are located outside the reactor cell, will therefore be connected directly to the cooler X-10 potable-water supply. The turbine oil coolers, turbine condenser, and vent condenser, which are not subject to chloride-induced stress corrosion, will continue to receive water from the cooling-tower basin.

The major piping changes which will be required by the modified design will be in the west valve pit, none being required within the reactor cell. The volume between the Monitrons on the main cooling-water outlets from the cell and the pneumatically operated control valves will be sufficient to provide a 3-sec holdup of water, allowing time for the valves to close should activity be detected in the cooling water.

2.2 CORROSION SPECIMEN HOLDERS

Figure 2.1 shows the positions of corrosion specimen holders in the core and blanket regions of the HRT pressure vessel; the method of mounting metallurgical specimens in the holders is shown in Fig. 2.2. Forty-eight specimens will be mounted in the core and exit from the core and 24 in the blanket.

The main structural member of the holder was designed with a Y cross section to obtain a maximum surface-area-to-volume ratio consistent with required strength. This permits better cooling of the member and minimizes the possibility of localized surface boiling. It is estimated that the maximum average surface temperature of the holder in the fuel side will be 314°F, and bulk boiling at the surface should not occur unless the total pressure falls below 1540 psia.[6]

The design of coffins and decontamination facilities for removal of hot corrosion specimen holders is complete. The coffin, which provides 7 in. of lead for gamma shielding, is approximately 10 ft long. A special roof plug (Fig. 2.3) will be installed over the pressure vessel and will have flanged openings to permit access to the pressure-vessel thimbles without extensive interference with the cell sealing membrane. It is estimated that the maximum induced activity in the fuel-side specimens and specimen holder will be 600 r/hr (at 6 ft), assuming reactor operation for one year at 10 Mw, or 120 r/hr (at 6 ft) after three months of operation at 5 Mw. The activity of fission products

[1] On loan from TVA.

[2] On loan from Kaighan & Hughes, Inc.

[3] On loan from Maxon Construction Co.

[4] On loan from Westinghouse Electric Corp.

[5] H. A. McLain, R. E. Aven, and R. C. Robertson, *HRT Cooling Water System Modifications*, ORNL CF-56-8-152 (Aug. 23, 1956).

[6] W. R. Gall and M. I. Lundin, *Monthly Report — Design Section — July and August, 1956*, ORNL CF-56-8-189.

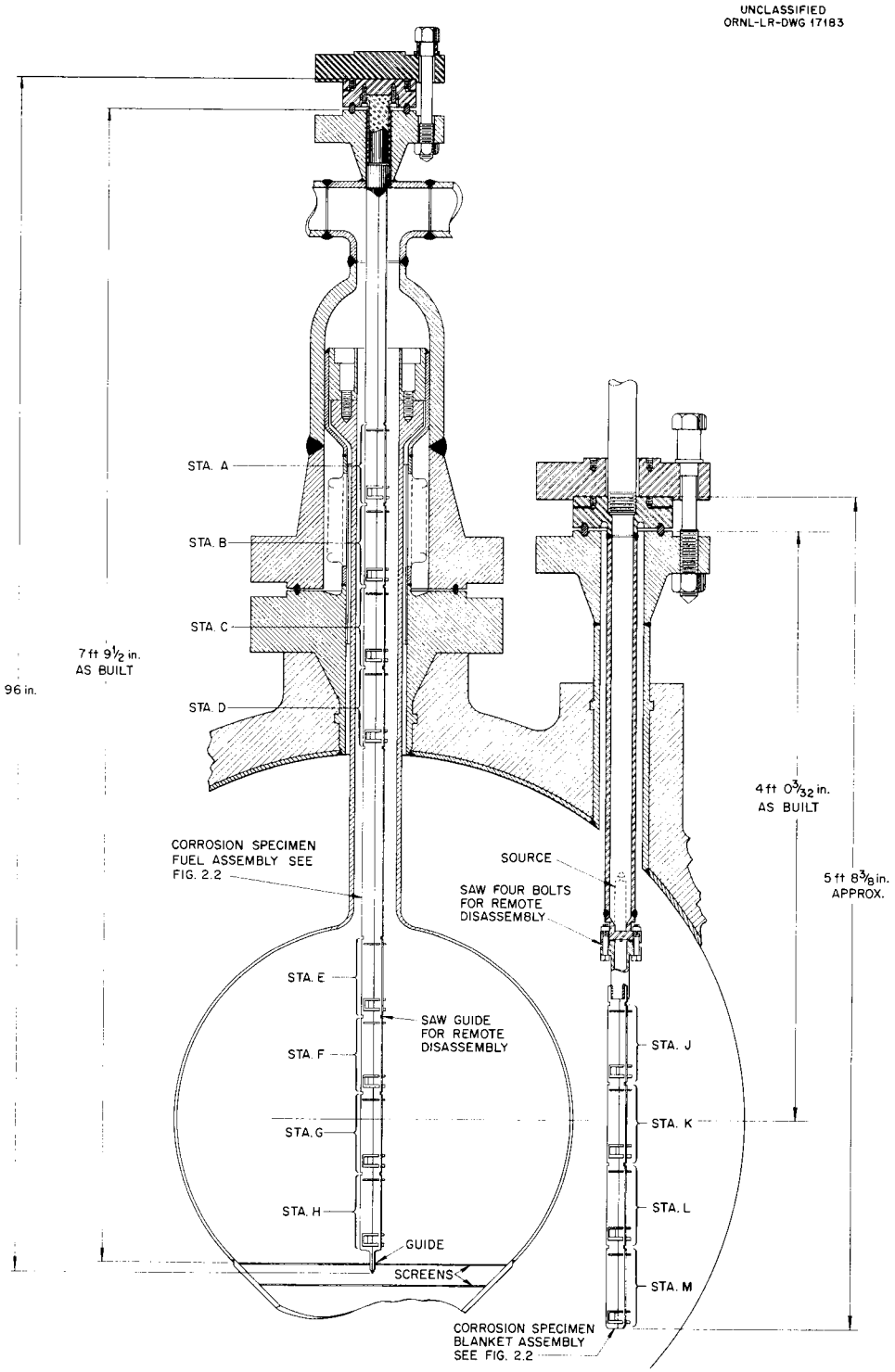

Fig. 2.1. Corrosion Specimen Holders in HRT Core and Blanket Regions.

UNCLASSIFIED
ORNL-LR-DWG 17184

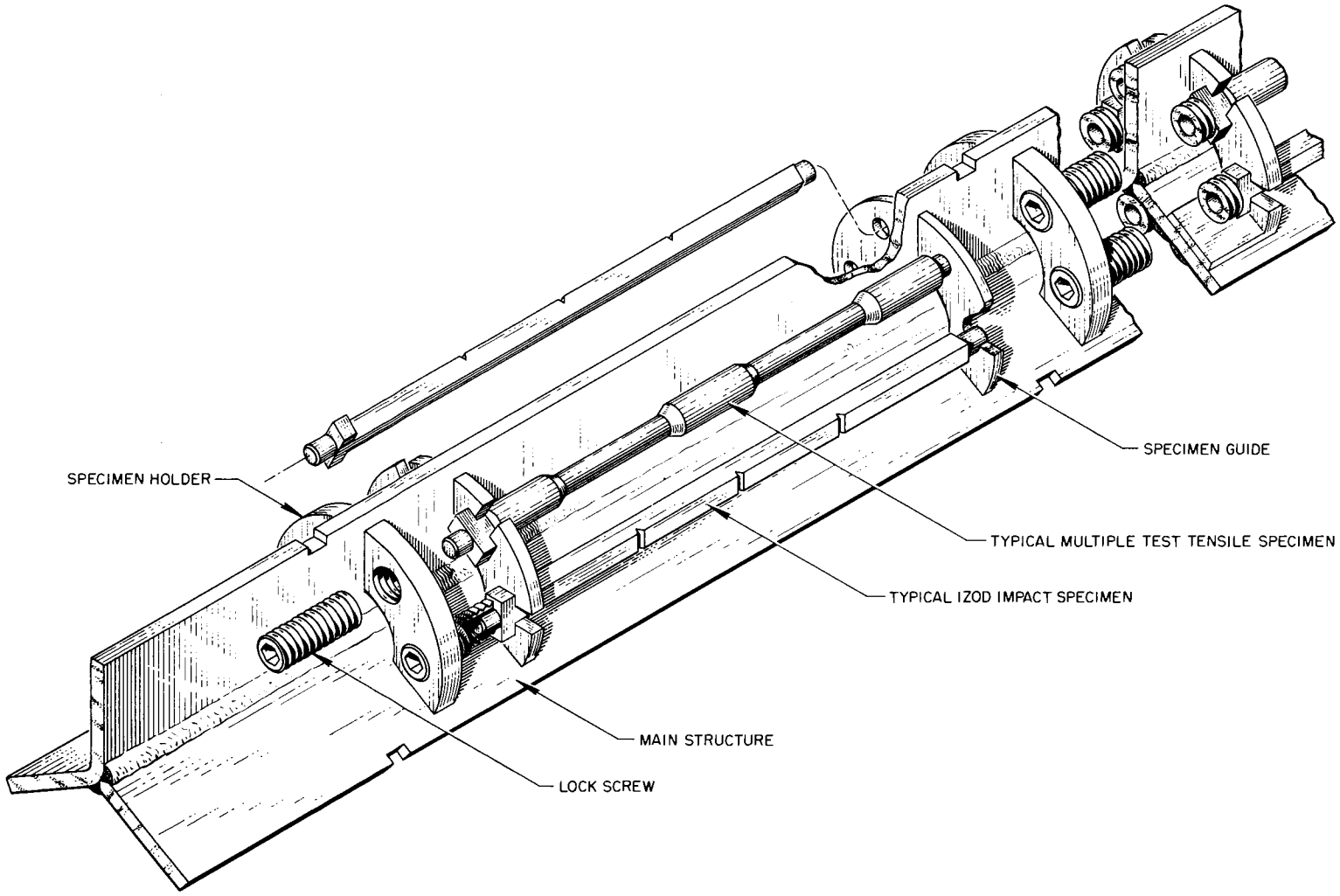

Fig. 2.2. Typical HRT Corrosion Specimen Station.

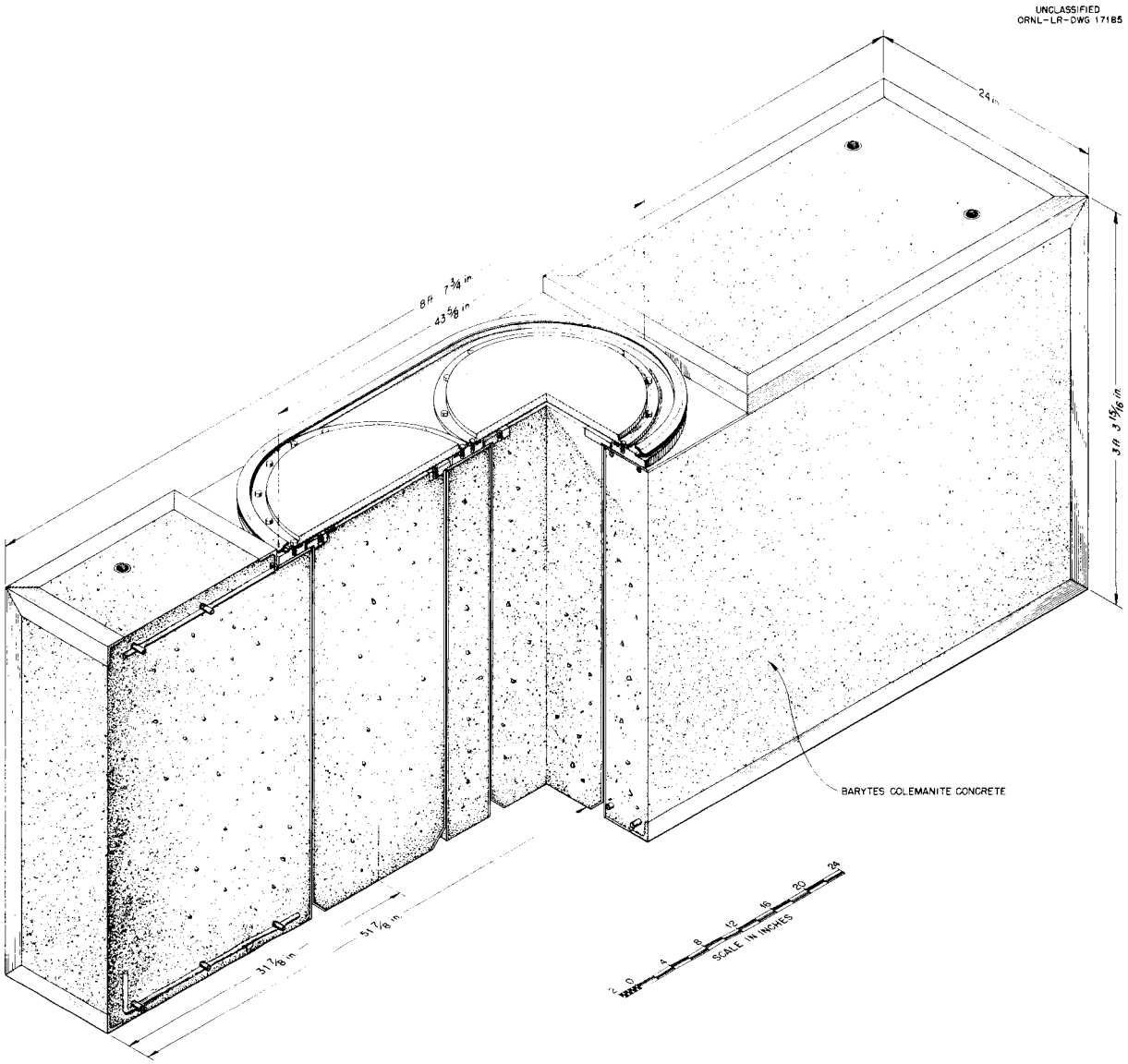

Fig. 2.3. Special Roof Plug with Reactor Access Opening.

adhering to the holder is estimated[7] at 60 r/hr at a distance of 6 ft.

2.3 SOURCE-HANDLING FACILITIES

A portable shield was designed in which the HRT source will be transported from the LITR and stored at the HRT during critical experiments preliminary to bringing the reactor to power. Gamma activity of the source, which has been irradiated in the LITR since May 25, 1956, will probably be about 160 curies; the neutron emission rate is estimated at 8×10^8 neutrons/cm^2·sec. The existing HRT sample carrier and a 300-gal tank will be used to provide 7 in. of lead for gamma shielding and 17 in. of borated water for neutron attenuation. Figure 2.4 is a sketch of the shield assembly.

[7] E. H. Gift, *Induced Activity in HRT Core Specimen Holder* (to be published).

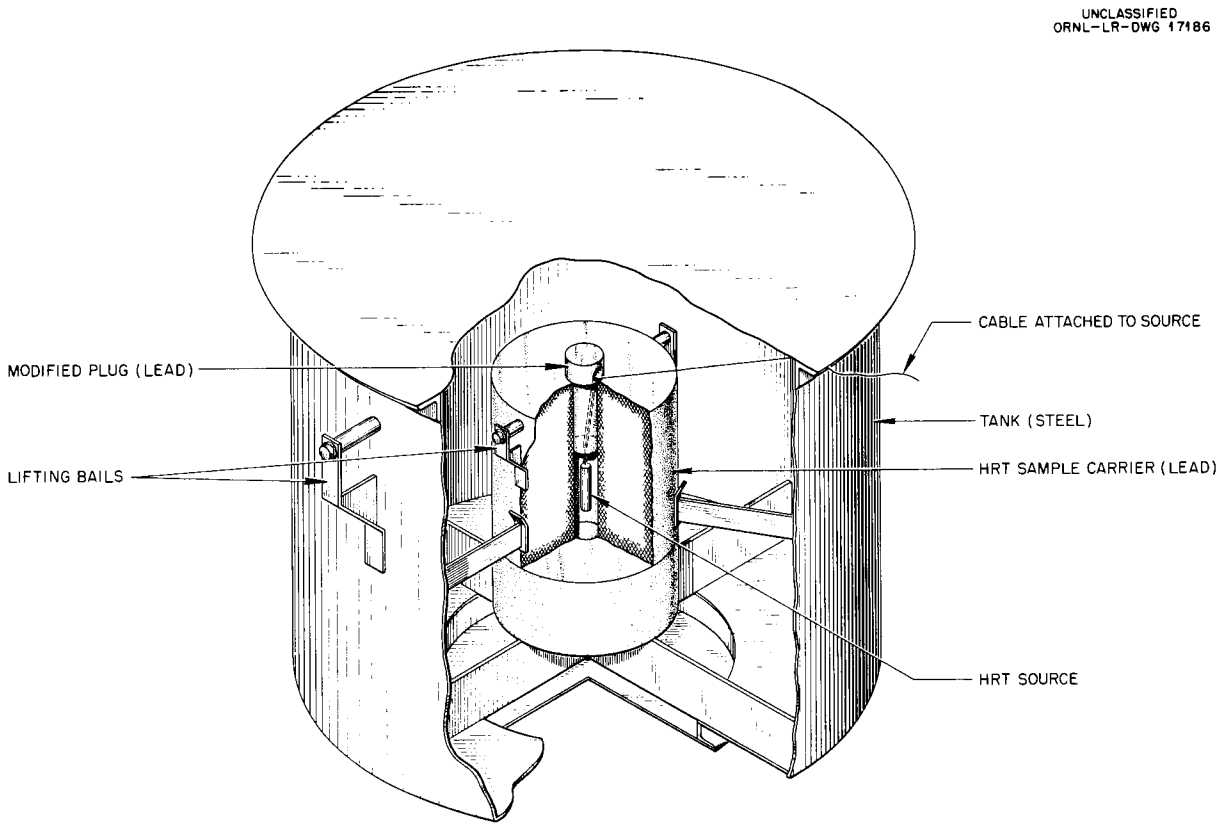

Fig. 2.4. Portable Shield for HRT Source.

2.4 PRESSURE-BALANCING SYSTEM

The rupture-disk assembly in the pressure-balancing system was modified slightly to facilitate removal of the disk holder and to permit the installation of screens opposite each disk.[6] The screens are provided to intercept pieces that may tear from the disks on rupture and to prevent such pieces from flowing into the system, where they might restrict flow or otherwise impair operation. A specification has been prepared and a contract let for the development and fabrication of gold rupture disks to be used with this assembly.

The design of the pressure-balancing valve accepted for the HRT (Fig. 2.5) is very similar to that of the 1-in. dump valve described previously,[8] with the exception that the pressure-balancing valve requires a considerably greater stroke ($\frac{3}{8}$ in.). As a result of tests made by the HRT Instrumentation and Controls Group, type 17-4 PH stainless steel will be used for the plug instead of Stellite. At the time of this report a test stem-seal bellows had been subjected to more than 30,000 cycles at a pressure of 2000 psig, a temperature of from 650 to 705°F, and a valve stroke in excess of $\frac{3}{8}$ in.

Estimates of the radiation activity to be expected in the rupture-disk holder following two years of operation of the HRT at a power level of 5 Mw are (at 4 hr after shutdown):[9]

	Gamma Radiation (r/hr)	
	At 6 in. from Holder	At 6 ft from Top of Biological Shield
Neutron-induced activity (in metal of entire assembly)	500	6.5
Fission-product activity (in holder only, assuming fuel solution in contact with the rupture disk)	7800	55

[8] D. S. Toomb *et al.*, *HRP Quar. Prog. Rep. July 31, 1956*, ORNL-2148, pp 19, 23.

[9] R. E. Aven, *Radiation Problem in Removing Rupture Disc Assembly After Operation of HRT*, ORNL CF-56-9-35 (Sept. 10, 1956).

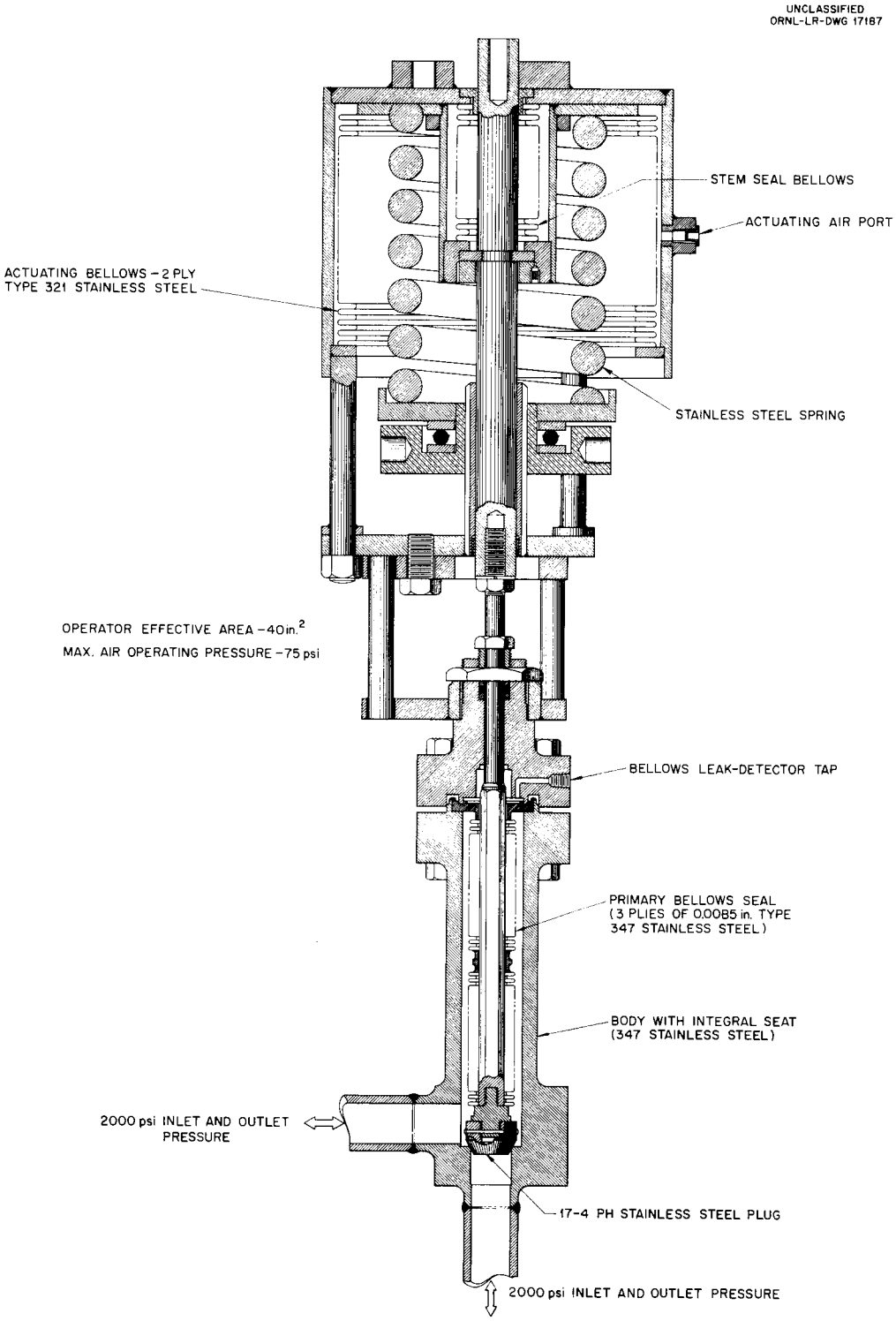

Fig. 2.5. HRT Pressure-Balancing Valve.

The greatest radiation hazard during the removal of the rupture-disk holder will occur when the holder is drawn from the biological shield into a coffin which provides 4 in. of lead gamma shielding. A special shielding plug, similar to that in Fig. 2.3, will provide access to the rupture-disk assembly without disturbance of the remainder of of the cell seal membrane.

2.5 FLANGE BOLTING[10]

Figure 2.6 shows a typical variable-elasticity bolt assembly that was recommended for installation in all high-pressure flanges in the HRT. The ferrule lengths and reduced bolt shanks were specified to increase the elasticity of the bolt assembly to 2.5 times that of the original full-shank HRT bolts.

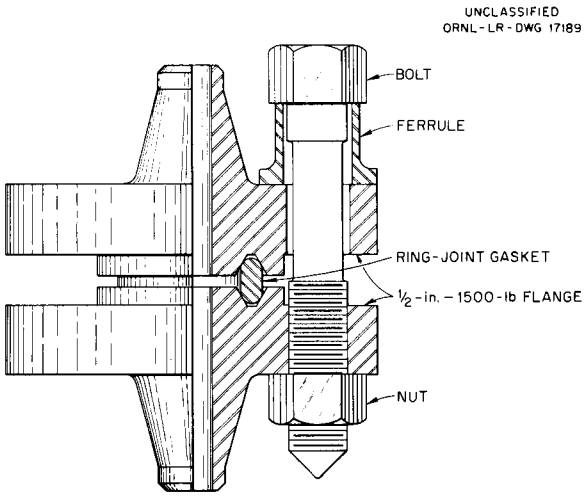

Fig. 2.6. Typical HRT Variable-Elasticity Bolt Assembly.

Tables were prepared giving the recommended and maximum torques to be applied to the AISI 4140 steel bolts in order to restrict maximum tensile stresses to 20,000 to 30,000 psi (the yield stress is 90,000 psi).

2.6 DRY MAINTENANCE

Several advantages of dry, as compared with underwater, maintenance of the HRT have led to a study of the problem involved in such procedures. Figure 2.7 indicates a concept of a shielded roof plug with built-in crane and manipulator to provide motion in the three planes. The operations would be observed by use of periscopes or television or through high-density glass windows in the plug. Maintenance operations would be carried out with the presently designed HRT tools attached to the manipulator. The dimensions of the manipulator plug would permit its insertion at any point over the reactor cell.

2.7 MISCELLANEOUS

Minor redesign of the pressurizer heaters was completed to improve the clamping mechanism. Tests of a single heater under conditions simulating those expected in the HRT indicated that a sustained heat transmission rate of 4.5 kw at a maximum aluminum matrix temperature of 730°F will be possible with the Calrods that are installed in these heaters.

A proposal was issued describing the equipment and procedures for removal of the tie-beams in the HRT cell in the event that installation of temporary shielding in the cell should become necessary.

A natural-convection flange test facility was designed and constructed to investigate the problem of bolted closures under thermal cycling. Flanges will be tested with various combinations of insulation, bolting, and gaskets.

All drawings of the leak-detector system were brought up to date to incorporate the changes necessary to convert the system from D_2O to O_2 operation.

ORNL Central Files reports issued by the Design Section during the quarter are listed below.

Report No.	Author	Title
56-7-127	W. F. Taylor	TBR Plant Turbo-generator Systems Study
56-8-102	C. L. Segaser	Design Study – HRT Pressurizer Level Float
56-8-134	F. C. Zapp	HRT Drawings – Cross Reference Listing
56-8-152	H. A. McLain	HRT Cooling Water System Modification
56-8-175	C. Michelson	Flow Characteristics for HRT Pressure-Balancing Control Valve
56-9-36	C. A. Burchsted	Prices of Type 347 Stainless Steel Shapes
56-9-35	R. E. Aven	Radiation Problem in Removing Rupture Disc Assembly after Operation of HRT

[10] J. N. Robinson, memo to S. E. Beall, *HRT Flange Bolting*, Sept. 10, 1956.

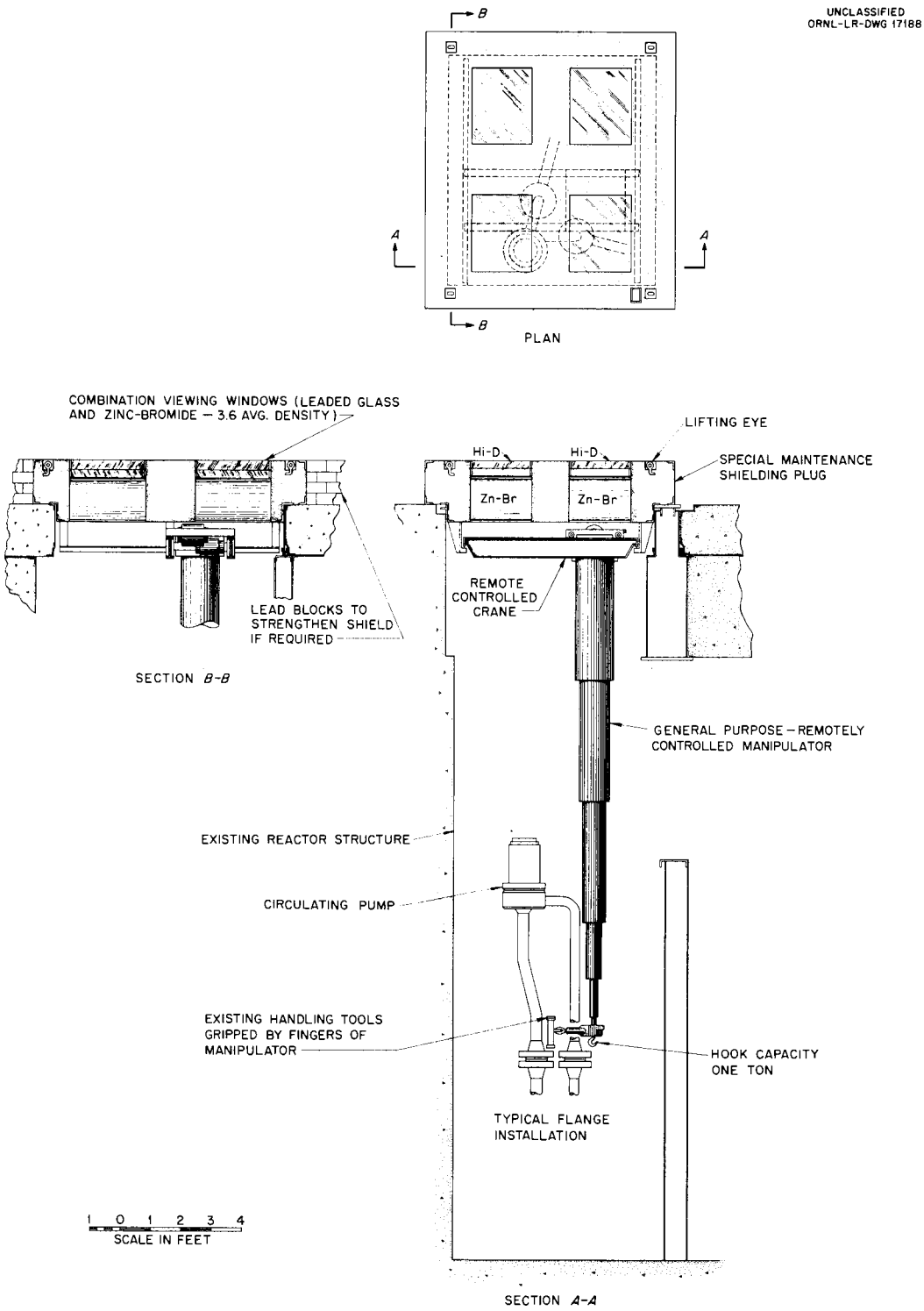

Fig. 2.7. Conceptual Dry-Maintenance Facility.

3. HRT COMPONENT DEVELOPMENT

I. Spiewak

R. Blumberg
B. D. Draper[1]
C. H. Gabbard
B. A. Hannaford
P. H. Harley
E. C. Hise
J. C. Moyers
P. F. Pasqua[2]
W. L. Ross
D. E. Willis
H. D. Wills

3.1 PUMP DEVELOPMENT

3.1.1 400A-1 Pump and Loop

The 400A-1 Westinghouse pump, which contains a titanium impeller and a stainless steel thermal barrier with a titanium wear-ring insert, has operated for 4400 hr since the thermal barrier was welded to the stator flange. For 4278 hr, a solution of 0.04 *m* UO_2SO_4, 0.005 *m* $CuSO_4$, and 50 mole % excess H_2SO_4 was circulated at 255°C. Heat-balance checks on the pump cooling water indicated no leakage around the thermal barrier. Chemical analyses indicated a generalized over-all corrosion rate of 0.15 mpy during the run.

3.1.2 400A-2 Pump and Loop

The 400A-2 pump is being operated in the 400A-2 test loop in a test of various thermal-barrier gasket designs and materials. The pump was operated for 204 hr with water at 250 to 275°C while fitted with a $\frac{3}{16}$-in.-wide Teflon thermal-barrier gasket. During this operation the pump was subjected to three thermal cycles. No leakage was indicated during operation or after disassembly.

A $\frac{1}{16}$-in.-wide gold-plated stainless steel gasket is currently being tested. The narrow design permits higher unit seating force on the gasket with no increase in bolt loading. The pump, while fitted with the new gasket, was subjected to a series of ten thermal cycles on water. Pump cooling-water heat-balance checks indicated no leakage around the gasket.

Bolting materials for use with titanium and stainless steel thermal barriers are being investigated. Difficulty has been experienced in socket-head failures with cap screws made of titanium alloy RC-130-AM and precipitation-hardened 322W stainless steel.

[1]On loan from TVA.

[2]Consultant.

3.1.3 300A-1 Pump

Since the thermal barrier and the main flange were seal welded, the 300A-1 pump has operated in the HRT mockup for 4983 hr, including 4590 hr in uranyl sulfate solution at 300°C. An increase in solution concentration has been noted in the motor cavity, indicating possible leakage around the seal weld or excessive shaft-seal wear or corrosion.

3.1.4 Spare Reactor Fuel Pump and 400A-2 Test Loop

The spare reactor fuel pump with titanium parts operated for a total of 1300 hr on a solution containing 0.04 *m* UO_2SO_4, 0.005 *m* $CuSO_4$, and 50 mole % excess H_2SO_4 at 250°C. Because of high power indication during operation, the pump was dismantled for inspection. The Graphitar thrust-runner surface was generally abraded (Fig. 3.1) and showed one gouge (Fig. 3.2). Very little loss of material occurred. The cast Stellite 19

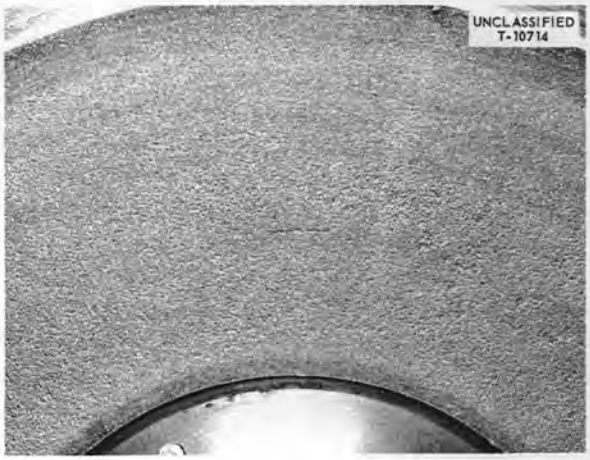

Fig. 3.1. Abraded Surface of Thrust Runner of Spare Reactor Fuel Pump.

thrust shoes were cracked and "burned" in some areas as shown in Fig. 3.3. The failure could have been caused by gas binding in the back of the pump, resulting in excessive bearing temperatures. The thrust runner was replaced, and new stainless steel shoes faced with Stellite 12 deposits were installed. The pump was then operated for 261 hr in cold water prior to being shipped to the 7500 Area.

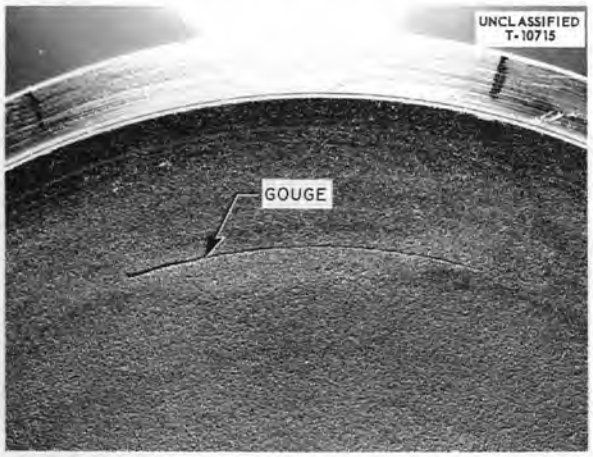

Fig. 3.2. Gouge in Thrust Runner Spare Reactor Fuel Pump.

Fig. 3.3. Damage to Thrust-Bearing Shoes of Spare Reactor Fuel Pump.

3.2 HRT SPARE HEAT EXCHANGER[3]

The contract for fabrication of a 5-Mw spare heat exchanger was awarded to Babcock & Wilcox Co. An acceptable design for the external header was agreed upon.

3.3 DIAPHRAGM PUMPS

3.3.1 HRT Feed Pumps

Diaphragm deflection studies were completed for the standard welded head; results indicated that 0.031-in.-thick diaphragms of type 347 stainless steel would be preferred to the 0.019-in. diaphragms now being used. Use of the thicker diaphragms would result in slightly higher theoretical stresses (24,000 vs 16,000 psi) but would eliminate the wave motions which exist in the 0.019-in. material. Therefore, because the actual operating stresses are lower, longevity should be enhanced. A detailed report is being issued covering the above work and other feed-pump development.[4]

Since there are no corrosion-fatigue data available for materials operating in uranyl sulfate solution, a subcontract is being placed with Ohio State University for a study of the fatigue properties of annealed and work-hardened type 347 stainless steel in that medium.

Feed pump loop No. 1 is being used for diaphragm endurance testing in water. At the present time an annealed 0.019-in. diaphragm has been tested for 1541 hr and a $^1/_4$-hard 0.031-in. diaphragm for 611 hr. These diaphragms will be tested until they fail.

Feed pump loop No. 2 was completed and put into operation. Several difficulties in the bolted-head design and in the loop piping are being corrected.

3.3.2 HRT Purge Pump

A prototype HRT purge pump is being run continuously at 2000 psi and 200 strokes/min on

---

[3]C. B. Graham *et al.*, *HRP Quar. Prog. Rep. July 31, 1956*, ORNL-2148, p 13.

[4]R. Blumberg, C. H. Gabbard, and E. C. Hise, *Diaphragm Feed Pump Development Program Progress Report*, ORNL CF-56-10-114 (Oct. 29, 1956).

an endurance test. The diaphragm has been operated for a total of 5330 hr to date.

The cause of the eroded discharge-check-valve seats[5] has not yet been fully determined. The microstructure of the seat material (Stellite 6) was found to differ from that of the material that gave excellent service in the HRE Lapp Pulsafeeder pumps. Samples of both materials were sent to Haynes Stellite for identification.

3.4 HRT DUMP TEST

The two-region dump tests on the $\frac{1}{18}$-scale model of the HRT were completed.[6] Initial conditions were usually 300°C and 2000 psi in both systems.

With simulated HRT control of vent and dump valves, it was possible to maintain the pressure balance to within 50 psi, with the system pressure decreasing at a maximum rate of 50 psi/sec.

A test was conducted with the core system charged with nitrogen at 2000 psi and the blanket charged with pressurized water as usual. During this test, which was considerably more severe than the normal operating condition, the control system was able to maintain the pressure balance to within 75 psi. The studies show that the HRT control system should be able to maintain the core and blanket pressures to within 50 psi as required.

3.5 HRT SAMPLER

Additional runs were made with the prototype HRT sampler. The limit switches for flask-holder position and isolation-chamber stem position were found to work satisfactorily.[7]

3.6 FREEZE JACKETS

The freeze-jacket test assembly was modified to operate at temperatures up to 300°C and pressures to 2000 psi. Conditions similar to several existing in the HRT can now be reproduced.

Tests were made on a $\frac{5}{16}$-in.-OD, type 347 stainless steel refrigerant coil welded around a $\frac{1}{2}$-in. vertical pipe. The pipe was an appendage on a piping system through which fluid was circulated at 300°C and 2000 psi to simulate the condition on the reactor where line 167 to the chemical plant leaves the main circulating loop. Water leaking at a maximum rate of 11 cc/min was frozen off in an average time of 20 min, with a refrigerant temperature of −40°C.

Maximum leak rates at which water could be frozen at 2000 psi and various loop temperatures are listed in Table 3.1. Heat was removed by the refrigerant at a rate of 8 to 16 Btu/min. The average rate at which Freon refrigerant passed through the coil was 1.7 gpm.

3.7 NATURAL-CIRCULATION RECOMBINER

A natural-circulation recombiner[8] was constructed[9] (Dwg. TD-E-2955) and tested. A similar recombiner will be installed on the fuel storage tanks in the HRT.

[5] C. B. Graham *et al.*, *HRP Quar. Prog. Rep. July 31, 1956*, ORNL-2148, p 15.

[6] C. H. Gabbard, *HRT Dump Test*, ORNL CF-56-10-73 (Oct. 29, 1956).

[7] C. B. Graham *et al.*, *HRP Quar. Prog. Rep. July 31, 1956*, ORNL-2148, p 16.

[8] C. B. Graham *et al.*, *HRP Quar. Prog. Rep. Oct. 31, 1955*, ORNL-2004, p 65.

[9] C. H. Wodtke, *Inspection of Recombiner*, memorandum to S. E. Beall, dated Sept. 18, 1956.

TABLE 3.1. RESULTS OF FREEZE-JACKET TESTS

Insulation: aluminum foil
Pressure: 2000 psi

Loop Temperature (°C)	Refrigerant Temperature (°C)	Maximum Leak Rate (cc/min)	Time to Freeze (min)
300	−40	11	20
200	−39	14	12
100	−40	22	4.5
24	−41	70	2.5

The design capacity was 8.26 standard liters per minute of D_2. The unit was operated satisfactorily with H_2 fuel at 156% of capacity, with O_2 and air used as diluents.

The efficiency of the recombiner as an H_2 burner was 99.9% at a flow of 17 liters per minute of stoichiometric gas, with an excess O_2 input of 0.57 liter/min bled off through the vent. With the vent valved off and no excess O_2 flow, recombination was 100% complete, as indicated by a steady recombiner pressure.

Before the H_2 and O_2 were introduced, circulation was started by use of 225-psi steam in the tubing at the bottom of the chimney.

3.8 HRT MOCKUP

3.8.1 Operation

The HRT mockup operated for 1628 hr during the period covered by this report. In a continuation of a run started previously,[10] the mockup operated for 275 hr at 2000 psi and 300°C, with a solution concentration of 0.042 *m* UO_2SO_4, 0.021 *m* H_2SO_4, and 0.005 *m* $CuSO_4$. The O_2 concentration was 500 ppm, except for the final 190 hr, when it was reduced to 130 ppm. The run was terminated by a bellows failure in a ½-in. Fulton Sylphon block valve.

Following an inspection and maintenance period, operation was begun at 1400 psi and 280°C, with a solution concentration of 0.04 *m* UO_2SO_4, 0.024 *m* H_2SO_4, 0.02 *m* $CuSO_4$, and 500 ppm O_2. These are the conditions proposed for the initial power operation of the HRT. The lower pressure permitted high-pressure O_2 addition from gas cylinders. The latter run has continued for 1353 hr without requiring maintenance shutdowns.

3.8.2 Inspection

Before the 1400-psi operation was started, the loop was subjected to a major inspection; 1843 operating hours, mostly at 300°C, had elapsed since the previous inspection. Stainless steel corrosion coupons removed from the high-pressure stream showed corrosion rates of 0.15 to 0.19 mpy; the titanium was attacked at 0.04 mpy. Type 347 stainless steel coupons in the vertical leg from the loop to the pressurizer showed rates varying from 0.04 mpy at the top in steam to 0.24 mpy at the bottom. These results compare with a generalized rate of 1.5 mpy obtained from nickel analyses.

Parts of the high-pressure loop that could be inspected visually appeared to be in good condition. The horizontal pipe connection to the pressurizer contained 350 g of finely divided corrosion- and fission-product solids which had settled in that low-velocity region. Only 1.2% of the deposit was uranium. The only serious corrosion was found in the cap that was removed from the end of the horizontal pressurizer header. It contained stress-corrosion cracks extending through about one-fourth the wall thickness. The cause of the cracking has not been determined. The cracks occurred on the bottom of the cap, near a weld, and were covered with solids which contained 25 ppm of Cl^- and 2000 ppm of F^-. The cap was made from bar stock, not necessarily of HRP quality.

The gas separator was in good condition, and the area between the separator and the pipe wall was not plugged.

The O-ring groove of one pair of flanges in the main loop showed small pits when dye-checked. A new ring was installed and the joint was tightened. The flanges will be dye-checked again during the next major shutdown.

3.8.3 Component Failures

A feed-pump pulsator housing failed after being in service for 2870 hr. The failure was in the side wall near the closed end of the housing and was similar to housing failures reported previously.[11]

The bellows in a ½-in. Fulton Sylphon block valve failed after 190 hr of service. Solution conditions at the time of failure were: 130 ppm of O_2, a temperature between 240 and 280°C, and 5 ppm of Cl^- in the solution. The corrosion,

[10] C. B. Graham *et al.*, *HRP Quar. Prog. Rep. July 31, 1956*, ORNL-2148, p 17–18.

[11] H. L. Falkenberry and I. Spiewak, *Pulsafeeder and Purge Pump Failures on the HRT Mockup*, ORNL CF-56-3-173 (March 1, 1956).

which appeared to be a general attack with some stress cracking, was localized in the top of the bellows. The failure is still being studied by the Metallurgy Group. There was no uranium precipitation, such as would be expected in an oxygen-deficient solution.

3.8.4 Special Tests

A study of solids removal was made in the mockup, using a hydroclone installation similar to that which is installed on the HRT. Results of these studies are reported by the Chemical Technology Division in Sec. 15.1.

4. HRT REACTOR ANALYSIS

P. R. Kasten

H. C. Claiborne T. B. Fowler M. W. Rosenthal

4.1 EXPLOSION HAZARD IN HRT REACTOR CELL

Rupture of the HRT high-pressure system would result in the release of hot fluid, deuterium, and oxygen into the containment cell. Under this circumstance the maximum cell pressure attained would be dependent upon the volume of hot fluid exposed to cell conditions, the total energy release, the rate of energy release, and the thermodynamic conditions. Of particular importance are the amount of D_2 and O_2 present, which would be affected by the occurrence of a zirconium-water reaction, and the pressure rise associated with a D_2-O_2 explosion. In this study[1] the energy release, explosion hazard, and cell pressures developed with and without an explosion were examined for a number of situations following rupture of the high-pressure system.

4.1.1 Zirconium-Water Reaction

Studies of metal-water reactions[2] have revealed that very high temperatures and fine dispersions are necessary to achieve appreciable Zr-H_2O reaction. However, the reaction of Zircaloy-2 with the fuel solution in a radiation field is at present uncertain.

If all the zirconium in the reactor core tank were to react according to Eq. 1, about 10^6 Btu of energy would be released.

$$(1)\quad Zr + 2D_2O \longrightarrow ZrO_2 + 2D_2 + \text{Energy}$$

If the D_2 evolved from this reaction were to combine with O_2 in the reactor cell, an additional 10^6 Btu would be released. Because of the improbability of a Zr-D_2O reaction when the metal is present in massive form, complete reaction does not appear to be a reasonable assumption. If 10% or 1% of the zirconium reacted in accordance with Eq. 1, the energy release would be 10^5 or 10^4 Btu, respectively; these values can be compared with 1.5×10^6 Btu, which is the thermal energy (above a liquid temperature of 100°C) stored in hot fluid in the core and blanket high-pressure systems.

The maximum cell pressure would be dependent upon the fraction completion of the metal-water reaction. With zero metal-water reaction, the maximum cell pressure following adiabatic expansion of all fluid in the high-pressure systems has been calculated by Wood[3] to be 35.5 psia. If the energy from complete reaction of the core tank without recombination of D_2 were added to the thermal energy of the water, the static cell pressure following a rupture would be 55 psia. Reaction of 10% of the zirconium would result in a peak pressure of 38 psia, and for 1% reaction the maximum pressure would be about 36 psia. About 50% reaction would be required to exceed the 45 psia at which the cell has been tested.[4]

4.1.2 Explosion Hazards in Reactor Cell

The concentrations of D_2 which would occur in the HRT reactor cell following rupture of the high-pressure systems have been computed for a number of situations. If both the core and blanket fluids were saturated with dissolved D_2, the concentration of D_2 existing in the cell after rupture would be 2 mole % if the steam condensed completely and 0.5 mole % if the steam expansion were adiabatic. If the D_2 from a complete Zr-D_2O reaction were included, the concentrations for the above conditions would be 24 and 7 mole %, respectively; for 10% Zr-D_2O reaction the mole fractions would be 5 and 1.2%, while 1% reaction would add little D_2 relative to that dissolved in the core and blanket fluids.

The lower explosive limit for D_2 is in excess of 4% in air and 10% in steam.[5] Therefore it appears that an explosion in the cell would not occur

[1] M. W. Rosenthal, *Hazard to HRT Containment Cell from Zirconium-Water Reaction or D_2 Explosion*, ORNL CF-56-8-156 (Aug. 24, 1956).

[2] H. M. Higgins, AGC-2914-2 (April 30, 1956) (Secret).

[3] P. M. Wood, *HRP Quar. Prog. Rep. Jan. 31, 1955*, ORNL-1853, p 6.

[4] J. N. Robinson, *Test of HRT Cell Preliminary Report*, ORNL CF-55-11-62 (Nov. 9, 1955).

[5] D. W. Kuhn *et al.*, Y-731 (March 1, 1951) (Secret).

unless there were at least 10% metal-water reaction, accompanied by condensation of steam.

The above computations assumed complete mixing of gases in the reactor cell, since circulation of air in the cell is afforded by the space-cooler blowers, which have a total capacity of about 20,000 cfm. Although improbable, it is conceivable that a D_2 leak from the reactor into an air pocket could result in accumulation of a combustible mixture.

4.1.3 Pressure Rise from D_2-O_2 Explosions

The static pressure which exists in a fixed-volume, adiabatic system following a hydrogen explosion varies from about 4 to 11 times the initial pressure over a wide range of hydrogen concentrations in diluents of air or steam.[6] Although detonation cannot be sustained in a three-dimensional system, the impact pressure on a container wall from an ordinary explosion may be 2 to 4 times as great as the equilibrium static pressure, or between 8 and 44 times the pressure before the explosion. At the time of an explosion the pressure existing in the HRT cell could be between 7.5 and 55 psia, dependent upon the fraction completion of the metal-water reaction. However, the likelihood of an explosive mixture is less for the higher initial pressures.

The preceding values apply to explosions in a container filled with a uniform mixture of explosive gas. As indicated in the preceding section, attainment of an explosive mixture which fills the cell is highly unlikely, but an explosion might be possible in a limited volume within the cell. All the D_2-O_2 from the reactor following a 10% zirconium-water reaction would occupy 1.8% of the cell volume if accumulated as a stoichiometric mixture. If it were to explode before any steam condensation occurred elsewhere in the cell, the maximum static pressure would be about 50 psia. With no metal-water reaction the D_2-O_2 normally in the reactor (accumulated as a stoichiometric mixture) would occupy less than 0.5% of the cell; if this were to explode, the maximum static pressure would be about 41 psia.

[6] T. H. Pigford, ORNL-1322 (Aug. 14, 1952) (Secret).

4.2 RADIATION LEVEL WITHIN HRT CELL

After reactor shutdown the radiation level within the HRT cell would be due to the induced activity in the shield materials and equipment, and to fission products adhering to the inner surfaces of the equipment. Initial results from calculations show that induced activity in the shield or equipment would be small in comparison with fission-product activity, even if only a small percentage of the total fission products were retained on equipment walls. The activation of the shield and of the steel liner of the cell would contribute only about 3 r/hr to the cell radiation level 4 hr after reactor shutdown following one year of operation at 5 Mw.

5. HRT CONTROLS AND INSTRUMENTATION

D. S. Toomb

A. M. Billings
J. D. Grimes[1]
J. C. Gundlach
R. L. Moore
L. R. Quarles[2]
W. P. Walker[2]
K. W. West

5.1 COMPONENT AND SYSTEM TESTING

5.1.1 Remote-Radiation-Monitoring System

In the HRT, service lines from the reactor are to be monitored for activity by remote radiation-detection elements (small gamma ionization chambers). Ten such units will be connected to a central control-panel chassis and power supply. Two of these assemblies were received from the Victoreen Instrument Company and were accepted after performance testing at the ORNL Health Physics Division calibration facility. They will be installed in the HRT during the next quarter.

5.1.2 Oxygen-Injection System[3]

The oxygen-injection system shown in Fig. 5.1 controls and meters the gas flow from a high-pressure liquid-oxygen converter to the reactor high-pressure system. The gas flow is first restricted by the snubbing capillary to prevent damage to the differential pressure cell by the sudden application of pressure. This transmitter provides an electrical signal proportional to the flow by sensing the differential pressure produced by the gas flow through the metering capillary. The electric flow signal is transduced to an air signal, which is recorded in the control room and which provides a means of actuating the bellows-sealed needle-type flow-control valve. The actuator is adjustable to provide a stroke of from 0.010 to 0.150 in. for a 3- to 15-psi control signal.

5.1.3 Pressurizer-Level Control System

In order to optimize control of the pressurizer level in the HRT, a frequency-response analysis was conducted on the pressurizer-level control system in the HRT mockup facility. The elements of this control loop are shown in Fig. 5.2. The level is controlled by the letdown valve, which throttles a mixture of gas and liquid out of the high-pressure circulating system into the low-pressure storage tanks and gas recombiners. The continuously operating feed pump provides a constant makeup liquid flow.

The pulsating action of the feed pump and the vibrational sensitivity of the displacer-type transmitter produced an air signal to the recorder-controller which contained too much "noise." The control was improved by minimizing the noise in this signal so that the derivative element of the controller could be used to the best advantage.

After the optimum magnitude of damping was found, the system performed as indicated below; the data are compared with the criteria for stability set forth in the literature.[4] The results indicate that the system is now slightly underdamped and marginal with respect to gain.

	System	Criteria for Stability
Phase margin (open loop)	60 deg	Exceed 30 deg
Gain margin (open loop)	0.62	Exceed 0.60
Maximum offset ratio (closed-loop step response)	1.67	~1.5

The design of the piping from the level-transmitter housings to the pressurizers is being reviewed by the Mechanical Design Section. Resistance to flow in this connecting piping results in a lag in level change which is added to the pneumatic transmission lags and must be minimized for optimum control.

5.1.4 Dump Tests

Temporary pneumatic recorders with fast chart drives have been provided for the dump tests of the HRT. These tests have as their purpose the evaluation of the controls utilized to maintain the differential pressure between the reactor core

[1]On loan from TVA.

[2]Consultant from University of Virginia.

[3]D. S. Toomb *et al.*, *HRP Quar. Prog. Rep. July 31, 1956*, ORNL-2148, p 19.

[4]G. A. Coon and W. I. Caldwell (eds.), *Frequency Response for Process Control*, Taylor Instrument Companies, Rochester, N.Y., 1955.

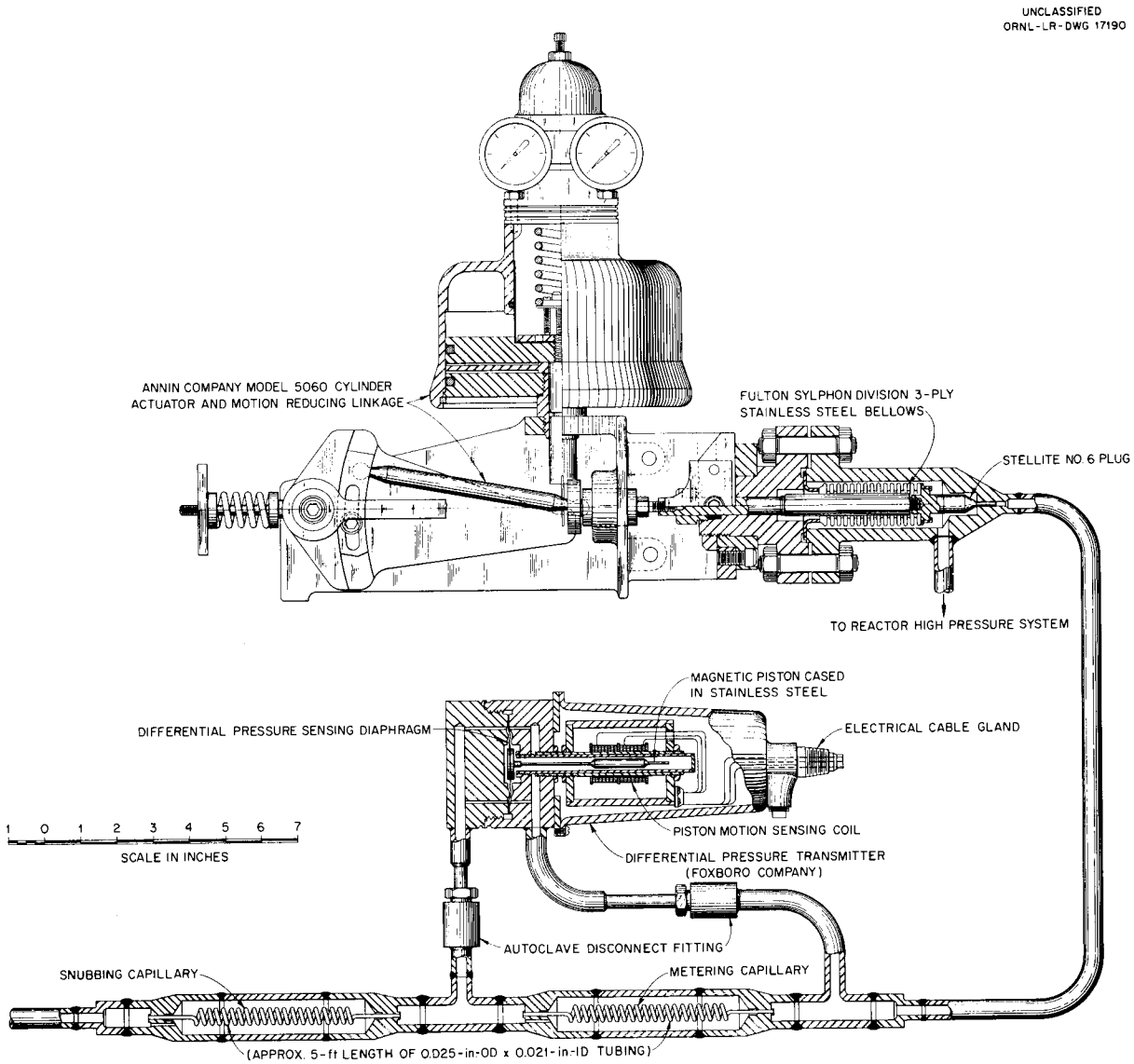

Fig. 5.1. Oxygen Metering and Control System.

and blanket systems during the time of an emergency shutdown. During such a shutdown the contents of the high-pressure systems must be rapidly drained through the dump valves to the low-pressure storage tanks. Whenever possible, existing system transmitters have been used; however, an electric-transmission differential-pressure transmitter has been provided to sense the core-blanket differential pressure in order to obtain a faster system. The pneumatic transmitter, which is permanently installed, was specified because it is operable from the emergency air system during power failures. Slide-wires for transmitting valve position have been added temporarily to key valves to provide information on valve response times. The speed of response of the dump valves has been increased by adding an air capacity tank on the upstream side of the solenoid pilot valves.

5.1.5 Disconnects for Valve-Actuator Air Lines

In the HRT, provision was made for remote removal of the control valves when replacement is necessary. This necessitated the use of

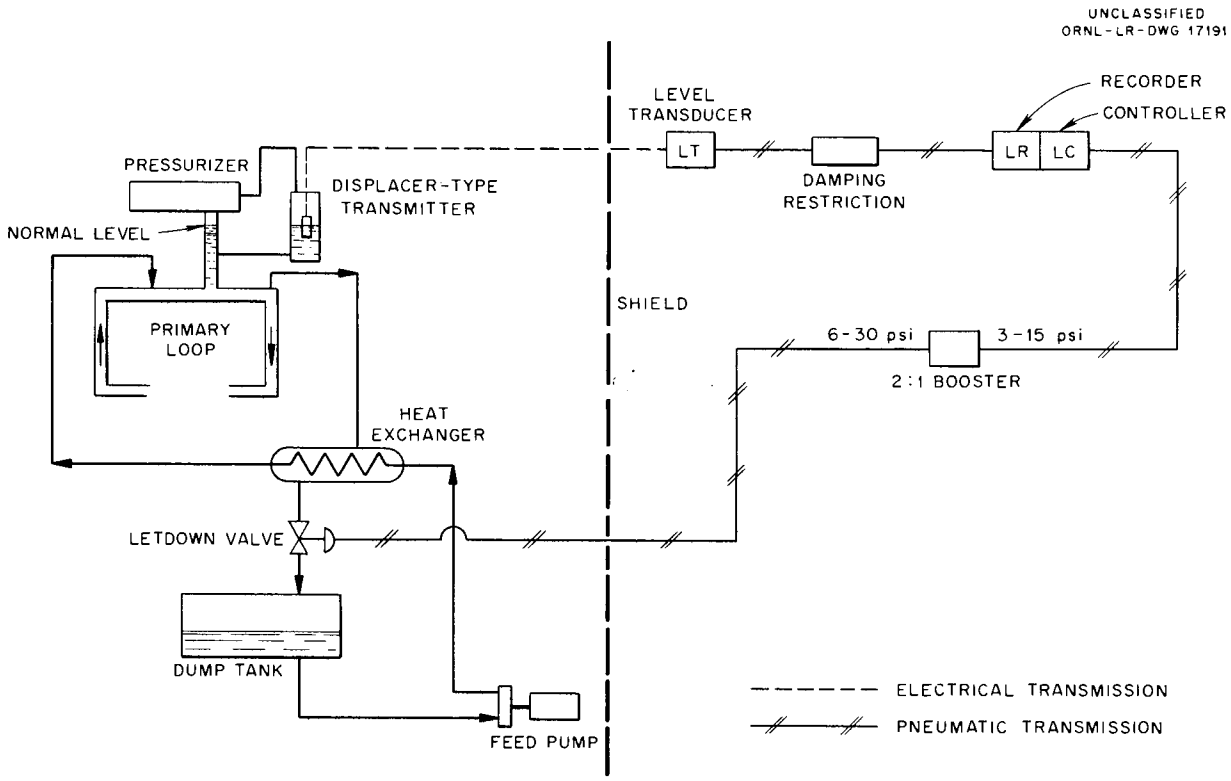

Fig. 5.2. HRT Pressurizer-Level Control Loop.

"quick" disconnects in the air lines to each valve actuator. A long-term leakage test of these disconnects, which use natural-rubber packers for seals, was completed. The unit showed no detectable leakage while being held at 150°F for two and one-half months.

5.1.6 Heat-Balance Flowmeters

The differential-temperature system for measuring feed and purge water flow rates was calibrated at known flows and found to be satisfactory, although it has an inherently slow response. This type of system is used because it introduces no pressure drop, involves no regions of high fluid velocity, and meters without the use of moving parts.

5.1.7 Sample Stations

The reactor system has two stations for remotely controlling the withdrawal of radioactive samples of the fuel and blanket solutions. These sample-station control circuits were revised to provide better operating knowledge of valve and chamber positions. The assemblies were tested at 2000 psi, and overrange did not shift the zero of the pressure transmitters.

5.1.8 Emergency Air System

The emergency air system automatically provides nitrogen for control during periods of power or compressor failure. The emergency nitrogen tank supply and controls were tested and found satisfactory. The nitrogen regulator took over at 55 psig and provided sufficient gas for the operation of the entire reactor pneumatic control system for 28 min before the dump-valve loading pressure dropped to 48 psig and closed the dump valves.

5.1.9 Conduit Leakage Tests

All thermocouple conduits penetrating the north shield were leak tested and showed no leakage through the sealing Unilet at the shield. The leakage rate into the conduit inside the shield was acceptably low. However, tests show that

the power conduits will have to be sealed beyond the Fiberglas conductors to prevent leakage at the shield face.

5.2 DESIGN

5.2.1 Waste Disposal System

The design of the instrumentation for the radioactive-waste disposal system was completed. This system will be installed when construction time permits.

5.2.2 Control Circuits

The electrical system for the oxygen generator was revised so that controls and instruments could be placed inside the building.

Control-circuit drawings are being revised for the addition of a gas-recombination delay stage to the dump system, rearrangement of dump circuitry for greater reliability, change of oxygen-addition circuitry for high-pressure addition, and inclusion of the additional circuitry and controls required by cooling-water-system revisions.

6. HRT PROCESSING PLANT

W. E. Unger

T. A. Arehart
G. B. Berry
B. F. Bottenfield
N. C. Bradley
N. A. Brown
W. D. Burch
W. L. Carter
S. D. Clinton
W. J. Clossey
J. L. Gory
P. A. Haas
C. C. Haws
R. H. Horton
F. C. McCullough
E. O. Nurmi
A. M. Rom
W. F. Schaffer
H. O. Weeren
R. H. Winget

6.1 CORE FUEL PROCESSING – FLOWSHEET

The insoluble contaminants in the reactor fuel solution will be removed centrifugally from a small stream which bypasses the reactor heat exchanger. The solids, along with a quantity of reactor fuel, will be discharged periodically to a dissolver, dried to recover the heavy water, and dissolved in sulfuric acid for sampling.

The dissolution of the solids, ZrO_2, Fe_2O_3, Cr_2O_3, etc., in boiling 10.8 *M* H_2SO_4, is essentially a metathesis. An insoluble sulfate layer forms on the surface of the oxide particles and prevents complete conversion of the oxide to the sulfate. The insoluble sulfate layer must be removed; this is accomplished by diluting the dissolver solution to 4 *M* H_2SO_4, which dissolves the sulfate layer and exposes the surface of the unconverted oxide to the dissolver solution. The diluted dissolver solution can be reconcentrated by evaporation to 10.8 *M* H_2SO_4 for the second and final dissolving.

The dissolving cycle now consists of the following:

1. dissolving for 6 hr in boiling 10.8 *M* H_2SO_4,
2. diluting to 4 *M* H_2SO_4,
3. refluxing for 4 hr in 4 *M* H_2SO_4,
4. evaporating to 10.8 *M* H_2SO_4,
5. dissolving for 6 hr in boiling 10.8 *M* H_2SO_4,
6. diluting to 4 *M* H_2SO_4,
7. refluxing for 1 hr in 4 *M* H_2SO_4.

The dissolver is being constructed of a type 347 stainless steel 6-in. pipe lined with 0.020-in.-thick tantalum (see Fig. 6.1). Tantalum nozzle sleeves which pass through the stainless steel cover are anchored to the cover with Swagelok fittings and are welded to the tantalum cover sheath. The dissolver and cover flanges are sealed with a flat gold gasket, but provision has been made for a peripheral seal weld of their liners.

The 4 *M* H_2SO_4 dissolver contents will be transferred to a hold tank for sampling (see Fig. 6.2) and then dropped back to the dissolver. After sampling, the dissolver contents, followed by water washes, will be transferred to one of two decay tanks for storage. Approximately 13 weeks of decay is desired before the solution is transferred from the cell to an external carrier for subsequent processing for recovery and decontamination of the uranium.

The 4 *M* H_2SO_4 is far more corrosive if boiled; therefore the use of steam as an inert diluent for transporting radiolytic hydrogen and oxygen to a catalytic recombiner is not practical. Instead, the oxygen atmosphere of the decay tank will be used and will be continuously circulated through the recombiner by thermal convection; a heater and cooler on a loop above each decay tank will be used to promote the convection.

The decay tanks will be constructed of Carpenter-20 stainless steel pipe, jacketed for steam and cooling water (see Fig. 6.3). They will be sufficiently remote from the high-pressure equipment that liquid-level sensing by oxygen bubbler lines is deemed acceptable. In order to minimize the amount of oxygen discharged to the off-gas system, the bubblers will be operated only when accurate liquid-level readings are desired. Automatic valves in the bubbler lines at the cell wall will be closed on signals from radiation monitors to prevent the escape of radioactivity beyond the shielding wall.

6.2 CONSTRUCTION STATUS

Construction of the HRT Core Processing Plant was completed during August. Figure 6.4 shows a view of the cell just before construction was completed. High-pressure equipment is located

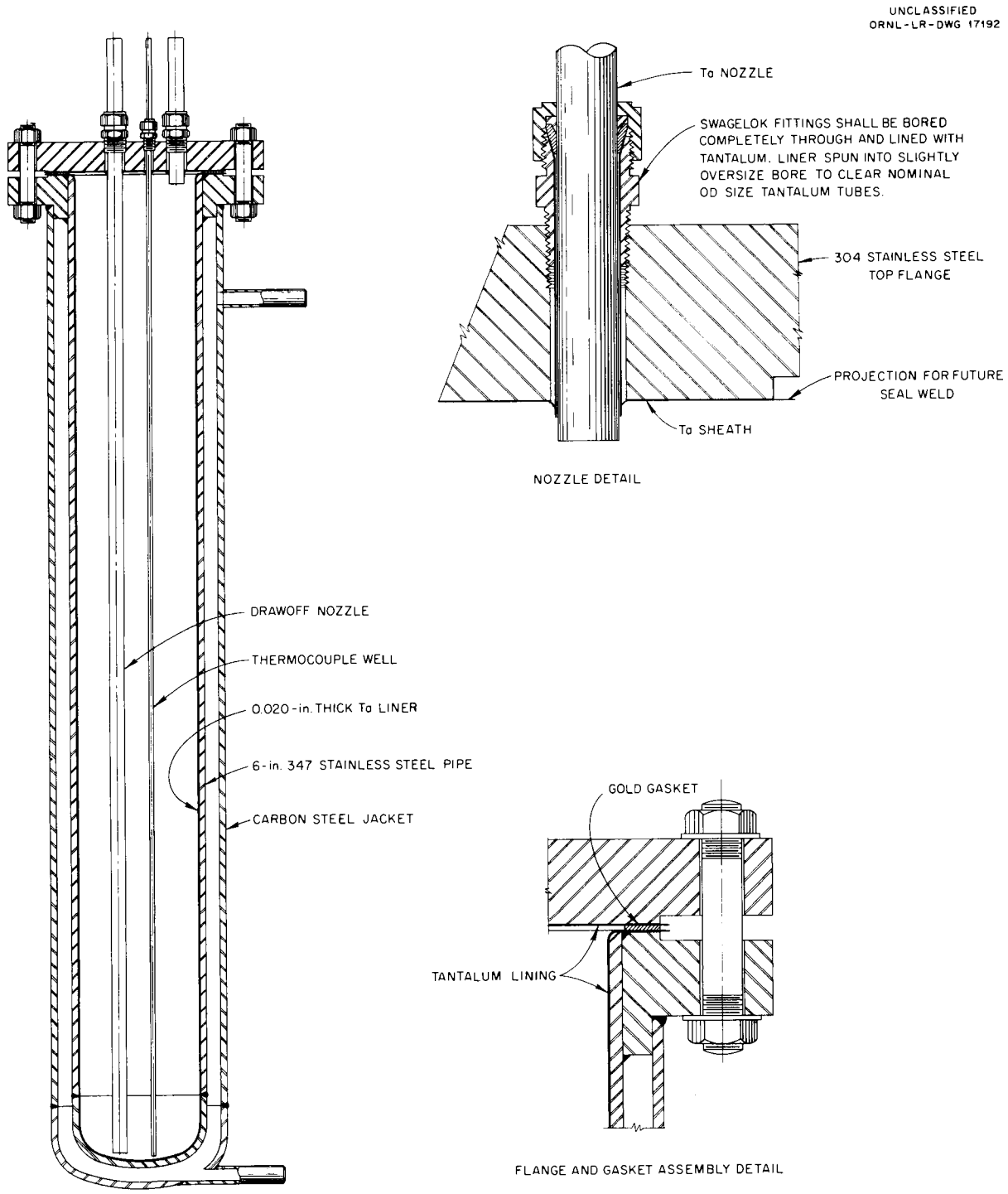

Fig. 6.1. HRT-CP Tantalum Dissolver.

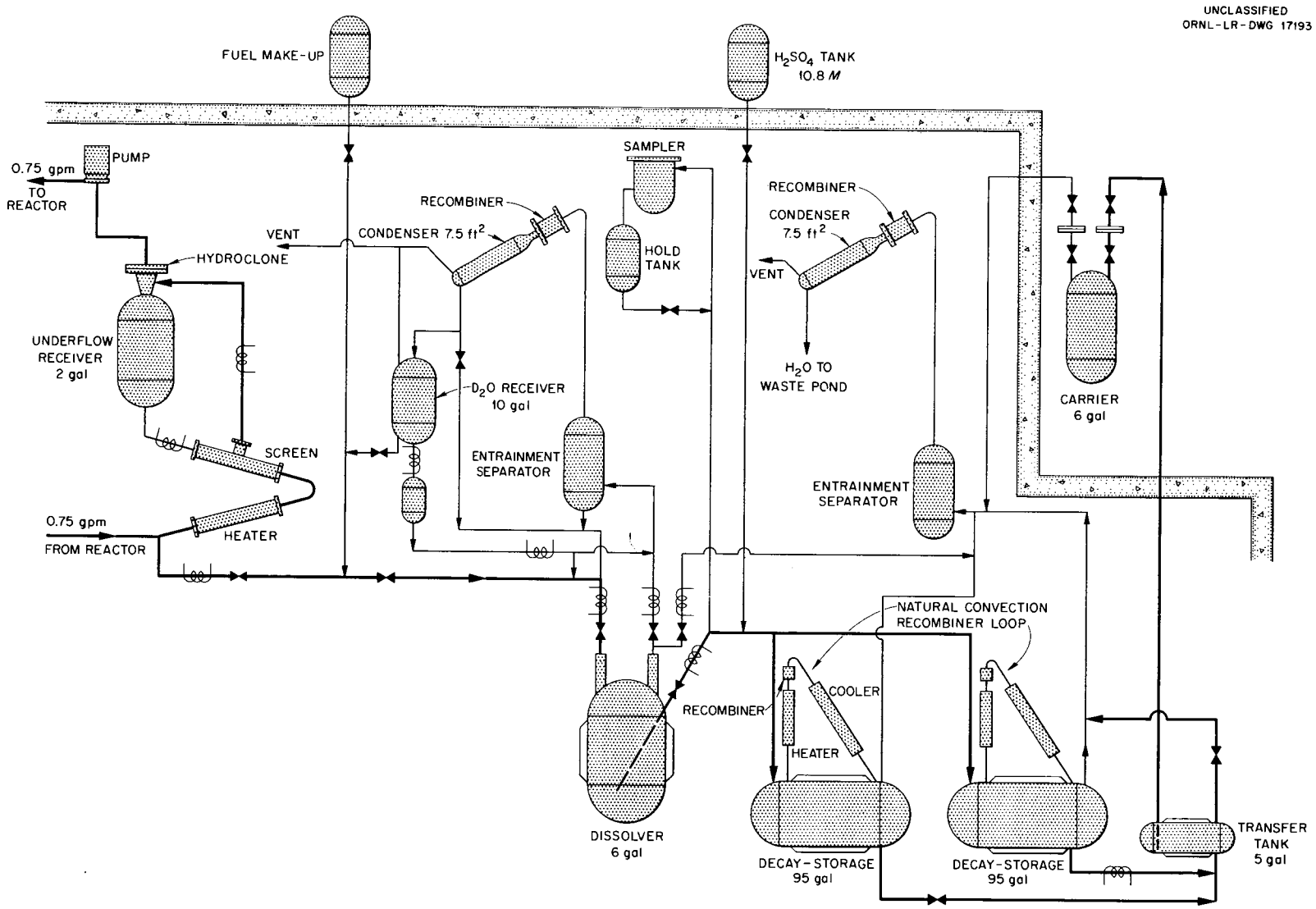

Fig. 6.2. Schematic Flowsheet of HRT Core Processing Plant.

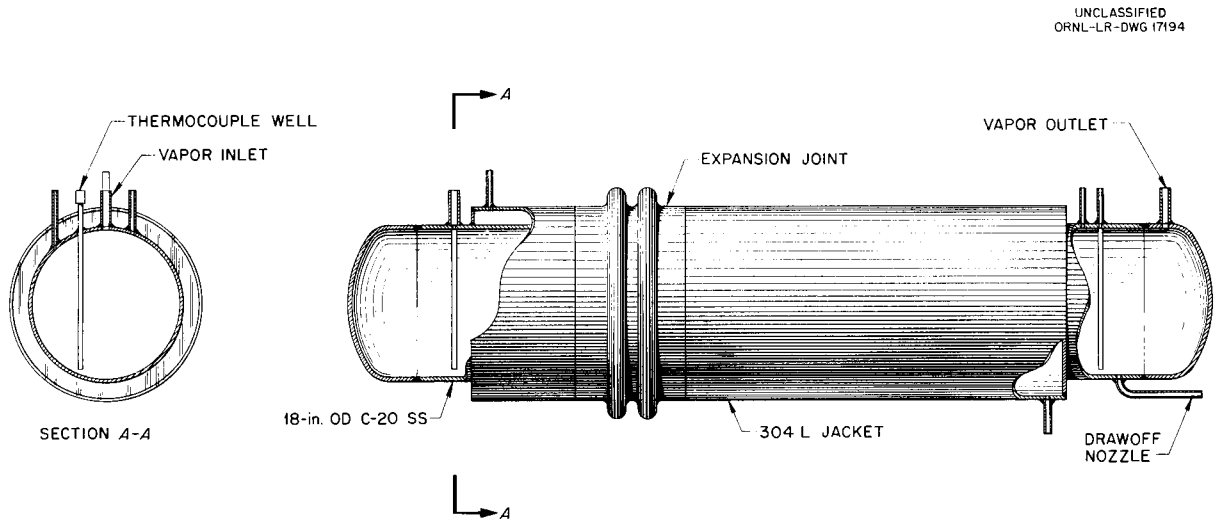

Fig. 6.3. Decay Tanks T-21 and T-22.

on the right side of the photograph, with low-pressure equipment in the upper left part of the picture. Visible in the right foreground are portions of the insulated high-pressure piping. Directly below and just to the left of the circulating pump is the hydroclone and underflow-receiver assembly; the hydroclone is installed in a specially machined flange located immediately below the mating and sealing flange[1] visible in the picture.

Modifications to the low-pressure equipment incidental to the proposed dissolving system have not been started. A dissolver, two decay storage vessels, and a condensate tank will be located on the lower level of the cell, with a new sampler, similar to existing designs, in the top northwest corner of the cell. Shop fabrication of the tanks is under way, and field installation will begin as soon as all are available.

6.3 ENGINEERING TESTS AND SHAKEDOWN OPERATIONS

Engineering tests and shakedown of the plant are under way, with emphasis on equipment in the service areas and within the high-pressure system, which will not be affected by the dissolver-system installation. Results of tests completed are summarized in the following subsections.

6.3.1 Refrigeration System[2]

Although performance of the refrigeration system has been satisfactory, minor difficulties were experienced with solenoid valves in lines to individual freeze coils and with mechanical seals on the circulating pumps in the secondary Freon "brine" system. However, all freeze coils have been frozen regularly with process equipment at normal operating temperatures. Even within the high-pressure system, freeze plugs can be easily maintained at −25°C with Freon at −35°C and process equipment at 275°C.

6.3.2 Hydrostatic Test

All high-pressure piping and equipment, including the shakedown loop,[3] were subjected to a hydrostatic test at 300 psi. During the test a faulty seal weld was located and repaired on a valve where the bellows-poppet assembly is welded to the valve body. No equipment failures occurred during the test.

6.3.3 Trisodium Phosphate and Nitric Acid Rinses

The high-pressure equipment, the shakedown loop, and a small portion of the low-pressure

[1] W. E. Unger *et al.*, *HRP Quar. Prog. Rep. April 30, 1956*, ORNL-2096, p 48.

[2] R. E. Brooksbank, *Testing Procedures for HRT-CP Refrigeration System — HRT-CP Engineering Test P-13 and P-14*, ORNL CF-56-7-139 (July 11, 1956).

[3] B. H. Hamling, *Design of Solids Feed Loop for Shakedown of the HRT Chemical Plant*, ORNL CF-56-3-34 (March 5, 1956).

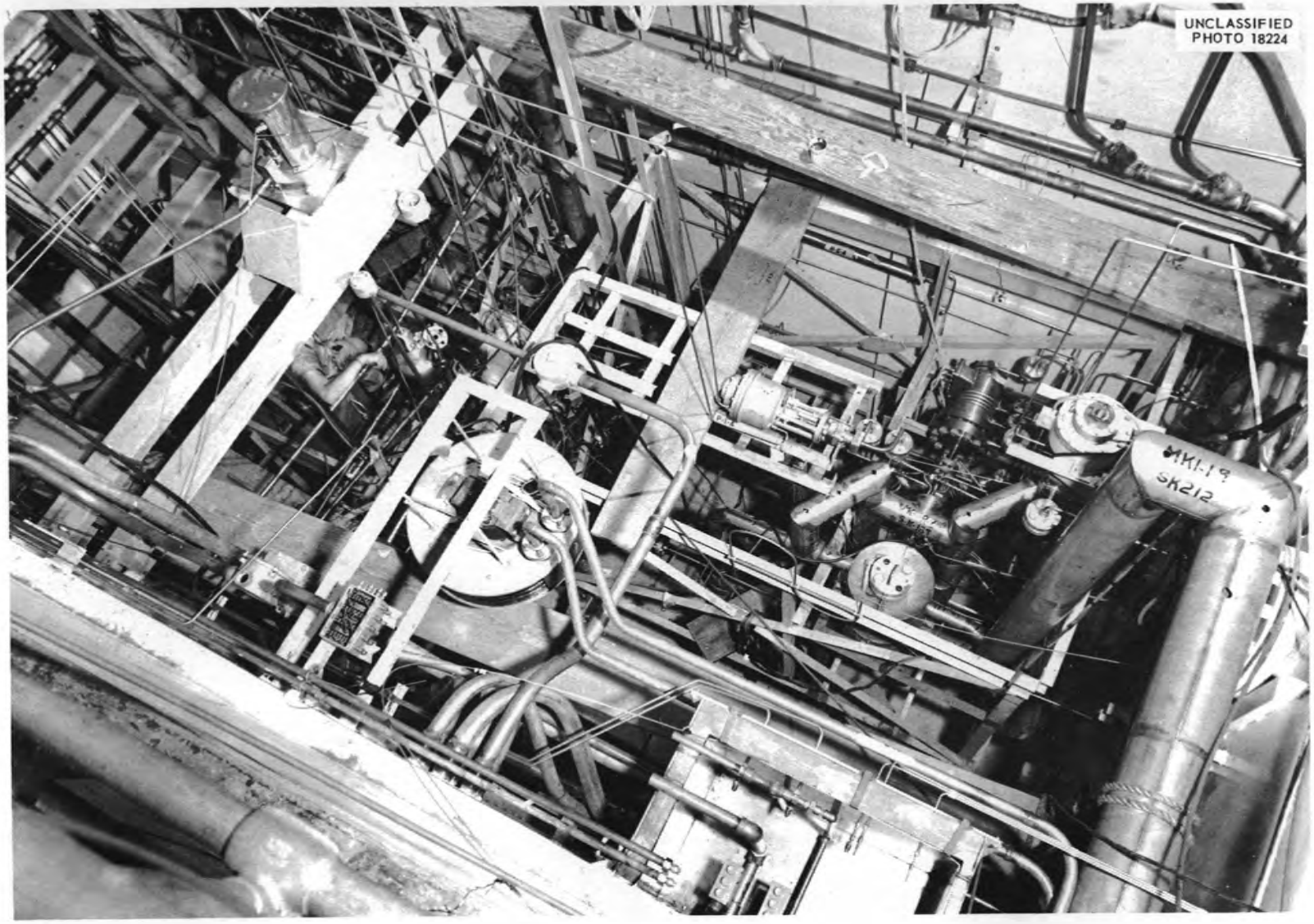

Fig. 6.4. HRT Core Processing Cell.

equipment were treated for 3 hr at 100°C with a 3% trisodium phosphate solution and then with 5% HNO_3 for 48 hr at 85°C as a check for off-specification material. None was indicated.

6.3.4 Westinghouse Circulating Pump

Tests previously outlined[4] for the Westinghouse circulating pump have been performed with generally satisfactory results. Minor difficulties with overheating in the motor end of the pump were due either to gas binding or to leakage across the thermal-barrier gasket. The original stainless steel hollow O-ring was replaced with a gold-plated solid gasket of rectangular cross section. To date no detectable leakage has occurred past this gasket. The problem with gas binding, both in the motor end and in the scroll, has not been entirely eliminated in the test loop but is not expected to be a problem during operation with the reactor, because the stream circulated from the reactor should be gas-free.

6.3.5 D_2O-Storage-Tank Calibrations[5]

Preliminary calibrations of the weigh cell and thermal level probe on the 10-gal D_2O storage tank have disclosed severe limitations to the instrumentation on this vessel. The weigh cell was shown to be temperature sensitive due to rigidity of the drain line, but minor piping changes will minimize this effect. The 30-min response time of the thermal level probe limits its usefulness to long-term inventories.

6.3.6 Shakedown-Loop Operation[3]

The maximum temperature attainable with the net mechanical work input of the 400A circulating pump was 225°C. Approximately 6 kw of additional heat from resistance heaters was added to the shakedown loop and raised the operating temperature to 260°C. Excessive transfer of oxygen gas from the pressurizer to the circulating stream, attributed to dissolution rather than to entrainment, has caused gas binding of the pumps, particularly the 1-gpm model. The pressurizer exit line was enlarged from $\frac{1}{8}$ to $\frac{1}{2}$ in. pipe size to ensure that the pressurizer would operate at pump suction pressure. Strip heaters were added to the pressurizer to raise the temperature a few degrees, thus increasing the steam vapor pressure and lowering the oxygen content required in the gas space to maintain pressure.

6.3.7 Oxygenated-Water Runs

Three runs, each of approximately two days' duration, with oxygenated water at temperatures above 250°C were completed, with minor difficulties. Operation simulated normal startup, continuous operation of the hydroclone, and shutdown.[6] With the system hot some difficulty was experienced in freezing plugs because of thermal-convection circulation set up within the closed loop in the high-pressure system, which contains no valves. However, after the plugs were frozen, they held without difficulty.

After approximately 100 hr the Graphitar thrust bearing of the 400A pump in the temporary solids feed loop failed and had to be replaced.

6.3.8 Flange Leakage During Thermal Cycles

All flanges in the high-pressure system were subjected to a series of six thermal cycles, ranging from 100 to 275°C, within a 36-hr period. Leakage, as determined by the leak-detector system pressurized to 2500 psi with air, was insignificant. All $\frac{1}{2}$-in. flanges were sealed with octagonal ring gaskets. The $1\frac{1}{2}$-in. hydroclone flange contained an oval-ring gasket.

6.4 REMOTE-MAINTENANCE TOOLS

Following the nitric acid rinse, the hydroclone and clone retainer plug were installed in the specially machined flange above the underflow receiver with the tools[7] designed for this maintenance operation. Figure 6.5 shows the operation being performed from above the cell. The total time required was less than 2 hr.

A manually operated, light-weight, right-angle remote starting wrench (Fig. 6.6) was designed to facilitate insertion and engagement of horizontal bolts. The bolts will be tightened with the pneumatically operated right-angle remote bolt wrench

[4] P. E. Novak, *HRT-CP Engineering Test Procedure, P-1, Westinghouse Circulating Pump*, ORNL CF-56-8-120 (Aug. 15, 1956).

[5] J. D. Perret, Jr., *Calibration of D_2O Receiver (T-2) Weigh Cell and Thermal Level Probe*, ORNL CF-56-7-128 (July 27, 1956).

[6] R. B. Lindauer, *Operating Procedure for the HRT Chemical Plant*, ORNL CF-56-3-22 (March 5, 1956).

[7] W. E. Unger *et al.*, *HRP Quar. Prog. Rep. July 31, 1956*, ORNL-2148, p 26.

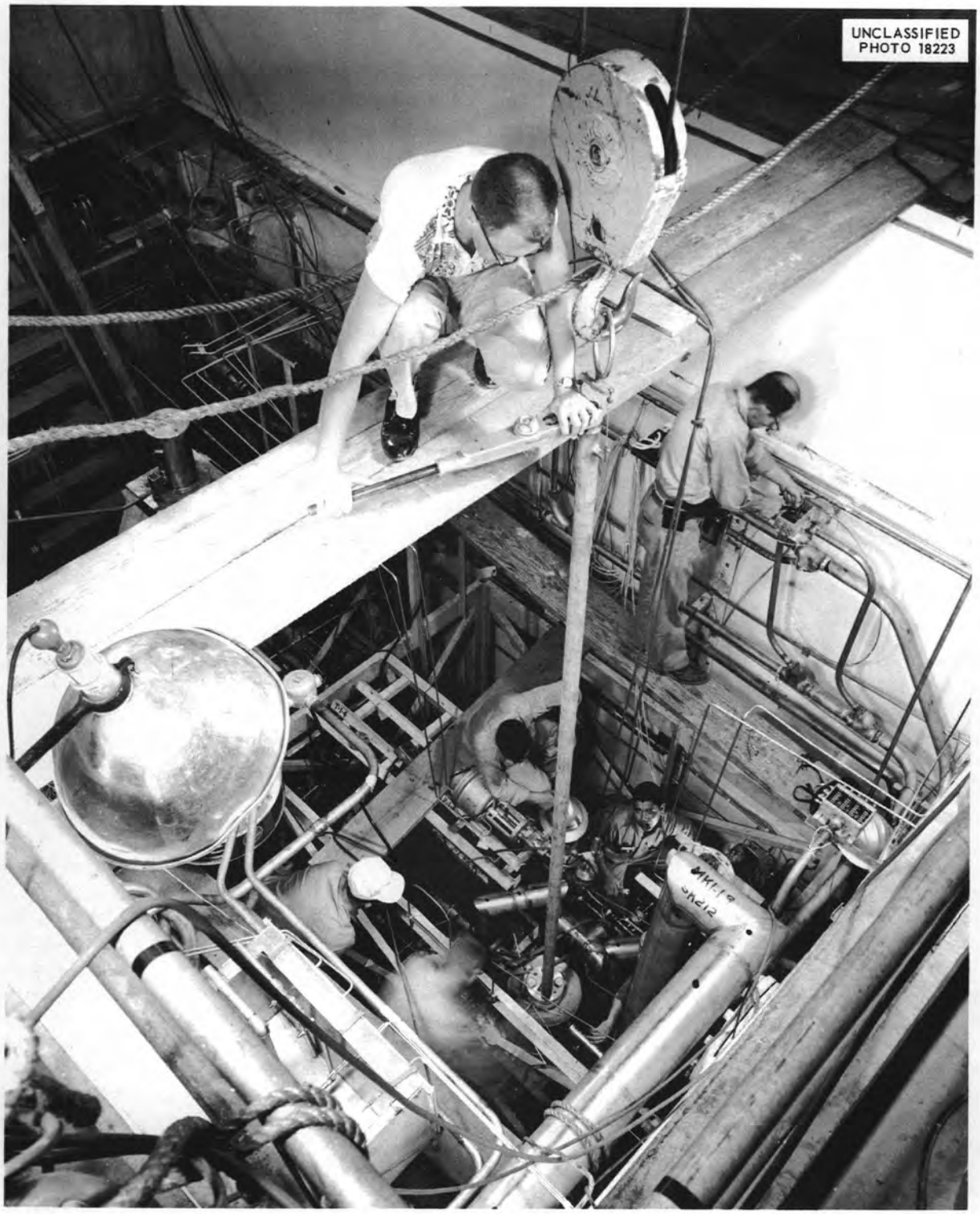

Fig. 6.5. Installation of Hydroclone.

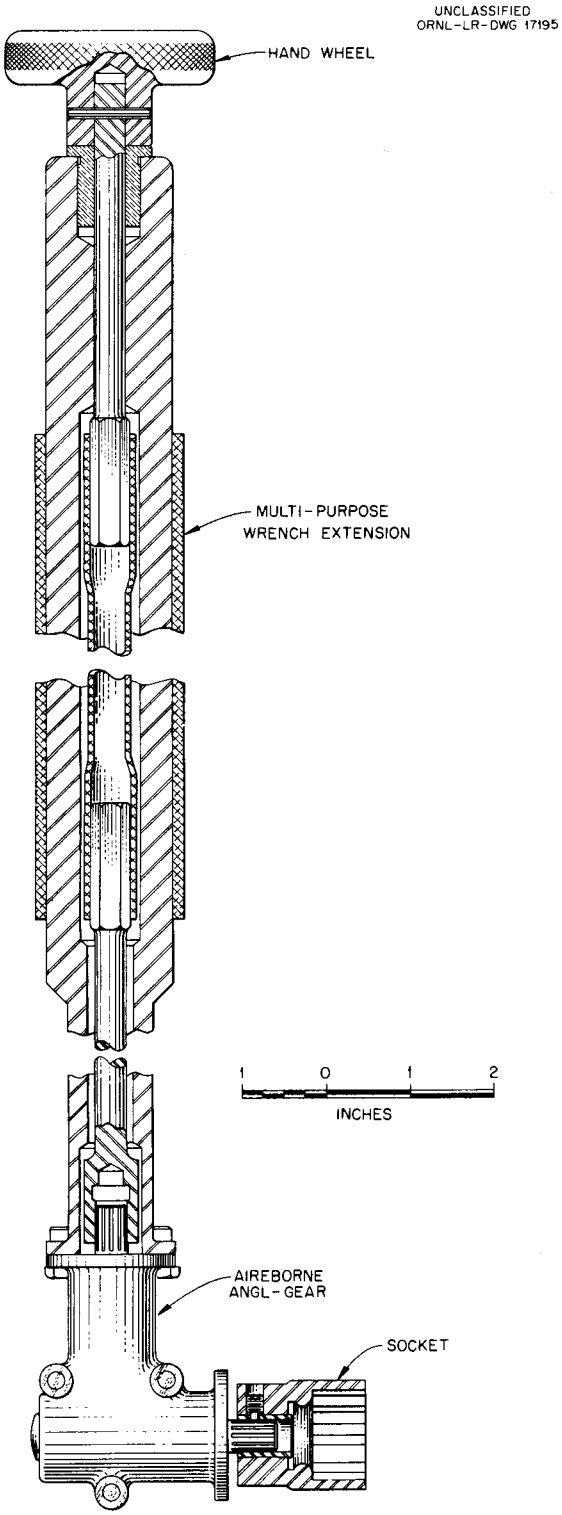

Fig. 6.6. Remote Right-Angle Starting Wrench.

(Fig. 6.7), which is scheduled for completion on November 1. The wrench is operated by an air piston, which reciprocates a slotted drive shaft, which in turn operates the ratchet socket.

The removal of process equipment fitted with a number of thermocouples can be facilitated if the thermocouple leads can be severed near the process equipment. A remote thermocouple-lead cutter has been designed (Fig. 6.8) which makes use of the multipurpose wrench extension. The cutter head consists of notched concentric sleeves rotated with respect to each other to provide a shearing action to cut the $\frac{1}{8}$-in.-OD stainless-steel-sheathed thermocouple leads.

6.5 CORROSION AND COMPONENT TESTS

The procurement of Carpenter-20 stainless steel for the decay tanks and of tantalum for the dissolution equipment was based on preliminary order-of-magnitude corrosion tests, reported in Sec. 11.2 and abstracted in Table 6.1.

The dissolver is constructed of tantalum, which exhibits consistent resistance to corrosion by sulfuric acid under all conditions that will be encountered in the plant. The Carpenter-20 decay tanks will be satisfactory for 4 *M* H_2SO_4 decay storage solution only at room temperature and under an oxygen atmosphere.

6.5.1 Flange Tests

Four $\frac{1}{2}$-in. flanges and gaskets that had been used previously were reassembled and tested for leak-tightness. Although all the flanges sealed successfully against 3000 psi in a hydrostatic test, on temperature cycling three developed leaks. The leaks were not continuous, were generally of short duration, and occurred below 100°C and on the cool-down portion of the temperature cycle. The bolt loadings of the leaking flanges were halved by the temperature cycling, but no permanent elongation of the bolts was detectable. This indicates permanent distortion of the flange or gasket surfaces and confirms the need for increasing the extensibility of the bolts, either by using extension sleeves and longer bolts or, preferably, by employing Belleville-type spring washers under the bolt heads. Belleville springs designed to provide a reasonably flat load-vs-deflection curve and fabricated of Inconel to minimize temperature effects have been procured for tests.

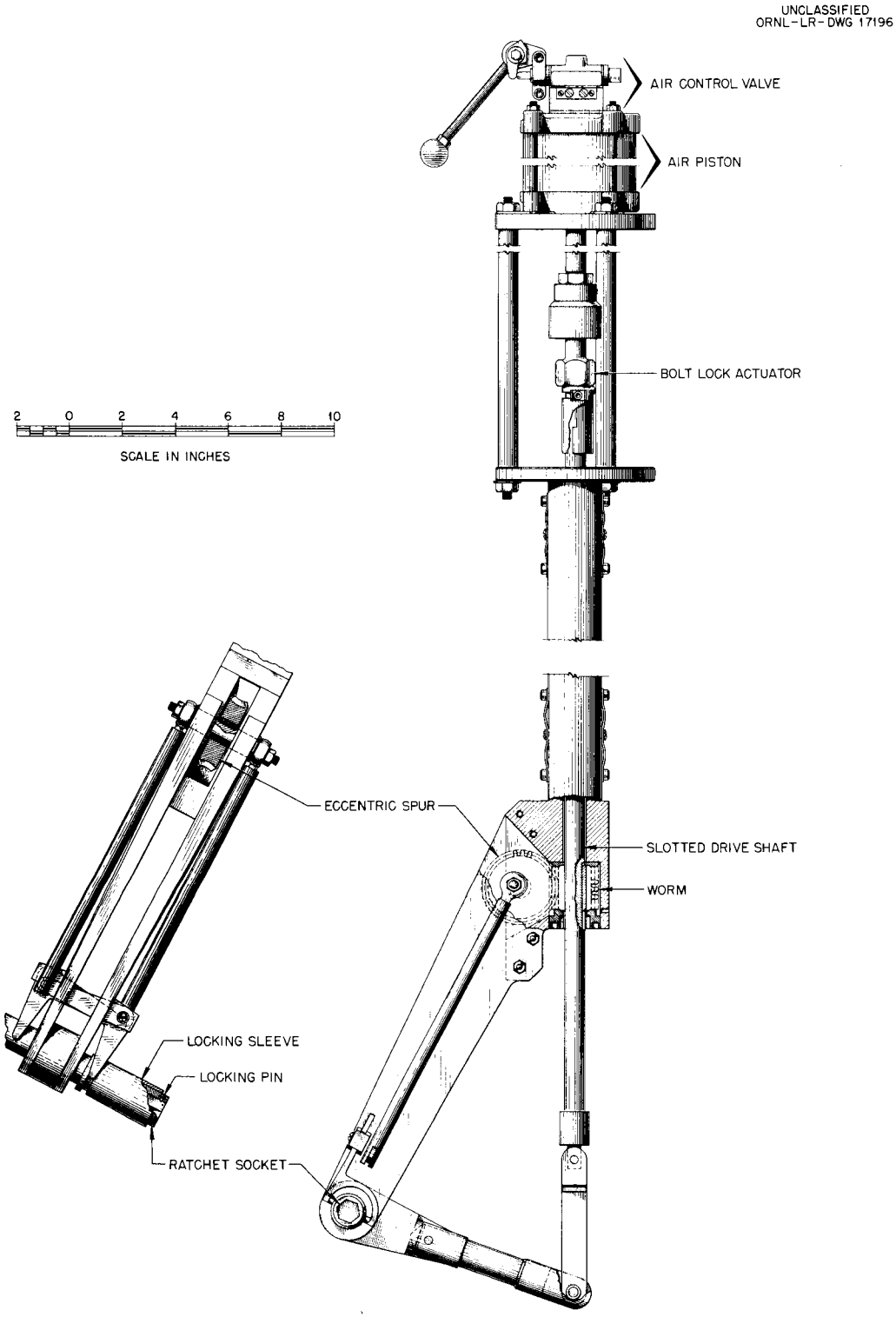

Fig. 6.7. Remote Right-Angle Bolt Wrench.

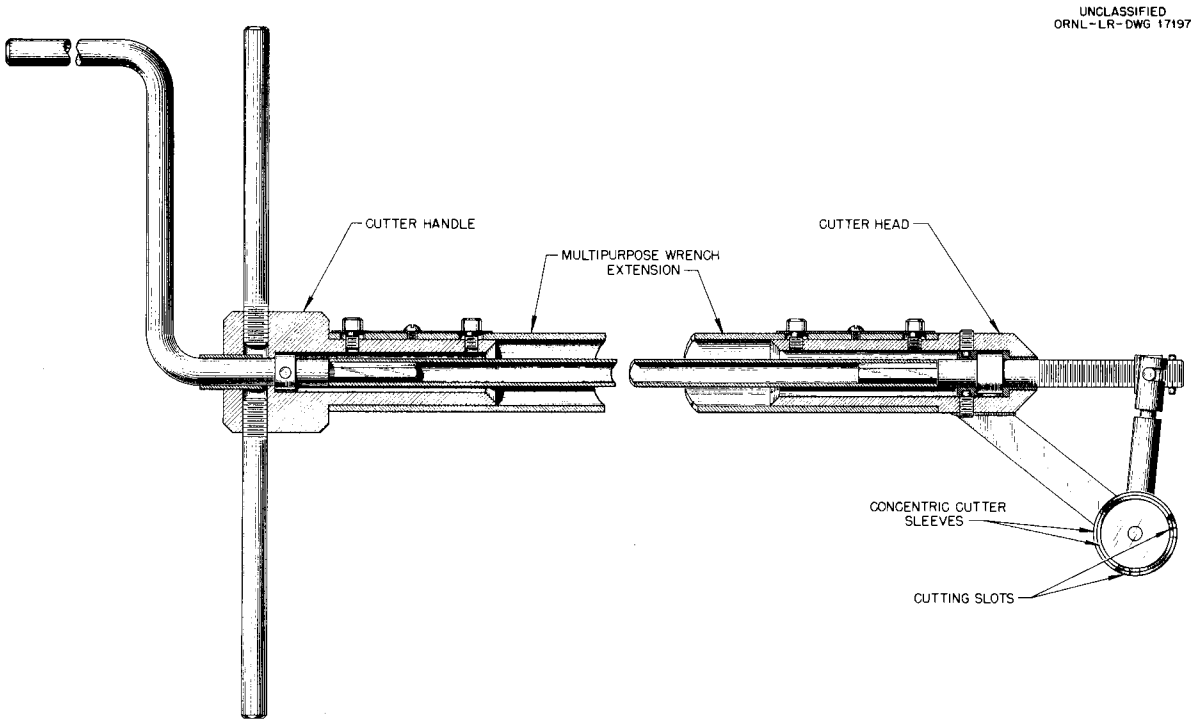

Fig. 6.8. Remote Thermocouple-Lead Cutter.

TABLE 6.1. CORROSION (mpy) IN SULFURIC ACID[a]

	Acid Concentration						
	4 *M*				10.8 *M*		
Temperature	109°C	109°C	111°C	39°C	157°C	157°C	159°C
Atmosphere	He	He	O_2	He		O_2	O_2
Contaminants		Ru[b]	FP's[c]				FP's[d]
Tantalum	0		0	0	0.1	0.2	0.6
Carpenter-20-Cb	38	170	1.5	0.4	39,000	22,000	
Type 347 SS	2500		5				
Type 316 SS	2000		5	0			
Zircaloy-2	0		0.3	0	19	5.4	200
Zirconium	0	1	0.3	0	8	11	700
Al_2O_3	10		8.2	Gain			

[a]Extract of corrosion data reported by H. C. Savage *et al.*, *Quarterly Report of Solution Corrosion Group for the Period Ending Oct. 31, 1956*, ORNL CF-56-10-13.

[b]Solution contained 25 to 50 ppm ruthenium.

[c]Contained fission and corrosion products and uranium to simulate expected HRT-CP conditions (Zr, 56; Fe, 75; Cr, 24; Ru, 0.4; Cu, 1.5; U, 28; in g/liter of corresponding sulfates).

[d]Contained fission and corrosion products and uranium to simulate HRT-CP conditions (Zr, 152; Fe, 208; Cr, 65; Ru, 1.2; Cu, 4; U, 50; in g/liter of corresponding sulfates).

Bolts plated with cadmium for rust protection were found to have been badly corroded after service on insulated flanges. Torque in excess of 200 ft-lb was required to disassemble the flanges. Improved protection of the bolts, perhaps by zinc plating, is required to ensure that the process flanges can be disassembled remotely.

6.5.2 Hydroclone Tests

The HRT-CP hydroclone–underflow-receiver unit is designed so that the hydroclone insert may be removed remotely and replaced with inserts of varying effective dimensions.

Assorted replacement inserts have been operated under comparable conditions to establish their operating characteristics, which are given in Table 6.2. The 0.4-in.-dia hydroclone has about three times the throughput capacity of the 0.25-in.-dia unit at the same pressure drop (see Fig. 6.9).

It is expected that the optimum combination of capacity, concentration-factor efficiency, and port size for the HRT installation will be obtained with a 0.40-in.-dia by 2.4-in.-long insert.

6.6 BLANKET PROCESSING – FLOWSHEET

The continuous processing of the HRT natural-uranium blanket solution will concentrate insoluble plutonium and corrosion products in a small quantity of purge solution and in this sense is similar to the continuous processing of the core solution. Plutonium and the corrosion products

TABLE 6.2. INDUCED UNDERFLOW AND EFFICIENCIES OF FLANGED HYDROCLONES

Material: TM-Y ThO_2 at room temperature; 80 wt % between 0.6 and 3 μ
Pressure differential: 44 psi

Unit No.	Dimensions (in.)		Percentage Efficiency with Forced Underflow, $B/F^* = 0.1$	Percentage Efficiency with Induced Underflow	B/F^* for Induced Underflow
	Diameter	Length			
FL-25-11	0.25	1.50		49	0.014
				58	
**	0.25	1.50	44**		0.015
			53**		
			42**		
FL-25-1	0.25	1.50			0.014
FL-25-2	0.25	1.50			0.017
FL-40-7	0.40	2.40	39		0.014
			44		0.013
			42		
FL-40-10	0.40	3.14		40	0.0056
				36	
TM-Ti-21**	0.40	3.14			0.0062**
**	0.40	3.14	37**		
			43**		
			34**		

*B/F, ratio of the underflow rate to the feed rate.

**Nonflanged units, included for comparison purposes; efficiencies should be similar for flanged units.

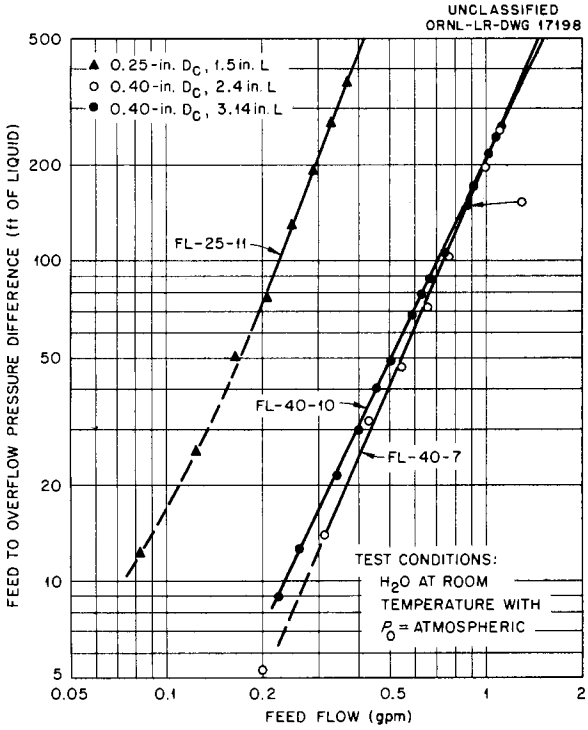

Fig. 6.9. Characteristics of HRT-CP Integrally Flanged Hydroclones.

chromium, iron, and zirconium hydrolyze and precipitate as oxides at the blanket operating temperature. Once they are precipitated, temperature has little effect upon the apparent solubility of these oxides, so that their removal from the blanket solution by centrifugation may be carried out at room temperature. This will minimize the corrosion of process equipment by the concentrated uranium blanket solution. The schematic process flowsheet is shown in Fig. 6.10.

A bypass stream of approximately 1 gpm from the high-pressure side of the reactor heat exchanger is fed to a hydroclone, after first being passed through a heat exchanger and cooler to lower its temperature and through a screen to protect the hydroclone ports from plugging. The clarified overflow from the hydroclone is transferred by a booster pump through the feed heat exchanger and then back to the low-pressure side of the reactor heat exchanger. At intervals, the blanket process equipment will be isolated from the reactor by closing the isolation valves, and the underflow receiver will be discharged by gravity to a dissolver, where the heavy water will be recovered by evaporation. The dissolver will then be isolated from the heavy-water system by a combination of valves and freeze plugs. The plutonium and corrosion products will then be dissolved in a light-water solvent, sampled, and discharged to the decay storage tank for radioactive decay pending transfer to a carrier for transportation to a solvent-extraction facility.

Investigation of a suitable solids-dissolution scheme is being carried out for both a sulfuric acid system similar to that to be used in the core plant and for one employing concentrated phosphoric acid. The choice between the two systems will depend upon the relative corrosion problems, the ease of operation, and the seriousness of cross-contamination with the blanket solution.

Procurement of materials and equipment items that will require considerable time for delivery has been initiated in advance of the issuance of a detailed flowsheet or equipment design.

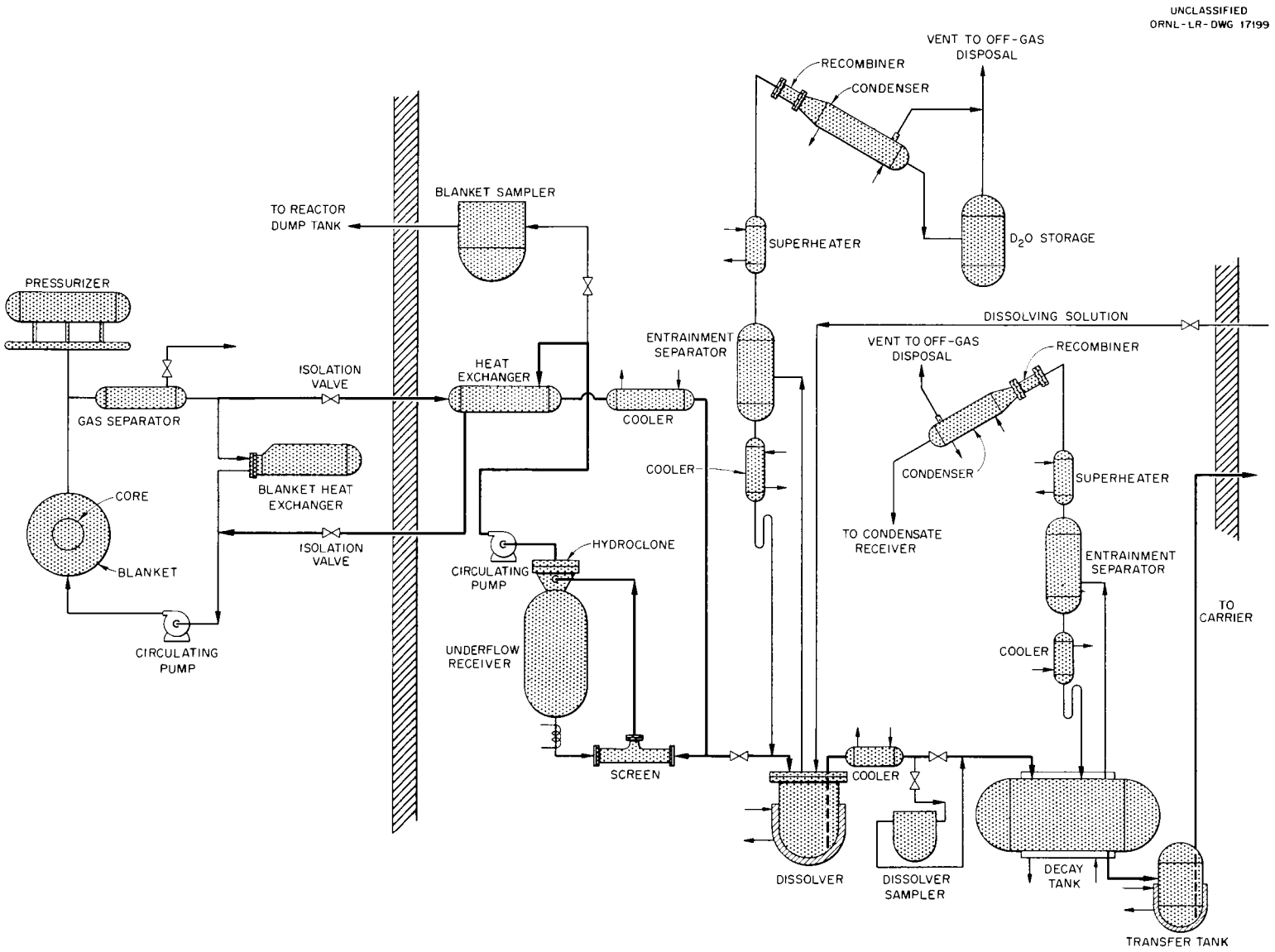

Fig. 6.10. Schematic Flowsheet of HRT Blanket-Processing Plant.

Part II

REACTOR DESIGN AND ANALYSIS

J. A. Lane

7. REACTOR ANALYSIS

P. R. Kasten

T. B. Fowler
S. Jaye
M. P. Lietzke
C. W. Nestor, Jr.
M. W. Rosenthal
M. Tobias

7.1 TWO-REGION SLURRY REACTOR STUDIES

Some nuclear characteristics of two-region reactors having D_2O-ThO_2-$U^{233}O_2$ slurries in both regions have been computed. As in the previous studies,[1] two-group calculations were applied to reactors having pressure vessels with inside diameters of 10 and 12 ft, variable core diameters, and ½-in.-thick Zircaloy-2 core tanks. Fission-product and isotope buildup and protactinium losses were not considered in these initial calculations. The value of η was taken as 2.25, $\sigma_f^{23}/\sigma_a^{23}$ as 0.90, and the reactor temperature as 280°C. The maximum U^{233} concentration in the blanket region was 5 g/liter.

Typical information obtained is given in Table 7.1 for two of the cases considered. For all cases the total reactor power was assumed to be 100 Mw, and the values for power density, flux, and blanket and core power are normalized to that value.

[1] C. W. Nestor, Jr., and M. W. Rosenthal, *HRP Quar. Prog. Rep. April 30, 1956*, ORNL-2096, p 60–62.

TABLE 7.1. SLURRY-REACTOR CHARACTERISTICS

Pressure-vessel inside diameter, ft	10	10
Core inside diameter, ft	7	7
Core thorium concentration, g/liter	100	200
Blanket thorium concentration, g/liter	1000	2000
Blanket U^{233} concentration, g/liter	3	5
Total power, Mw	100	100
Blanket power, Mw	8.5	4.2
Critical core concentration, g of U^{233} per liter	3.0	6.0
Breeding ratio	1.18	1.21
Power density at core center, kw/liter	43	45
Power density at core wall, kw/liter	5.4	4.9
Flux at core center $\times 10^{-14}$	5.5	2.9
Neutron absorptions in core wall, %	0.7	0.3

Increasing the total power would increase these values in direct proportion.

For all reactors having thorium concentrations of at least 100 g/liter in the core and 500 g/liter in the blanket, the neutron absorption by the core-tank wall was less than 1% of the total absorptions.

The variations of breeding ratio and wall power density with core size, thorium concentration, and blanket U^{233} concentration are plotted in Figs. 7.1 through 7.6 for the 10-ft reactors. When the fuel concentration in the blanket was greater than that

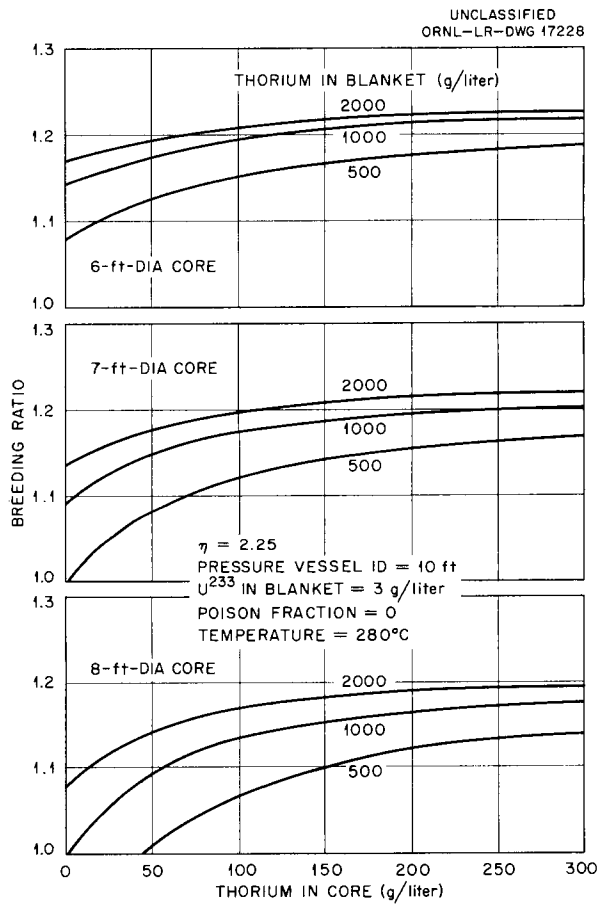

Fig. 7.1. Effect of Core Thorium Concentration on Breeding Ratio of Two-Region Slurry Reactor.

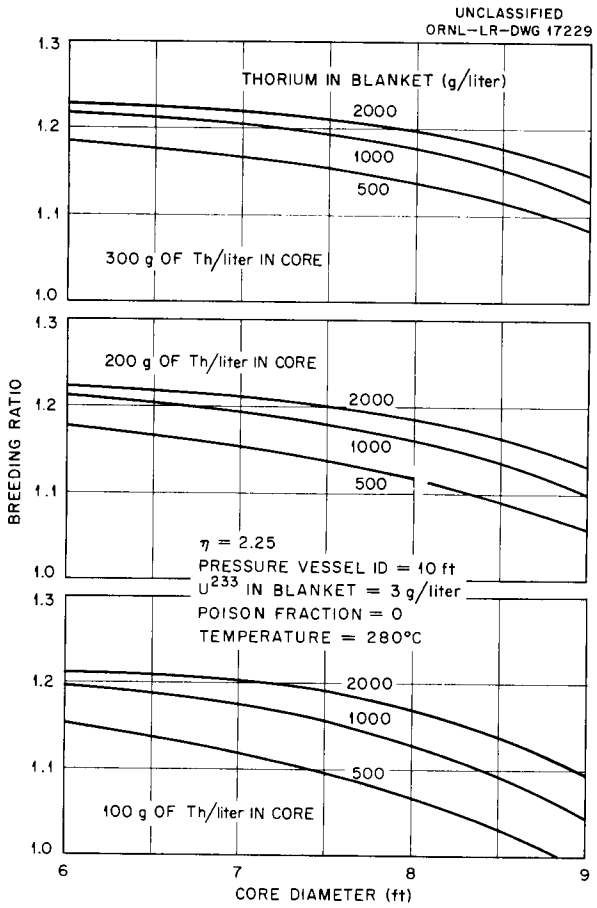

Fig. 7.2. Effect of Core Diameter on Breeding Ratio of Two-Region Slurry Reactor.

in the core region, the power density on the blanket side of the core-tank wall was sometimes greater than that on the core side. In the above figures the greater value was plotted, as indicated in Fig. 7.4.

The values of breeding ratio for the two-region reactors given in Table 7.1 may be compared with those given below for a one-region reactor having the same size of pressure vessel:

Thorium Concentration (g/liter)	Breeding Ratio
100	0.875
200	0.993
300	1.037

The results for the two-region 10-ft-dia reactors may be summarized as follows:

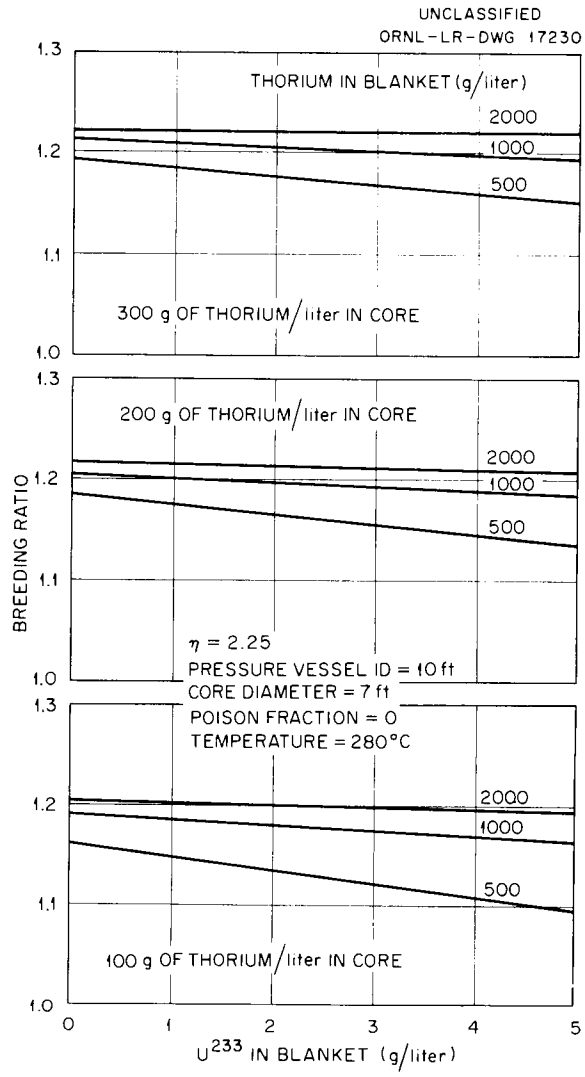

Fig. 7.3. Effect of Blanket U^{233} Concentration on Breeding Ratio of Two-Region Slurry Reactor.

1. The breeding ratio increased when the thorium concentration was increased in either the core or blanket region; however, it did not change appreciably for thorium concentrations above 200 g/liter in the core and 2000 g/liter in the blanket.

2. The core-wall power density decreased when the thorium concentration was increased in the blanket region; the wall power density had a minimum value when the thorium concentration in the core was about 90 g/liter, for 3 g of U^{233} per liter in the blanket.

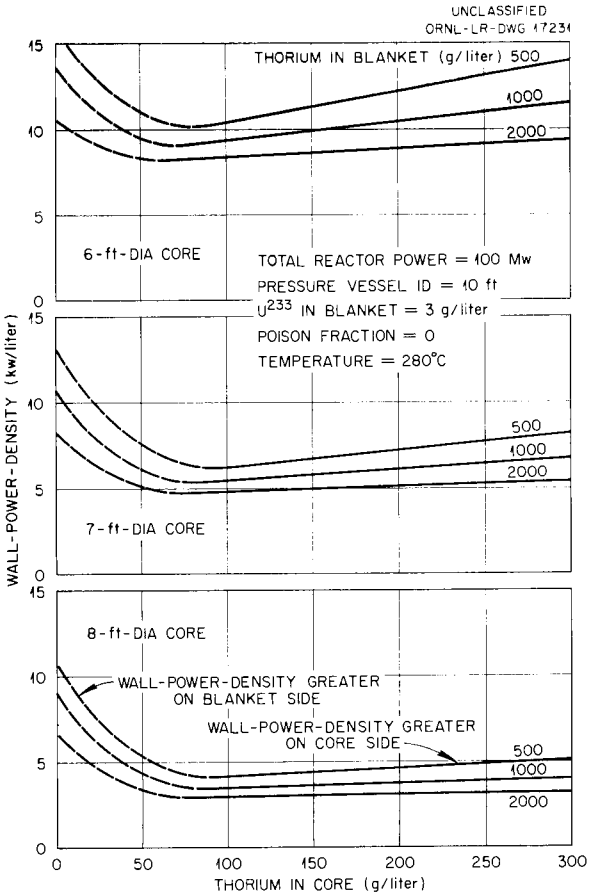

Fig. 7.4. Effect of Core Thorium Concentration on Wall Power Density of Two-Region Slurry Reactor.

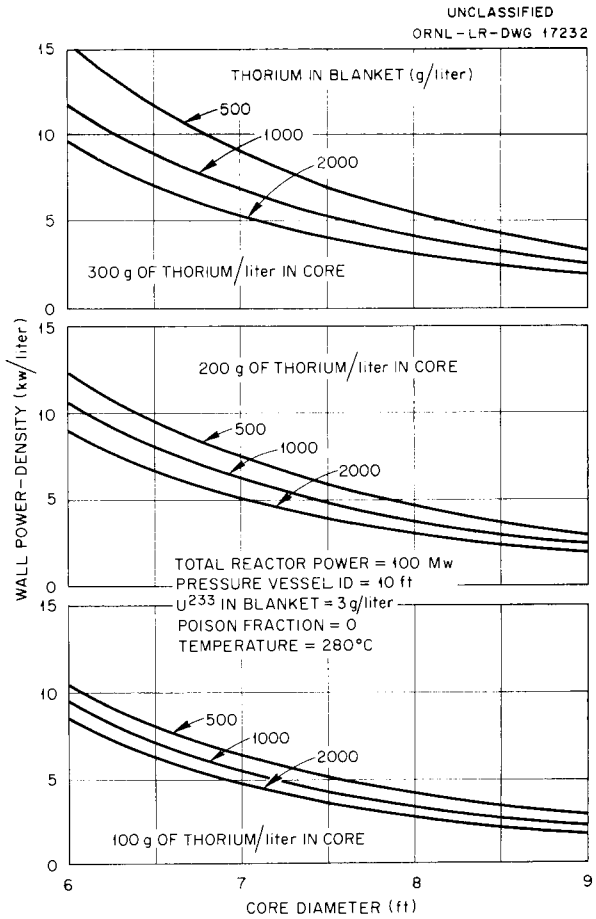

Fig. 7.5. Effect of Core Diameter on Wall Power Density of Two-Region Slurry Reactor.

3. Decreasing the core size increased the breeding ratio but also increased the power density at the core wall.

4. Increasing the blanket U^{233} concentration decreased the breeding ratio; however, at the higher blanket thorium concentrations the effect was slight.

5. The wall power density was relatively insensitive to changes in the blanket fuel concentration for specified thorium concentrations greater than 100 and 500 g/liter in the core and blanket, respectively.

7.2 EFFECT OF U^{233} RESONANCE ABSORPTION ON BREEDING RATIO AND CRITICAL MASS

If η is lower in the resonance energy region than in the thermal energy region, neglect of fuel resonance effects in thorium breeder reactor calculations could give breeding ratios significantly higher than would actually be the case. To examine this effect, calculations were carried out for a single-region reactor containing ThO_2, $U^{233}O_2$, and D_2O at 300°C.[2] Neutron leakage was neglected. The thorium concentration and the resonance value for η^{23} were considered as parameters in evaluating the breeding ratios which would exist in these unpoisoned reactors. The results are given in Figs. 7.7 and 7.8. Figure 7.7 shows how the critical mass would increase if the average value for η^{23} in the resonance energy region were to decrease (in all cases the value for η^{23} in the thermal energy region was taken as 2.25) for various concentrations of thorium; Fig.

[2] S. Jaye, *Effect of U^{233} Resonance Absorption on Breeding Ratio and Critical Mass* (to be issued).

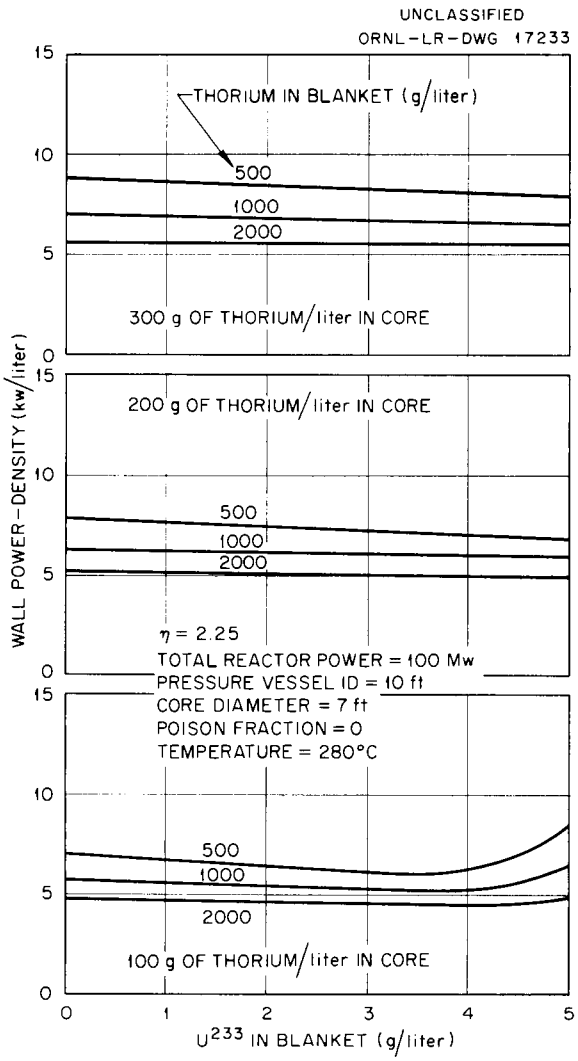

Fig. 7.6. Effect of Blanket U^{233} Concentration on Wall Power Density of Two-Region Slurry Reactor.

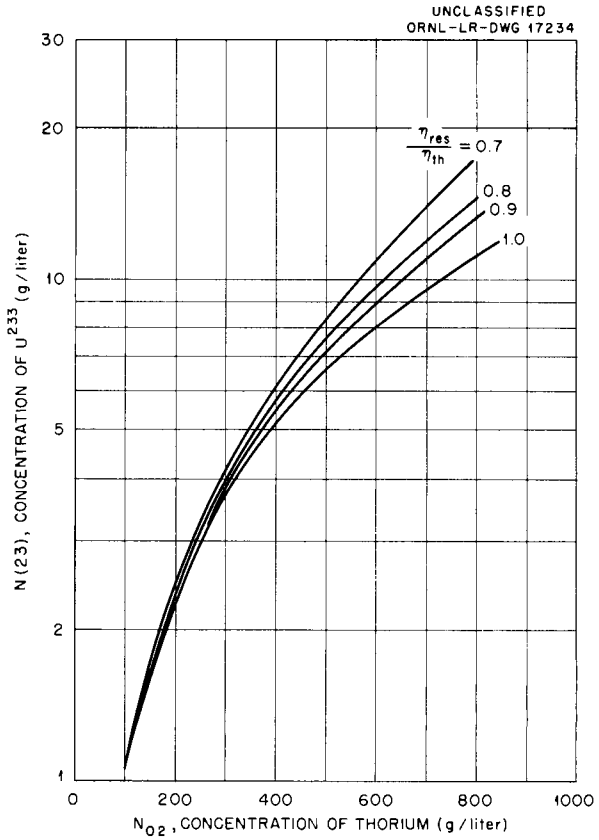

Fig. 7.7. Critical Concentration of U^{233} as a Function of Thorium Concentration and Value for η_{res}/η_{th} (Reactor Operating Temperature, 300°C; Neutron Leakage Neglected).

7.8 indicates the decrease in breeding ratio for the same conditions.

The value for η_{res} has not been firmly established. Russian broad-spectrum results indicate that $\eta_{res} \approx \eta_{th}$; however, results obtained at Harwell and at the MTR[3] indicate that η^{23} oscillates in the ev range, with $\eta(2.5\text{ ev}) \approx 1.4$ and $\eta(3.0\text{ ev}) \approx 2.4$. Based on available data, η_{res}/η_{th} lies between 0.90 and 1.0.

[3]Results presented at meeting of the Neutron Crass Section Advisory Group, ANL, Sept. 24–26, 1956.

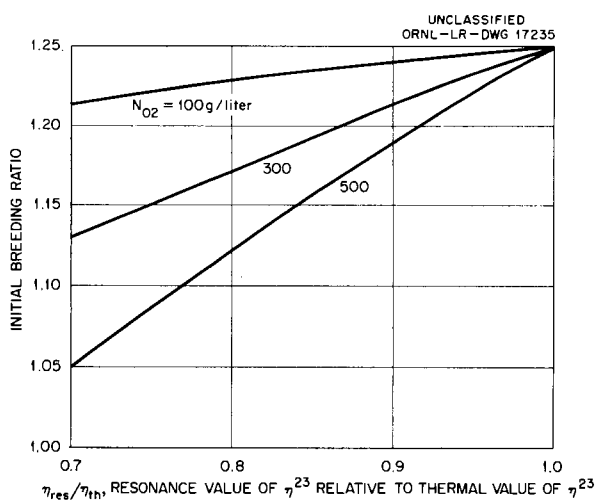

Fig. 7.8. Initial Breeding Ratio as a Function of Thorium Concentration and Value for η_{res}/η_{th}.

If the reactor were initially fueled with U^{235}, the initial breeding ratio would have a maximum value of 1.08, rather than 1.25. However, the curves would have about the same shape as those presented in Fig. 7.8. With U^{235} as the fuel, the value for η_{res}/η_{th} would be between 0.8 and 0.9.

7.3 NATURAL-CIRCULATION REACTORS

A major question concerning large nuclear reactors is whether a reactor system can be repaired and maintained as needed to yield a long operating life. For homogeneous reactors the long-term operability of large fuel-circulating pumps is one source of concern. It is possible, however, to eliminate the major pumps from a reactor system by using natural circulation of fuel solution rather than forced flow – at the expense of lowering the power output from a given system. To provide a comparison between power capabilities of forced- and natural-circulation systems, computations were performed[4] for present and modified designs of the HRT and TBR and for the present design of the HRR. The proposed modifications were such as to increase the power obtainable by natural-circulation flow. The pertinent features of the systems studied are listed below, and the results of the calculations are presented in Table 7.2. The symbols employed have the following meanings:

Δp_0 = pressure drop around system for flow at design rate,
T_2 = core exit temperature,
T_b = boiling temperature in heat-exchanger shell,
W = fuel circulation rate,
P = reactor power.

The existing design of the Homogeneous Reactor Test (HRT) has the following features:

heat exchanger 5.2 ft above core,
heat-exchanger tube length = 20 ft,
Δp_0 = 35.2 psi,
T_2 = 300°C,
T_b = 244°C.

In the modified design the following changes were assumed:

heat exchanger 20 ft above core,
heat-exchanger tube length = 8 ft,
pipe sizes increased,
gas separator eliminated,
all regions streamlined,
Δp_0 = 9.6 psi.

[4]M. W. Rosenthal, *Natural Circulation Homogeneous Reactors*, ORNL CF-56-10-53 (Oct. 16, 1956).

TABLE 7.2. POWER LEVEL AS A FUNCTION OF SYSTEM DESIGN AND TYPE OF FLOW

	Fluid Flow Rate, W (gpm)	Reactor Power, P (kw)	Power Level Relative to Forced-Flow Power
HRT			
Present design, forced flow	400	5,000	1
Present design, natural circulation	24	380	0.08
Modified design, natural circulation	102	1,300	0.26
TBR			
Present design, forced flow	26,500	357,000	1
Present design, natural circulation	2,700	59,000	0.16
Modified design, natural circulation	3,200	65,000	0.18
HRR			
Present design, forced flow	35,300	500,000	1
Present design, natural circulation	3,700	62,000	0.12

The Thorium Breeder Reactor (TBR), as presently conceived, has the following design characteristics:

heat exchanger 22 ft above core,
heat-exchanger tube length = 24 ft,
Δp_0 = 68.1 psi,
T_2 = 300°C,
T_b = 225°C.

In the modified design the following changes were assumed:

gas separator eliminated,
all regions streamlined,
Δp_0 = 55.1 psi.

The Homogeneous Research Reactor (HRR), as presently conceived, has the following pertinent features:

heat exchanger 12 ft above core,
Δp_0 = 31.1 psi,
T_2 = 275°C,
T_b = 214°C.

For the present designs the natural-circulation power relative to the forced-flow power was the highest for the TBR and the lowest for the HRT, mainly because of the difference in fluid height between the heat exchanger and the core for the two systems. By modifying the system designs so as to increase the driving force and decrease the resistance to fluid flow, the natural-circulation power relative to forced-flow power increased to 26% for the HRT and to 18% for the TBR.

The heat exchangers included in the modified systems contained tubes of the same diameter and number as those in the present designs. Although somewhat higher power levels could be attained by changing the tube size and number of tubes present, this effect would not be appreciable. For example, if the number of tubes used in the exchanger of the modified HRT were doubled and their length halved, the change in reactor power would be only 3%.

Thus any maintenance advantage obtained by elimination of a large-capacity pump would be accompanied by a reduction in power output relative to that in a forced-flow system of the same size. Based on the results here, between one-fifth and one-third of the power output of a pumped system can be obtained by natural circulation, with the use of the same core and the same heat-exchanger area. Increasing the volume of the reactor system would increase the power level. Concomitant with the reduced power of the natural-circulation system is reduced power density in the reactor core. If the power density were already restricted by radiation-induced corrosion, then no additional penalty may be associated with the use of natural circulation. A corollary benefit results from the low flow rate, which would restrict the rate at which reactivity could be introduced into the core (by cold-fluid addition).

The operating dependability associated with natural-circulation flow may recommend it for reactors in which high power density is not required. At remote installations in particular, economic factors and the necessity for maintenance-free operation may favor its use.

7.4 PHYSICAL-PROPERTY DATA FOR HOMOGENEOUS REACTOR SOLUTIONS AND SLURRIES

Physical-property data concerning aqueous homogeneous reactor solutions and slurries have been compiled for use in nuclear calculations.[5] The materials considered are light and heavy water and their mixtures, uranyl sulfate solutions, uranyl sulfate–lithium sulfate equimolal solutions, uranyl sulfate–beryllium sulfate equimolal solutions, and slurries of uranium dioxide, uranium trioxide, and thorium oxide. Most of the information presented deals with density on a mass or atomic basis, but data concerning viscosity, thermal conductivity, heat capacity, and vapor pressure are also included. The values are reported mostly in graphical form, with notations pointing out areas of actual experimental knowledge. A large amount of extrapolation has been necessary in order to cover regions of interest in which no property measurements have been made. Estimates of accuracy are included where possible.

7.5 HRP MATHEMATICS AND COMPUTATION

Analytical solutions for the time behavior of fuel concentrations in single-region reactors containing either U^{235}, U^{238}, Pu^{239}, and fission-product poisons or U^{233}, U^{235}, Th^{232}, and fission-product poisons have been coded for the Oracle.

[5] M. Tobias, *Physical Property Data for Homogeneous Reactor Solutions and Slurries* (CF memo to be issued).

Oracle codes have been devised to calculate the fraction of gamma rays originating from a shielded source which would escape through a hole in the shield as a result of air scattering and wall scattering. It was assumed that there was no direct line of sight between the gamma source and positions outside the shield. Only a single scattering was assumed in the air-scattering calculations. In the wall-scattering calculations the scattering of gamma rays penetrating into the wall of the hole, as well as surface scattering, was considered. Only that surface of the hole which had direct line of sight with the source and the shield volume enclosed by the extremes of this line of sight were considered in the calculation.

Part III

ENGINEERING DEVELOPMENT

J. A. Lane

8. DEVELOPMENT OF FUEL-SYSTEM COMPONENTS

I. Spiewak

C. H. Gabbard
B. A. Hannaford
P. H. Harley
P. P. Holz
R. G. Meza
I. K. Namba
W. L. Ross

8.1 HIGH-PRESSURE RECOMBINER LOOP

In a resumption of the testing in the high-pressure recombiner loop (constructed of type 347 stainless steel), titanium and Zircaloy-2 specimens were exposed in the system for 90 hr to determine the effect of hydrogen absorption in these metals. This test was a repetition of one reported previously.[1] During the 90 hr of operation, one leak occurred in a weld and one in a straight pipe, possibly as a result of stress-corrosion cracking induced by KOH entrainment.

8.2 SMALL REACTOR COMPONENTS

8.2.1 20-cfm Canned-Rotor Blower

The 20-cfm canned-rotor blower, with its hollow metallic O-ring seals, passed the required performance and hydrostatic tests at Allis-Chalmers and was received at ORNL on October 17, 1956.

Performance tests included 50 starts and stops and operation for 135 hr at atmospheric pressure; the operation was trouble-free. The characteristics given in Table 8.1 were observed with impellers of various diameters. Since the design specifications called for 160 ft of head at 20 cfm, the blower is equipped with the 7½-in.-dia impeller.

The blower loop, which will operate under simulated reactor conditions, has been constructed and is ready for installation of the blower.

[1] G. M. Adamson *et al.*, *HRP Quar. Prog. Rep. July 31, 1956*, ORNL-2148, p 107–108.

TABLE 8.1. RESULTS OF PERFORMANCE TESTS ON IMPELLER FOR 20-cfm CANNED-ROTOR BLOWER

	Impeller Diameter		
	6½ in.	7½ in.	8 in.
Motor input, kw (440 v, 6 amp)	2.44	2.48	2.52
Speed, rpm	3525	3525	3540
Developed head at 20 cfm, ft of air	104	194	264

8.2.2 Small Circulating Pumps

Operation of three 5-gpm canned-rotor ORNL pumps with series-connected stator windings was continued. Two of the pump loops were changed from operation with water to operation with UO_2SO_4 solution (10 g/liter). One of the loops has since operated continuously for 900 hr without incident. The initial corrosion rate of 1.3 mpy decreased to less than 0.7 mpy during this time. Chemical analyses of samples from the other loop, however, indicated a corrosion rate of 3.7 mpy, and the loop was shut down after 139 hr of operation. Disassembly of the pump revealed severe pitting on the inside of the 60-mil wall of the stator can; some of the pits are estimated to be 15 to 20 mils deep. This localized corrosion is as yet unexplained; no excessive temperatures were noted during the run.

The 5-gpm pump operating on cold water has now run for 13,220 hr without incident.

8.3 4000-gpm LOOP

Disassembly of the Byron Jackson 4000-gpm pump was completed, and it was revealed that the Stellite in the cooler regions of the pump had not been so severely attacked as that in the hotter regions.[2] Figure 8.1, showing the bottom case wear ring, illustrates the corrosion which occurred. The thrust and radial bearings were in satisfactory condition.

In order to continue operation of the pump with uranyl sulfate solution, seven of the eight Stellited wearing surfaces were replaced with new, type 347 stainless steel, parts. The existing Stellited upper-thrust-shoe wearing ring had negligible corrosion and was re-used.

During the overhaul, components of the 4000-gpm loop were also inspected. The water entrance line to the main-pump balance accumulator was clogged with rubber deposits, indicating decomposition of the accumulator bag. This accumulator

[2] C. B. Graham *et al.*, *HRP Quar. Prog. Rep. July 31, 1956*, ORNL-2148, p 49.

Fig. 8.1. Bottom Case Wear Ring.

was replaced with a new unit, as was the accumulator at the discharge of the seal pump. A visual inspection of the coils of the loop water cooler indicated no serious signs of corrosion. The reassembled pump operates satisfactorily.

8.4 TITANIUM PROGRAM

The construction of the titanium-lined pipe by Crane Co. and the small heat exchanger by The Pfaudler Co.[3] is still being delayed because of lack of materials. The current delivery dates are December 1956 for the pipe and January 1957 for the heat exchanger.

Preliminary design has begun on a 400-gpm pump loop to be constructed of titanium alloy A-110-AT, if available. This loop will provide construction and operating experience on a titanium piping system and will serve to test the 3½-in. titanium-lined pipe.

8.5 HEAT-EXCHANGER TUBE-JOINT TEST

Reports of stress-corrosion attack on austenitic stainless steel tubes in steam-generating service indicate that the most severe attack occurs in the tube-to-tube-sheet joint, where the tendency to concentrate solids by boiling is most pronounced. Because of the potential seriousness of this problem in steam generators operating with boiler water containing radiolytic oxygen, a program was started to investigate different tube-joint designs from the standpoint of design and

[3] *Ibid.*, p 50.

materials which will offer maximum resistance to this type of attack.

For the initial tests several five-tube heat exchangers have been fabricated; $\frac{3}{8}$-in.-dia type 347 stainless steel tubes are attached to 2-in.-thick carbon-steel tube sheets clad with $\frac{1}{2}$-in. layers of type 347 stainless steel. A test unit is shown in Fig. 8.2. Variables being studied in this group of test units are the counter-boring of tube holes in the tube sheet from the secondary side and the nickel-plating of the tube ends which form a crevice with the tube sheet. Boiler-water composition has been tentatively set at 50 ppm oxygen and 5 ppm chloride in order to provide a severe stress-cracking environment. Boiling will be accomplished by injecting 250-psi steam into the primary side of the tubes.

A single unit is undergoing preliminary testing so that the operating procedures for the remaining units can be fixed.

8.6 HIGH-PRESSURE FLANGE TEST

Thermal cycling of the 4-in. 1500- and 2500-lb flanges was continued.[3] Each cycle consisted of a 4-hr heatup period from ambient conditions to 2000 psi and 636°F, a hot period of from 2 hr to eight days, and a 16-hr cooling period. The cycling was repeated six times with the flanges uninsulated and twice with nine layers of aluminum foil around the flanges. The leak rates remained extremely low throughout the tests, with a maximum for the 1500-lb flange of 10^{-4} g of water per day. This occurred during the cold portion of the second cycle with insulated flanges. The 2500-lb flanges experienced minimum leakage throughout the cycles.

Following these thermal cycles, the bolts were loosened and their lengths determined with C-clamp extensometers. A permanent elongation, which varied between 0.0016 and 0.0043 in., was noted on all the bolts. The bolts originally tightened the most showed the greatest permanent set. The reason for the peculiar bolt behavior is not known, since the yield point of the bolts should not have been exceeded in the tests.

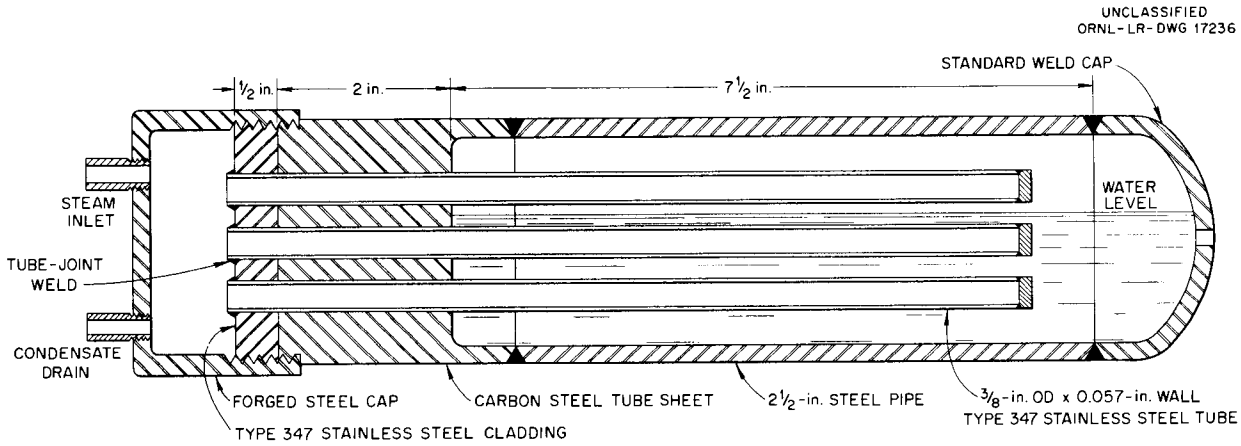

Fig. 8.2. Tube-Joint Test Unit.

9. DEVELOPMENT OF REACTOR SLURRY SYSTEMS

R. B. Korsmeyer

D. G. Davis
H. L. Falkenberry[1]
R. B. Gallaher
A. S. Kitzes
C. G. Lawson
I. M. Miller
C. S. Morgan
R. H. Nimmo
L. F. Parsly
M. Richardson
A. N. Smith
D. G. Thomas
C. F. VandenBulck[2]
R. P. Wichner

9.1 INTERIM STANDARD SLURRY

9.1.1 Preparation

Specifications for an interim standard slurry were drawn up for the purpose of providing a reproducible reference material whereby the work of the groups participating in the HRP slurry program could be compared. Three batches of the slurry were prepared according to the standard procedure,[3] which in general specifies the dispersion of very pure, 800°C-calcined thorium oxide in distilled water by circulation in the 200-A loop for 100 hr within the temperature range of 150 to 200°C. The standard concentration is 500 g of thorium per kilogram of H_2O. In the preparation of each batch of slurry, the loop was charged to give a slurry concentration of 500 g of thorium per kilogram of water with no additives except 50 psig of oxygen. The slurries were circulated at 200°C for approximately 100 hr with no difficulties encountered.

From the results obtained thus far, the three batches of slurry prepared in runs 200A-6, -7, and -8 appeared to be identical in chemical composition and also in physical appearance when observed under a microscope. The particles were found to be roughly spherical after 100 hr of circulation and varied in diameter from 8 to 30 μ, with an estimated average diameter of approximately 15 μ. Figures 9.1 through 9.4 show the formation of the spheres as a function of circulation time. Figure 9.1 is a photograph of the slurry after 15.4 hr of circulation at 200°C, at which time no spheres are apparent. Figure 9.2 indicates the appearance of the slurry after 22.6 hr of circulation and shows the spheres beginning to form. The spheres are more sharply defined after 46.9 hr of circulation (Fig. 9.3) but are not yet fully formed; extremely fine material can be seen still adhering to the surfaces of the spheres. After 101 hr of circulation, however, the spheres appear to be fully developed (Fig. 9.4).

9.1.2 Physical Properties

The effect of settled-bed depth and container diameter on the standard-slurry settled-bed concentration is shown in Fig. 9.5 for containers

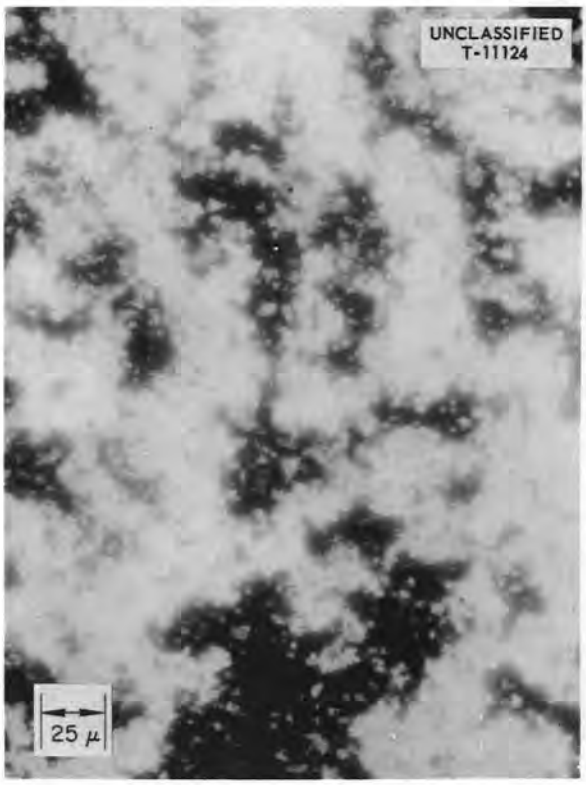

Fig. 9.1. Condition of ThO_2 in Run 200A-6 After 15.4 hr of Circulation at 200°C. 400X. Reduced 9%.

[1]On loan from TVA.

[2]On loan from Union Carbide Nuclear Company, New York Office.

[3]R. B. Gallaher and A. S. Kitzes, *Preparation of Standard Oxide*, ORNL CF-56-10-8 (Oct. 3, 1956).

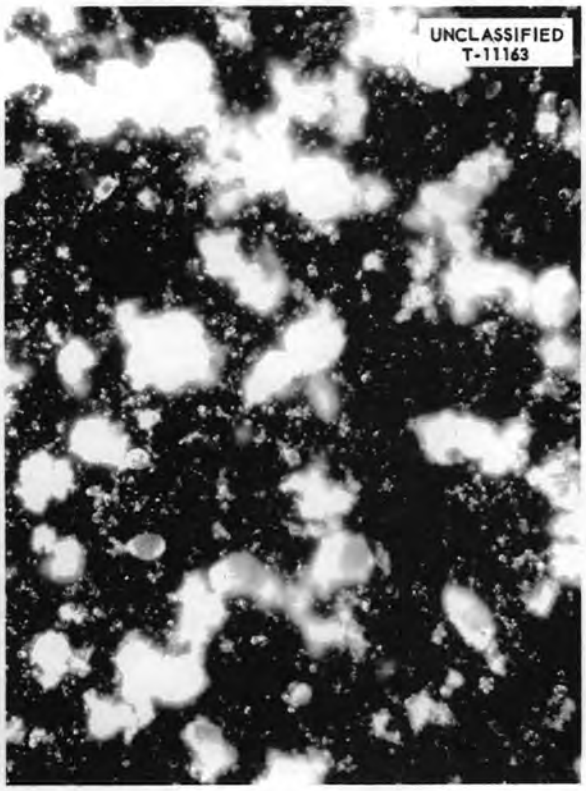

Fig. 9.2. Formation of Spheres in Run 200A-6 After 22.6 hr of Circulation at 200°C. 400X. Reduced 9%.

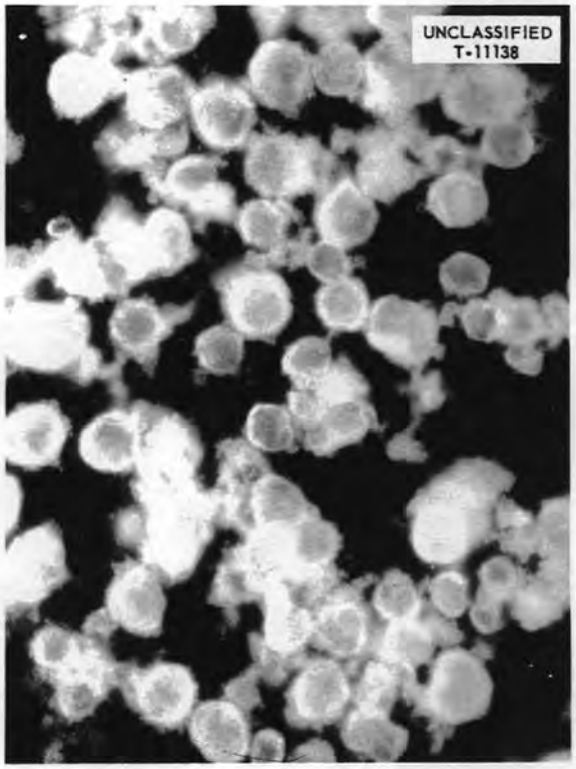

Fig. 9.3. Appearance of Slurry in Run 200A-6 After 46.9 hr of Circulation at 200°C. 400X. Reduced 11%.

having diameters of from 1.6 to 4.7 cm and for bed depths of from 1 to 17 cm. The settled-bed concentration appears to be independent of container diameter and increases by a factor of only 1.37 for a 17-fold increase of bed depth.

An average particle density of 5.1 g/cc was estimated from settled-bed data extrapolated to zero bed depth. A bed voidage of 39.5% was assumed,[4] and simultaneous equations including the effect of water incorporated in the individual particles, as well as in the interstices between the particles, were solved for the particle density. For comparison an average particle density of 4.8 g/cc was estimated by comparing mean particle diameters obtained by gravitational sedimentation[5] (D_{pmw} = 11 μ) with those obtained by measuring particle diameter with an optical microscope (D_{pmw} = 16.7 μ). The agreement between the densities estimated from the two different sets of data appears to be satisfactory.

The settling rates at room temperature for different concentrations of standard slurry are shown below:

Initial Slurry Concentration (g of Th per kg of H_2O)	Settling Rate (cm/sec)
310	0.26
750	0.12
1600	0.031
3300	0.0033

[4]G. Herdan, *Small Particle Statistics: An Account of Statistical Methods for the Investigation of Finely Divided Materials*, p 244, Elsevier, Amsterdam, 1953.

[5]Particle-size distributions on a weight basis were calculated by means of Stokes' law by assuming a ThO_2 density of 9.67. Thus the true average density of the particles based on the optically determined diameter is $(\rho - 1)/8.67 = (11/16.7)^2$.

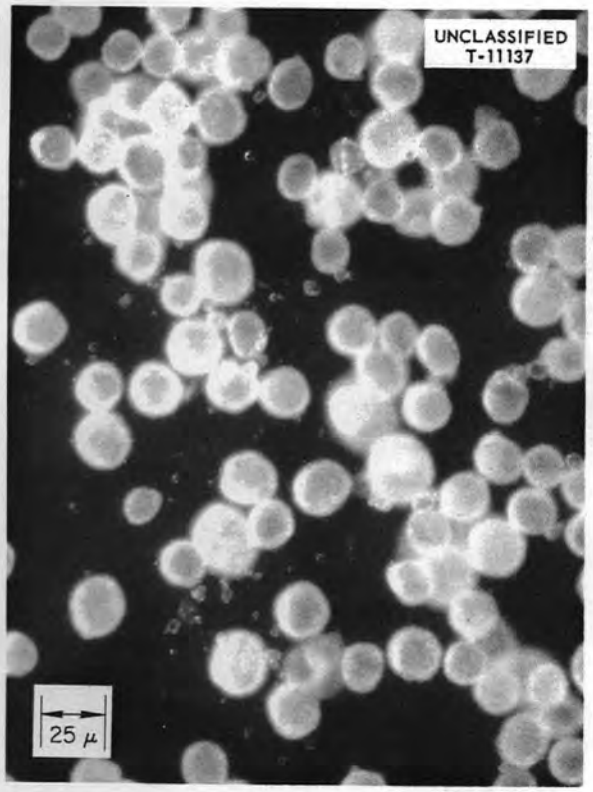

Fig. 9.4. Fully Formed ThO_2 Spheres in Run 200A-6 After 101 hr of Circulation at 200°C. 400X. Reduced 9%.

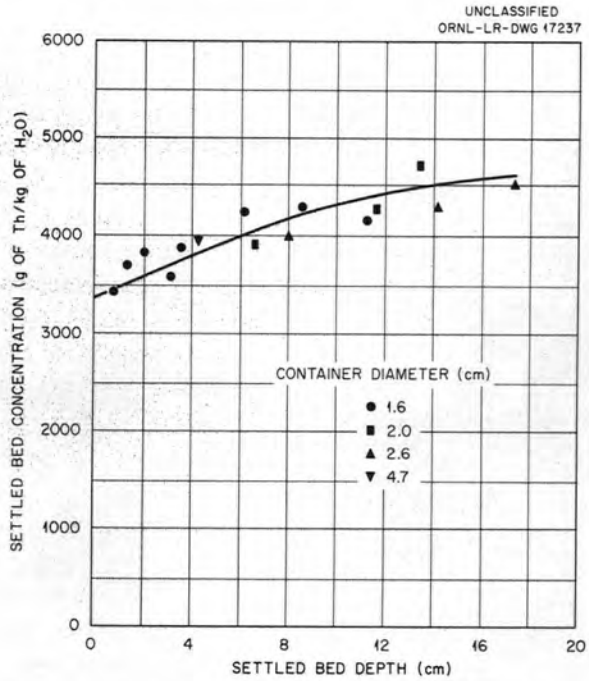

Fig. 9.5. Effect of Settled-Bed Depth and Container Diameter on Settled-Bed Concentration.

Richardson and Zaki[6] have shown that the settling rate of uniformly sized particles greater than 100 μ in diameter may be expressed as

$$\frac{V_c}{V_o} = \epsilon^n \ , \tag{1}$$

where n was found to be 7.65 experimentally (other symbols are defined in the Nomenclature, attached at the end of this chapter). The settling-rate data for standard slurry are shown in Fig. 9.6 as settling-rate, V_c, plotted against voidage, ϵ, with a line of slope 4.65 drawn through the data. It appears that Eq. 1 may be used for determining the effect of concentration on the settling rate for slurries of essentially uniform particle-size distribution and particle diameters as small as from 15 to 20 μ.

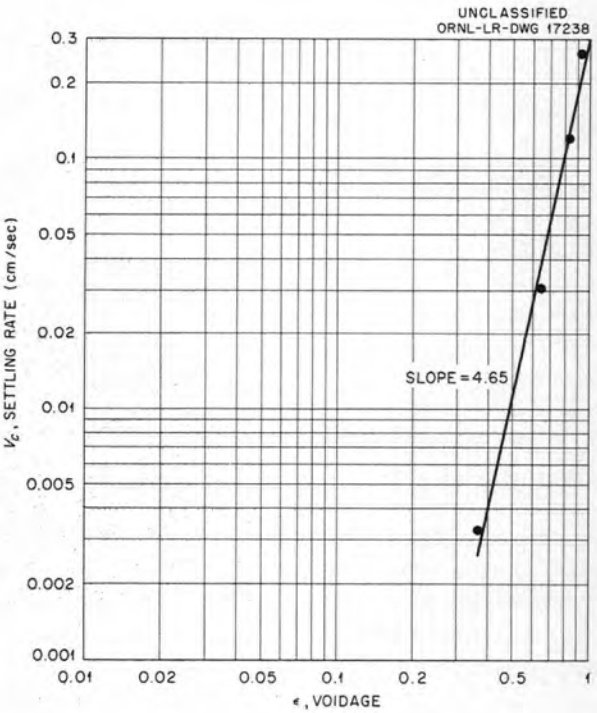

Fig. 9.6. Effect of Concentration of Suspended Solids on Rate of Settling.

[6] J. F. Richardson and W. N. Zaki, *Trans. Inst. Chem. Engrs. (London)* **32**, 35–53 (1954).

9.1.3 Rheology

Pseudo-shear diagrams for samples of interim standard slurry having solids concentrations in the range 250 to 2500 g of thorium per kilogram of H_2O were determined at room temperature in a capillary-tube viscometer. The slurries tested included the materials prepared in each of the three loop runs (200A-6, -7, and -8), the composite mixture of these batches, and concentrates obtained by decanting off various amounts of supernatant liquid. The rapidity with which the solids settled out of these slurries, especially at low concentrations, resulted in stratified flow, pulsing flow, or complete plugging at low rates of shear. Hence in some runs insufficient data were obtained in the laminar flow region to determine the slurry yield stress, τ_y, and the coefficient of rigidity, η. The results obtained are listed in Table 9.1, and the pseudo-shear diagrams obtained with a tube 0.0985 in. in inside diameter and 8.03 ft long are shown in Fig. 9.7. It may be seen that the interim standard slurry is characterized by having a low yield stress and a low coefficient of rigidity, even at thorium concentrations greater than 1000 g per kilogram of H_2O.

The instability of the "snowball" structure of the particles in the interim standard slurry was evidenced in a series of tests made with slurry which had been handled in a recirculating sampling system. This system comprised an Eastern Midget pump (the open-type centrifugal impeller rotating at 5000 rpm) and $\frac{3}{8}$-in. copper tubing for recirculating the slurry to the carboy to obtain homogeneity or for pumping a charge into the viscometer head tank. Air sparging was employed to keep the solids agitated in the carboy. As may be seen from the data in Table 9.2, and the pseudo-shear diagram in Fig. 9.8, both the yield stress and the coefficient of rigidity for the slurry pumped with the Midget pump are higher than the values for the standard slurry. The yield stress of this material appeared to decrease with continued use. Passing this material through a 200-mesh screen to remove any air-dried flakes gave a slurry having a shear diagram substantially the same as that for the unpumped standard slurry. The reason for this change is unknown at present.

TABLE 9.1. VISCOMETRIC DATA FOR STANDARD ThO_2 SLURRIES AT ROOM TEMPERATURE

Slurry Concentration (g of Th per kg of H_2O)	Tube Length (ft)	Yield Stress (lb/ft^2)	Coefficient of Rigidity (centipoises)	Notes
265	8	0.041	0.89	Composite slurry from loop runs 200A-6, -7, and -8
215	6	0.034	1.04	
265	4	0.030	1.04	
560	8	Insufficient data in laminar region		Loop run 200A-6
515	4	Insufficient data in laminar region		Loop run 200A-6
478	8	Insufficient laminar data		Loop run 200A-7
475	8	Insufficient laminar data		Loop run 200A-8
1000	8	Insufficient lominar data		Composite slurry
1600	6	0.041	2.08	Composite slurry
1540	8	0.038	2.16	Composite slurry
2520	8	0.049	3.50	Composite slurry
2430	6	0.045	3.53	Composite slurry

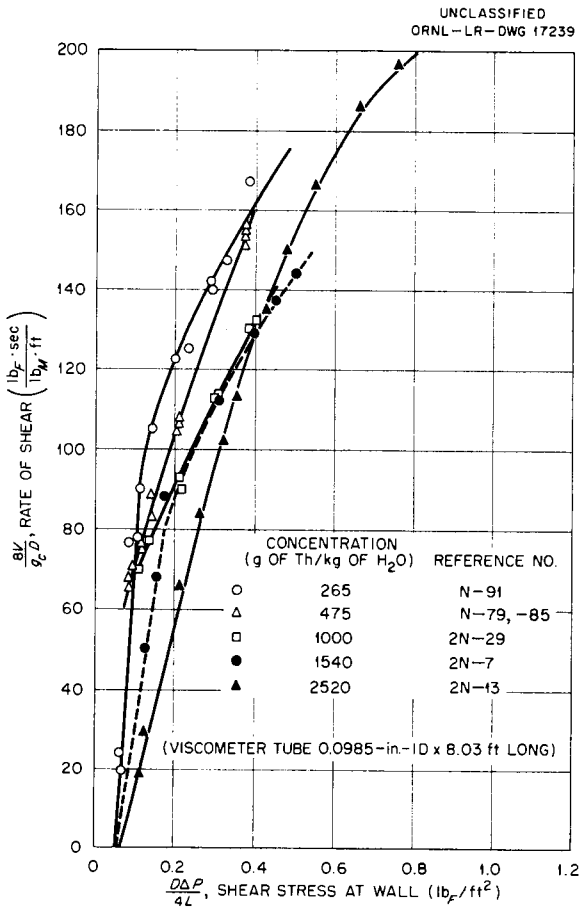

Fig. 9.7. Influence of Concentration on Pseudo-Shear Diagrams for Standard Slurry.

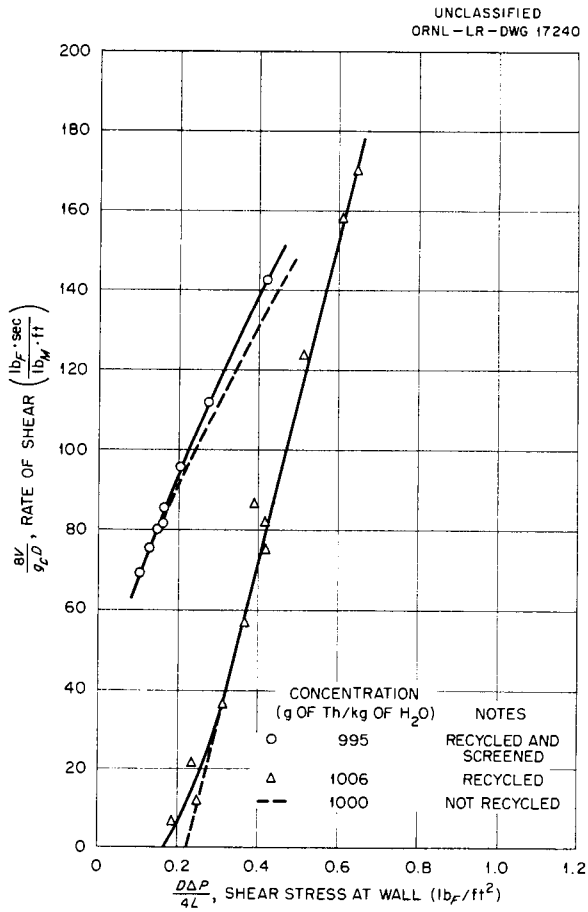

Fig. 9.8. Pseudo-Shear Diagram for Standard Slurry After Recirculation in Sampling System.

TABLE 9.2. VISCOMETRIC DATA FOR STANDARD ThO_2 SLURRIES AFTER RECIRCULATION IN SAMPLING SYSTEM

Slurry Concentration (g of Th per kg of H_2O)	Tube Length (ft)	Yield Stress (lb/ft^2)	Coefficient of Rigidity (centipoises)	Notes
1006	4	0.165	3.71	Composite slurry from loop runs 200A-6, -7, and -8
1080	8	0.165	3.71	
1015	8	0.139	4.37	
1022	8	0.120	3.95	
1016	6	0.094	3.78	
995	4	Insufficient laminar data		Screened through 200-mesh screen

9.2 HEAT-TRANSFER MEASUREMENTS

An analysis of the effect of the rheological properties of Bingham plastic slurries on slurry heat-transfer coefficients indicated that experimental data in the turbulent region could be correlated by an equation of the form

$$\frac{hD}{k} = 0.023\left(\frac{C_p\eta}{k}\right)^{1/3}\left(\frac{DV\rho}{\eta}\right)^{0.8}\left(1 - \frac{\tau_y}{\tau_w}\right)^n\left(\frac{\mu_{H_2O}}{\eta}\right)^m , \tag{1}$$

where n was taken to be $5/3$, based on a momentum–heat-transfer analogy. Preliminary data, taken with a 1-in. sched-40 black-iron-pipe heat-transfer system containing a highly flocculated thorium oxide slurry, are shown in Fig. 9.9. Curve A is drawn through data taken with slurries having a yield stress, τ_y, of 0.16 lb/ft^2 and a coefficient of rigidity, η, of 1.4 centipoises; curve B is drawn through data taken with a slurry having a yield stress of 0.34 lb/ft^2 and a coefficient of rigidity of 2.0 centipoises; curve C is drawn through data taken with the slurry of curve B after it was deflocculated with sodium silicate; curve D is drawn through data taken with water. The Wilson-plot method was used to evaluate the heat-transfer coefficients.

Figure 9.10 is a generalized plot of the heat-transfer data with exponents $n = 5/3$ and $m = 0.2$ in Eq. 1. The data corresponding to low values of $1 - (\tau_y/\tau_w)$ deviate further from the theoretical line than data for higher values of $1 - (\tau_y/\tau_w)$. This suggested that either the exponent n was greater than $5/3$ or that the data were taken in the transition region where the length-to-diameter ratio is important. Figure 9.11 is a generalized plot of the data with exponents $n = 3$ and $m = 0$. Although this relationship gives the best fit to the data, it must be considered preliminary until more accurate data are obtained with tubes of different diameters and lengths and over a wider range of velocities.

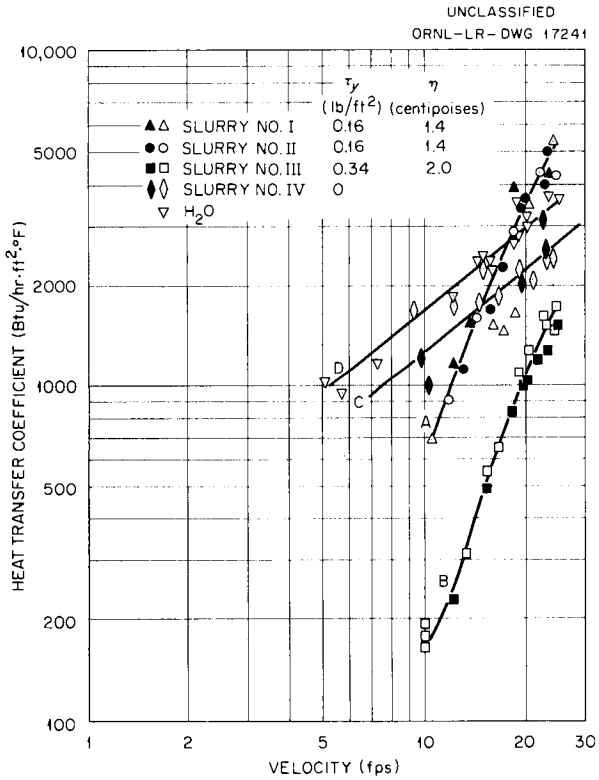

Fig. 9.9. Effect of Velocity on Slurry Heat-Transfer Coefficient.

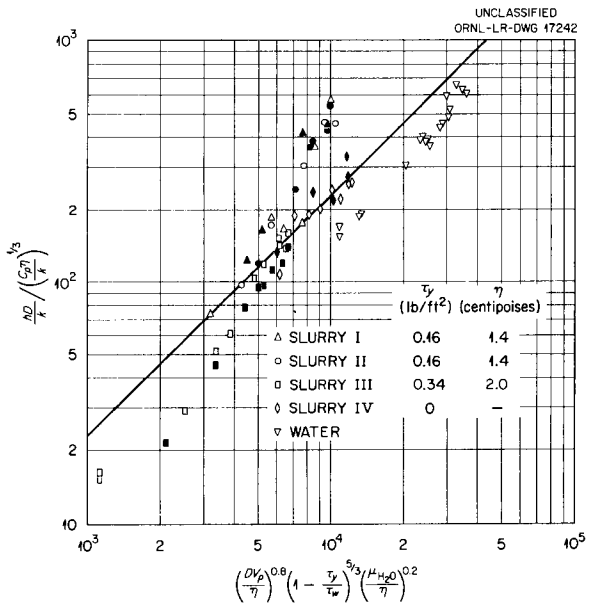

Fig. 9.10. Comparison of Slurry Heat-Transfer Data with Derived Equation for Bingham Plastics.

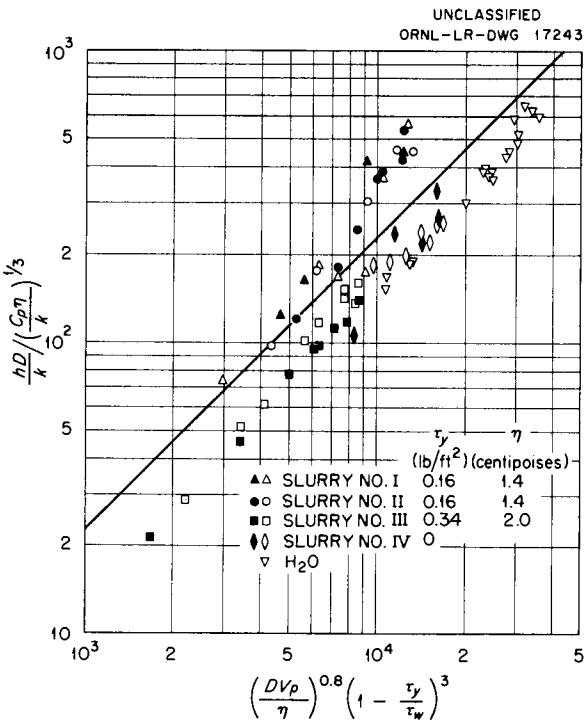

Fig. 9.11. Empirical Modification of Derived Heat-Transfer Equation for Turbulently Flowing Bingham Plastics.

On the basis of these results and by use of the equation for laminar-flow heat transfer previously reported,[7] the generalized heat-transfer plot shown in Fig. 9.12 was prepared.

9.3 THERMAL STABILITY OF A DEFLOCCULATED SLURRY

A thermally stable deflocculated thorium oxide slurry would possess many physical properties desirable for use in a blanket system. Previous static bomb tests at 250°C indicated that a slurry treated with sodium silicate was thermally stable;[8] however, all attempts to circulate silicate-treated slurries in 5-gpm loops were unsuccessful.[9] Because of the improved heat-transfer characteristics indicated in Sec. 9.2 for a silicate-treated slurry, it seemed desirable to re-examine the high-temperature stability of such a slurry.

Loop T was charged to a concentration of 750 g of thorium per kilogram of H_2O, 2000 ppm of oxygen was added, and the test (T-79) was started.[10] After 3.8 hr of circulation at 290°C, 0.3 wt % $Na_2O{\cdot}SiO_2$ (based on the total weight of slurry) was added to the system through a Pulsafeeder; the test was continued uneventfully for another 88.6 hr. The loop was then cooled to below 100°C, and the slurry was allowed to settle. After standing for two days, the system was heated to 290°C, and within 1 hr after the pump was started (i.e., after reaching 290°C), the slurry was essentially resuspended. Similar results were obtained in a subsequent circulation and shutdown cycle in which the loop was allowed to stand overnight. Samples withdrawn at intervals during the test were essentially Newtonian, and the room-temperature settling rate was less than 10^{-4} cm/sec. The attack-rate data for this test are compared with data from previous tests[11] in loops S and T in Table 9.3.

TABLE 9.3. COMPARISON OF ATTACK RATE IN TEST T-79 WITH RANGE OF ATTACK RATES IN PREVIOUSLY REPORTED TESTS IN LOOPS S AND T

Type of Rate*	Previous Results			T-79
	Min	Median	Max	
Y_1	1	15	23	18
Y_2	13	39	47	44

*Y_1 = 10 log [(10) (linear attack rate) (av ThO_2 conc.)]; Y_2 = 10 log [(parabolic attack rate) (av ThO_2 conc.)^2].

The titanium hubs of the stainless steel impeller were attacked under the seal rings (Fig. 9.13), the impeller losing 13 g during the test. However, the titanium seal rings were not appreciably attacked, the inside diameter increasing only 0.002 in.

[7] C. G. Lawson, *HRP Quar. Prog. Rep. July 31, 1956*, ORNL-2148, p 56.

[8] R. N. Lyon *et al.*, *HRP Quar. Prog. Rep. Oct. 31, 1954*, ORNL-1813, p 126.

[9] R. N. Lyon *et al.*, *HRP Quar. Prog. Rep. April 30, 1955*, ORNL-1895, p 144–145.

[10] P. H. Hayes and D. G. Thomas, *The Thermal Stability of Sodium Silicate Treated Thorium Oxide Slurry in Dynamic Tests*, ORNL CF-56-11-2 (to be issued).

[11] D. G. Thomas, *Attack of Circulating Aqueous-ThO_2 Slurries on Stainless Steel Systems*, ORNL CF-56-1-21 (Jan. 5, 1956).

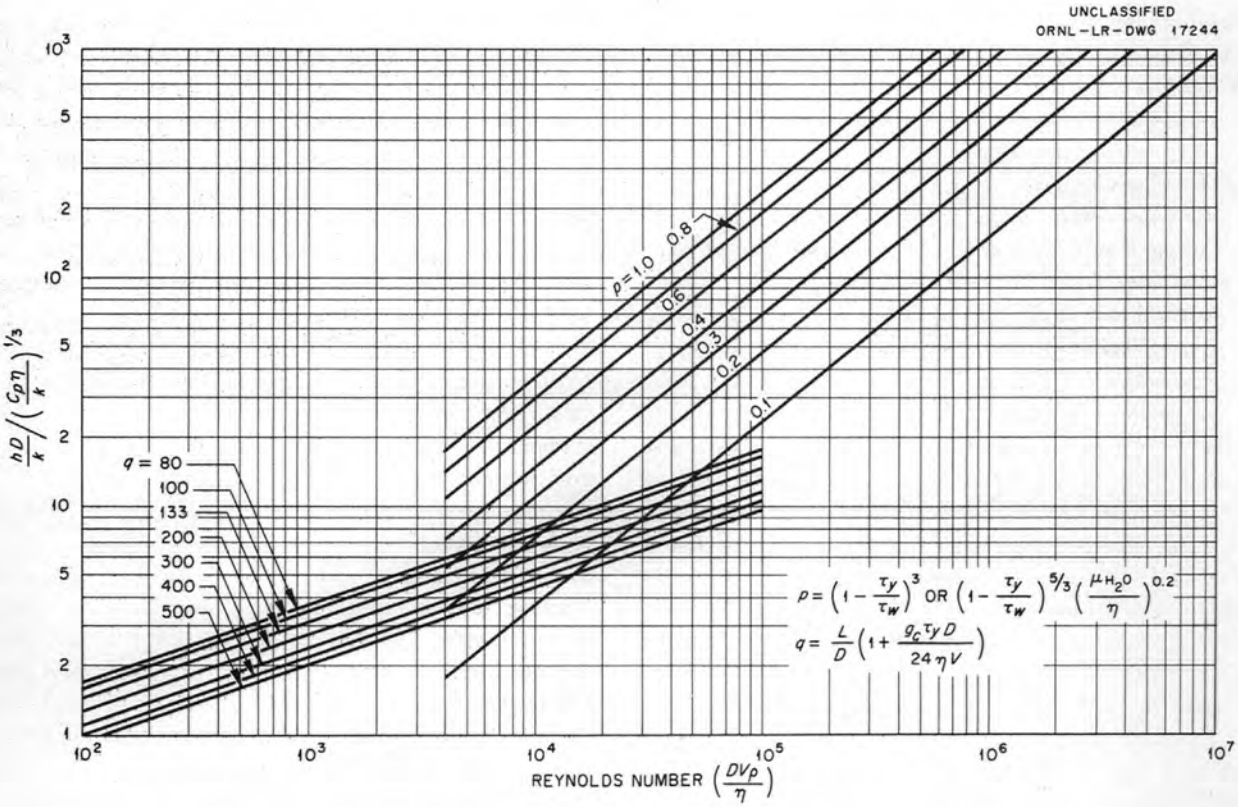

Fig. 9.12. Generalized Heat-Transfer Diagram for Bingham Plastic Slurries.

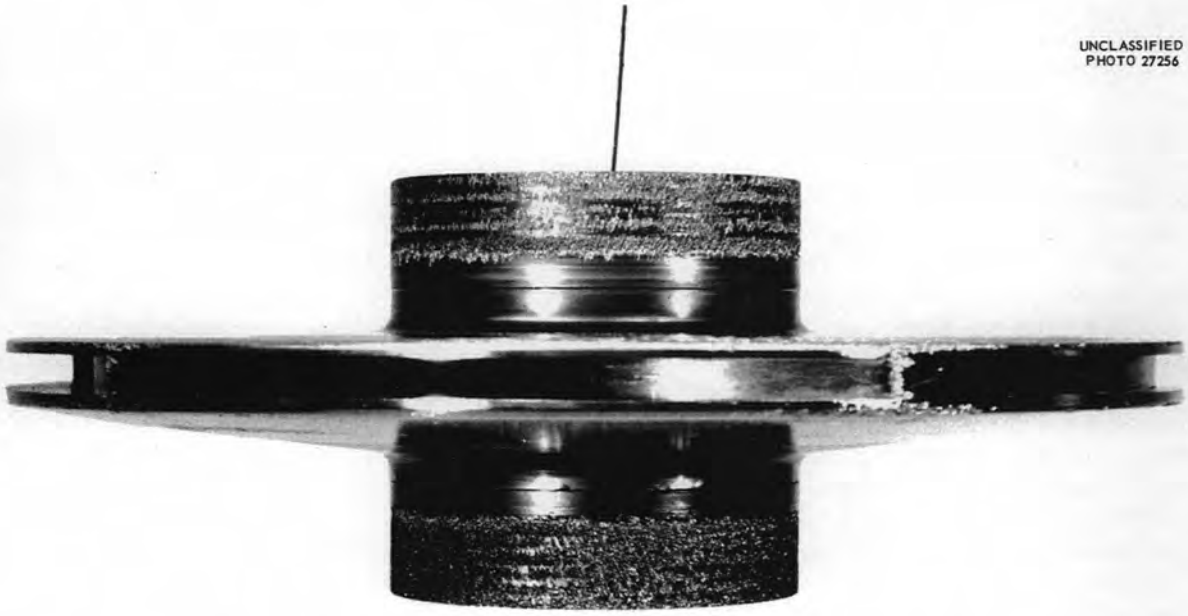

Fig. 9.13. Impeller from T-loop After Silicated Slurry Run (T-79).

during the test. The room-temperature pH of the slurry was 11.3 after the addition of the sodium silicate, essentially all the sodium being in the supernatant liquid.

9.4 COMPONENT DEVELOPMENT

9.4.1 Effect of Sulfate and ThO_2 Concentration on Slurry Behavior

Run 208A-9 – to determine the feasibility of circulating concentrated slurries containing little or no sulfate at 300°C – was completed in the 200A loop during the quarter. The loop was loaded initially with unsulfated oxide to give a thorium concentration of 500 g per kilogram of H_2O, and O_2 was charged to a partial pressure of 50 psi. The thorium concentration was increased to 1350 g per kilogram of H_2O in three increments by adding fresh, unpumped slurry to the loop at room temperature. After each addition, the mixture of pumped and fresh slurry was circulated at 300°C for at least 100 hr.

The initial charge of slurry containing 500 g of thorium per kilogram of H_2O was circulated at 200°C for 59 hr before the loop temperature was raised to 300°C to determine whether the spheres which were formed during circulation at 200°C were thermally stable at 300°C. Upon microscopic examination, it was found that the spheres had grown after 35 hr of circulation at 300°C. The average diameter of the spheres was approximately 15 μ at 200°C and was about 25 μ at 300°C. Microscopic examination of the samples is still continuing to determine whether or not the spheres continued to grow during the last 64 hr of circulation at 300°C.

During the run with the slurry containing 500 g of thorium per kilogram of H_2O, the loop was cooled to room temperature after 47 hr of operation at 300°C so that the main pump flanges could be seal welded in order to eliminate a leak which developed when the temperature was raised from 200 to 300°C. During the startup after the seal-welding operation, the pump began to vibrate slightly and continued to vibrate during the remaining runs. These vibrations, however, did not appear to affect the operation of the pump, except for small fluctuations in the power demand, which increased with each addition of fresh oxide and reached a maximum of 0.24 kw as the concentration was increased to 1350 g/kg. It is now believed, after an inspection of the pump at the termination of the run, that the vibrations and the fluctuations in the power demand were a result of solids accumulated in the pump scroll and/or in the impeller vanes, causing the pump to become dynamically unbalanced.

When the slurry concentration was increased to 750 g of thorium per kilogram of H_2O, samples taken from three different sampling points varied in concentration by a factor of 3 to 4, indicating that the slurry was not circulating homogeneously. In addition, the sample bombs often plugged before the sample could be drained. Inspection of a plugged bomb revealed that the plugging was not due to caking but occurred as a result of the solids settling rapidly to a high bed density. This slurry was circulated at 300°C for 132 hr.

Increasing the thorium concentration to 1000 and then to 1350 g per kilogram of H_2O did not eliminate the large variations in sampling which were noticed with the above slurry. With both concentrated slurries, wide variations in concentration were still found in the samples taken from the three loop-sampling points.

The 1000-g/kg slurry was circulated at 300°C for 107 hr. The 1350-g/kg slurry, however, was circulated at 300°C for 138 hr, and then 0.1 *N* H_2SO_4 was added at temperature to determine the effect of the sulfate on the handling characteristics of pumped slurries.

Before the sulfuric acid was added to the 1350-g/kg slurry, a vertical concentration gradient was found in the horizontal pipe run by using a scintillation head in combination with a Hewlett-Packard counter and an oscilloscope to measure the attenuation of the gamma rays from Co^{60} in passing through the pipe. The results of several vertical traverses indicated that the larger part of the slurry was flowing (or present) along the bottom of the pipe, as can be explained by the work of Newitt *et al.*,[12] who have described the different types of flow encountered with suspensions of uniform particles. They have established criteria both theoretically and experimentally for the transition velocities differentiating between homogeneous fully suspended flow and heterogeneous fully suspended flow and between heterogeneous fully suspended flow and suspended flow

[12] D. M. Newitt *et al.*, *Trans. Inst. Chem. Engrs.* (*London*) 33, 93–113 (1955).

with a moving bed. The values of these transition velocities were calculated for the conditions of the 200A-9 test (by using the value of the settling rate determined at room temperature corrected to operating conditions by the application of Stokes' law[13]) and were found to be 11.5 and 1.8 fps, respectively. The order-of-magnitude agreement between these transition velocities and the nominal velocity in loop 200A (10 fps) indicates that the observed vertical concentration gradient may be explained entirely on the basis of the large working particle size of the slurry and the accompanying high settling rate.

The sulfuric acid was added in two increments; the first addition increased the sulfate content from 0 to 250 ppm based on water, and the second addition brought it up to 750 ppm. The pump power demand showed an immediate increase of 0.24 kw with each acid addition, but the vertical concentration gradient was not noticeably affected until 12 hr after the second addition, at which time the solids appeared to be layered on the bottom of the pipe. While the loop was being cooled for an examination of the character of the apparent "layer of solids," the solids appeared to resuspend when the loop temperature reached 150°C; so the run was continued at this temperature to determine whether complete resuspension would occur. The run was terminated when the behavior of the pump became extremely erratic.

On inspection, it was found that the 3-in. pipe of the circulating loop was completely filled with sludge. There was no apparent settling of solids even though the system was allowed to remain quiescent for 70 hr prior to dismantling. However, solids were deposited in the throat and on both faces of the orifice plates. The solids deposited on the downstream face of the orifices were layered; the layer next to the metal was yellow, and the layer wetted by the slurry was gray. After the loop was flushed with water, a thin, relatively hard film, approximately 0.030 in. thick, still adhered to the pipe walls; this film was removed by mechanical means.

Inspection of the pump revealed a similarly layered cake on all the wetted surfaces of the volute, which, however, could not be removed by flushing. Photographs showing the deposit, the thickness of the two layers, and the general character of the deposits are presented in Figs. 9.14 and 9.15. Four of the five impeller channels and the eye of the impeller were also plugged with solids, as shown in Fig. 9.16.

Some pump components suffered wear. The titanium seal rings in the pump liner were worn slightly. There was no damage to the Kingsbury thrust bearing, but both the front and rear radial bearings were severely worn. Both the front and rear journals were damaged, and the Stellite overlaid on stainless steel cracked in several places.

The thermal barrier and impeller were also severely damaged, as shown in Figs. 9.17 and 9.18. Apparently, when the cake formed in the volute and in the channels of the impeller, the impeller was forced against the thermal barrier, removing a considerable amount of metal. Steel shavings and slivers from the thermal barrier were embedded in the cake found in the eye of the impeller.

9.4.2 Modifications to Loop 200A

The modifications being made to loop 200A to improve the operation of the system are approximately 80% complete. Included in the modifications are the following:

1. a venturi to meter the slurry flow; water obtained by condensing steam from the pressurizer will be used to purge the pressure taps and the manometer lines;
2. a capillary-tube or letdown-type sampling system; the tube, 0.059 in. in inside diameter and 30 ft long, is jacketed for water cooling to minimize flashing as the sample is taken;
3. installation of an in-line sampling system, capable of isolating 300 ml of slurry, as a bypass across the pump discharge and suction lines;
4. installation of a slurry-addition system, previously described,[14] to control the inventory of the system;
5. two densitometers using a scintillometer in combination with a counter to measure the attenuation of gammas from a Co^{60} source; one densitometer will be used to determine the homogeneity of the slurry circulated in the

[13] J. H. Perry (ed.), *Chemical Engineers Handbook*, p 1019, 3d ed., McGraw-Hill, New York, 1950.

[14] E. L. Compere *et al.*, *HRP Quar. Prog. Rep. April 30, 1956*, ORNL-2096, p 87.

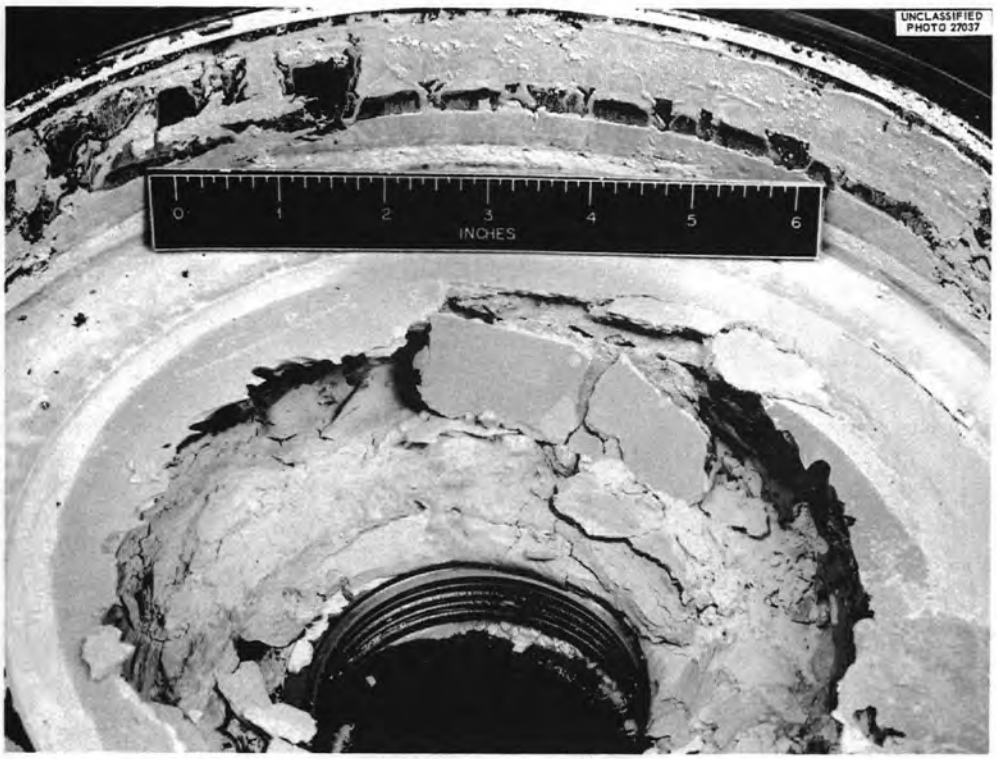

Fig. 9.14. Cake Deposited in Pump Volute in Run 200A-9.

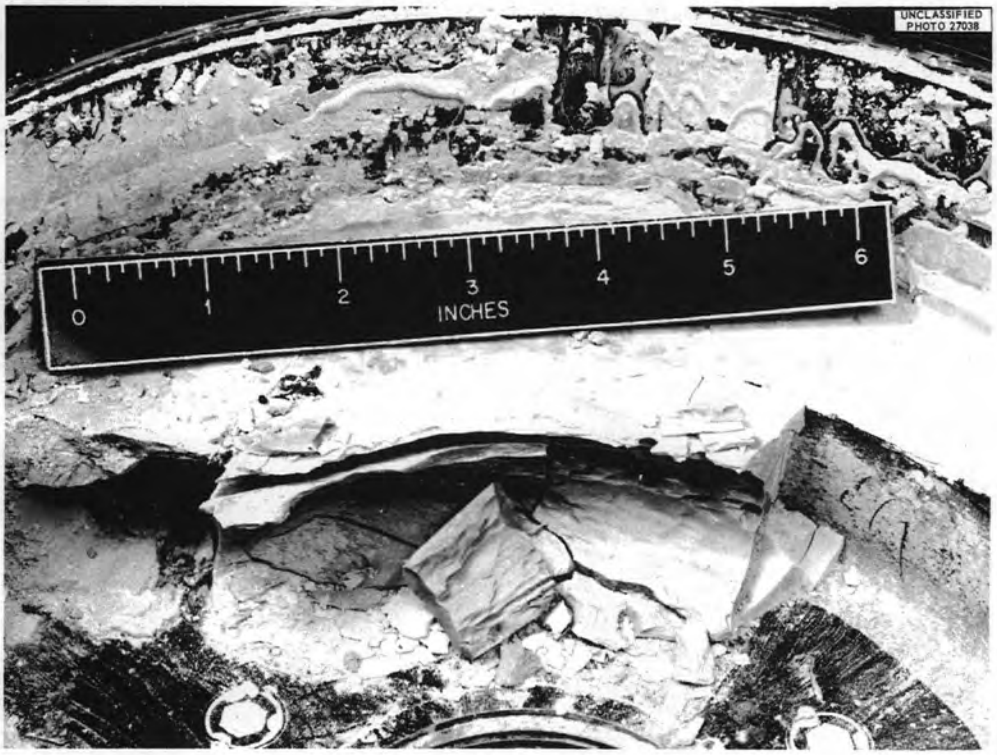

Fig. 9.15. Cake Formation in Pump Volute in Run 200A-9.

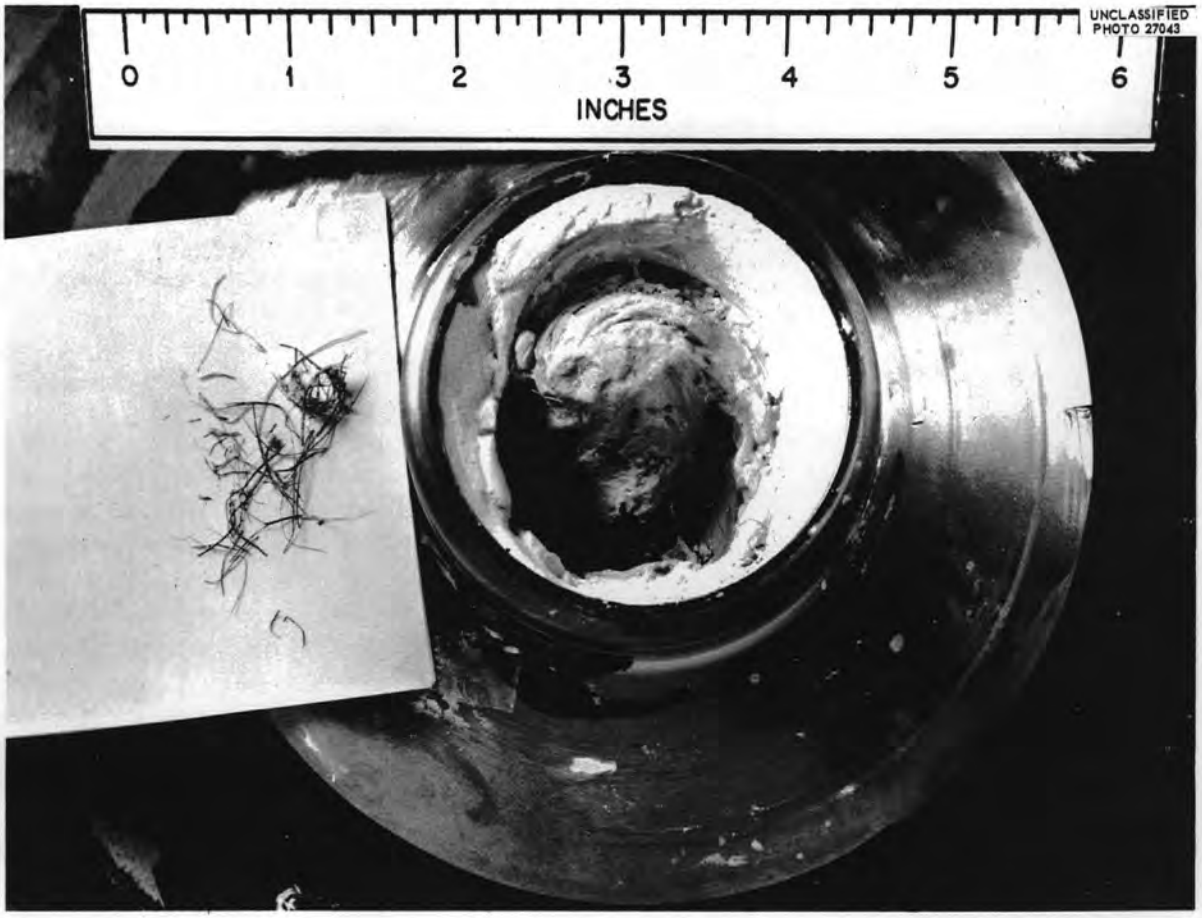

Fig. 9.16. Cake Formation Found in the Eye of the Impeller. Fibers are type 347 stainless steel removed from thermal barrier and found embedded in cake.

loop, and the other will be used to determine the liquid level and slurry level in the pressurizer under operating conditions.

9.4.3 Venturi Flowmeters

During the quarter a run was completed in loop S (100 gpm), in which the feasibility of metering slurry flow at elevated temperatures was demonstrated by use of a venturi in combination with continuous flushing of the manometer lines. For this run the loop[15] was revised by placing the venturi downstream from the pressurizer so that condensate from the pressurizer could be used to flush the venturi pressure taps.

A slurry containing 440 g of thorium per kilogram of H_2O was circulated for 72 hr at temperatures ranging from 218 to 288°C, with continuous flushing of the venturi taps. The purge-water rate was maintained at approximately 8 cc/min, and it was found upon inspection at the end of the run that the manometer lines stayed clean at this purge rate. No difficulty was encountered in controlling the flow of the purge water.

9.4.4 Survey of Graphitar-Radial-Bearing Life in 100A Pumps

A survey was made of Graphitar-radial-bearing life in 100A pumps circulating solutions and slurries; included were total cumulative operating

[15] R. N. Lyon *et al.*, *HRP Quar. Prog. Rep. Oct. 31, 1953*, ORNL-1658, p 128.

UNCLASSIFIED
PHOTO 27255

Fig. 9.17. Condition of Thermal Barrier at the End of Run 200A-9, Showing Damage Done by Impeller.

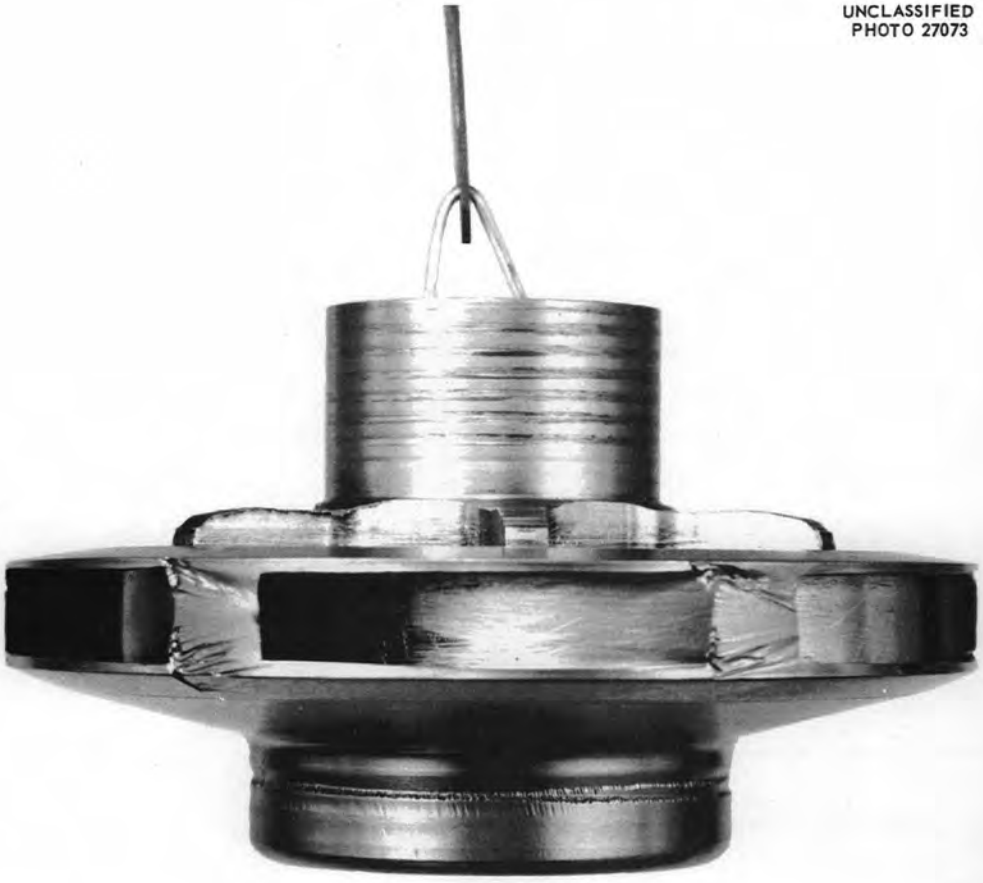

Fig. 9.18. Condition of Titanium Impeller at End of Run 200A-9, Showing Damage to Back Ribs.

times in excess of 80,000 hr for solution pumps[16] and 16,000 hr for slurry pumps.[17] During these times the bearings were inspected at the end of every run, and when the inside diameter had increased more than 0.005 in., the bearing was replaced. Chipped and cracked bearings were also replaced. Experimental data on the radial bearing life in the pumps are plotted in Fig. 9.19 on logarithmic-probability coordinates. As can be seen, the bearings give longer service in solution loops than in slurry loops. That this is an effect attributable to the presence of slurry is indicated by a ratio of mean front-bearing lives of 5.6 compared with the ratio of mean rear-bearing lives of 2.7. (The rear radial bearings of 100A pumps are continously flushed with a supply of condensate from the pressurizer, whereas the circulating stream is separated from the front radial bearing only by seal rings.) The performance which will be achieved by a particular bearing is, of course, not predictable.

[16] H. C. Savage *et al.*, *HRP Quar. Prog. Rep. Oct. 31, 1955*, ORNL-2004, p 80.

[17] D. G. Thomas, *Attack of Circulating Aqueous-ThO_2 Slurries on Stainless Steel Systems*, ORNL CF-56-1-21 (Jan. 5. 1956).

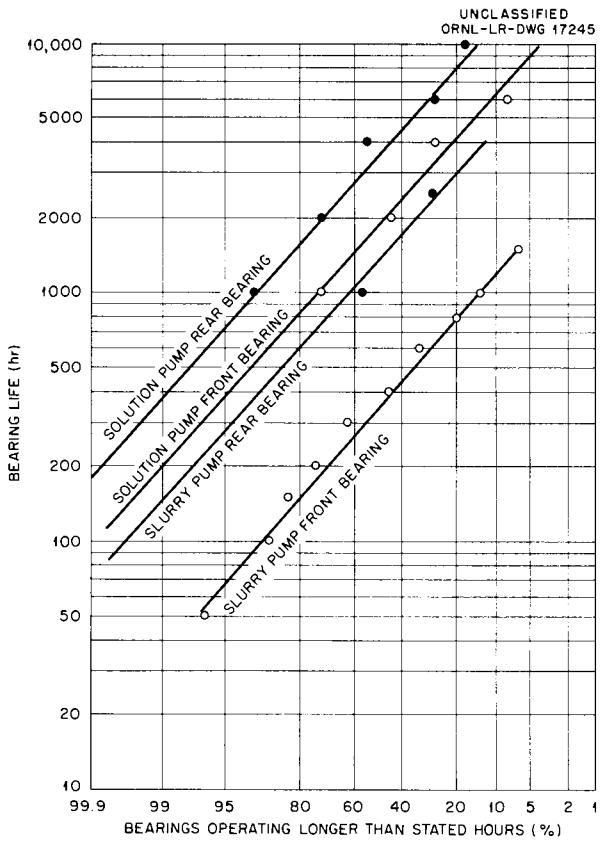

Fig. 9.19. 100A Pump Graphitar-Radial-Bearing Life While Circulating Uranyl Sulfate Solutions or Thorium Oxide Slurries.

9.5 BLANKET-SYSTEM DEVELOPMENT

9.5.1 High-Pressure-System Run

The first slurry run was made in the blanket test facility during the quarter. The high-pressure loop was operated with a slurry concentration of 500 g of thorium per kilogram of water without additives, at a system pressure of 1800 psi, and at loop temperatures of 200 and 300°C. The high-pressure heat-exchanger loop plugged after 4 hr of operation, and then, after being unplugged, it plugged again in 3½ hr. The run was terminated after 127 hr of operation.

After the loop was charged at room temperature, the system was brought to 1000 psi by heating the liquid in the pressurizer, and the pump and line heaters were then started. After 2 hr it was necessary to interrupt the run to repair a leaky valve. When repairs to the valve had been completed and the run restarted, some difficulty was experienced with pressure-temperature control, apparently owing to excessive liquid in the loop. Two level instruments, a displacement type and a differential-pressure type, were in service, and both indicated a normal operating level. However, after a sufficient quantity of liquid had been discharged, normal pressure control was re-established and good performance of the main circulating loop was achieved for the balance of the run. The run had to be terminated after 127 hr, because a leak again developed in the valve which had caused the difficulty during the initial startup.

The heat-exchanger loop (Fig. 9.20) gave difficulty throughout the run. During the initial 2-hr startup, evidence of a plug starting to form was observed. Flow and pressure-drop data obtained during this period showed that flow through the exchanger was laminar, whereas with water in the system the flow had been turbulent. The velocities were found to be 6 fps in the exchanger tubes and 3.6 fps in the connecting lines. When the run was restarted after repair of the leaking valve, the pressure leads to the flowmeter in the heat-exchanger loop became plugged and no further flow data were obtained. Later, the exchanger loop was frozen and the material plugging the loop was forced out the sample connection. A quantity of very thick slurry, of a consistency similar to calking compound, was discharged which assayed 1650 g of thorium per kilogram of H_2O. In each case of plugging, the pressure drop through the exchanger decreased gradually, finally dropping to zero. Thus it is concluded that the plug first formed in the ½-in. connecting lines rather than in the exchanger, since the main-loop flow nozzle furnished a constant head for the exchanger loop. Since the heat exchanger could not be brought to steady state, no heat-transfer data were obtained.

On termination of the run the inventory was released to the 125-gal slurry storage tank through the letdown valve, and the loop was immediately refilled with water.

9.5.2 Low-Pressure-System Shakedown

Three water-rinse runs to recheck loop performance were made following the slurry run, and the system was shut down and converted to low-pressure operation with the blanket and low-pressure heat

exchanger in service. The high-pressure heat-exchanger loop was removed for redesign. During the conversion a very fluid slurry about 1 in. deep was noted in the 3½-in. piping. It was easily removed by water flushing, and there was no evidence of caking.

The low-pressure system was given three shakedown water runs totaling 300 hr to check system performance and to gain operating experience. A number of shortcomings in instrument performance and equipment were discovered and corrected. Several aluminum rupture disks failed prematurely, so that the design is being changed to provide relief valves downstream of the disks to prevent emptying the entire system in the event of disk failure. Also, a nitrogen cylinder station was installed to provide gas pressurization of the core as an alternative to steam pressurization.

With steam pressurization of the core all loop heat requirements were easily supplied by transfer of heat through the core wall to the blanket stream. From heat-balance calculations the core supplied 39 kw of heat, and the over-all heat-transfer coefficient between the core and the blanket was 212 Btu/hr·ft^2·°F with water circulating in the blanket.

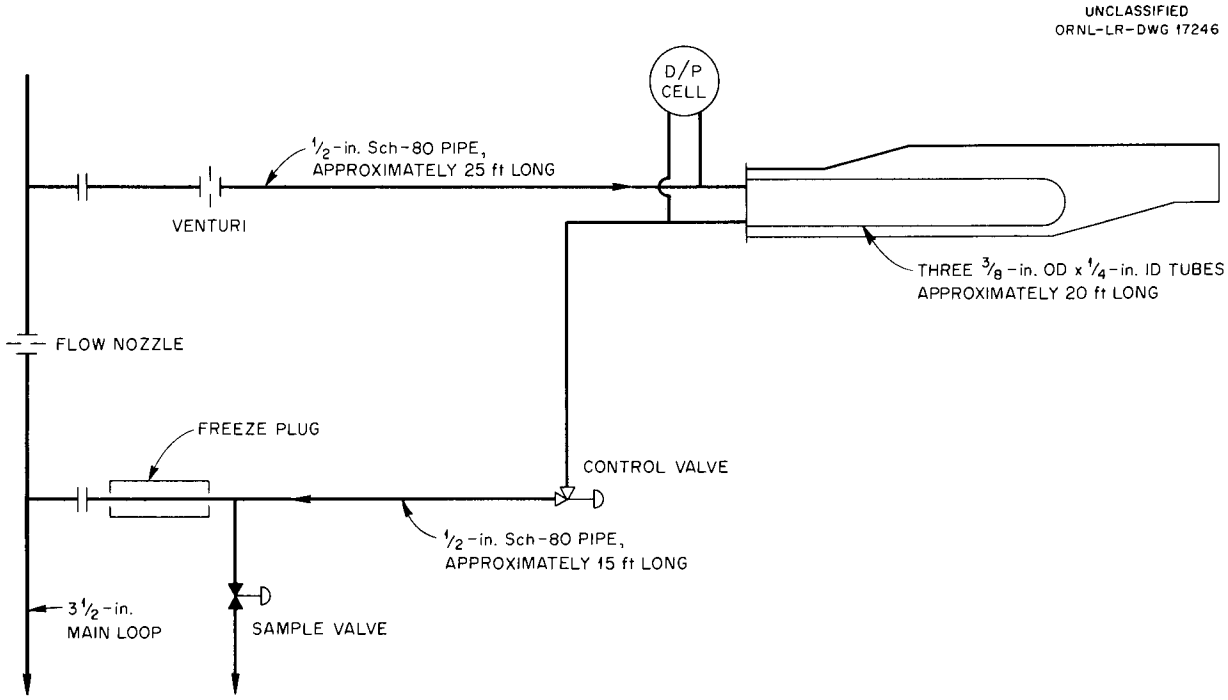

Fig. 9.20. Blanket-System Test; Heat-Exchanger Loop.

NOMENCLATURE

C_p	Specific heat	Btu/lb·°F
D	Diameter	ft
D_{pmw}	Mean particle diameter on a weight basis	ft
h	Heat-transfer coefficient	Btu/hr·ft^2·°F
k	Thermal conductivity	Btu/hr·ft·°F
m	Exponent	Dimensionless
n	Exponent	Dimensionless
V	Velocity	fps
V_c	Settling rate of concentrated suspension	cm/sec
V_o	Stokes' law settling rate	cm/sec
ϵ	Voidage	Dimensionless
η	Coefficient of rigidity	Centipoise or lb-mass/ft·sec
μ_{H_2O}	Viscosity of water	Centipoise or lb-mass/ft·sec
ρ	Density	lb/ft^3
τ_w	Shear at the wall	lb/ft^2
τ_y	Yield stress	lb/ft^2

10. INSTRUMENT AND VALVE DEVELOPMENT

D. S. Toomb

A. M. Billings H. D. Wills

10.1 INSTRUMENT DEVELOPMENT

10.1.1 Liquid-Level Transmitters

Two linear differential transformers have been ordered from the Crescent Engineering Corp. for test and evaluation. The coils are designed for continuous operation at 250°C, contain no organic material, and are hermetically sealed. Temperature resistance and radiation resistance are provided by the silver wire, ceramic insulation, and stainless steel jacket construction. Electrical and physical specifications are such as to make the transformer a direct replacement for the transformers utilized in the HRT displacement-type level transmitters.[1]

10.2 VALVE DEVELOPMENT

10.2.1 Sealing Bellows

In continuation of the bellows-life tests described earlier,[2] six HRT-type bellows manufactured of HRP specification material by Fulton Sylphon Division are being tested in uranyl sulfate at 200 psig and 300°C with a $\frac{1}{8}$-in. stroke. To date, five units have been cycled to destruction, with an average life of 25,000 strokes.

10.2.2 Valve Trim

In a continuation of the investigation of materials for valve-trim use,[3] four sets of trim fabricated from type 17-4 PH hardened to RC-39 have been checked for performance in the valve test loop, with results approximating those obtained by using type 347 stainless steel trim. Figures 10.1 and 10.2 show the "before" and "after" condition of a typical type 17-4 PH trim set. Localized wear and galling occurred in the seating area but to an extent much less than is experienced with Stellite 6. This particular set of trim was subjected to 402 dumping cycles with uranyl sulfate at 1200 psig and 250°C.

10.2.3 Actuators

Three all-metal bellows-type actuators of 23-in.^{2} area were procured from Fulton Sylphon Division for test and evaluation as remote actuators for small valves. This actuator, shown in Fig. 10.3, is rated at 30 psig operating pressure with a

UNCLASSIFIED
T-10832

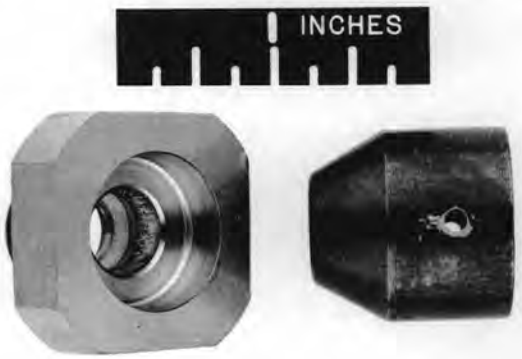

Fig. 10.1. Type 17-4 PH Stainless Steel Valve Trim Before Test.

UNCLASSIFIED
T-11067

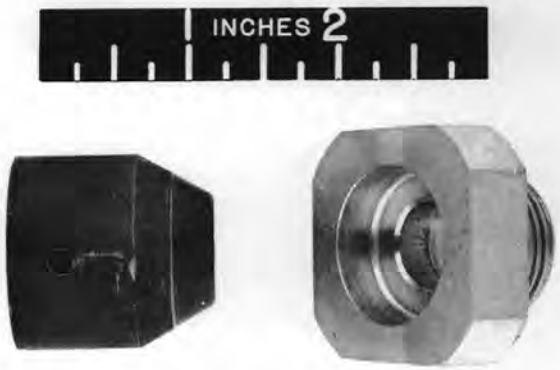

Fig. 10.2. Type 17-4 PH Stainless Steel Valve Trim After Test.

[1] D. S. Toomb *et al.*, *HRP Quar. Prog. Rep. April 30, 1956*, ORNL-2096, p 32.

[2] *Ibid.*, p 75.

[3] A. M. Billings, *HRP Experimental Valve Program*, ORNL CF-56-2-42 (Feb. 14, 1956).

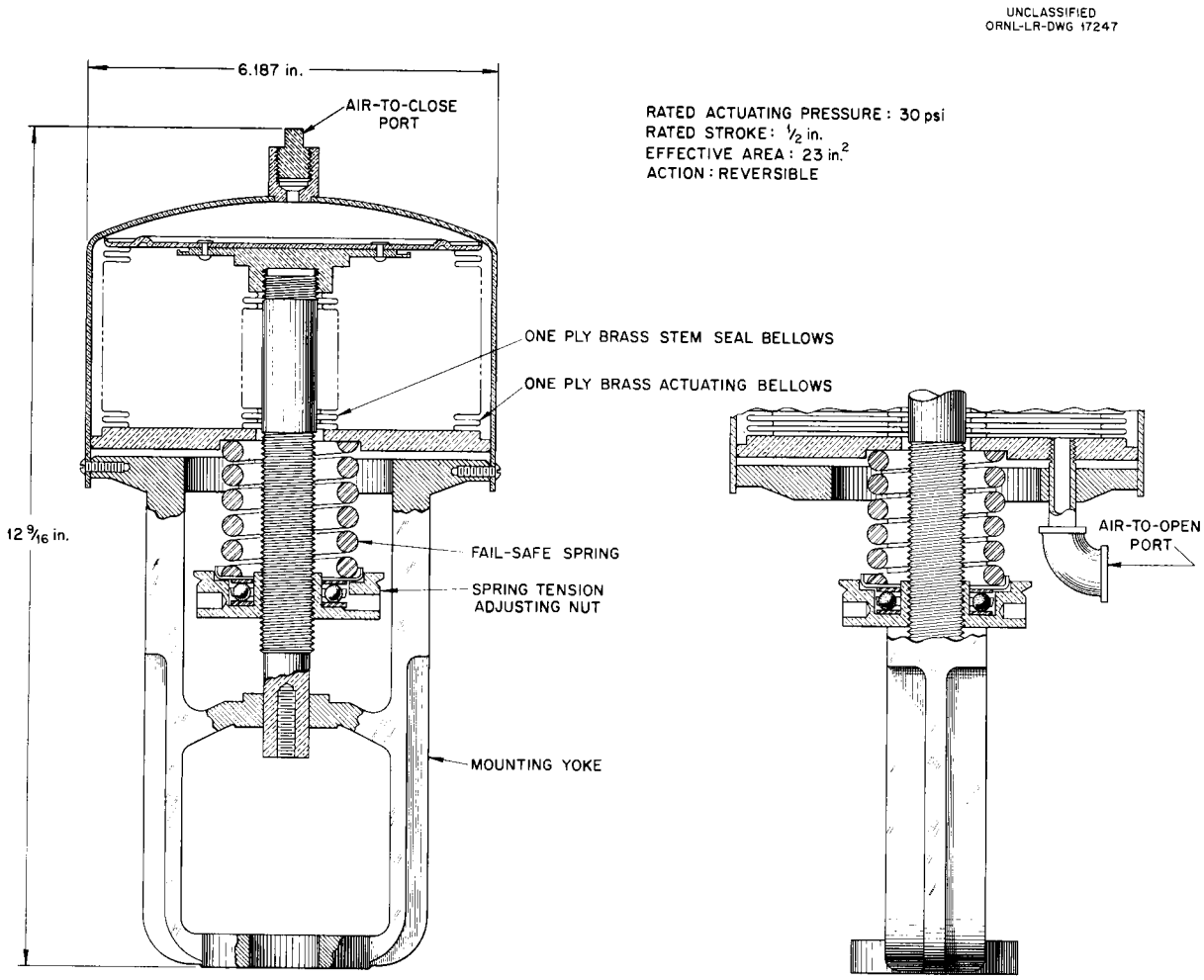

Fig. 10.3. All-Metal Small-Valve Actuator.

½-in. stroke and is reversible. The all-metallic construction allows the unit to be installed in zones of high radiation.

Two units have been tested to destruction at higher-than-rated actuating pressures and longer-than-rated stroke, with the following results:

Pressure (psig)	Stroke (in.)	Life (cycles)
75	¾	600
45	¾	1300

The third unit will be tested at the manufacturer's recommended operating conditions.

Part IV

CORROSION AND MATERIALS

E. G. Bohlmann

11. SOLUTION CORROSION[1]

H. C. Savage J. C. Griess

S. R. Buxton D. J. Krause
J. L. English T. H. Mauney
R. S. Greeley R. M. Pierce[2]
E. F. House J. A. Russell

W. C. Ulrich

11.1 PUMP LOOPS

11.1.1 Loop Engineering

(a) Loop F – Mockup of HRT Core-Vessel Expansion Joint and Zircaloy-2–Stainless Steel Gasket. – The mockup of the Zircaloy-2–stainless steel transition and expansion joint, previously described,[3] as used in the HRT reactor vessel was tested under conditions simulating reactor startup, operation at temperature, and shutdown. Fifty thermal cycles and mechanical deflections during 1240 hr of operation in uranyl sulfate solution were completed, and a preliminary examination of the unit was made.

After the transition and expansion joint had been installed in 100A dynamic corrosion loop F, the loop was treated with 3% trisodium phosphate solution at 100°C for 7 hr, rinsed, and treated with 5% nitric acid solution at 100°C for 9 hr. A final treatment with 1000 ppm oxygen in water at 300°C for 28 hr was made. The loop was then filled with the desired volume of fuel solution containing 0.04 *m* UO_2SO_4, 0.005 *m* $CuSO_4$, and 0.02 *m* H_2SO_4.

During a complete test cycle of the expansion and transition joint, the loop temperature was cycled between 100°C at 100 psig to 300°C at 1550 psig, and the expansion joint was extended $\frac{5}{16}$ in. and compressed $\frac{5}{16}$ in. for a total traverse of $\frac{5}{8}$ in. Heating was accomplished in 4 hr, operation at 300°C and 1550 psig was for 16 hr, and the cooling-down to 100°C was accomplished in 4 hr. The bellows joint was extended during heatup and compressed during the cooling period, both in $\frac{1}{8}$-in. increments. During the third test cycle a faulty mechanical jack being used to extend and compress the bellows failed. This allowed the bellows to be compressed ~$\frac{3}{8}$ in. in excess of the design allowable.

The flow rate of the fuel solution from the main circulating loop through the pressure vessel in which the bellows and transition joint were housed was ~1 gpm. Flow was external to the expansion bellows, into the transition-joint bore, and then back into the main circulating loop. The differential pressure across the bellows from outside to inside and across the gasket in the transition joint was maintained at 45 to 55 psi throughout the run. The interior of the expansion joint was filled with distilled water throughout the run. Daily samples of the distilled water were taken and were analyzed for uranium to determine whether leakage across the test gasket or expansion joint had occurred.

After the 50-cycle test the loop was shut down and the outer pressure vessel removed; visual examination failed to reveal any cracks or damage beyond a partial collapse of the uppermost convolution of the bellows. A leak test, in which 50-psig helium pressure was applied inside the expansion joint, failed to reveal any leakage as measured by a mass-spectrograph type of leak detector. Further examination of the bellows and transition joint to determine additional information relative to the mechanical reliability of this joint as presently installed in the HRT is being made.

Visual examination of the loop and bellows assembly after partial dismantling revealed one area of significant corrosion. The stainless steel bellows is prevented from flexing at the end welds by tightly fitting rings (see Fig. 11.1). Near the top and bottom of the crevice between the ring and the bellows several pits were observed in the bellows material, one of which appeared to be 10 to 15 mils deep. Further investigation is being made into the causes and extent of this attack. Over-all loop corrosion rate and corrosion specimen results are discussed in Sec. 11.1.2. Photographs of the bellows and transition joint and of

[1] Reported in greater detail by J. C. Griess *et al.*, *Quarterly Report of the Solution Corrosion Group for the Period Ending October 31, 1956*, ORNL CF-56-10-13 (to be issued).

[2] On loan from TVA.

[3] J. C. Griess *et al.*, *HRP Quar. Prog. Rep. July 31, 1956*, ORNL-2148, p 73 and Figs. 11.1 and 11.2.

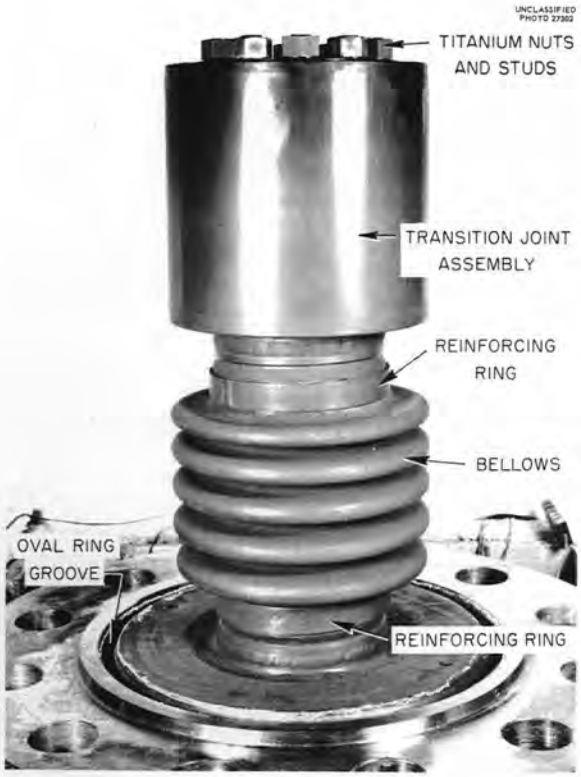

Fig. 11.1. Photograph of Bellows and Transition Joint Assembly After 1250-hr Operation.

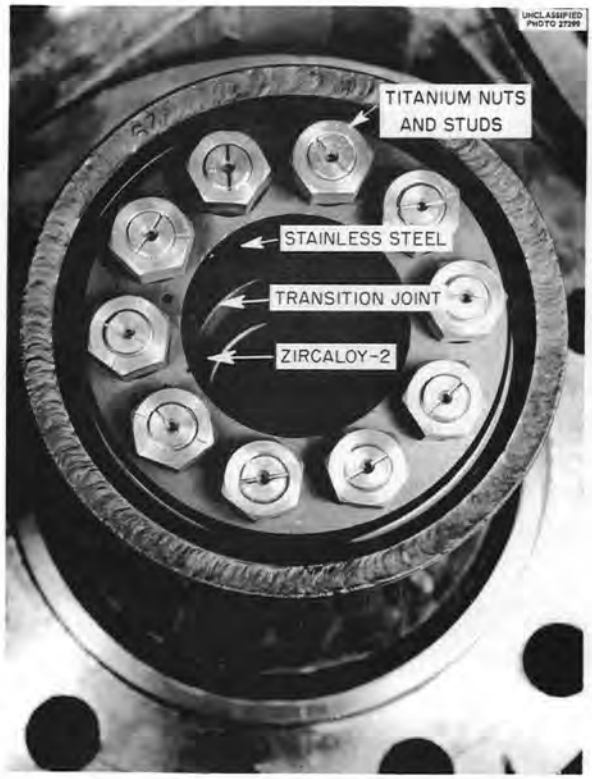

Fig. 11.2. Photograph of Interior of Transition Joint After 1250-hr Operation.

the test-vessel flange are presented in Figs. 11.1 and 11.2.

Prior to disassembly the 10-in. IPS test-vessel oval-ring-gasketed joint was leak tested at 500-psig helium pressure with a mass-spectrograph type of leak detector without evidence of leakage. The flanges are 1500-lb, 10-in. IPS, standard type with oval ring No. R-54 of type 304 stainless steel. Bolts are $1\frac{7}{8}$-in. per ASTM-A193-52T, grade B-7, threads 8N8, class 3 fit. Nuts are per ASTM A194-53, grade 2H, threaded 8N8, class 2 fit. To assure a tight joint, the as-received flange grooves were remachined to remove tool chatter on mating surfaces and to mate pitch diameters to the gasket. The initial bolt stresses were $28–30 \times 10^3$ psi, with ~2500 ft-lb torque applied to obtain this stress.

Examination of the 10-in. IPS flange groove and gasket after the 50 thermal cycles showed that leakage of fuel solution into the oval-ring groove had occurred. A black deposit identified as uranium dioxide and ferric oxide was found in the bottom of the groove and on the curved surface of the gasket – probably resulting from oxygen depletion in the stagnant region between the inner and outer sealing surfaces. However, preliminary examination of the oval ring and groove revealed no pitting or other evidence of excessive corrosion attack.

(b) Loop O – Beryllium Solution Loop. – Loop O, designed to handle solutions of uranyl sulfate containing beryllium salts as additives, was placed in operation during the past quarter, and a beryllium-containing solution was circulated at 250°C in a preliminary run. Prior to operation with the beryllium solution, the loop shielding was tested for adequate containment of toxic material in the event of a loop failure. This was done by charging the loop with a 0.17 *m* uranyl sulfate solution, bringing the loop up to 250°C and 1000 psia (partial pressure of oxygen was approximately 400 psi), and then opening three loop valves, thus discharging the loop contents into the shield. The area immediately surrounding the loop shielding, as well as the filtered off-gas system, was monitored by Health

Physics Division personnel for escape of any uranium activity. Since no leakage of activity was observed, the shielding was considered adequate.

11.1.2 Loop Test Results

Previous reports[4] have shown that when a solution containing 0.04 *m* UO_2SO_4 and 0.005 *m* $CuSO_4$ (the concentrations proposed for use in the HRT) was circulated in a stainless steel loop at 250 and 300°C, some uranium and copper precipitated from the solution, even when as much as 0.015 *m* H_2SO_4 was added to the solution. During the past quarter, therefore, three new runs (at 200, 250, and 300°C) were initiated with 0.04 *m* UO_2SO_4–0.005 *m* $CuSO_4$, with the acid concentration increased to 0.02 *m*.

At the end of approximately 2000 hr all three runs were interrupted so that the corrosion specimens could be examined. During the first 2000 hr all solutions remained completely stable; there was no loss of uranium or copper, and the pH did not change. It thus appears that a sulfuric acid concentration of 0.02 *m* will be sufficient to ensure stability; however, all runs are being continued to verify this conclusion.

The corrosion specimens were examined in the as-removed condition and were then returned to the loop. The following qualitative observations were made:

1. All the pins that had been exposed in previous runs and that had not been defilmed gained weight. Most of these pins had been exposed to 0.04 *m* UO_2SO_4 containing 0.005 *m* $CuSO_4$ and various amounts of sulfuric acid for over 14,000 hr at velocities between 8 and 42 fps. All the previously exposed stainless steel pins retained a protective film under conditions where new stainless steel pins formed no film (e.g., 36 and 42 fps at 200°C and 34 fps at 250°C). This protection by a previously formed film has been observed and discussed before.[5]

2. New stainless steel pins exposed at flow rates lower than the critical velocities (listed in the next paragraph) corroded more during the period of film formation than in previous runs with less acid. The new pins exposed at flow rates above the critical velocity remained at least partially free of film and corroded at high rates.

3. New stainless steel coupons (exposed in these runs only) indicated critical velocities of 15 to 20 fps at 200°C, 25 to 30 fps at 250°C, and 40 to 45 fps at 300°C.

4. Titanium and zirconium alloys showed excellent corrosion resistance under all conditions. Niobium pins exposed at low flow rates at 200 and 250°C lost little weight, but one pin at 42 fps at 200°C corroded at approximately 6 mpy.

5. Stress-corrosion specimens of types 347 and 309 SCb stainless steel, titanium, and Zircaloy-2, all stressed to 75% of their room-temperature yield strength, were exposed in each run. No evidence of stress-corrosion cracking was found. These same specimens have now been exposed to dilute uranyl sulfate solutions for over 7000 hr with no evidence of cracking.

A number of corrosion specimens were exposed in loop F during the HRT bellows-flange mockup test. As a result of the manner in which the test was operated, all specimens were subjected to a daily thermal cycle between 100 and 300°C. In one case previously reported,[6] corrosion had been observed to be slightly more severe when the temperature of the system was cycled than when it remained constant. Therefore it was of interest to observe the corrosion of specimens in loop F after 1240 hr. The solution used in the test was 0.04 *m* UO_2SO_4. Materials under test included titanium and several of its alloys, Zircaloy-2, zirconium, types 347 and 309 SCb stainless steel, and Incoloy. The types of specimens were pin, coupon, coupled, and stressed specimens. While none of the specimens were defilmed at this time, the following observations were made: pin-type specimens did not appear to corrode to a greater extent than in the absence of thermal cycling. The type 347 stainless steel coupons indicated a critical velocity of 60 to 70 fps, a value substantially higher than that normally found in the absence of the temperature cycling; however, the increased critical velocity could have resulted from the pretreatment which the system received before the run with uranyl sulfate solution began. There was no visual evidence of crevice, galvanic, or stress-cracking corrosion. All specimens have been returned to the system for further testing.

[4] *Ibid.*, p 77; also, J. C. Griess *et al.*, *Quarterly Report of the Solution Corrosion Group for the Period Ending Jan. 31, 1956*, ORNL CF-56-1-167, p 24.

[5] J. C. Griess *et al.*, *HRP Quar. Prog. Rep. July 31, 1956*, ORNL-2148, p 77.

[6] J. C. Griess *et al.*, *Quarterly Report of the Solution Corrosion Group for the Period Ending Jan. 31, 1956*, ORNL CF-56-1-167, p 29.

The increase in nickel concentration in the solution during the run indicated a generalized corrosion rate of nearly 1 mpy. A similar run at 300°C without thermal cycling had a generalized rate of about 0.1 mpy. Therefore, although the corrosion specimens indicated no effect of thermal cycling, the generalized corrosion rate did indicate an increase in attack rate.

In the last quarterly report[7] the results of a study in which controlled amounts of chromium(VI) were added to 0.17 *m* UO_2SO_4 circulated in a titanium loop at 250°C were reported. During the past quarter a similar study was made at 275°C. The experimental conditions were the same as in the previous study; that is, all runs were made in a titanium loop (loop G) for 100 hr, and the oxygen concentration was 1000 to 2000 ppm. Two type 347 stainless steel pins were exposed at 10 to 12 fps and two at 68 to 70 fps.

Figure 11.3 shows the results; for comparison the data obtained previously at 250°C are also shown. The data show that the addition of chromium(VI) to 0.17 *m* UO_2SO_4 at 275°C has the same general effect as at 250°C; that is, the higher the chromium(VI) concentration, the higher the film-free corrosion rate and the lower the average corrosion rate at low velocity. However, at 275°C at the same chromium(VI) concentration the corrosion rate of the film-free stainless steel was higher and the filmed-over corrosion rate was lower than at 250°C. No more than 200 ppm chromium(VI) was added at 275°C, because the critical velocity would have been in excess of 70 fps. It thus appears that the addition of chromium(VI) has the same effect as raising the temperature and that the two effects are additive.

At the suggestion of the Chemical Technology Division, an attempt was made to descale a stainless steel loop by use of a solution containing 2 wt % phosphorous acid and 2 wt % sodium hypophosphite. The solution was circulated for 26 hr in loop D at 170°C under helium pressurization. Loop D had been exposed for over 9000 hr to various uranyl sulfate solutions at temperatures between 200 and 350°C and was heavily coated with scale.

[7] J. C. Griess *et al.*, *HRP Quar. Prog. Rep. July 31, 1956*, ORNL-2148, p 79.

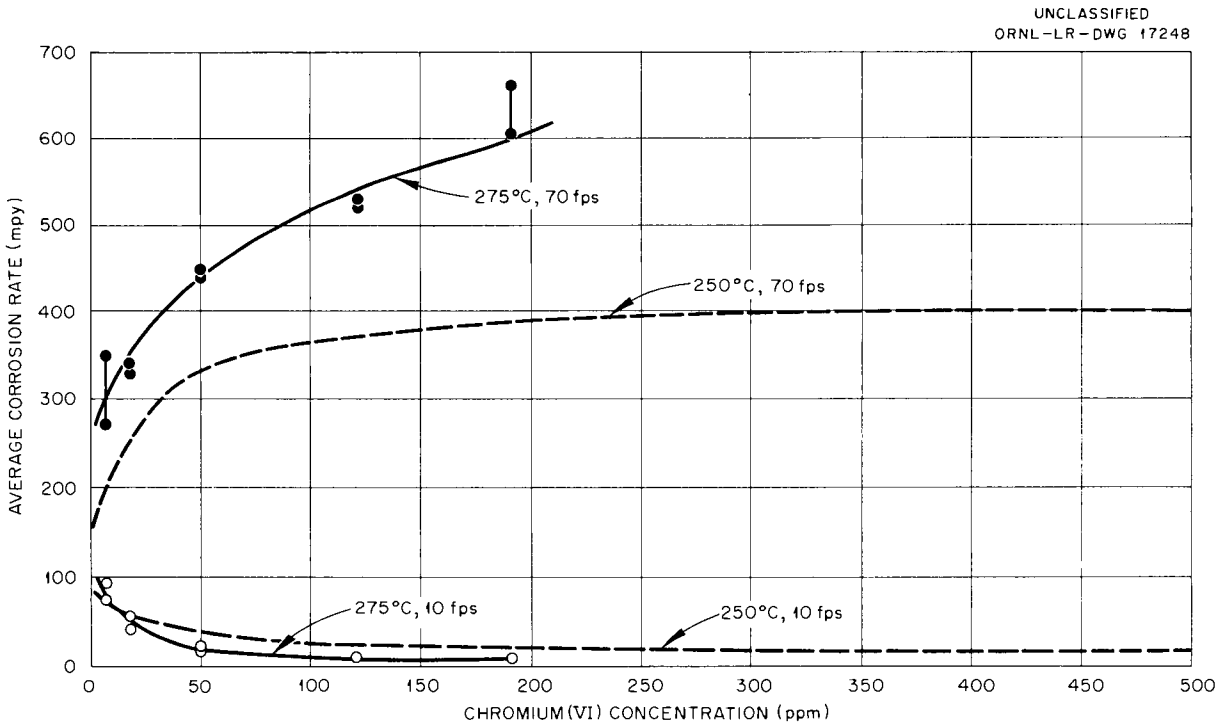

Fig. 11.3. Corrosion of Type 347 Stainless Steel Pins in 0.17 *m* UO_2SO_4 Containing Chromium(VI).

Solution samples taken during the run gave erratic results, presumably due to the insolubility of iron, nickel, and chromium phosphates. The final concentration of iron in the solution corresponded to 54 g of Fe_2O_3 dissolved, although the iron concentration after 18 hr corresponded to 96 g of Fe_2O_3 dissolved. However, visual examination of the loop after the run indicated that descaling was far from complete. All observable areas of piping were still covered with oxide scale. Also, four pins with scale on their surfaces were exposed during the run, two at 17 fps and two at 68 fps. Each pin lost some weight, but all retained most of their oxide. Hence, the phosphorous acid–sodium hypophosphite solution was not so effective a descaling solution under the test conditions as was the chromous sulfate solution employed previously.[8]

11.2 LABORATORY SERVICE CORROSION

A small-scale, steam-heated stainless steel evaporator designed for the study of stress-corrosion cracking of type 347 stainless steel in boiling uranyl sulfate solutions has been operated for a total of 10,000 hr. The exposure time represents an increase of 1870 hr since corrosion data were reported last.[9] Detailed information on the design of the evaporator experiment and preliminary corrosion data have been reported previously.[10,11]

After 7630 hr of exposure in boiling (101 to 102°C) 0.04 *m* UO_2SO_4 containing 0.005 *m* $CuSO_4$ and 0.004 *m* H_2SO_4, during which time no evidence of stress-corrosion cracking was observed, 60 ppm chloride as sodium chloride was added to the system and the test was continued. All previously exposed corrosion specimens remained in the evaporator, and, in addition, one new assembly of type 347 stainless steel was placed in the solution phase and one in the vapor phase. All assemblies were examined after 500 hr of operation with the chloride-containing solution.

All specimens which had been exposed before the addition of chloride showed no evidence of cracking or pitting and continued to corrode at about 0.1 mpy, the same rate that had been observed in the absence of chloride. The new specimen exposed to the vapor phase also showed no unusual attack. The new specimen immersed in the solution, however, showed several small cracks near the area of maximum applied stress (20,000 psi); random pitting and blistering were observed on all surfaces of the stress assembly. The generalized corrosion rate of the assembly was 3.8 mpy.

After a total of 2380 hr of operation with the chloride-containing 0.04 *m* UO_2SO_4 solution, the results were not appreciably different from those that had been obtained after 500 hr of exposure. Four large cracks were present on the new solution-exposed stress specimen of type 347 stainless steel, and numerous pits and blisters appeared on all surfaces. The generalized corrosion rate for the 2380-hr exposure was 4.1 mpy, as compared with 3.8 mpy for the first 500-hr period.

The stress assemblies that had precorroded in the chloride-free solutions showed slight weight gains at the completion of the test. No evidence of pitting or cracking could be found. The complete absence of pits or cracks on the precorroded stress assemblies suggests that the film formed on the specimens during the 7630 hr of chloride-free exposure possessed characteristics of uniformity and compactness that successfully prevented attack by chloride ions. The nature and composition of the protecting film have not been determined to date.

At the request of the Chemical Technology Division, a number of corrosion tests were carried out to find a material suitable for construction of a tank for dissolution and storage of the solids collected in the HRT hydroclone. Corrosion tests were run in 4 *M* sulfuric acid at its boiling point (109°C) and at 39°C and in boiling (157°C) 10.8 *M* sulfuric acid. In addition, some tests were made in the above solutions to which simulated corrosion and fission products had been added.

The results, to date, have shown that only tantalum has adequate corrosion resistance to boiling 10.8 *M* sulfuric acid containing substantial quantities of iron, chromium, and zirconium sulfates and lesser quantities of uranyl, copper, and ruthenium sulfates. In the absence of the added salts both zirconium and Zircaloy-2 have adequate corrosion resistance (<20 mpy), but the addition of

[8] J. C. Griess *et al.*, *HRP Quar. Prog. Rep. April 30, 1956*, ORNL-2096, p 85.

[9] J. C. Griess *et al.*, *Quarterly Report of the Solution Corrosion Group for the Period Ending Jan. 31, 1956*, ORNL CF-56-1-167, p 38.

[10] E. L. Compere and J. L. English, *HRP Quar. Prog. Rep. July 31, 1954*, ORNL-1772, p 94–95.

[11] E. L. Compere and J. L. English, *HRP Quar. Prog. Rep. July 31, 1955*, ORNL-1943, p 134–136.

the above salts increased their corrosion rates to greater than 100 mpy. Lead, Illium-R, and Hastelloy B had excessive corrosion rates, particularly in the presence of the added salts.

In boiling 4 *M* H_2SO_4 from which oxygen was excluded, tantalum, Zircaloy-2, and zirconium showed essentially no corrosion, and lead corroded at 1 mpy. Hastelloy B, Illium-R, and Carpenter 20-Cb corroded at the following average rates during the approximately 500-hr test period: 3.2, 15, and 32 mpy, respectively; all three alloys showed corrosion rates that tended to increase slightly with time. In addition, Carpenter 20-Cb showed a strong tendency toward stress-corrosion cracking in regions of localized stress. Types 347 and 316 stainless steel and Stellites 98M2 and 6 corroded at very high rates and were tested for very short periods. Graphitar-14 showed excellent resistance to the 4 *M* H_2SO_4 solution, but sintered aluminum oxide corroded at an average rate of 10 mpy.

To determine the effects of traces of ruthenium on the corrosion of Carpenter 20-Cb, Hastelloy B, and zirconium, one specimen of each alloy was exposed in boiling 4 *M* H_2SO_4 containing about 25 to 50 ppm ruthenium sulfate. The average corrosion rates for 44-hr runs were: Carpenter 20-Cb, 170 mpy; Hastelloy-B, 41 mpy; and zirconium, 1.0 mpy. In all cases the rates appeared to be decreasing, but with Hastelloy B and Carpenter 20-Cb the rates were much greater than in the absence of the trace of ruthenium.

The same alloys discussed above were also tested in boiling 4 *M* H_2SO_4 to which had been added the following salts: $Fe_2(SO_4)_2$, 75 g/liter; $Zr(SO_4)_2$, 56 g/liter; $Cr_2(SO_4)_3$, 24 g/liter; $Ru(SO_4)_2$, 0.4 g/liter; UO_2SO_4, 28 g/liter; and $CuSO_4$, 1.5 g/liter. In addition, oxygen was bubbled through the solution during the test. Carpenter 20-Cb corroded at a rate of 1.5 mpy, a rate considerably less than in the absence of the added salts. In addition, there was no evidence of stress-corrosion cracking during the 500-hr test period. On the other hand, Hastelloy B corroded at a rate of 5300 mpy, an increase of a factor of 1600 over the rate observed in the absence of the added salts. Another striking effect of the added salts was the reduction in the corrosion rates of types 347 and 316 stainless steel; in the absence of the added salts both alloys corroded at a rate of approximately 2000 mpy, but in the presence of the added salts they corroded at 5 mpy. The corrosion rates of Stellites 98M2 and 6 were reduced from 140 and 1100 mpy, respectively, in the absence of the additives to 27 and 240 mpy, respectively, in the presence of the salts. Graphitar-14, aluminum oxide, tantalum, zirconium, Zircaloy-2, and lead showed comparable rates in both environments.

The only tests completed to date in 4 *M* H_2SO_4 at 39°C have been in the absence of oxygen and added salts. Under these conditions all the above-discussed alloys except type 316 stainless steel (type 347 was not tested) and Stellite 6 corroded at rates well under 1 mpy. Stellite 6 showed localized attack and had an average corrosion rate of 12 mpy; type 316 had an average corrosion rate of 8 mpy; both rates were decreasing substantially with time.

Of the alloys tested, only tantalum showed adequate corrosion resistance to boiling 10.8 *M* H_2SO_4 containing added corrosion products. In boiling 4 *M* H_2SO_4 types 316 and 347 stainless steel and Carpenter 20-Cb had good corrosion resistance when the solution contained the added salts. However, since Carpenter 20-Cb is susceptible to stress-corrosion cracking and since types 316 and 347 showed high corrosion rates in the absence of the added salts, these materials should be tested further before their use is considered.

12. SLURRY CORROSION

E. L. Compere H. C. Savage
S. R. Buxton S. A. Reed
G. E. Moore J. A. Russell, Jr.
R. M. Pierce[1] R. M. Warner
D. B. Weaver[1]

12.1 PUMP LOOPS

12.1.1 100A Pump Loops

During the quarter five dynamic slurry corrosion tests were made in 100A pump loops BS and CS at circulating concentrations of approximately 350 to 500 g of thorium per kilogram of water.

Two tests, runs BS-5 and BS-6, were made at 250°C with the addition of oxygen and with a new lot of 800°C-calcined thorium oxide prepared at ORNL. During circulation the slurry appeared to develop essentially into fractions of two sizes. One fraction, which circulated freely, was composed of spherical agglomerates ranging in size from 7 to 20 μ in diameter, while the second fraction, composed principally of particles 2 to <1 μ in diameter, formed hard, tenacious deposits in the centrifugal pump and on the corrosion specimens and specimen holders exposed at the higher velocities.

In loop CS one test, run CS-28-29, was made at 300°C with the addition of oxygen to study the effects of the use of previously pumped slurry on particle degradation and corrosion.

A test with oxygen at 300°C, run CS-30, was made with "standard" slurry (a previously circulated material composed of spherical agglomerates ranging from 8 to 30 μ in diameter); this test was terminated after 26.3 hr of slurry operation because of deposition of thoria in the centrifugal pump and pump cavity.

The third test in loop CS was made at 300°C with slurry prepared from the new lot of ORNL-produced thorium oxide. The system was operated under a reducing atmosphere provided by the addition of about 2 atm of hydrogen. This test was terminated after approximately 83 hr of circulation because of heavy deposits of thoria in the pump scroll and impeller.

In each test slurry was added to the loops in increments while operation proceeded at the selected temperature. The 100A pumps in both systems were equipped with aluminum oxide bearings and journals.

In run BS-5, the initial slurry test in loop BS,[2] three sets of corrosion specimens were inserted in the loop. One set of pin specimens and a set of coupon specimens were placed in the main line at a flow rate of 13.5 gpm; one set of pin specimens was placed in the return line at a flow rate of 31.5 gpm. Flow through the mixing line was 18 gpm. All flow measurements were made with water at room temperature.

In accordance with usual practice, the system was operated with oxygenated water at 250°C for a period of 97 hr before slurry was added. The system was then charged, while operating at 250°C, with two batch additions of slurry prepared from batch LO-14 thorium oxide to provide a calculated circulating concentration of 500 g of thorium per kilogram of water. The thorium oxide had been made at ORNL from especially pure thorium nitrate by oxalic acid precipitation at 70°C and calcination at 800°C. Before being used to charge the loop, the slurry was passed while wet through a 200-mesh screen.

The initial slurry sample was withdrawn from the system after 4.3 hr of operation. By chemical analysis it contained 563 g of thorium per kilogram of water. A second sample, taken after 21.5 hr of circulation, contained 584 g of thorium per kilogram of water.

Immediately after the second sample was withdrawn from the system, the flow of purge water to the rear of the pump ceased and the pump power demand became very erratic. Therefore the test was terminated after a total of 21.9 hr of operation on slurry. The system was cooled to room temperature, drained, flushed thoroughly with water, and disassembled for inspection.

A thin, hard, tenacious deposit of thoria had formed in the channels of the three specimen holders and on the specimens themselves. Also,

[1]On loan from TVA.

[2]A detailed description of loop BS is given by E. L. Compere *et al.*, *HRP Dynamic Slurry Corrosion Studies: Quarter Ending April 30, 1956*, ORNL CF-56-4-139.

a wedge-shaped deposit of thoria had formed on the upstream surface of each pin specimen exposed in the return-line sample barrel.

Similar hard deposits of thoria were found adhering to the front hub of the titanium impeller, in the impeller vanes, and in the weep holes in the rear hub. A total of 28 g of thoria was removed from the impeller surface.

The suction nozzle of the centrifugal pump was also uniformly coated with a layer of thoria, the consistency of which was similar to that of dried plaster of paris. No other deposits were found in the system.

Chemical- and spectrographic-analysis data of the slurry charge, of the samples withdrawn from the system, and of the deposits showed no evidence of foreign constituents in the material, other than the expected levels of the corrosion ions, iron, chromium, and nickel. However, sedimentation particle-size data of the same materials indicated that a gradual increase in particle size had occurred during circulation. These data were confirmed by microscopic examination of the materials. While the slurry charge to the system contained only discrete crystalline particles of thoria, the samples withdrawn from the system during operation were composed of spherical opalescent agglomerates of slurry which appeared to have increased in size and number with circulation time. The agglomerates ranged from about 7 to 20 μ in diameter.

No agglomerates could be detected in the deposits. Sedimentation particle-size data showed them to be composed primarily of particles ranging from 2 to <1 μ in diameter. Photographs of the materials are shown in Figs. 12.1 to 12.3.

Run BS-6 was essentially a continuation of run BS-5. After the system was reassembled and a short performance run was made on oxygenated water, the slurry drained from run BS-5, which contained 6694 g of thorium oxide, and an additional 2035 g of raw thorium oxide from the same batch, LO-14, were charged to the system to provide a calculated concentration of 530 g of thorium per kilogram of water. A sample taken from the loop 2 hr after the addition of thoria contained 565 g of thorium per kilogram of water.

After 10 hr of operation with slurry, the pump power demand increased rapidly and a pulsating noise was noted in the pump. Therefore the run was terminated after 11.1 hr of slurry circulation.

Inspection of the system after it was drained and was rinsed with water revealed deposits almost identical with and in the same locations as those described previously for run BS-5. Although chemical-analytical data are incomplete, preliminary information indicates that the circulating sample was composed of spherical bodies of slurry, whereas the deposits again consisted of very fine material.

Pin specimens exposed for a total of 33 hr in the combined runs showed relatively high attack rates; for example, at 19 fps the austenitic stainless steels corroded at rates of from 5 to 28 mpy; platinum, 24 mpy; titanium and its alloys, 0 to 16 mpy; and Zircaloy-2, 8 mpy. Attack rates of coupon specimens exposed at a relative velocity of 11 fps were the following: austenitic stainless steels, 2 to 5 mpy; welded austenitic stainless steel, 12 mpy; Armco iron, 120 to 280 mpy.

Run CS-28-29 was made to observe the effects of the use of previously circulated slurry on particle-size degradation and corrosion. The slurry charge, prepared from batch LO-2 thorium oxide, had been circulated previously in loop CS for approximately 300 hr.

Corrosion data obtained in loop CS with slurry prepared from batch LO-2 thorium oxide have been reported previously.[3] In these tests, however, raw slurry with no previous pumping history was used to charge the loop. In each test considerable degradation of the thoria particles had occurred during the first 10 to 30 hr of circulation, after which time thoria of an average particle size of about 0.6 μ was being circulated. Differential corrosion rates determined for various periods of a nominal 200- to 300-hr test have shown the highest rates of attack to occur during this period of particle attrition, with a gradual leveling off thereafter. Therefore it was of interest to obtain attack rates at the same conditions but with the use of slurry which had been previously circulated.

The three loop barrels contained pin-type corrosion specimens exposed to the slurry at relative velocities of 13, 22, and 43 fps. The system was charged with four batch additions of pumped slurry while operating at 300° C on oxygenated water.

The system was temporarily shut down 73 hr after the initial slurry addition because of erratic

[3] E. L. Compere *et al.*, *HRP Quar. Prog. Rep. July 31, 1956*, ORNL-2148, p 83.

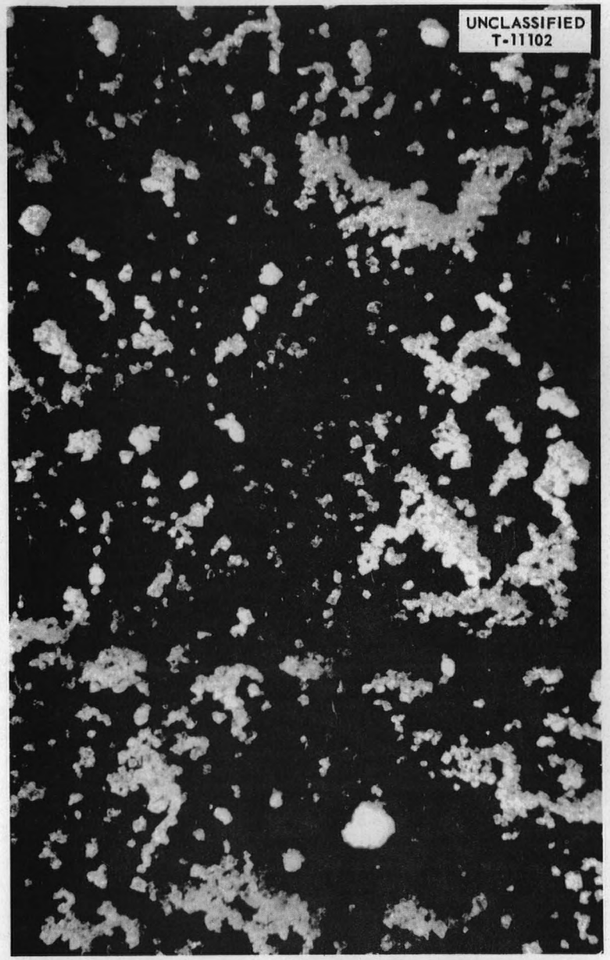

Fig. 12.1. Original Slurry Charge for Run BS-5. 400X.

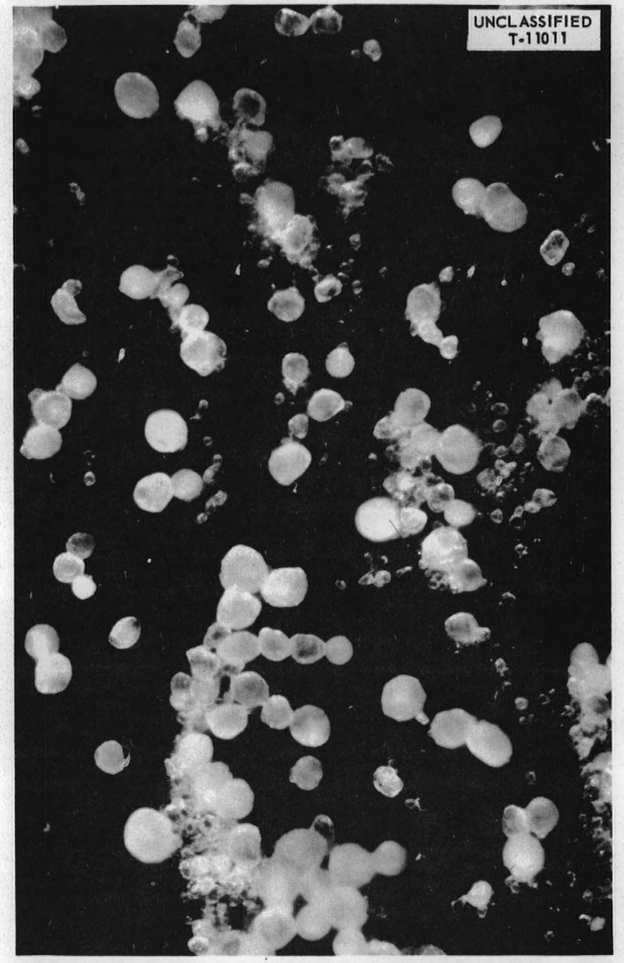

Fig. 12.2. Agglomerates of Slurry Formed After 21.5 hr of Circulation in Run BS-5. 400X.

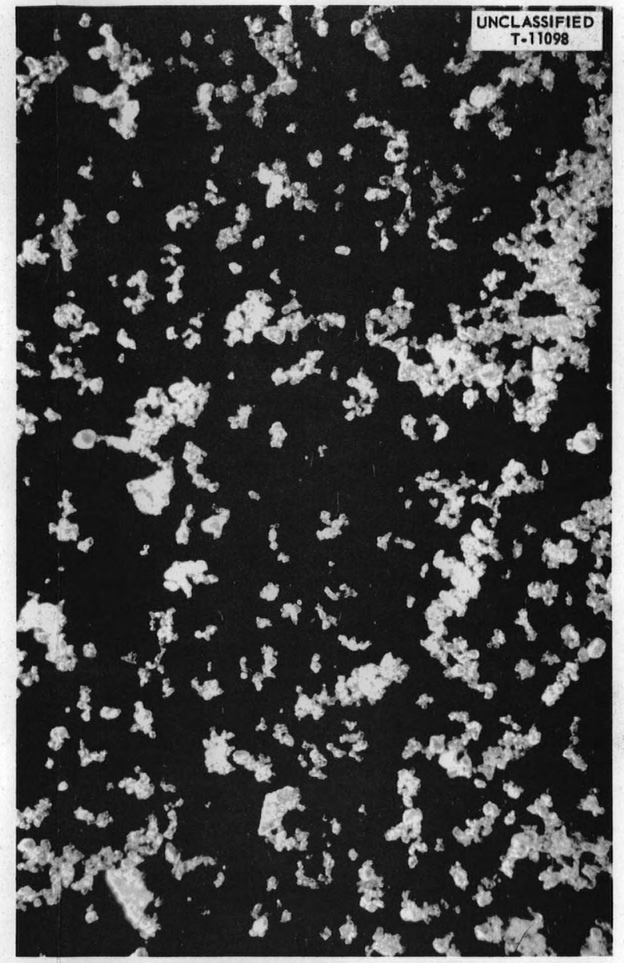

Fig. 12.3. Thoria Deposit Removed from Pump Impeller After Run BS-5. Slurry circulated for 21.5 hr. 400X.

pump performance. After the pump was repaired, the test was resumed. Slurry was again charged to the system while operating on oxygenated water at 300°C, and the test loop was operated routinely for an additional 192 hr. At run hour 264, one of the high-pressure sample valves on the system could not be secured satisfactorily. Consequently, it was necessary to terminate the run. Slurry had been circulated in the system for a total of 266 hr (for both run CS-28 and -29) at shutdown. Corrosion rates are shown in Table 12.1.

The slurry charge for run CS-30 had also been circulated in a loop system. The material was prepared by the Engineering Research Section as an experimental "standard" slurry by circulating an ORNL-produced, 800°C-calcined oxide at 200°C for a period of 100 hr in a 200A pump loop. The slurry was of an unusual character in that it was composed of spherical agglomerates ranging from approximately 8 to 30 μ in diameter. The detailed preparation of the material is outlined in ORNL CF-56-10-8.

It was thought to be of interest to compare the corrosion characteristics of this material at 300°C with those of other slurries which had been previously pumped in loop CS. Three sets of pin-type corrosion specimens were exposed during the test at flows, measured on water at room temperature, of 6, 14, and 24 gpm (10, 24, and 40 fps, respectively). Flow through the loop mixing line was 11 gpm.

The loop was charged initially, at room temperature, with 16.6 liters of supernatant liquid from the standard slurry and 120 psig of oxygen. Thoria was to be charged to the system as a concentrated slurry, containing approximately 1100 g of thorium per kilogram of water, in two batch additions while operating at 300°C. A total of 9850 g of thorium oxide was required to provide a calculated circulating concentration of 500 g of thorium per kilogram of water.

Both additions were made with difficulty. Ten hours was required to charge the first portion of slurry, which contained about 7400 g of thoria. The normal charging schedule for such additions is 2 hr. The ¼-in. tubing which connected the addition tank to the loop plugged repeatedly. Flow through the line could be maintained only by using a Pulsafeeder and by frequent back-washing of the line with liquid from the loop.

A Pulsafeeder was used continuously while making the second addition; however, the ¼-in. line and high-pressure valve soon became plugged. An attempt was made to complete the addition through a sample valve on the system, but the valve and associated tubing also were plugged. Consequently, a total of only 7800 g of thorium oxide was charged to the system.

Twenty-six hours after the initial addition of slurry the flow of purge water to the rear of the pump stopped. Coincident with this the pump power demand became extremely erratic and actuated the pump override automatic control, which shut down the system. Total operation with slurry in the system was for 26.3 hr.

After the system was drained and was thoroughly flushed with water, hard, tenacious deposits of thoria were found on both outer impeller surfaces and in the impeller suction and vanes. Similar material had been deposited around the weld pads on the pump head and on the thermal barrier. Photographs of deposits are shown in Figs. 12.4 and 12.5. A softer deposit had filled the weep holes in the impeller.

The header to the No. 4 sample barrel contained a heavy deposit of pasty solids. The annulus between the header and the specimen holder was partially filled with a sticky deposit of slurry, and porous plugs of thoria had formed over both ends of the specimen holder. Flow through this section of the system was approximately 24 gpm. Chemical and particle-size data are not yet available for the deposits.

Corrosion data calculated from weight losses of the pin specimens exposed during the test are of questionable value, since the blockage in the No. 4 sample barrel would undoubtedly change the flow characteristics in the entire loop system. The rates were unusually high, however; for example, at 10 fps, rates for the austenitic stainless steels ranged from 7 to 14 mpy.

Run CS-31 was made in order to study the attack by aqueous thoria slurry under reducing rather than oxidizing conditions. Heretofore all dynamic slurry corrosion tests made in loops BS and CS were made under oxidizing conditions (oxygen concentration of ~500 to 1000 ppm).

The loop was charged at room temperature with 17.3 liters of water and then purged for approximately 30 min with argon gas to remove air from the system. After purging, 10 ml of 85% hydrazine hydrate for removal of trace oxygen (estimated

TABLE 12.1. COMPARATIVE CORROSION RATES AT 300°C

	Run CS-25 (ThO_2 Batch LO-2)			Run CS-27 (ThO_2 Batch LO-2)			Run CS-28-29 (ThO_2 Batch LO-2)			Run CS-31 (ThO_2 Batch LO-14)		
	Corrosion Rate, mpy											
	11 fps	21 fps	41 fps	10 fps	22 fps	41 fps	13 fps	22 fps	43 fps	13 fps	25 fps	41 fps
Austenitic SS	2–4	5–9	18–23	1	2–4	6–9	0.5	0.5	2–4	1–2	4–6	10–12
Gold	0.4	0.4	4	0.1	0.1	0.6	0.03	0.08	0.90	0.1	1	2
Titanium and alloys	1	3–5	7–11	0.2	2	6	0.1	1.0	4–5	2	4	3–6
Zircaloy-2	0.1	1	6	0.1	0.1	2	<0.1	<0.1	1	<0.3	4	13
Mild steel	150	165	205	11	13	24	21	21	21	40	42	48
Average loop corrosion rate, mpy		4.5			1.5			0.8				
Duration of test, hr		49			301			266			83	
Average circulating concentration (g of Th per kg of H_2O)		543			348			346			409	
pH of slurry		6.5			7			7			9.5	
Additive		O_2 (~1000 ppm)			O_2 (~1000 ppm)			O_2 (~1000 ppm)			H_2 (~15 ppm) N_2H_4 (420 ppm)	
	Average Sedimentation Particle Size, wt %											
Approximate Circulation Time (hr)	>3 μ	1–3 μ	<1 μ	>3 μ	1–3 μ	<1 μ	>3 μ	1–3 μ	<1 μ			
0	48	27	25	59	26	15	3	32	65	Sedimentation particle size not available; microscopic examination revealed formation of spheroid agglomerates of approximately 6- to 20-μ diameter formed during circulation		
5	8	25	67									
20	7	20	73	7	26	67						
30	5	21	74	7	25	69	7	28	65			
50	2	30	67	7	17	76	2	22	76			
150				8	36	56	7	42	51			
200				5	26	69						
300				3	32	65	2	21	77			

Fig. 12.4. Thoria Deposits on Titanium Pump Impeller After Run CS-30. Standard slurry, 300°C, 26 hr.

Fig. 12.5. Thoria Deposits on Pump Thermal Barrier After Run CS-30. Standard slurry, 300°C, 26 hr.

20-fold in excess of requirement) and 30 psi hydrogen were injected into the system. The loop was heated to 300°C and operated for a period of 74 hr before slurry was added. A sample withdrawn from the system during this period contained, by chemical analysis, <1 ppm oxygen and 24 ppm hydrogen.

Two batch additions of slurry were charged to the system to obtain a calculated circulating concentration of 500 g of thorium per kilogram of water. Batch LO-14 thorium oxide was used. Five milliliters of 85% hydrazine hydrate was added to each slurry charge. After 26.7 hr of operation with slurry in the system, the sampled concentration was 509 g of thorium per kilogram of water.

At run hour 46 the pressure drop to the back of the pump had changed, and the flow of purge water to the pump bearings stopped. Flow was reestablished by employing a Pulsafeeder, which was used for the duration of the run. Pump operation became quite erratic.

After slurry was circulated for a period of 70 hr, the sampled concentration of the loop had decreased to 344 g of thorium per kilogram of water. A third addition of slurry was made at that time in an attempt to increase the circulating concentration to the original level. System operation was very unstable after the addition, and the pump power demand increased rapidly. Consequently, the run was terminated after 82.9 hr of slurry circulation.

Final disassembly and inspection of the system are not complete. In a preliminary examination of the pump, heavy deposits of hard thoria were observed on the pump scroll and thermal barrier. Similar material was found in the impeller vanes and on the impeller surface adjacent to the front hub. Portions of the hard deposits, which had apparently been dislodged from the pump cavity, were located throughout the loop piping. A photograph of the pump thermal barrier and impeller is shown in Fig. 12.6. In general, the deposits were gray,

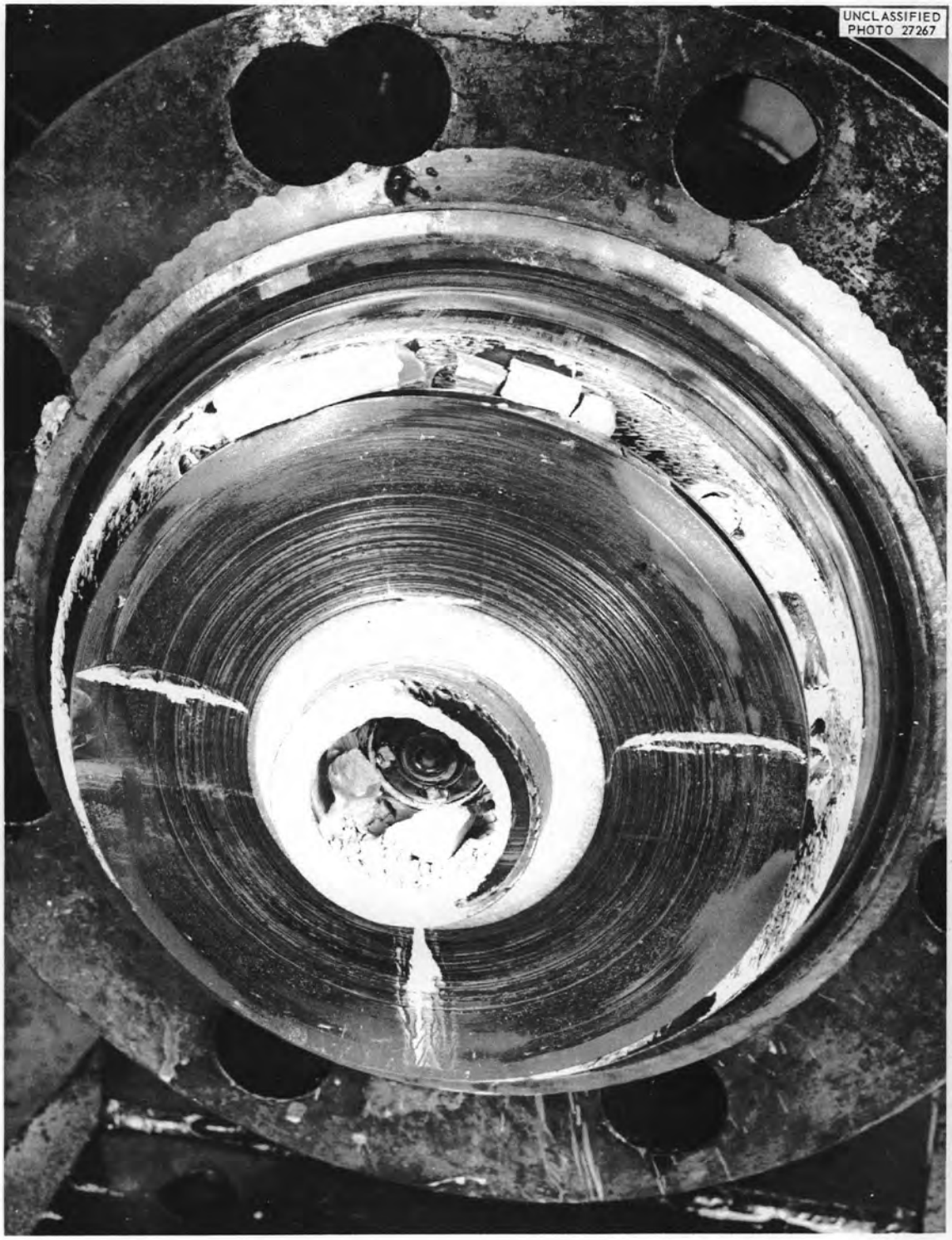

Fig. 12.6. View of 100A Pump Impeller and Thermal Barrier After Run CS-31. LO-14 slurry, 300°C, H_2, 83 hr.

appeared to be very dense, and were difficult to remove from the metal surfaces.

Average corrosion rates during the 83-hr test are shown in Table 12.1. It is interesting to note that attack on the mild-steel specimens exposed in run CS-31, as well as those exposed in the previous tests using oxygenated slurry, appears to be relatively insensitive to slurry velocity. Furthermore, if the data are normalized, by taking the product of the run time and corrosion rate, the attack on mild steel appears to diminish with increasing pH and in the presence of a reducing atmosphere. Additional tests will be made in order to study these factors.

The effect of particle degradation on the attack of materials by previously circulated slurry is shown in Table 12.1. Comparative data are presented which show the average attack rates and particle degradation in run CS-28-29, along with those observed in two previous runs, CS-25 and CS-27,[4] made under similar conditions.

Average attack rates in run CS-28-29 were, with the exception of the mild steel, about 50% lower than those observed in run CS-27, in which raw slurry was used. Also, in run CS-27, degradation of thoria particles took place during the first 20 to 30 hr of circulation; in run CS-28-29, particle-size distribution remained essentially unchanged.

The effect of particle degradation is also strongly borne out in comparing corrosion rates in run CS-25, a 49-hr test, with those in run CS-27, a 300-hr test. The rates are generally about half as great in run CS-27, indicating that both highest corrosion rates and greatest particle degradation are associated with the early hours of the runs.

There is no clear explanation for the absence of a velocity effect on mild-steel specimens exposed in run CS-28-29. The data suggest, however, that the attack was mainly chemical in nature and at a sufficiently high rate to preclude any effect from the abrasive action of the slurry particles, but the data also indicate that corrosion rates for this material become substantially lower as the run durations are increased.

[4]Summaries of runs CS-25 and CS-27 are given by S. A. Reed *et al.*, *HRP Dynamic Slurry Corrosion Studies: Summary of Runs CS-24W and CS-25*, ORNL CF-56-8-88 (Aug. 10, 1956); S. A. Reed *et al.*, *HRP Dynamic Corrosion Studies: Summary of Runs CS-26W and CS-27*, ORNL CF-56-8-89 (Aug. 21, 1956).

12.1.2 In-Pile Slurry Loop Development

Several short-term slurry runs were made in the experimental in-pile slurry loop during the past quarter. One objective of these runs was to evaluate the performance of the revised slurry-addition tank. Satisfactory operation of the addition system was demonstrated by two successful additions of thorium oxide slurry to the loop during loop operation at approximately 250°C and 600 psia. Briefly, this was accomplished by adding thorium oxide slurry to the tank, which was isolated from the loop; the tank was then opened to the loop, and the slurry in the tank was flushed into the loop and replaced by clean water condensate from the condensate system incorporated in the loop system. In both additions all the slurry in the tank was transferred to the loop circulating stream.

In the several runs made with thorium oxide slurry, difficulty was encountered in maintaining the calculated theoretical thorium concentration in the loop circulating stream. In two cases, partial plugging of the loop piping was also observed shortly after the thorium oxide was added. In one instance plugging did not occur, but the thorium concentration was lost. In this run sodium silicate was used as a dispersion agent. No improvement was noted when the system flow rate was increased from ~3.4 to ~4.9 gpm, based on water calibration.

12.2 TOROIDS

Attention has continued to be directed at three variables which are believed to affect considerably the behavior of thorium oxide slurries. These variables are the maximum temperature of calcination of the thorium oxide, the size of the thorium oxide particle in its environment, and the solution in which the oxide particle is immersed. These variables are not independent in their effects but are so closely related that it is often difficult to study any one of them independently of the others.

Some studies of the attack rate of certain metals by thorium oxide slurries circulated in toroids have been completed and reported; in these studies an attempt was made to correlate the rate of attack with the calcination temperature of the oxide,[5]

[5]E. L. Compere *et al.*, *Dynamic Slurry Corrosion Studies: Quarter Ending January 31, 1956*, ORNL CF-56-1-168, p 33.

the size of the oxide particle,[6] or, in certain cases, the presence of phosphate ions in the aqueous slurry system.[6] Certain phases of these studies have now been investigated further.

12.2.1 Particle-Size Degradation

Examination of certain of the data obtained in toroids has suggested a correlation between the maximum calcination temperature of the thorium oxide and its degradation during circulation, as well as a possible correlation between some slurry properties and the ultimate size of the oxide particle after circulation. Earlier studies[7] had indicated that a smaller ultimate size of thorium oxide was obtained as the maximum calcination temperature decreased and as the velocity of circulation increased.

Because the thorium oxide particles constituting an aqueous thorium oxide slurry often became degraded upon circulation,[7,8] it was difficult[6] to evaluate the effect of the particle size upon attack of materials. However, an interesting dependence of the degree of particle degradation upon the maximum calcination temperature of the thorium oxide and on its original size was observed during the course of this investigation in toroids. The changes in size of thorium oxide particles during circulation in toroids as aqueous slurries at a concentration of 1000 g of thorium per kilogram of water, 26 fps relative velocity, 250°C, and under an oxygen atmosphere were considered. The oxide used was produced by the Chemical Technology Division by the thermal decomposition of thorium oxalate; certain of these oxides were then recalcined and were sized by gravitational sedimentation[6] or had been circulated in loop CS prior to use. Thus data were obtained under the above-described conditions for thorium oxides of maximum calcination temperature from 650 to 1600°C and of average original particle diameters from about 0.3 to 5.1 μ. Particle-size distributions were obtained by gravitational sedimentation in 0.001 *M* $Na_4P_2O_7$ by using the neutron-activation technique.[9]

[6] E. L. Compere *et al.*, *HRP Dynamic Slurry Corrosion Studies: Quarter Ending July 31, 1956*, ORNL CF-56-7-51.

[7] E. L. Compere *et al.*, *HRP Dynamic Slurry Corrosion Studies: Quarter Ending April 30, 1956*, ORNL CF-56-4-139, p 16.

[8] C. E. Schilling, *HRP Quar. Prog. Rep. Oct. 31, 1955*, ORNL-2004, p 179.

[9] G. W. Leddicotte and H. H. Miller, *Anal. Chem. Semi-ann. Prog. Rep. Oct. 20, 1954*, ORNL-1788, p 21.

The size distribution of the thorium oxide was also determined after circulation times between 174 and 475 hr (85% of the runs for 238 ± 44 hr) in toroids under the described conditions. The results are illustrated in Fig. 12.7, in which the original average particle diameter is plotted against the average particle diameter after circulation at 26 fps relative velocity, 250°C, 1000 g of thorium per kilogram of water, and under an oxygen atmosphere. By choosing the same units for both coordinates, points lying on or very near the 45-deg line represent slurries whose particle size had not detectably altered during circulation. Points lying below the 45-deg line represent slurries whose particles had become degraded during circulation. Since a growth of particles was never observed in these tests, no points are found significantly above the 45-deg line. The maximum temperatures of calcination of the thorium oxide and the times of recalcination at 1400°C are represented by appropriate symbols on the figure.

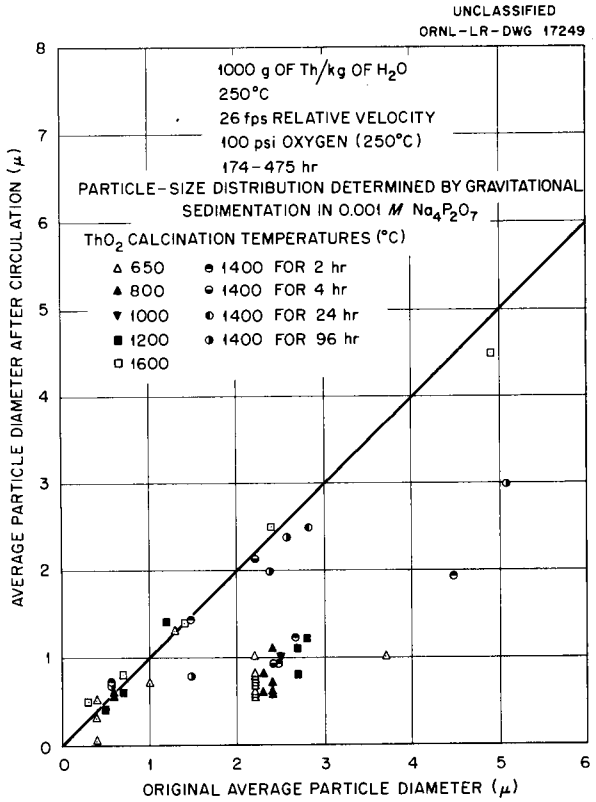

Fig. 12.7. Extent of Degradation of Thorium Oxide Upon Circulation of Aqueous Slurries in Toroids.

Certain generalizations are apparent from the graph. Particles about 1.3 μ or smaller in original diameter appeared not to degrade appreciably during circulation; this lack of degradation applied to all oxides calcined from 650 to 1600°C. However, degradation of particles having original diameters greater than about 1.3 μ appeared to be dependent upon the maximum temperature of calcination; it was also somewhat dependent upon the length of time at maximum temperature, as illustrated in the experiments in which the time of recalcination (at 1400°C) was studied. In no case did the oxide that was recalcined at 1600°C for 4 hr appear to degrade upon circulation (within the limits of determination of the particle-size distribution). Thus even 475 hr of circulation did not alter the size of the 1600°C oxide, whereas only 41 hr of circulation was sufficient to decrease the size of an 800°C oxide from an original diameter of 2.4 μ to an ultimate size of 0.9 to 1.0 μ.

In general, oxides recalcined up to 1200°C (7 hr) were degraded upon circulation when their original particle diameter was larger than approximately 1.3 μ. The ultimate size after circulation was then approximately 0.6 to 1.2 μ. In contrast, oxides recalcined at 1400°C for at least 4 hr or at 1600°C generally showed greater resistance to degradation.

During the course of these experiments a definite trend in properties of the circulated slurries was noted which was correlated with the final size of the thorium oxide particle. Table 12.2 summarizes the data accumulated during circulation of 48 different slurries. It is realized, of course, that this particular correlation exists only for the system described; changes in the system (for example, the introduction of a dispersing additive) would most likely alter the behavior of the slurry.

Although the behavior of a particular slurry system is, apparently, governed by the combination of many factors, it becomes evident that the particle size of the thorium oxide and its changes during circulation contribute strongly to the particular properties observed. In addition, the maximum calcination temperature of the oxide becomes important either directly (through changes in the surface area and/or structure of the oxide) or indirectly (through its influence on the particle behavior during circulation).

12.2.2 Dispersing Additives

The addition of electrolytes to aqueous thorium oxide slurries appears attractive for at least two reasons:

1. Often a more fluid (deflocculated) slurry results.
2. By the proper choice of additives a system may be realized that is more resistant to changes in the operating conditions of the system; desirable stability might thus be imparted to the system.

On the other hand, there are advantages to the use of a flocculated slurry; the relative merits of both systems have been discussed from engineering considerations.[10] In any event, the attractiveness

[10] D. G. Thomas, *The Relationship of Slurry Physical Properties to the Engineering Characteristics of a Slurry System*, ORNL CF-56-5-69 (May 11, 1956).

TABLE 12.2. CORRELATION OF PROPERTIES OF CIRCULATED THORIUM OXIDE SLURRIES WITH ULTIMATE PARTICLE SIZE

Circulation conditions: 1000 g of thorium per kilogram of water
26 fps relative velocity
250°C
100 psi oxygen
Type 347 stainless steel toroids

Average Diameter After Circulation (μ)	Relative Slurry Character After Circulation		
	Fe:Th Ratio (mg/g·day)	Thickness	Settling Rate
4.5–2.0	0.3–1.5 (av 0.9)	Thin	Fast
1.9–1.2	0.2–1.2 (av 0.6)	Thin to moderately thick	Slow to fast
1.1–0.1	0.0–1.1 (av 0.3)	Thick	Slow

of dispersing additives warrants careful investigation.

Previous investigations[6] in toroids with circulating thorium oxide slurries have shown that titanium can be severely attacked by both neutral and alkaline phosphate buffer solutions at 250°C under either oxygen or hydrogen atmospheres. Because the attack was dependent upon the concentration of phosphate, further investigations were carried out at phosphate concentrations believed to be low enough not to affect adversely the titanium and yet sufficient to influence the behavior of a thorium oxide slurry at a concentration of 1000 g of thorium per kilogram of water. This concentration appeared to be about 0.02 *M* phosphate.

In collecting data on phosphate systems at this concentration level, studies of 0.01 *M* Na_2SiO_3 were included, since this salt has also shown interesting dispersive effects on thorium oxide slurries.[11] Both hydrogen and oxygen atmospheres were used in an effort to determine the influence of this variable on the attack of type 347 stainless steel, A-212 carbon steel, titanium 75A, and Zircaloy-2. Each combination of electrolyte and atmosphere was studied at a slurry concentration of 1000 g of thorium per kilogram of water, 250°C, and 26 fps relative velocity for 330 hr. A previously pumped thorium oxide (CS-21) was used in order that the oxide might possess a relatively small, stable particle size from the very beginning of the circulation.

Table 12.3 summarizes the results of this investigation. Certain discrepancies are obvious

[11] D. G. Thomas, J. D. Perret, and R. Buxton, *HRP Quar. Prog. Rep. Oct. 31, 1954*, ORNL-1813, p 125; D. E. Ferguson *et al.*, *loc. cit.*, p 145.

TABLE 12.3. EFFECT OF VARIOUS ADDITIVES UNDER OXYGEN OR HYDROGEN ATMOSPHERES ON THE ATTACK BY AQUEOUS THORIUM OXIDE SLURRIES CIRCULATING IN TOROIDS

Conditions: 1000 g of thorium per kilogram of H_2O (CS-21 ThO_2)
250°C
26 fps relative velocity
330 hr

Additive	Atmosphere	Molarity	Slurry pH		Attack Rate (mpy)[a]				Final Slurry		
			Initial	Final	347 SS	A-212	Ti	Zr-2	Settling Rate	Resuspension	Character
NaOH	O_2		11	7.6	6	5[b]	6		Slow[c]	Difficult	Thick
			10	7.0	4	5[b]	7	0		Easy	Thin
NaOH	H_2		11	9.5	17[d]	4	4		Slow	Easy	Thick
			10	8.1	20[d]	4	8		Slow	Easy	Thick
				8.8	18[d]	11	8		Slow	Easy	Thick
$Na_4P_2O_7$	O_2	0.01	11	7.3	4	4[b]	5	0	Dispersed	Difficult	Thin
	H_2			9.8	9[d]	6	3	0	Slow		Thin
Na_2HPO_4	O_2	0.01	10	6.7	3	4[b]	2	0	Dispersed	Difficult	Thin
$+ NaH_2PO_4$	H_2			9.2	17[d]	6	3	0	Dispersed	Easy	Thin
Na_2SiO_3	O_2	0.01	10	6.7	7	8[b]	20[d]	0	Dispersed	Easy	Thin
Na_2SiO_3[e]	H_2	0.01	10		(6)	(6)	(4)	(0)			Thick

[a] Calculated on basis of uniform general corrosion of pins.

[b] Localized pitting was observed.

[c] A "slow" rate indicates a flocculated system in compaction settling. The notation "dispersed" indicates that after at least 16 hr of undistrubed settling at room temperature, although some solids may have accumulated by settling, much solid remained dispersed throughout the aqueous phase.

[d] Severe localized attack was present.

[e] Since there is some evidence that a leak occurred during this experiment, the reported results may not be valid; the values are therefore enclosed in parentheses.

from the table and require reinvestigation; nevertheless, certain conclusions do seem to be valid. Type 347 stainless steel appeared to be severely attacked in the presence of hydrogen; although the generalized rate (assuming uniform attack) gave values from about 10 to 20 mpy, the attack was quite localized in that a severe attack occurred near the root of the pin. Therefore the true attack rate was probably more of the order of 50 to 200 mpy. The attack of the type 347 stainless steel toroid itself was also greater in these cases (2 to 4 mpy) than is normally found (1 mpy and less).

The presence of a hydrogen rather than an oxygen atmosphere seemed to improve the appearance of the A-212 carbon steel exposed to circulating aqueous slurries. Attack rates of about 5 to 10 mpy were observed on the carbon steel under hydrogen; the attack appeared to be uniform and did not change in character or magnitude in the presence of the additives used in these experiments. Although the generalized attack rates of A-212 carbon steel in the presence of oxygen were little different from those in the presence of hydrogen, when oxygen was used an intensified etch or very localized pitting attack was observed both in the absence and presence of the added electrolytes.

In the absence of additives the attack of titanium was slightly greater, based on microscopic examination of the pins, when hydrogen was used as the blanket gas than when oxygen was used; weight-loss data gave approximately the same rate of attack in the presence of both gases. As predicted, the concentration levels of 0.01 *M* $Na_4P_2O_7$ or of 0.01 *M* NaH_2PO_4 plus 0.01 *M* Na_2HPO_4 were low enough so that no enhanced attack on titanium was found when these electrolytes were used. However, somewhat severe attack of titanium occurred in the slurry system which contained 0.01 *M* Na_2SiO_3 and oxygen. The results in the corresponding experiment with hydrogen used in place of oxygen are probably invalid since there was some evidence of a leak in the system during circulation.

In all the experiments Zircaloy-2 showed negligible attack, both from weight-loss data and from microscopic examination of the corrosion pins.

The original slurries of 1000 g of thorium per kilogram of water adjusted to pH 10 to 11 with sodium hydroxide were quite thick in contrast to those slurries of the same concentration containing 0.02 *M* phosphate or 0.01 *M* silicate; the latter slurries were quite thin and fluid. Circulation did not appear qualitatively to alter this property of the slurry.

12.2.3 Toroid Examination

During the past two years 12 type 347 stainless steel toroids have been used to circulate thorium oxide slurries. Although these toroids were giving satisfactory service, they have been removed from service and replaced with entirely new units for use in future studies because of considerable mechanical wear on the Parker fittings, through which corrosion pin specimens are inserted. It was considered desirable to replace the toroids at a convenient time rather than to experience unscheduled shutdowns or loss of experimental data as a result of leaks at the mechanical closures.

Several of the replaced toroids, each of which has circulated thorium oxide slurries under a wide range of conditions for from about 4000 to 5000 hr, have been sectioned for examination. Preliminary examination has revealed only slight attack of the toroid walls, with certain areas of much greater metal loss.

Figures 12.8 and 12.9 are photographs of the inside surface of the outer wall of a type 347 stainless steel toroid after 4909 hr of circulation of aqueous thorium oxide slurries; approximately 4100 hr was at 250 or 300°C, 26 fps relative velocity, 1000 g of thorium per kilogram of water, and with oxygen atmospheres. These photographs

UNCLASSIFIED
T-11154

(*a*) DOWNSTREAM

Fig. 12.8. Inner Surface of Outside Half of Type 347 Stainless Steel Toroid After Exposure to Circulating Aqueous Thorium Oxide Slurries for Approximately 4900 hr (Downstream from Weld).

(*b*) UPSTREAM

Fig. 12.9. Inner Surface of Outside Half of Type 347 Stainless Steel Toroid After Exposure to Circulating Aqueous Thorium Oxide Slurries for Approximately 4900 hr (Upstream from Weld).

overlap the area of the circumferential weld of the toroid and include the areas adjacent to two ports through which the corrosion pin specimens were introduced; the combined photographs thus show a little over one-quarter of the area of the outer half of the pipe. The direction of circulation in the toroid was from right to left. The areas immediately downstream from protuberances (corrosion pins and welds) showed bright, shiny, polished bare metal, whereas areas immediately upstream from these points were covered with a thin, dark, (presumably) metal oxide film. The inner half of the pipe, however, was generally covered with a dark, apparently thin metal oxide film. The only areas of bare metal on the inner half were immediately opposite the holes through which the corrosion pin specimens had been introduced. When the opening was used as a thermocouple well and no pin had ever been present, the area opposite the port was covered with the dark, thin film.

On the basis of the photographs and the descriptions just given, it is apparent that areas near protuberances, which are likely sources of turbulence, are relatively free of film and are apparently subjected to a very mild polishing action by the slurry. However, areas immediately adjacent to such protuberances (as near the corrosion pin entrances) or the protuberances themselves (welds and often pin specimens) showed relatively greater metal loss than other areas. This is particularly apparent in Fig. 12.9 at the pin port; the circumferential weld was also attacked much more than other areas, although this is not clearly shown in the photograph.

A more quantitative assay of the damage may be obtained when the metallographic examination of parts has been completed. The source or cause of the small striae and the small comet-shaped depressions in the outer walls of the toroids (Figs. 12.8 and 12.9) will also be pursued during further metallurgical examination.

12.2.4 Circulation of "Standard" Slurry

A number of experiments in toroids have been carried out in an attempt to learn the behavior and fate of the oxide particles of standard slurry[12,13] during circulation under a variety of conditions of temperature, velocity, and slurry concentration. In general three techniques have been employed to evaluate the slurry character after such circulations:

1. determination of particle-size distribution by gravitational sedimentation[9] in 0.001 *M* $Na_4P_2O_7$ using the neutron-activation technique or a higher viscosity medium of glycerol-water and 0.005 *M* $Na_4P_2O_7$,
2. optical photography of the slurry of 400-dia magnification,[14]
3. measurement of the rate of subsidence of the thorium oxide particles either in their supernatant liquid after circulation or in pure water.

Of these methods the optical photographs were perhaps the most revealing, for this was the only one of the three techniques which disclosed the shape or character of the individual oxide particle. The chief disadvantage of the method was the difficulty of locating a microscopic field representative of the entire sample.

Table 12.4 summarizes the toroid runs which have been completed in the study of the standard slurry, while the photographs in Figs. 12.10 through 12.16 record the character of the thorium oxide particles at appropriate points during the investigation.

Figure 12.10 is a photograph of the LO-12 thorium oxide used to charge the 200A loop, while Fig. 12.11 is a photograph of the standard slurry.

[12] R. B. Gallaher and A. S. Kitzes, *Production of Standard Oxide*, ORNL CF-56-10-8 (Oct. 3, 1956).

[13] R. B. Korsmeyer, *Standard Thorium Oxide Slurry*, Letter to Slurry Program Committee, June 1, 1956.

[14] The optical photography was performed by R. S. Crouse of the Y-12 Metallography Section of the ORNL Metallurgy Division.

TABLE 12.4. RESULTS OF CIRCULATION OF 200A STANDARD SLURRY IN TYPE 347 STAINLESS STEEL TOROIDS UNDER OXYGEN

Relative Velocity (fps)	Temperature (°C)	Circulation (hr)	Slurry	Concentration (g of Th per kg of H_2O)	Attack Rates[a] (mpy)			Final Supernatant pH[b]	Average Particle Diameter[c] (μ)		Figure (Photograph) Reference
					347 SS	Ti-75A	Zr-2		Before	After	
10	200	97	LO-12	500	2,5	0	0	7.9	3.3	1.4	12.12
			Standard	500	2,6	+	1	7.3	9	19–26	
				1000	2	+	0	7.4	9	24–27	12.13
				1500	1,1	0	2	(8.4)	10	24–26	
20	200	97	LO-12	500	5,5	2	1	(8.2)	3.3	0.8	
			Standard	500	1,2	1	+	6.7	9	19	
				1000	5	+	+	(7.3)	9	19–21	
				1500	2,2	0	2	6.5	10	6.5–14	
20	300	100	LO-12	500	3,3	7,8		7.7	3.3	1.2	
			Standard	500	1,1	+,+		7.5	9	14	
				1500	1,1	+,+		8.3	9	18	12.14
26	200	100	LO-12	500	2,5	1		7.6	3.3	<1[d]	
			Standard	500	0,1	+,+		7.1	9	<1	
				1000	1,1	+,+			9	1	12.15
				1500	1,1	1		7.5	9	3	
26	250	225	LO-12	1000	3,3	4		(6.9)	3.3	0.5	
			Standard	1000	4,4	7	3		9–15	0.6	12.16

[a]The two values that are given for type 347 stainless steel represent rates obtained for two different corrosion specimens; the + sign represents a weight gain.

[b]In cases where the pH value of the supernatant liquid was not available, the pH of the slurry is shown in parentheses; where both values were measured the difference was less than 1.3 pH units.

[c]By gravitational sedimentation in $Na_4P_2O_7$ solutions of water or glycerol-water mixtures.

[d]Particle-size distribution data not yet completed; values are estimates from determinations still in progress.

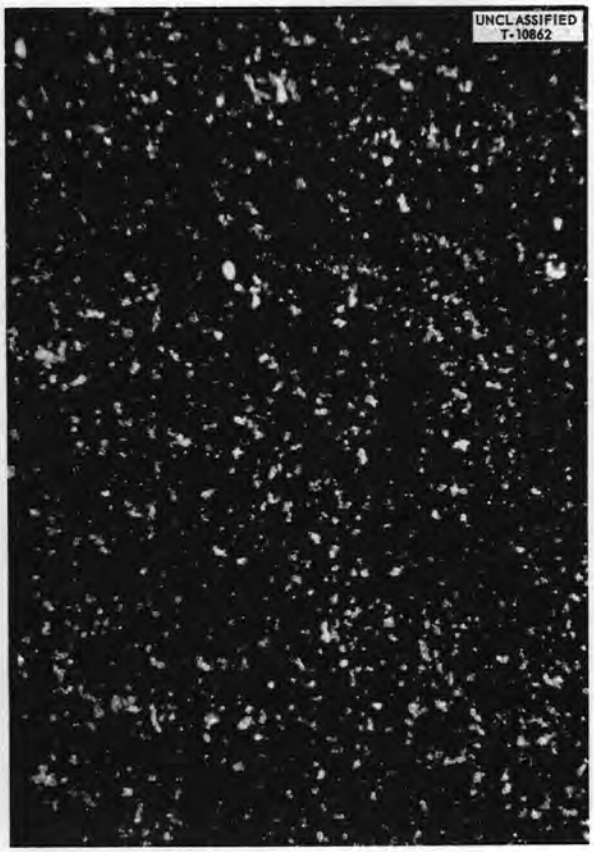

Fig. 12.10. LO-12 Thorium Oxide Used to Charge Loop 200A for Production of Standard Slurry and to Charge Certain Toroid Runs. 400X.

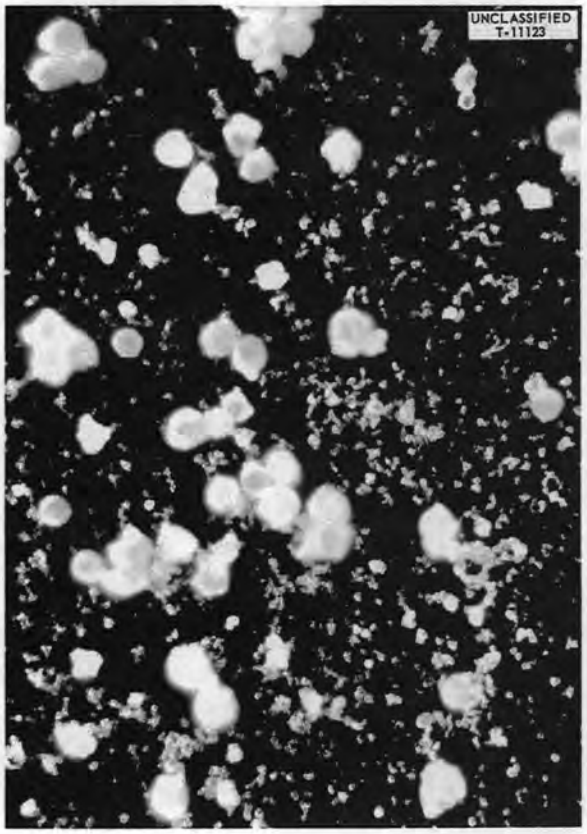

Fig. 12.11. Thorium Oxide Produced in Loop 200A as Standard Slurry. 400X.

Figures 12.10 through 12.16 were taken at 400-dia magnification, so that 1 mm represents 2.5 μ (prior to any reduction associated with reproduction). The production of such large, single particles of thorium oxide from "normal" thorium oxide (produced by the Chemical Technology Division) has not been duplicated in toroids under a variety of conditions, as is shown in Table 12.4 and illustrated in Fig. 12.12.

On the other hand, the behavior of the standard slurry upon circulation in toroids was entirely different from that of any other oxide thus far studied. Its behavior appeared to depend upon the relative velocity of circulation and to be relatively independent of the temperature and slurry concentration; the presence of corrosion pin specimens, which served as surfaces of direct impact for the circulating oxide particles, also seemed likely to have influenced the behavior and character of the thorium oxide.

Table 12.4 demonstrates that in no case under the conditions of circulation in the toroids was it possible to produce a larger-sized particle from LO-12 thorium oxide. On the other hand, when the standard slurry (already containing large-sized particles) was circulated, much larger-sized particles were produced at the lower velocity (10 fps, Fig. 12.13), while higher velocities (20 fps, Fig. 12.14) appeared not only to produce larger-sized particles but also to shatter some of the particles into irregular-shaped chips or fragments (note hemisphere in Fig. 12.14). At the highest velocity studied (26 fps), in one run this same growth and destruction were evident (Fig. 12.15), while, in the extreme, complete destruction to very small-sized particles appeared to have occurred (Fig. 12.16).

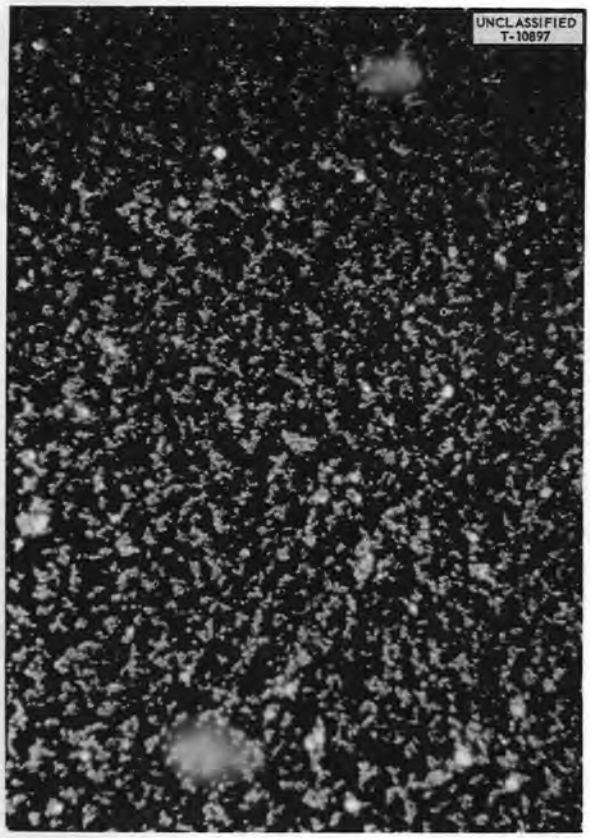

Fig. 12.12. LO-12 Thorium Oxide After Being Circulated in Toroid at 10 fps Relative Velocity, 200°C, 500 g of Th per Kilogram of H_2O, in Oxygen for 97 hr. 400X.

Examination of the pin specimens exposed during the runs summarized in Table 12.4 showed very slight attack. In this aspect the results are quite surprising. A larger attack by thorium oxide particles which maintained such large size during circulation would have been expected on the basis of previous results,[6] even at the lower velocities and certainly at the 26-fps level. It is believed, however, that the present results do not refute the previous postulate but rather are another reflection of the unparalleled properties shown by the standard slurry.

Perhaps even more significant, however, were the observations that those pins exposed to the circulating standard slurry invariably accumulated a deposit of thorium oxide (except in the run at 26 fps for 225 hr). These deposits ranged from hard, adherent, thin, transparent layers to bulky waxlike deposits that could not be removed by mere scrubbing with a bristle brush. The deposition did not appear to show preferential orientation with respect to the direction of circulation. An illustration of these deposits is shown in Fig. 12.17. No noticeable deposits of thorium oxide were found on pins exposed to the LO-12 oxide under the same conditions.

The results of this investigation have not thus far shed any light on the method of formation of large-sized thorium oxide particles (as seen in the standard slurry) from small-sized oxide (e.g., LO-12) upon circulation. The experiments, however, have shown the singular qualities exhibited by the standard slurry: the ability to produce a very large, spherical thoria particle; unexpectedly low attack rates by such large particles; and the accumulation of hard thorium oxide deposits upon surfaces exposed directly into the circulating medium.

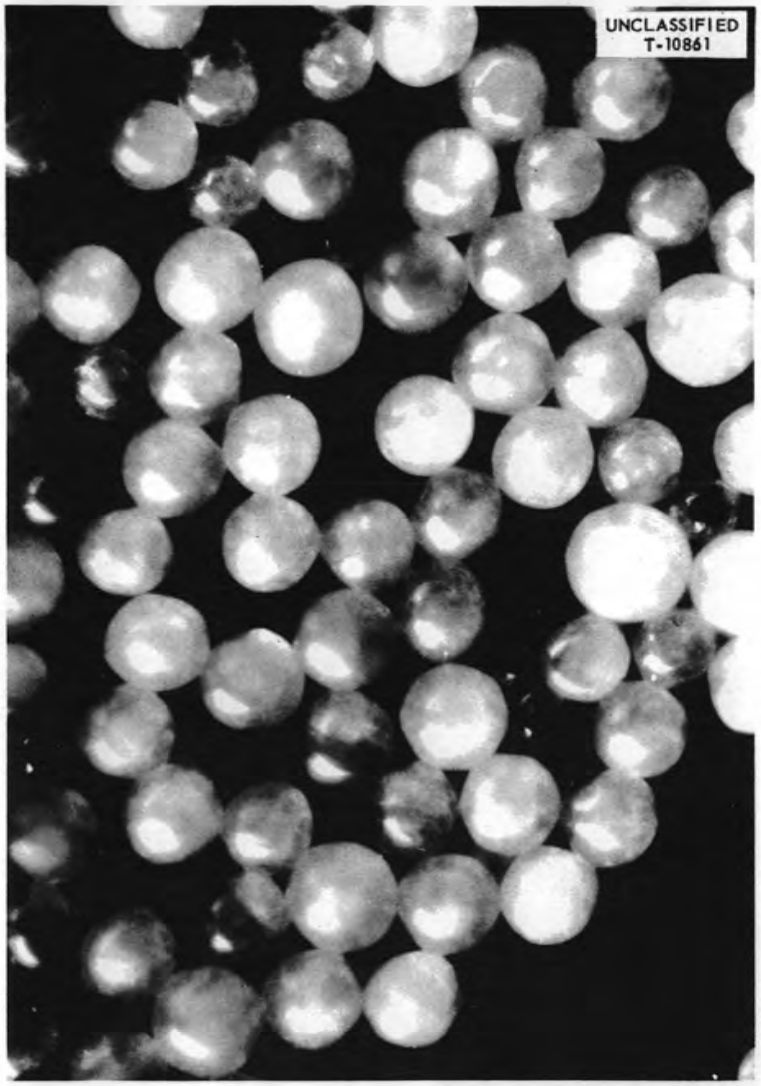

Fig. 12.13. 200A Standard Slurry After Being Circulated in Toroid at 10 fps Relative Velocity, 200°C, 1000 g of Th per Kilogram of H_2O, in Oxygen for 97 hr. 400X.

Fig. 12.14. 200A Standard Slurry After Being Circulated in Toroid at 20 fps Relative Velocity, 300°C, 1500 g of Th per Kilogram of H_2O, in Oxygen for 100 hr. 400X.

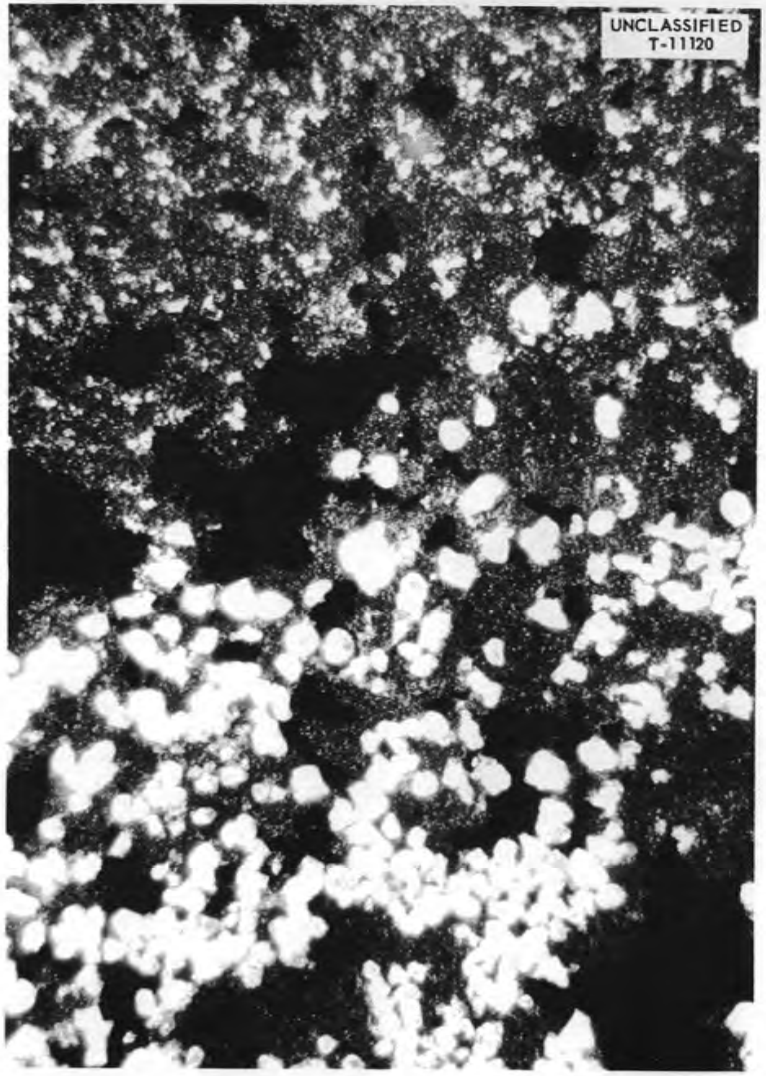

Fig. 12.15. 200A Standard Slurry After Being Circulated in Toroid at 26 fps Relative Velocity, 200°C, 1000 g of Th per Kilogram of H_2O, in Oxygen for 100 hr. 400X.

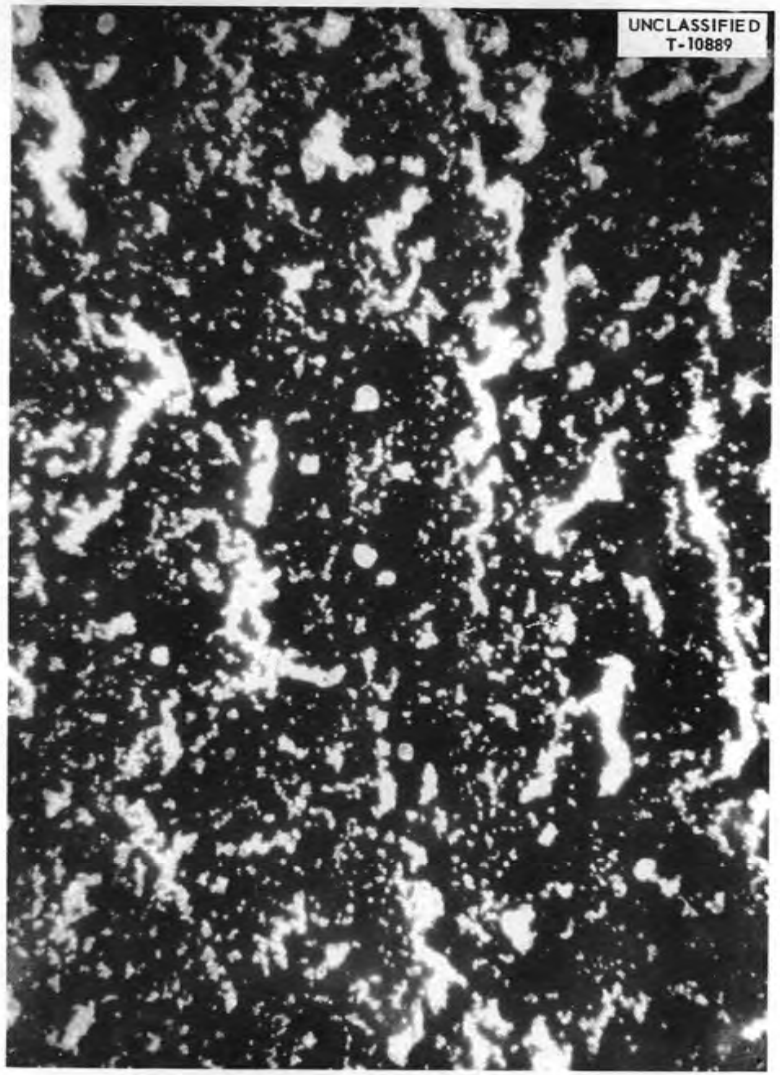

Fig. 12.16. 200A Standard Slurry After Being Circulated in Toroid at 26 fps Relative Velocity, 250°C, 1000 g of Th per Kilogram of H_2O, in Oxygen for 225 hr. 400X.

Fig. 12.17. Type 347 Stainless Steel Pin Exposed to Standard Slurry at 26 fps Relative Velocity, 1000 g of Th per Kilogram of H_2O, 200°C, in Oxygen for 100 hr. 12.5X.

13. RADIATION CORROSION

G. H. Jenks H. C. Savage

A. L. Bacarella
J. E. Baker
S. E. Bolt
R. J. Davis
V. A. DeCarlo
B. O. Heston
D. T. Jones
R. A. Lorenz
T. H. Mauney
J. R. McWherter
A. R. Olsen
R. M. Pierce
J. A. Russell
M. D. Silverman
F. J. Walter
K. S. Warren
R. M. Warner
D. B. Weaver[1]
S. H. Wheeler
L. F. Woo
W. C. Yee

13.1 IN-PILE LOOPS

13.1.1 Development and Construction

(a) General. – Construction of in-pile loop assemblies for operation in beam holes HB-2 and HB-4 at the LITR is continuing. A newly designed model of the loop cooler was installed on loop L-2-15. This cooler was tested and was found to be capable of removing an estimated 4.5 kw of heat from the loop, as compared with approximately 1 kw for the cooler previously used. Further development of the cooler is under way. The increased loop cooling capacity is required to remove the additional fission power generated by the higher neutron flux available in beam hole HB-2. The design layout of a loop package incorporating the Byron Jackson 5-gpm pump has been completed, but assembly of the loop is being delayed pending successful completion of the Byron Jackson pump test.

(b) HB-4 Loop Package. – Loop L-4-13[2] was installed and is in operation in beam hole HB-4 of the LITR. Loop L-4-16, which is fabricated of stainless steel and which will contain coupon corrosion specimens, impact specimens, and tensile specimens, is being constructed. The type 347 stainless steel tapered-channel coupon holders in the core and line positions will contain coupons of Zircaloy-2, type 55AX titanium, and type 347 stainless steel. In addition, two ladder-type holders (Fig. 13.1) in the core and one in the line position will contain coupons of nine different zirconium alloys, in addition to Zircaloy-2, and type 347

[1]On loan from TVA.

[2]G. H. Jenks *et al.*, *HRP Quar. Prog. Rep. April 30, 1956*, ORNL-2096, p 90.

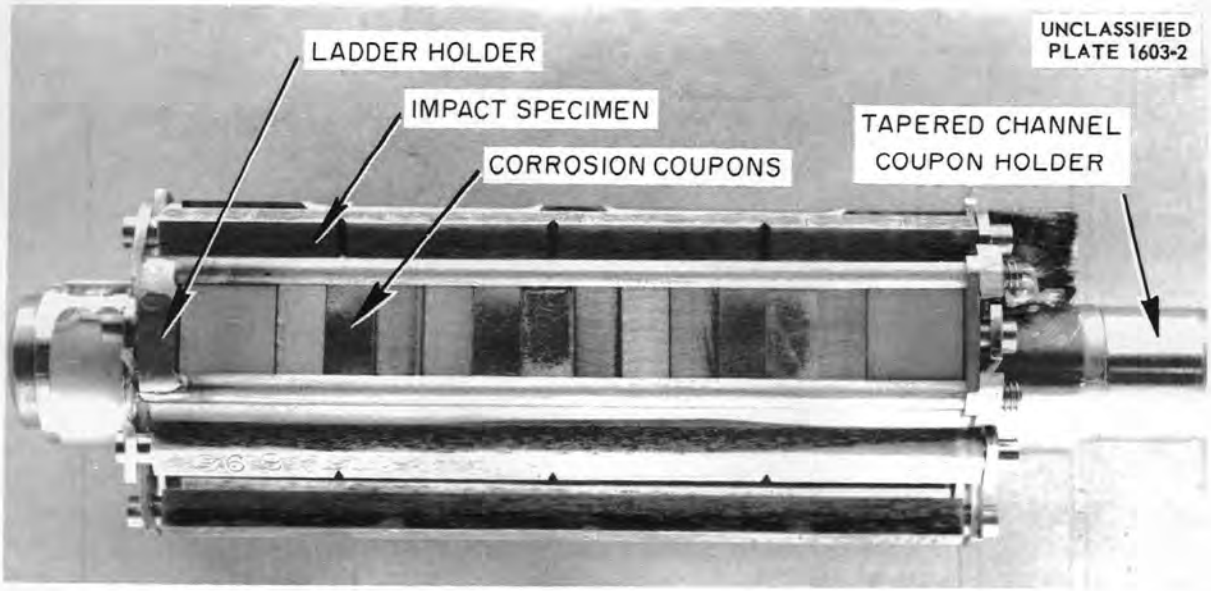

Fig. 13.1. Ladder-Type Specimen Holder.

stainless steel. Zirconium-alloy and titanium impact specimens will be located in the core and line positions. Titanium type 110AT tensile specimens will be located in the core and line holders.

(c) HB-2 Loop Package. – The construction, pretreatment operation, and initial testing of loop L-2-15 were completed. The loop is of type 347 stainless steel and contains coupon, tensile, impact, and stress-corrosion specimens. Zircaloy-2 tapered-channel coupon holders in the core and line positions contain Zircaloy-2, titanium type 55AX, and type 347 stainless steel coupons. Ladder-type holders in both positions contain type 347 stainless steel, Zircaloy-2, type 309 SCb stainless steel, titanium type 110AT, nickel-clad Zircaloy-2, platinum-clad Zircaloy-2, and platinum coupons. Tensile specimens of crystal-bar zirconium and of Zircaloy-2 are located in both positions, as are stress assemblies of titanium type 55AX. Present plans are to insert loop L-2-15 in the HB-2 hole at the LITR before loop L-2-14,[3] the all-titanium loop, which is also ready for installation.

(d) Byron Jackson Pumps. – One of the two 5-gpm pumps received has been tested in the pump test loop, DV-9. The total time accumulated on this pump is 261 hr. During 144 hr of this time, a solution of 0.17 *m* UO_2SO_4, 0.03 *m* $CuSO_4$, and 0.04 *m* H_2SO_4 was circulated at a loop temperature of 250°C. The remainder of the time was used in pretreatment and checkout of the loop and pump on 3% trisodium phosphate, 5% nitric acid, and distilled water.

At the end of the first 18 hr on uranyl sulfate, a pinhole was discovered in the seal-weld lip at the rear of the pump casing. This hole was repaired, but, upon pressure checking, a similar pinhole was detected in the seal-weld lip at the front of the pump case. Metallographic examination revealed that the pinholes were probably due to nonmetallic inclusions in the rod stock from which the pump case was made. After this second hole was repaired, the pump was operated on uranyl sulfate for 125 hr with no further evidence of leakage. Except for these leaks, operation of the pump has been satisfactory.

Further testing of the pump is being delayed for installation of an experimental loop core cooler in the system.

[3] J. R. McWherter *et al.*, *HRP Quar. Prog. Rep. July 31, 1956*, ORNL-2148, p 92.

(e) ORR Loop. – Design layout of the ORR corrosion test loop package was continued during the last quarter. A mockup of a core cooler for removing the gamma heat in the core wall was installed on the pump test loop. This cooler consists of 6 ft of ¼-in.-OD stainless steel tubing spiral-wrapped on the stainless steel core and cast in aluminum.

This experimental core cooler will be evaluated for incorporation in the in-pile loops designed to operate in the ORR. Removal of heat from the core wall is necessary to prevent boiling of the fuel solution in contact with the wall. It is estimated that 3 or 4 kw of gamma heat will be generated in the metal of the core wall.

13.1.2 General Description of In-Pile Loop Experiment L-4-12

Except for metallographic examination, the seventh in-pile loop experiment, L-4-12, has been completed. Details of this experiment and the results will be reported.[4] A summary is presented below.

One feature of loop experiment L-4-12 was the use of a titanium core in the otherwise all-stainless-steel loop. The titanium-75A core body was coupled to the type 347 stainless steel loop with mechanical fittings; titanium gaskets were used.

Identical sets of corrosion coupons (24 in each set) in titanium-75A tapered-channel coupon holders were installed in the core and in-line positions. Type 347 stainless steel, Zircaloy-2, and titanium-55AX were used for these coupons. One Inconel coupon was substituted for a type 347 stainless steel coupon in the in-line array. Six impact specimens, three of Zircaloy-2 and three of titanium RC-A-40, were placed in the core at positions surrounding the core coupon holder. Four impact specimens, two of Zircaloy-2 and two of titanium RC-A-40, were placed in the special line holder. In addition, the core and the special line holder each contained two stress-specimen assemblies. The stress specimens in the core and line were made of titanium alloy (6% Al, 4% V).

The pressurizer contained eight stress-specimen assemblies. These stress specimens were of titanium-C-130AM, titanium alloy (6% Al, 4% V), and type 17-4 PH stainless steel. Two of the eight

[4] J. R. McWherter *et al.*, *HRP Radiation Corrosion Studies, In-Pile Loop L-4-12*, ORNL-2163 (in press).

stress-specimen assemblies contained dissimilar stress-specimen pairs of titanium-C-130AM and 17-4 PH type stainless steel, while two others contained pairs of titanium alloy (6% Al, 4% V) and type 17-4 PH stainless steel. The pressurizer stress specimens were arranged so that four of the assemblies were exposed in the vapor region of the pressurizer and four matching assemblies in the liquid region.

The operating conditions employed in this experiment were similar to those reported for previous HB-4 loop experiments (loop at 250°C, pressurizer at 280°C).

Difficulty with the sample-withdrawal system resulting from two partially plugged valves necessitated a temporary loop shutdown after 773 hr of circulation time. The loop solution was drained to the weigh tank, and these two valves and another valve in the high-pressure gas line were replaced. The loop was recharged with fresh solution, and operation was continued for an additional 1247.5 hr. The total circulation time for the experiment was 2020.5 hr, of which 1917.5 hr was in the reactor. The energy output of the LITR during this time was 4375.5 Mwhr. The initial 191.6 Mwhr was liberated at the 1.5-Mw level and the remainder at the 3-Mw level.

The initial solution, the solution used when the loop was recharged, and the solution used to replace the samples withdrawn from the loop were of approximately the same composition: UO_2SO_4, 0.17 *m* (U^{235}/total U = 0.927); $CuSO_4$, 0.031 *m*; H_2SO_4, 0.04 *m*.

The average fission power during the first period of operation at 3 Mw, as determined from cesium analyses, was 755 w. For the three samples obtained during operation of the loop at the 1.5-Mw reactor level, the average was 388 w. Because of incomplete drainage of the original loop solution, cesium values obtained from the samples withdrawn during the second period of operation are not considered representative and are not given in this report. The power density at a given specimen position in the core was determined from measurements of the induced activities of the Zircaloy-2 core coupons. The power densities thus determined ranged from about 5.4 w/ml at the forward end of the core to 0.9 w/ml at the rear of the coupon holder.

The average corrosion rate of stainless steel as calculated from the oxygen data, which was in agreement with the rate based on nickel data, was 1.4 mpy for the 629-hr period of exposed operation with the initial solution. The average corrosion rate of stainless steel as calculated from oxygen data for the remainder of the run was 1.0 mpy.

13.1.3 Qualitative Results of Inspection and Evaluation of Loop L-4-12

All component surfaces outside the core were covered with a heavy rustlike scale. The scale deposit was heavier on the wall in the liquid-phase region of the pressurizer than in the vapor-phase region. Unlike the pressurizer wall, the stainless steel and titanium stress specimens located in the pressurizer vapor differed very little in appearance from those located in the liquid region. However, the specimens from the liquid region exhibited greater increases in the as-removed weights than did the specimens from the vapor region.

As with previous loop experiments,[5] all stainless steel surfaces in the core region were covered with a heavy black scale. The Zircaloy-2 impact specimens and stress-specimen holders located in the core annulus were covered with a thin film that produced interference colors. All titanium surfaces in the core region were covered with a brass-colored film. Both inside and outside titanium-holder surfaces and the interior titanium-core surface exhibited an additional, dark, rustlike scale at the low-flux end. The first three stainless steel coupons in the high-flux region of the core (positions 4, 5, and 7) were found to be missing when the core holder was opened. These specimens could not be found in any of the other loop components, and it is concluded that they were dissolved. Examination of the titanium holders revealed two disturbed film markings on each side of the channel, located approximately where the leading edge of two of the missing coupons should have been. These markings indicate that the coupons left the array before the in-pile run was terminated.

Five coupons located in consecutive positions near the outlet end of the in-line holder could not be identified from stamped identification numbers after disassembly. The coupons, two Zircaloy-2 (positions 20 and 23), two titanium-55AX (positions 19 and 22), and one type 347 stainless steel

[5] J. E. Baker *et al.*, *HRP Radiation Corrosion Studies, In-Pile Loop L-4-8*, ORNL-2042 (Aug. 8, 1956).

(position 21), showed absence of film and heavy attack on the clamped areas, which destroyed the identification numbers. Examination of these coupons with a stereoscopic microscope revealed evidence that they had not been held firmly in place. Previous out-of-pile experience in the 100A loops[6] has shown that when a specimen is not held firmly the vibration during operation may prevent the accumulation of a protective film on the clamped edges and lead to an increased attack in these areas. The mating surfaces of the two titanium-holder halves in the vicinity of the five coupons, unlike the remaining holder area, were not filmed over.

Two type 347 stainless steel in-line coupons, one adjacent to each end of the five-coupon group, showed heavy attack on their edges but were film-covered. The single Inconel coupon contained in the in-line holder was also heavily attacked.

This is the first in-pile loop in which localized attack of a loop component has been observed. The attack occurred in the type 347 stainless steel pump volute. A single pit was located in the surface of the recessed shoulder at the volute inlet. The pit appearance was typical of that found in stainless steel specimens located in the critical-flow-velocity range in out-of-pile experiments.[7]

Separation of the titanium core from the stainless steel inlet pipe was accomplished easily by unscrewing the coupling. The outlet pipe coupling from the titanium core to the stainless steel was sectioned without dismantling. No evidence of galvanic attack was noted on either coupling, and all sealing surfaces appeared to be in excellent condition.

As with all previous loops, cathodic defilming of the in-line coupons was only partially effective; some film was retained by the specimens. In fact, all Zircaloy-2 in-line coupons (excluding loose coupons in positions 20 and 23) showed weight increases or no weight changes following the final defilming. The core impact and the special in-line impact specimens were not defilmed but are to be examined metallographically in the as-removed condition.

[6] J. C. Griess, *HRP Quar. Prog. Rep. July 31, 1954*, ORNL-1772, p 78.

[7] J. C. Griess and R. E. Wacker, *HRP Quar. Prog. Rep. April 30, 1954*, ORNL-1753, p 76–77.

13.1.4 Quantitative Results of Inspection and Evaluation of Loop L-4-12

Unless otherwise specified, corrosion-rate values reported below were calculated from weight-loss data, with the exposed specimen area and total radiation time (equivalent to 1459 hr of LITR operation at 3 Mw) used as the basis for the calculations. Average solution velocities across the coupons contained in the tapered core and in-line holders were from 9.4 to 44.4 fps.

(a) Zircaloy-2. – The corrosion results obtained for Zircaloy-2 in this experiment were in good agreement with those obtained in previous loops. The Zircaloy-2 corrosion-rate data from all experiments to date are plotted against power density in Fig. 13.2. As before, the corrosion rates of the core specimens were dependent upon power density. Observed rates for the core coupons varied from 1 mpy at 1 w/ml power density to 3.7 mpy at 4.6 w/ml power density. As previously mentioned, the in-line Zircaloy-2 coupons showed either weight increases or no weight changes following the defilming.

(b) Titanium Alloys. – All titanium-alloy corrosion data obtained from this experiment are in general agreement with data from previous loop experiments.

With one exception the corrosion rate of the titanium-55AX core coupons varied from 0.7 mpy at 4.8 w/ml to 0.04 mpy at 1.0 w/ml. The exception, a coupon at 3.4 w/ml, exhibited a rate of 1.33 mpy. The average corrosion rate of all core coupons was 0.4 mpy. The coupons in the high-velocity region, 30 to 37 fps, and at power densities of 1.6 to 2.2 w/ml corroded at an average rate of 0.3 mpy. The average corrosion rate for the in-line coupons (excluding loose coupons in positions 19 and 22) was 0.10 mpy. There was no apparent effect of velocity on the attack of the in-line specimens.

The average corrosion rate of the four titanium (6% Al, 4% V) core stress specimens was 0.73 mpy. All four specimens were exposed to the same average power density of 2.4 w/ml. The average corrosion rate of the four special in-line specimens was 0.14 mpy. A single stress specimen located in the pressurizer liquid-phase region exhibited a corrosion rate of 0.17 mpy. The average corrosion rate for two similar stress specimens located in the pressurizer vapor-phase region was 0.19 mpy.

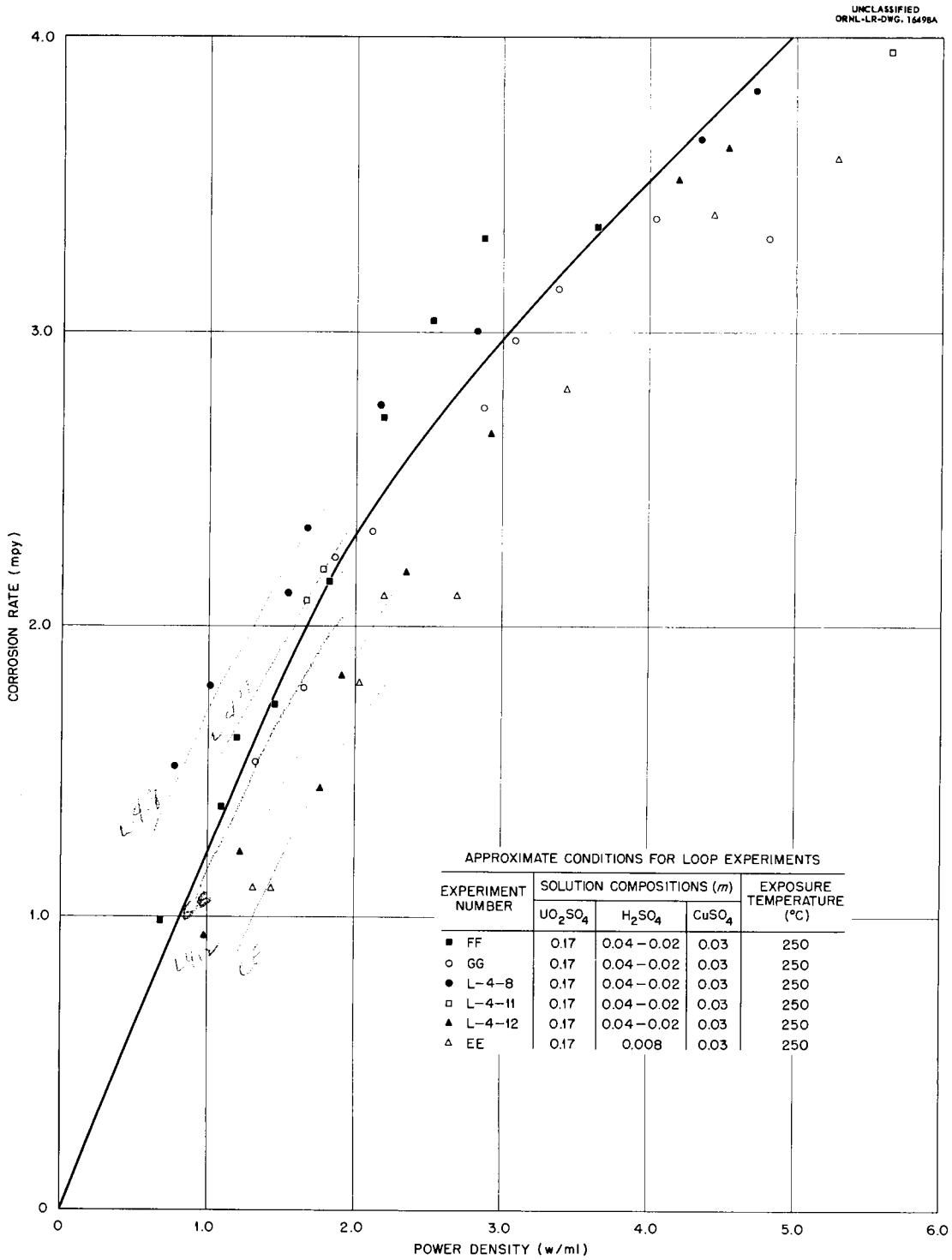

Fig. 13.2. Zircaloy-2 Core Coupon Corrosion Rates vs Power Density at Coupon Position.

Three titanium C-130-AM stress specimens located in the pressurizer liquid-phase region and three in the pressurizer vapor-phase region exhibited average corrosion rates of 0.26 and 0.07 mpy, respectively.

(c) Stainless Steels. – As mentioned previously, the first three coupons of type 347 stainless steel, in the high-power-density end of the core were missing. The power density at these coupons ranged from 4 to 3 w/ml and the velocity from 12 to 17 fps. A minimum corrosion rate of 186 mpy would have been required to completely dissolve these specimens during the time of irradiation. The fourth type 347 stainless steel coupon from the high-flux end of the core corroded at a rate of 3.4 mpy at a power density of 2.5 w/ml. The fifth coupon corroded at a rate of 0.8 mpy at a power density of 2.1 w/ml. The remaining three core coupons at power densities of 1.4, 1.1, and 0.9 w/ml corroded at rates of 0.1, 0.08, and 0.1 mpy, respectively. Excluding the loose coupon in position 21 and the coupons adjacent to the five damaged coupons mentioned previously, the average corrosion rate for the remaining four in-line type 347 stainless steel coupons was 0.16 mpy.

The four type 17-4 PH stainless steel stress specimens contained in the pressurizer exhibited corrosion rates of 0.54, 0.14, 0.76, and 0.03 mpy. The first two rates were obtained for specimens exposed in the pressurizer vapor-phase region and the latter two for liquid-phase-region specimens. Specimens two and four were stressed to lesser degrees than specimens one and three.

(d) Inconel. – The single Inconel in-line coupon exhibited a corrosion rate of 121 mpy. There were no Inconel specimens in the core.

13.1.5 Discussion of Results from Loop L-4-12

The results obtained for the over-all steel corrosion rate in loop L-4-12 differed markedly from those obtained in previous experiments with solution of the same initial composition (by over-all rate is meant the apparent rate which is calculated from nickel and oxygen data when it is assumed that all steel surfaces in contact with high-temperature solution corrode uniformly). The over-all rate in this loop, following the initial exposure to radiation, was 1.5 mpy. The rate dropped off slightly during the exposure and was about 1.0 mpy at the end of the experiment.

In contrast, the previous loops have exhibited appreciably higher initial rates and somewhat lower final rates. For loop L-4-8,[5] the initial and final rates were about 7 and 0.7 mpy, respectively. Similar high initial rates and low final rates were observed with loops GG[8] and L-4-11.[9] These results and comparisons clearly indicate that the high initial rates observed with previous experiments have been due primarily to a high rate of attack in the steel core at the start of radiation. Through the use of a titanium core in the present loop, the area of steel in the core was reduced to such a small amount that rapid attack of the core steel did not contribute appreciably to the initial over-all rate.

The existence of a very high corrosion rate for the three stainless steel specimens which were located in the three forward positions of the core holder is substantiated by a correlation of nickel and weight data. The average corrosion rate of the in-line stainless steel coupons (in positions 4, 5, 7, and 10) and of the stainless steel coupons in the low-flux end of the core (<2 w/ml) was 0.1 mpy. If the difference between this rate and the over-all rate based on nickel data is attributed to the three missing coupons in the core, the loose coupon in the in-line array, and the Inconel coupon, the corrosion rate of the three missing coupons would have been around 200 mpy, above the 186 mpy required to dissolve the specimens.

It appears likely that the high rate for these specimens is, in part at least, explained by an effect indicated by several loop data: The radiation-induced corrosion of steel by 0.17 *m* UO_2SO_4 solutions is severe when the concentration of excess H_2SO_4 is in the range 0.04 to 0.03 *m*. Concomitant with the high initial rates observed for previous loops was a rapid reduction in the concentration of excess acid. In general, the rates leveled off appreciably from the high initial rates when the calculated concentration of excess acid decreased to 0.02 *m* from the initial 0.04 *m*. As noted above, this behavior of the over-all rate probably reflects, in reality, the radiation corrosion in the core.

---

[8] G. H. Jenks *et al.*, *HRP Quar. Prog. Rep. July 31, 1955*, ORNL-1943, p 109–126.

[9] J. R. McWherter *et al.*, *HRP Radiation Corrosion Studies, In-Pile Loop L-4-11*, ORNL-2152 (in press).

In the present experiment, L-4-12, the concentration of excess acid did not decrease very rapidly because of the low over-all rate. The acid concentration was in the range 0.03 *m* to 0.04 *m* during most of the exposure. At these high acidities the steel specimens which were in the highest flux continued to corrode at rapid rates throughout the experiment.

It is of interest to estimate the corrosion rate in the core during the initial period for the previous loop L-4-8. Weight data from the core sleeve specimen of this loop indicate that only the forward 2 in. of the stainless steel core tank were heavily attacked (> 7 mpy average). The area of this portion of the core, including the impact-specimen holder and coupons in this region, is about 130 cm^2, as compared with the total loop stainless steel area of 3303 cm^2. Assuming that the 130 cm^2 of the stainless steel core in loop L-4-8 accounted for the high initial corrosion rate in that experiment, then the average corrosion rate on that portion would have been about 162 mpy.

In connection with experiment L-4-8, it should be mentioned that core-holder specimens which were in the high-velocity region corroded at average rates which were greater than those for the three specimens which were exposed at higher fluxes but at lower velocities. In loop L-4-12 the high-velocity specimens exhibited low corrosion rates. This difference is as yet unexplained. The higher acid in this loop had little effect on the corrosion rates of titanium and zirconium alloys.

13.1.6 In-Pile Loop L-2-10

Exposure of in-pile stainless steel experiment L-2-10 in the LITR has been completed. Total circulation time for the experiment was 1672 hr, of which 216 hr was accumulated outside the reactor. The energy output of the LITR during in-pile operation was 3764.9 Mwhr, and essentially all this power was liberated at the 3-Mw level. Disassembly of the loop and examination of the loop and specimens are in progress. The L-2-10 core contained specimens of stainless steel, Zircaloy-2, titanium-55AX, and platinum. Tapered-channel coupon holders fabricated of stainless steel type 347 were used in the core and in-line positions.

This is the first loop that has been irradiated in the HB-2 beam hole at the LITR. The solution used, which is similar to HRT solution, contained only one-fourth the uranium and copper concentrations of solutions used in previous loop experiments in the HB-4 beam hole. The solution charged to the loop for in-pile operation was of the following composition: UO_2SO_4, 0.04 *m* (U^{235}/total U = 0.927); $CuSO_4$, 0.0075 *m*; H_2SO_4, 0.02 *m*.

The makeup solution which replaced solution withdrawn as samples from the loop during operation contained 0.04 *m* excess acid, to replace acid consumed in corrosion, and 130 ppm chromium to inhibit corrosion of the type 420 stainless steel valve stems during solution additions. The operating temperatures of this loop were increased over those for previous loops and were as follows: mainstream temperature, 280°C; pressurizer temperature, 305°C.

Over-all stainless steel corrosion rates obtained from nickel and oxygen data showed only slight changes with operating time. As calculated from oxygen data, the corrosion rate during the first 300 hr of in-pile operation was 0.5 mpy. During the final 1385 hr the average rate was 0.4 mpy. The rates calculated for the same periods of time from the amounts of nickel found in solution were 0.3 and 0.2 mpy, respectively.

13.1.7 In-Pile Loop L-4-13

Stainless steel loop L-4-13 is now being exposed in beam hole HB-4 at the LITR. The core and in-line coupon holders are tapered-channel holders fabricated from type 347 stainless steel and contain coupon specimens of types 347 and 309 SCb stainless steel and crystal-bar zirconium. Impact specimens of zirconium alloy (20% Nb) and Zircaloy-3a are contained in the core and in-line positions. In addition, tensile specimens of Zircaloy-3a and titanium-A40 are contained in the core. For the first time, the solution charged to a loop for in-pile operation was made up by using heavy water. The solution composition for loop L-4-13 is as follows (for convenience in presenting concentrations it is assumed that the molecular weight of D_2O is the same as that of H_2O):

UO_2SO_4	0.17 *m* (U^{235}/total U = 0.927)
$CuSO_4$	0.031 *m*
H_2SO_4	0.02 *m*
D_2O/total water	0.998 *m*

The makeup solution used to replace solution withdrawn as samples from the loop contains 0.04 *m* H_2SO_4, to replace acid consumed in corrosion, and 100 ppm chromium to inhibit corrosion of the type 420 stainless steel valve stems during solution addition. This loop is operating at the same temperature as previous HB-4 loops (mainstream at 250°C and pressurizer at 280°C).

13.2 IN-PILE AUTOCLAVE TESTS – LITR TESTS

Three Zircaloy-2 experiments not previously mentioned, Z-21, Z-24, and Z-25, are reported, and the bomb data are presented in Table 13.1. Data from earlier experiments[10] are included in Table 13.1 to report recently available fission power densities and corrosion penetration from pin weight losses.

Experiments Z-11 and H-96 are reported again to show revised values of fission power densities. The previously reported power densities[10] represented slow-neutron fluxes which were significantly out of line with those found in all other recent HB-6 experiments. The check analysis yielded the fission power densities shown in Table 13.1, and since the corresponding slow neutron fluxes agree very well with other recent HB-6 values, these results are considered correct.

Following experiment H-97-2, which is not reported here, the HB-6 facility was modified to accept an experiment with a design similar to that of experiments presently conducted in HB-5.[11] The new installation is now in use. The various experiments are discussed briefly.

13.2.1 Experiment Z-21

Experiment Z-21 was conducted as a test of the effect of excess sulfate on the radiation-induced corrosion of Zircaloy-2. Excess sulfate was added as Li_2SO_4, with the lithium isotopes in natural abundance. The concentration of Li_2SO_4 was equal to that of the UO_2SO_4, 0.17 *m*. The experiment was prematurely terminated because of a capillary plug. No oxygen-pressure data were obtained during the 36-hr exposure, and the corrosion information in Table 13.1 on Z-21 is from pin weight-loss data only. The solution concentrations used in Z-21 are known to be in a range where precipitation might occur.[12,13] Chemical analyses of the solution and scale after exposure indicate that the lithium, copper, and uranium were all in solution at the time that the analyses were made. The brevity of experiment Z-21 tends to render the resulting pin data less accurate than pin data for the usual experiment. However, from a consideration of the corrosion rate of 23 mpy which may be predicted from the experimental conditions and the equation $CR = 3.8PD\,(1 - e^{-40/CR^{1.5}})$, discussed in Sec. 13.3, it may be concluded from this experiment that considerable protection from radiation corrosion was derived from the presence of the lithium sulfate. The measured rate is less, by a factor of 2, than that anticipated for a solution free of the excess sulfate.

13.2.2 Experiment Z-24

The surfaces of Zircaloy-2 specimens and bombs which are normally used in corrosion tests are in the as-machined condition. It was desired to ascertain whether a significantly different corrosion behavior characterized Zircaloy-2 which possessed a strain-free surface, as compared with the as-machined surfaces. To this end, experiment Z-24 was conducted in which three Zircaloy-2 pins were included which had been pickled in an HNO_3-HF mixture[14] to remove 3 to 5 mils of metal. This experiment was also designed as a test of the effect of nitrogen gas on the radiation corrosion of Zircaloy-2. In all but one of the previous bomb experiments, the bombs have contained air at a pressure of about 1 atm. It appears likely that the nitrogen in this air was fixed to some extent under radiation and, hence, may have played some part in corrosion or in the determination of corrosion through pressure measurements. Nitrogen was carefully excluded from the Z-24 bomb during assembly.

The average loss of weight of the etched specimens showed that they had suffered a penetration of 0.212 mil, whereas the average penetration

[10] R. J. Davis *et al.*, *HRP Quar. Prog. Rep. July 31, 1956*, ORNL-2148, p 99.

[11] G. H. Jenks *et al.*, *HRP Quar. Prog. Rep. Oct. 31, 1954*, ORNL-1813, p 86.

[12] J. C. Griess and R. S. Greeley, *HRP Quar. Prog. Rep. July 31, 1955*, ORNL-1943, p 84.

[13] J. C. Griess *et al.*, *HRP Quar. Prog. Rep. Oct. 31, 1955*, ORNL-2004, p 99.

[14] M. C. Udy, H. L. Shaw, and F. W. Boulger, BMI-711, p 136 (Feb. 20, 1952) (Secret).

TABLE 13.1. LITR IN-PILE BOMB DATA[a]

Bomb No.	LITR Beam Hole	Solution Composition (m)				Enrichment (% U^{235})	Exposure Temperature (°C)	Fission Power Density (w/ml)	Irradiation Time (hr) (1 hr = 3 Mwhr)	Total Penetration (mils)		Corrosion Rate O_2 Data (mpy)
		UO_2SO_4	$CuSO_4$	H_2SO_4	Other					O_2 Data	Pin Weight Data	
Z-21	HB-5	0.171	0.040	0	0.171 Li_2SO_4	93.2	280	18.8	36.4	[b]	0.042	10.0[c]
Z-24	HB-5	0.172	0.010	0		93.2	280	14.0	81.1	0.249	0.247[d] 0.212[f]	27.4[e]
Z-25	HB-5	0.0091[g]	0	0	0.129 Li_2CO_3	93.2	260	0.91	133.7	0.107	0.086	5.6[c]
Z-17	HB-5	0.169	0	0.040		6.0	250 250 280 250	1.51 0.75[n] 1.43 1.51	362.3 127.0[b] 165.7 107.8	0.167	0.150	2.17 1.0[b] 3.08 1.56
Z-18	HB-5	0.042	0.056	0.040	557 ppm Cr as CrO_3	93.2	280	4.9	158.9	0.177	0.16	9.9
Z-19	HB-5	0.160	0.010	0	546 ppm Mo as H_2MoO_4	93.2	280 300	17.1 16.4	53.5 18.1	0.215	0.22[i] 0.12[j] 0.12[k]	24.2[e] 32.8[e]
Z-20[l]	HB-5	0.168[m]	0.040[m]	0.040[m]		93.2	250	9.3[n] 18.6	128.0[b] 124.8	0.21	0.20	7.2[b] 9.7
Z-11	HB-6	0.172	0.010	0	0.0054 $KTcO_4$	93.2	232 250 280	10.2 9.8 9.2	116.0 51.1 125.1	0.275	0.288	5.6 7.64 16.1
H-96	HB-6	0.172	0.010	0	0.0011 $KTcO_4$	93.2	250	10.6	604.3	0.148	0.194	Variable
Z-1	HB-6	0.168	0.011	0.040		93.2	280	10.3	141.4	0.183	0.153	11.8

[a]The bomb material was Zircaloy-2 for all experiments except H-96, which was type 347 stainless steel.

[b]A capillary plug terminated the experiment after 35 hr; no oxygen-consumption data were obtained.

[c]Corrosion rate estimated from pin weight losses.

[d]Usual machined surfaces on "control" pins.

[e]Corrosion rate of Zr-2; i.e., observed oxygen data adjusted for lower rate of alloy pins indicated by pin weight-loss data.

[f]Machined surfaces removed by acid treatment.

[g]Concentration of UO_3.

[h]Rates based on 1.5-Mwhr radiation time scale. Reactor operated at 1.5 Mw.

[i]Zircaloy-2 pins.

[j]85% Zr–15% Nb pins.

[k]83.5% Zr–15% Nb–1.5% Sn pins.

[l]Deuterium replaced 96.9% of the light hydrogen in the solution.

[m]Concentrations calculated as moles solute per 1107 g of solvent D_2O.

[n]LITR operated at 1.5-Mw power level.

of the surfaces of three control pins in the same bomb was 0.247 mil. These data may indicate that the machined surface of Zircaloy-2 is subject to more rapid attack than the undisturbed metal beneath; however, reduction of the microscopic surface area by the chemical polishing treatment may also account for the approximately 12% difference in observed rates. The average corrosion rate of Zircaloy-2 in this experiment as determined from the oxygen data was about 27 mpy. The rate determined from the Zircaloy-2 pin data is in near agreement with that determined from the oxygen data. Agreement between the pin and oxygen data has also been found in the majority of the previous experiments. According to Fig. 13.3, a rate of about 20 mpy would be predicted for Zircaloy-2 under the conditions of this experiment if nitrogen has no effect. The difference between this predicted rate and the observed rate of 27 mpy is greater than would be expected from consideration of the usual spread of Zircaloy-2 data. Thus nitrogen may have some small effect on the radiation corrosion of Zircaloy-2. However, it is worth noting that for the previous experiment in which nitrogen was excluded, Z-1, the rate was not significantly different from that of other experiments which contained nitrogen but otherwise were similar. The exposure temperature for experiment Z-1, as for Z-24, was 280°C. The solution for Z-1 was 0.04 *m* in H_2SO_4; Z-24 contained no acid.

13.2.3 Experiment Z-25

Experiment Z-25 represents a distinct departure from the current series of uranyl sulfate solutions containing various additives. The corroding solution used in this Zircaloy-2 bomb was comprised of a lithium carbonate solution of natural isotopic distribution containing dissolved UO_3 and was pressurized with 800 psi of CO_2 measured at the test temperature of 250°C. No copper recombination catalyst was used, because it was anticipated that copper would not remain in solution. Atmospheric nitrogen was excluded from the bomb during filling. Experimental data by Loprest and Marshall[15] indicate that such a solution is stable at a temperature as high as 260°C. The experiment operated only with some difficulty regarding radiolytic-gas buildup, but after several hours of intermittent operation at 250 and 255°C, it was found that continuous operation at 260°C was possible, with a steady-state radiolytic gas pressure of about 700 psi A corrosion rate of 5.6 mpy was computed from the pin weight losses. It is convenient to compare this rate of 5.6 mpy with the corrosion rate obtained from the power-density curves (Fig. 13.3). The power density from uranium fission in bomb Z-25 is calculated to have been 0.9 w/ml. An additional 0.5 w/ml can be estimated (0.3 w/ml from fast-neutron energy and about 0.2 w/ml from lithium fission). A power density of 1.4 w/ml in a UO_2SO_4 solution without acid at 250°C would be expected to give a corrosion rate of 2.9 mpy. Suitable adjustment for an increase in temperature of ten degrees (to 260°C) yields an estimate of 3.6 mpy. The experiment thus indicates that the carbonate system is probably somewhat more corrosive under reactor radiation than the sulfate system is.

13.2.4 Experiment Z-17

Some results of experiment Z-17 were reported previously.[10,16] Additional data for this experiment are given in Table 13.1. The oxygen data have been re-evaluated, and the calculated rates reported here differ slightly from those previously reported. It may be noted that during 127 hr of the Z-17 experiment the reactor operated at half power (1.5 Mw). The corrosion rate during this half-power operation was about half that observed at full power. Thus a linear relationship between power density and corrosion rate is indicated by these results.

13.2.5 Experiment Z-20

Preliminary results of experiment Z-20 were reported previously.[10] This experiment was for testing the radiation corrosion in a D_2O solution. The power density which prevailed in this experiment has been evaluated, and the results are included in Table 13.1. By comparison with an extrapolation (Fig. 13.3) of Zircaloy-2 data with light-water solutions but with otherwise similar conditions (250°C, 0.17 *m* UO_2SO_4, and 0.04 *m* excess H_2SO_4), the results of Z-20 indicate that the rate in this D_2O solution is about 30% greater than that anticipated for the light-water solutions.

[15] C. H. Secoy *et al.*, *HRP Quar. Prog. Rep. Oct. 31, 1955*, ORNL-2004, p 203.

[16] G. H. Jenks *et al.*, *HRP Quar. Prog. Rep. April 30, 1956*, ORNL-2096, p 95.

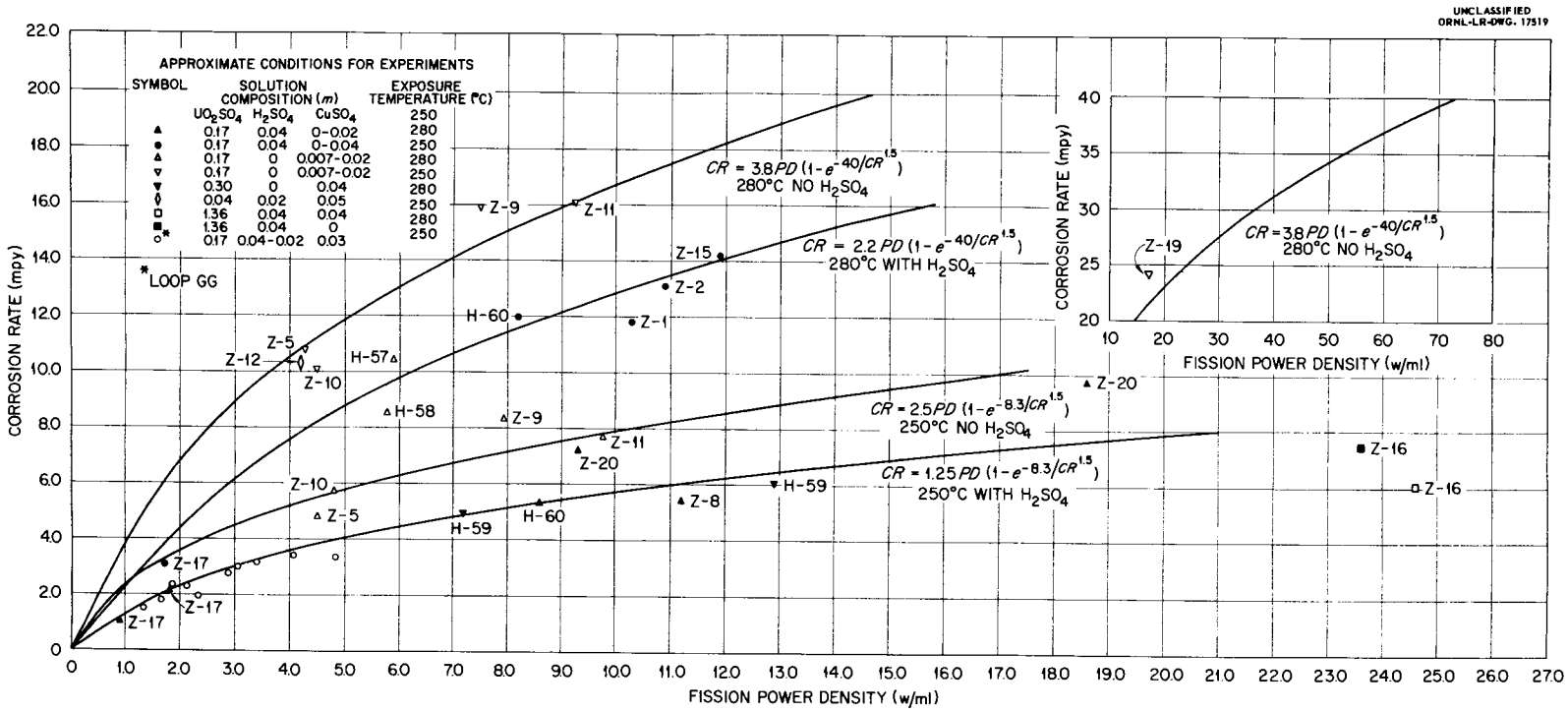

Fig. 13.3. Radiation-Corrosion Data for Zircaloy-2.

In contrast with Z-17, the results of the operations at two levels of reactor power in this experiment clearly indicate a nonlinear relationship between corrosion rate and power density.

13.3 CORRELATION OF ZIRCALOY-2 DATA

As discussed in the previous quarterly report,[10] the results of the various corrosion experiments in the LITR have provided evidence that the rate of radiation-induced corrosion of Zircaloy-2 by uranyl sulfate solution does not increase linearly with increasing power density in the solution. It was pointed out that the data from both loop and rocking-autoclave experiments can be expressed, approximately, by equations of the form

$$CR = K(PD)^{2/3} \tag{1}$$

where CR is the corrosion rate (mpy) based on radiation time, PD is the fission power density (w/ml) which prevails in solution during exposure, and K is a constant, the value of which depends upon temperature and solution composition.

Data presently available indicate that equations of the above form, with the exponent of power density equal to $\frac{2}{3}$, do not accurately represent the power-density–corrosion-rate relationship. The apparent exponent is smaller than $\frac{2}{3}$ at high power densities and corrosion rates and is greater than $\frac{2}{3}$ at low power densities and corrosion rates. The data to which reference is made are those for bomb experiments Z-17 and Z-20, which are listed in Table 13.1. During exposure of each of these experiments, the reactor operated at two different power levels, full power and one-half power. Experimental conditions other than those influenced by power density were maintained constant. It is believed that power-density–corrosion-rate relationships determined from the results of experiments of this type are the most accurate available.

As mentioned in Sec. 13.2, experiment Z-20 was operated at relatively high power densities. The results indicate a nonlinear relationship between power density and corrosion rate. If it is assumed that the results can be expressed by an equation of the form

$$CR = K(PD)^n \ , \tag{2}$$

the value of n which is calculated is 0.43. It is noteworthy that the results of an earlier experiment, H-59,[10] for which the reactor also operated at two different power levels, also yield a value of 0.43 for n. The power densities and corrosion rates which prevailed in experiment H-59 are in the neighborhood of those for the half-power operation in experiment Z-20.

As discussed in Sec. 13.2, the results of the low-power-density experiment, Z-17, indicate an approximately linear relationship between corrosion rate and power density. Fitted to an equation of the form of Eq. 2, the results yield a value of 1.1 for n.

All the loop exposures of Zircaloy-2 to date have been at fairly low power densities. As shown in Fig. 13.2, there is appreciable scatter among the results of different experiments. However, if the results of only one experiment are considered (e.g., those for GG or L-4-12), it appears that these results also indicate a linear relationship between corrosion rate and power density at low power densities. It is also evident that the relationship deviates from linearity at the higher power densities.

It has been found that the Zircaloy-2 corrosion data over the full power-density range which has been studied can be expressed by equations of the form

$$CR = A\,PD\,(1 - e^{-B/CR^{1.5}}) \tag{3}$$

where A and B are constants and the other symbols have the same meaning as in Eq. 1. At low corrosion rates this equation reduces to

$$CR = A'PD \ ; \tag{4}$$

at very high rates, Eq. 3 reduces to

$$CR = A''\,PD^{0.40} \ . \tag{5}$$

An equation of the form of Eq. 3 can be derived theoretically if certain postulates are made as to the mechanism of the radiation corrosion of Zircaloy-2. This derivation will be described in a forthcoming ORNL CF memorandum entitled *A Postulated Mechanism for the Radiation-Induced Corrosion of Zircaloy-2* by G. H. Jenks.

Data from the various rocking-autoclave experiments are plotted in Fig. 13.3. For the most part, these data are the same as those discussed and plotted in accordance with Eq. 1 in the previous report.[10] More accurate data are available for

some of the experiments, and hence some of the points are slightly changed. Some additional results are available and are included in this graph. The data from the in-pile loop experiment GG are included in this graph, because this set appears to be in nearest agreement with the bomb data. The lines in the graph are those which are represented by the equation adjacent to each line. Each equation is of the form of Eq. 3. The constants in the equation for the lower line were evaluated from the loop GG data and from the bomb data for Z-8, H-60, and Z-17. The data for this set of conditions (250°C, 0.17 m UO_2SO_4, with 0.04 m H_2SO_4) extend over a wide enough range so that the constants can be determined with reasonable accuracy. For the evaluation of constants for the data at 250°C without acid, it was assumed that the constant in the exponential term is equal to that for the lower line. The basis for this assumption is in the theoretical derivation mentioned above. Given the constant in the exponential term, the other constant, A, was evaluated from the data. The constants for the 280°C data were evaluated in a similar manner. The data for the set of conditions 280°C, 0.17 m UO_2SO_4, with H_2SO_4 extend over a wide enough range so that both constants can again be evaluated with reasonable accuracy. The equation for the line drawn through the in-pile loop data in Fig. 13.2 is the same as that for the lower line in Fig. 13.3, $CR = 1.25\ PD(1 - e^{-8.3/CR^{1.5}})$.

Conclusions as to the effect of variables other than power density on the corrosion of Zircaloy-2 within the conditions studied are not changed appreciably from those discussed in the previous report.[10]

13.4 SUPPORTING RESEARCH

13.4.1 Radiation Damage to Freon

Radiation damage to Freon-11 (CCl_3F) has been reported previously.[17] Therefore its use for the HRT refrigeration system was questioned and discussed.[18] It was deemed advisable to conduct a radiation experiment on Freon to determine the decomposition products and their amounts under conditions approximately those anticipated for the HRT. The results of this study have been reported by Silverman, Heston, and Rudolph.[19]

Thirty milliliters of Freon-11, contained in a pyrex cell and cooled to −70°C, was exposed to an electron beam from a Van de Graaff accelerator. Degreased copper and stainless steel turnings were included; therefore metal was present in both the liquid and gaseous Freon. The Freon received approximately 8% (2.63×10^{21} ev/ml) of the amount of the radiation exposure to be expected in the HRT refrigeration system.[17] In terms of the usual method for expressing irradiation decomposition, G values (molecules formed per 100 ev absorbed) of 0.31 and 0.082 were obtained for the production of chlorine and fluorine, respectively.

Since Freon in the HRT refrigeration system will be subjected to gamma radiation at temperatures from −40°C to room temperature, it is probable that the G value of 0.39 (for total halogen formation) will be raised by an order of magnitude. In view of these results and previous experience with Freon-11, it was recommended that refrigerants other than Freon-11, especially those which form noncorrosive decomposition products, be considered for use in the HRT secondary refrigeration system.

13.4.2 Effects of Electron Irradiation on the Corrosion of Zircaloy-2 in a Thermal Loop

The effect of ionizing radiation on the corrosion of Zircaloy-2 is being studied with the use of a Van de Graaff accelerator to provide a source of high-energy electrons.

It has been found[20] that the effect of ionizing radiation on the corrosion of stainless steel foils exposed to uranyl sulfate solution in a type 347 stainless steel thermal loop was negligible. Similar experiments[21] on Zircaloy-2 foil specimens contained in the same stainless steel loop were inconclusive. It is believed that the deposition of stainless steel oxides on the surface of the Zircaloy specimens may have in some manner affected their corrosion beneficially. In order to eliminate possible effects caused by the

[17] C. Michelson, *Radiation Damage to Freon*, ORNL CF-55-9-163 (Sept. 30, 1955).

[18] P. S. Rudolph, private communication to C. Michelson, Oct. 28, 1955.

[19] M. D. Silverman, B. O. Heston, and P. S. Rudolph, *Radiation Damage to Freon*, ORNL CF-56-8-198 (Aug. 27, 1956).

[20] J. A. Ghormley and C. J. Hochanadel, *Chem. Semi-ann. Prog. Rep. Dec. 20, 1953*, ORNL-1674, p 76.

[21] B. O. Heston and M. D. Silverman, *Effects of Electron Irradiation on the Corrosion of Zircaloy-2 in a Thermal Loop*, ORNL CF-56-2-2 (Feb. 2, 1956).

presence of stainless steel components in solution, a thermal-convection loop was fabricated of titanium.

Recently, in-pile autoclave experiments[22] have been conducted with solutions of depleted uranium. Since higher corrosion rates were observed for these experiments than in comparable out-of-pile studies, the importance of determining the effects of purely ionizing radiation is further emphasized.

(a) Experimental. – The system differed from the steel loop in having a larger pressurizer arranged so that the full flow of the loop passed through the pressurizer. Zircaloy-2 sheet machined down to about 8 mils was vacuum-annealed, polished with alumina (the abrasive was removed ultrasonically), and then etched with the standard nitric-hydrofluoric acid mixture commonly used for zirconium. A portion of the sheet was cut into foil specimens 0.25 by 0.070 in. Some specimens were later given a cathodic etch, wherein the specimen was made the cathode in a discharge tube with argon at reduced pressure and any adhering oxide film was reduced. Electron micrographs of replicas of the surface were made by T. E. Willmarth's group.

A number of runs were completed, both in the presence and absence of radiation. A film 400 Å thick (interference colors) was grown on the foil surface exposed to distilled water for 5 hr at 250°C. This corresponds to a penetration rate of 2.5 mpy, approximately the same as that observed in autoclave experiments. Approximately the same thickness of film was formed on specimens heated in distilled water for 2 hr at 250°C and then irradiated for 3 hr by using a current of 5 μa at 1.5 Mev.

The first cathodically etched specimen was irradiated for 2½ hr at 250°C in a solution of 0.04 *m* UO_2SO_4, 0.02 *m* H_2SO_4, and 0.01 *m* $CuSO_4$ under an excess oxygen pressure of 300 psi. A current of 16 μa at 1.5 Mev was used for the irradiation. This is equivalent to a current density of approximately 90 $\mu a/cm^2$. The specimen showed more film than was shown on any of the preceding samples for a similar amount of radiation. Microscopic examination did not reveal any crystal growth over the initial film formed on the original grain structure. However, a second similarly etched specimen, irradiated for 10 hr under the same conditions, was estimated by Willmarth to have formed a film approximately 1500 Å thick. The unetched portion of the specimen was not so heavily coated.

Another specimen, not cathodically polished, was irradiated for 41 hr in UO_2SO_4 under similar conditions. This sample received a total of 1025 whr (i.e. 17 μa at 1.5 Mev), or approximately 25% more than the specimen irradiated last summer (105 whr, 5 μa at 1.5 Mev) in the stainless steel loop. Willmarth estimates that the film thickness on the sample is about 2000 Å. This is roughly in agreement with out-of-pile autoclave experiments, where films of approximately 2500 Å are grown during a similar time period. Replicas of the film are now being studied. It is noteworthy that the film on the back or unpolished face of the specimen was far less adherent than that formed on the polished or front face.

(b) Discussion. – From the results reported above, it appears that ionizing radiation has little if any effect on the rate of corrosion of Zircaloy-2 under the conditions used. The previous history of the surface would presently appear to be a more important factor than either the composition of the solution or the amount of radiation energy.

In at least two aspects these results are incomplete. Further experiments should be performed to determine the effects of ionizing radiation at higher temperatures – up to 300°C, the design limit of the loop. The effect of increasing the radiation time should also be investigated, by using radiation periods of 100 hr or more.

Glick[23] has shown that the attack on crystal-bar zirconium in water is accelerated with increasing current density. In later work, however, he reports that the attack on Zircaloy-2 under similar conditions is at least an order of magnitude less than that observed for pure zirconium. Furthermore, his experiments were run at 315°C, whereas those reported here were conducted at 250°C.

[22] G. H. Jenks *et al.*, *HRP Quar. Prog. Rep. Jan. 31, 1956*, ORNL-2057, p 98.

[23] H. Glick (Westinghouse), personal communication.

14. METALLURGY

G. M. Adamson

R. G. Berggren
J. P. Hammond
W. J. Leonard
M. L. Picklesimer
J. J. Prislinger
R. L. Stephenson
J. K. White
J. C. Wilson
C. H. Wodtke
O. Zmeskal

14.1 PHYSICAL METALLURGY

14.1.1 Zirconium-Alloy Development

The objective of the zirconium-alloy development program is the development of a zirconium-base alloy with better radiation corrosion resistance to uranyl sulfate solutions than Zircaloy-2 has. From the results of in-pile corrosion tests, zirconium-niobium alloys have shown the most promise, and most of the work has been and will continue to be concentrated on a Zr–15% Nb base alloy. Alloys with bases of sponge and crystal-bar zirconium are being studied. The zirconium-niobium system appears to be quite a complex system and will require considerable metallurgical study before it can be recommended for reactor use.

Recent improvements in chemical polishes and etchants permitted the examination of the zirconium-niobium alloys heat treated below 600°C.[1] In general, the transformation, as revealed metallographically, of the beta-quenched alloys held below the eutectoid temperature of approximately 610°C was quite sluggish. Specimens that had been beta quenched have been held from 30 min to two weeks at temperatures of 300, 400, 500, and 600°C and water quenched. Metallographic examination has shown that the Widmanstätten plate phase occurring in the beta-quenched alloys will redissolve on heating to 400, 500, and 600°C and that it appears to fade out if held at 300°C, leaving a "ghost" structure reminiscent of the carbide "ghosts" occurring in a pearlitic steel held at a low austenitizing temperature for too short a period of time. This second phase in these alloys has not been definitely identified, but it is not alpha zirconium. At 600°C after the phase discussed above dissolves, a second transformation product starts appearing and grows slowly, so that complete transformation occurs between two days and two weeks at temperature (Fig. 14.1). The structure of the specimens held at 300, 400, and 500°C cannot be completely resolved with the optical microscope but, at 300 and 400°C, appears to consist primarily of retained beta, with another phase that cannot be resolved at all contributing to the large increase in hardness. At 500°C no structure of any type can be seen. Etching-technique development is continuing in an attempt to resolve the structures. Specimens aged at 300°C reached a hardness of 470 DPH in two weeks as compared with an as-beta-quenched hardness of 211 DPH. The age-hardening mechanism occurring at the three lower temperatures is believed to be different from the transformation occurring at 600°C.

The rate at which Zr–10% Nb base alloys transform is faster than that of the 15% Nb alloys. The addition of molybdenum as a ternary alloying element decreases the rate of transformation of all the alloys, while the addition of iron increased the rate appreciably. Ternary additions of palladium and platinum increased the rate of transformation but not so much as did additions of iron.

The first series of heat treatments were exploratory in nature, since very little is known about the zirconium-niobium alloys. Further heat treatments have been scheduled to fill out the data required for time-temperature-transformation (TTT) diagrams for these alloys.

The effects of mechanical working and subsequent heat treatment on the transformation kinetics and mechanical properties have been evaluated in a cursory manner during the preparation of tensile and impact specimens for in-pile radiation damage and corrosion studies. The effect of cold or warm working during fabrication seems to be an increase in the rate of transformation and a change in the location of the TTT curves on the temperature axis of the plot. Considerable difficulty has been encountered in subsequent fabrication and annealing. The material seems to be much harder and

[1] M. L. Picklesimer, *HRP Quar. Prog. Rep. July 31, 1956*, ORNL-2148, p 106–107.

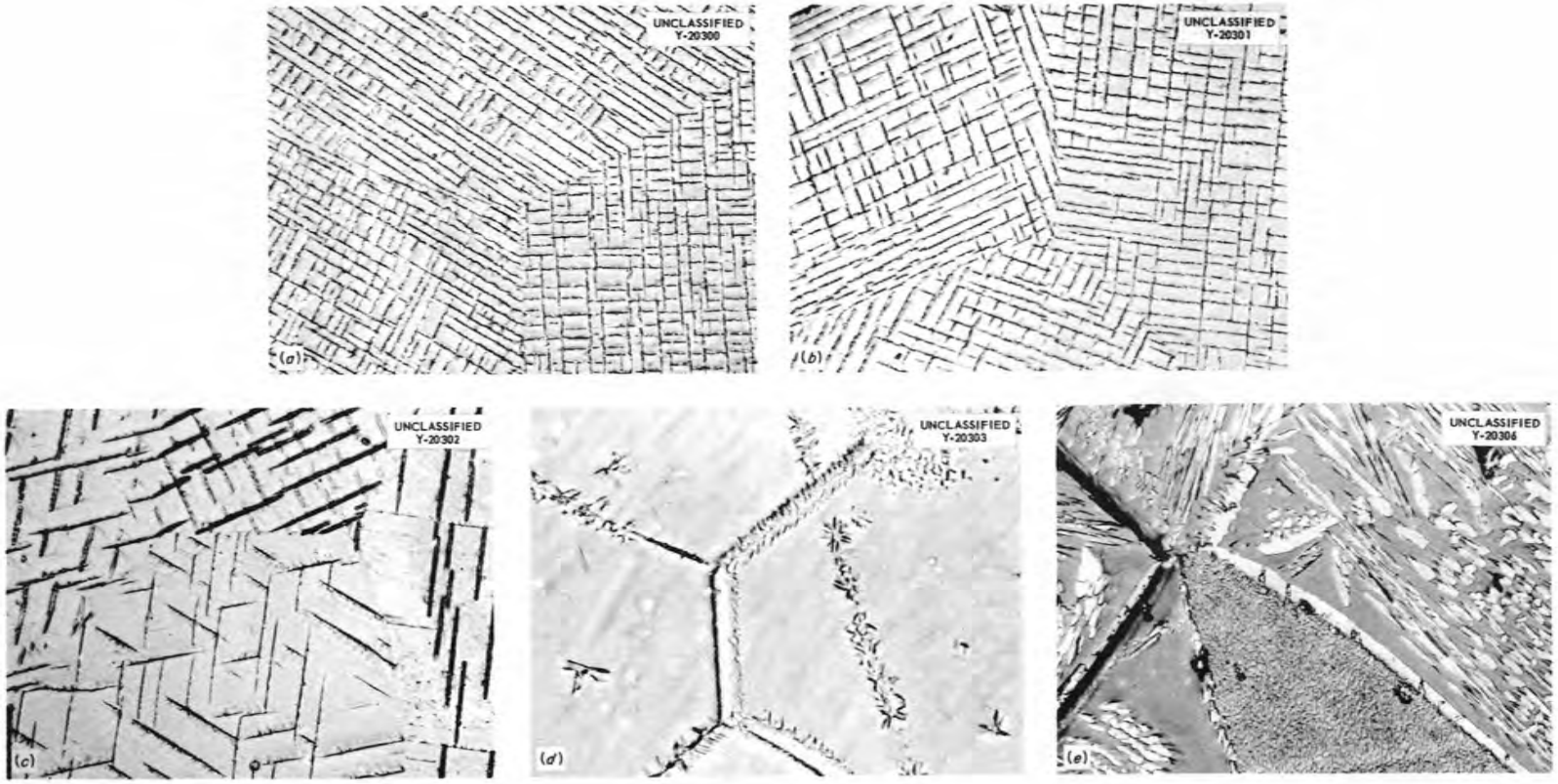

Fig. 14.1. Change in Structure of Beta-Quenched Zr-Nb Alloys After They Were Held for 1 hr at 885°C, Water-Quenched, and Aged for Various Times at 600°C. (*a*) As quenched; (*b*) aged for 15 min; (*c*) aged for 30 min; (*d*) aged for 1 hr; (*e*) aged for two weeks.

tougher after intermediate anneals. A series of controlled experiments to evaluate the effect of fabrication methods with intermediate anneals is scheduled.

14.1.2 Morphology of Zircaloy-2

In the metallographic examination of the Zircaloy-2 impact specimens from in-pile loop GG, an apparent second phase was noted in some of the grain boundaries. While these specimens were supposed to have been heated only into the alpha range, similarities in structure with alloys heated into the alpha/beta range were noted. Since the impact curve for these samples had not shown a transition region,[2] a series of tests was carried out to determine whether these effects can be caused by heat treatment.

Typical micrographs from both ends of a specimen from loop GG are shown in Fig. 14.2. The second phase is more apparent in the section from the low-flux end of the sample than in the one from the high-flux end, and this was noted in all samples examined.

Specimens of Zircaloy-2 rod, from the same stock from which the in-pile loop GG specimens were made, were heat treated in the furnace at 810, 820, and 830°C for 5, 10, and 15 min and were air cooled. The specimens were mounted, polished, and examined metallographically. Micrographs are presented in Fig. 14.3. The specimens held at 810°C showed only a recrystallization of the partially cold-worked structure of the original material, with some "clearing" of the microstructure. Those held at 820°C showed the appearance of a very thin platelike phase (needles in the micrograph) in the grain boundaries, with no particular change with time at temperature. The specimens held at 830°C, however, showed, with time at temperature, an increasing amount of a grain-boundary "film" second phase. This phase is believed to be the iron, nickel, and chromium intermetallics, deposited when the beta phase, present in the grain boundaries at 830°C, decomposed upon air cooling.[3]

Round, multibreak, subsize, impact specimens, similar to those from loop GG, were capsulated in

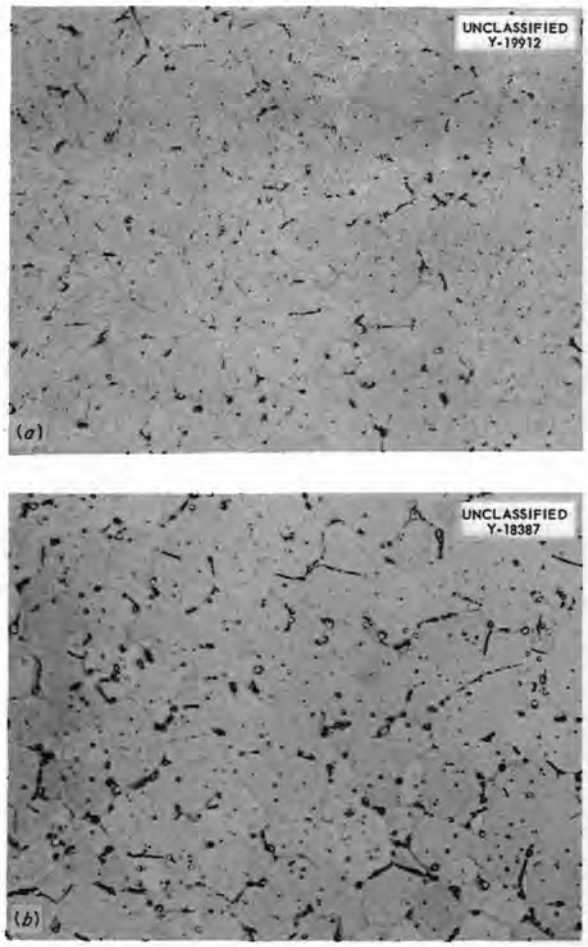

Fig. 14.2. Structure of Zircaloy-2 Impact Specimens 84 from In-Pile Loop GG. (*a*) High-flux end; (*b*) low-flux end. Bright field. Appearance, especially at the low-flux end, of a second phase in the grain boundaries can be seen.

Vycor tubing in a partial atmosphere of purified argon, held for 15 min at 800, 810, 820, and 830°C and for 5 min at 830°C, and air cooled in the capsule. The specimens were broken on an Izod-type subsize impact machine. The experimental results are presented in Fig. 14.4 and Table 14.1. From these data it is apparent that a significant reduction in impact energy was found in the specimens held at 820 and 830°C for 15 min. Although sufficient data are not available for complete proof, it also appears that the transition region has been moved approximately 100°C to a higher temperature. The data for the specimens held for 5 min at

[2]W. J. Fretague, *HRP Quar. Prog. Rep. July 31, 1955*, ORNL-1943, p 167–168.

[3]M. L. Picklesimer and G. B. Wadsworth, *HRP Quar. Prog. Rep. Jan. 31, 1956*, ORNL-2057, p 102.

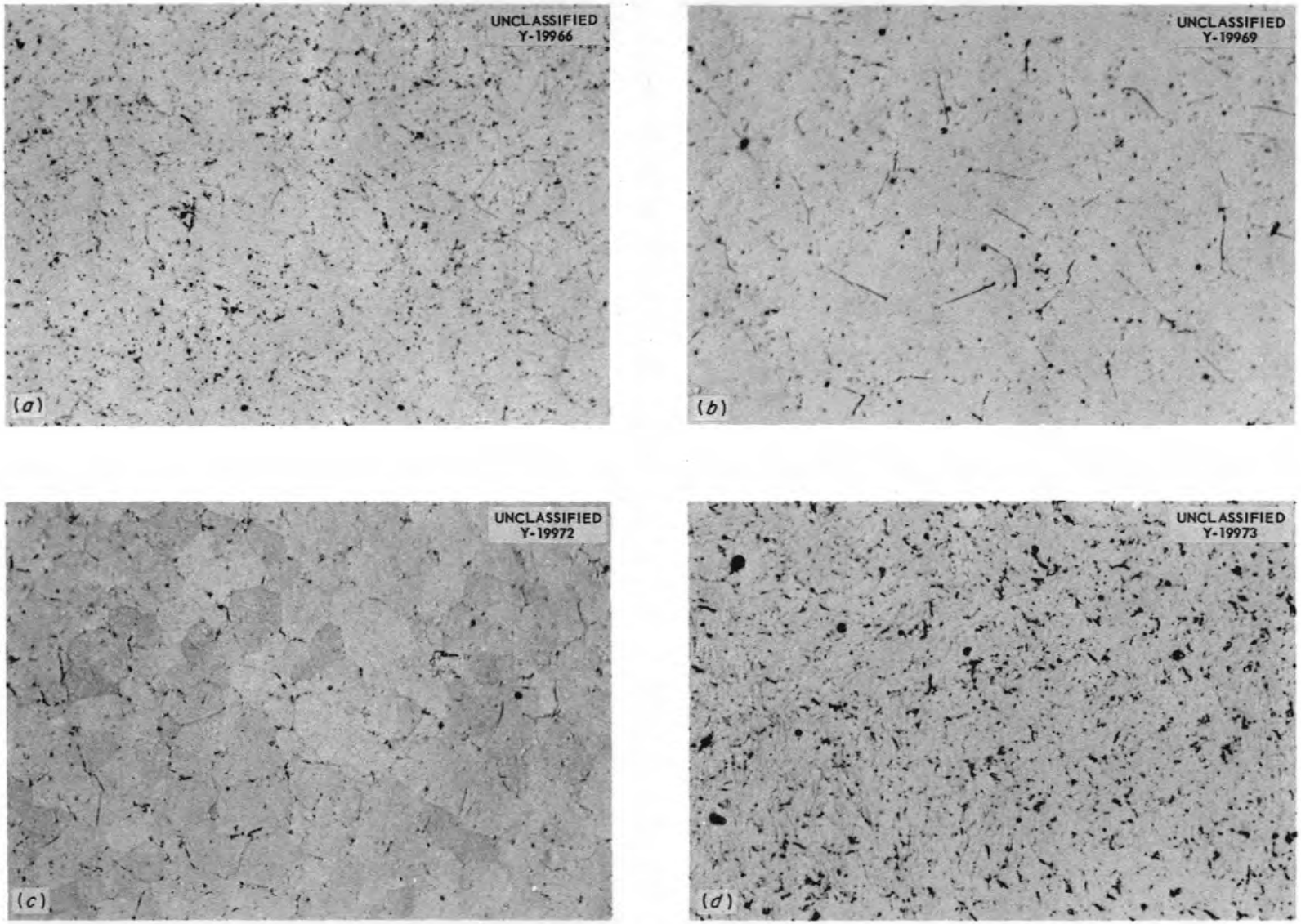

Fig. 14.3. Structure of Zircaloy-2 Heat-Treated for 15 min at (*a*) 810°C, (*b*) 820°C, and (*c*) 830°C; (*d*) as-received. Bright field. A second phase can be noted in the grain boundaries of (*b*) and (*c*). 750X.

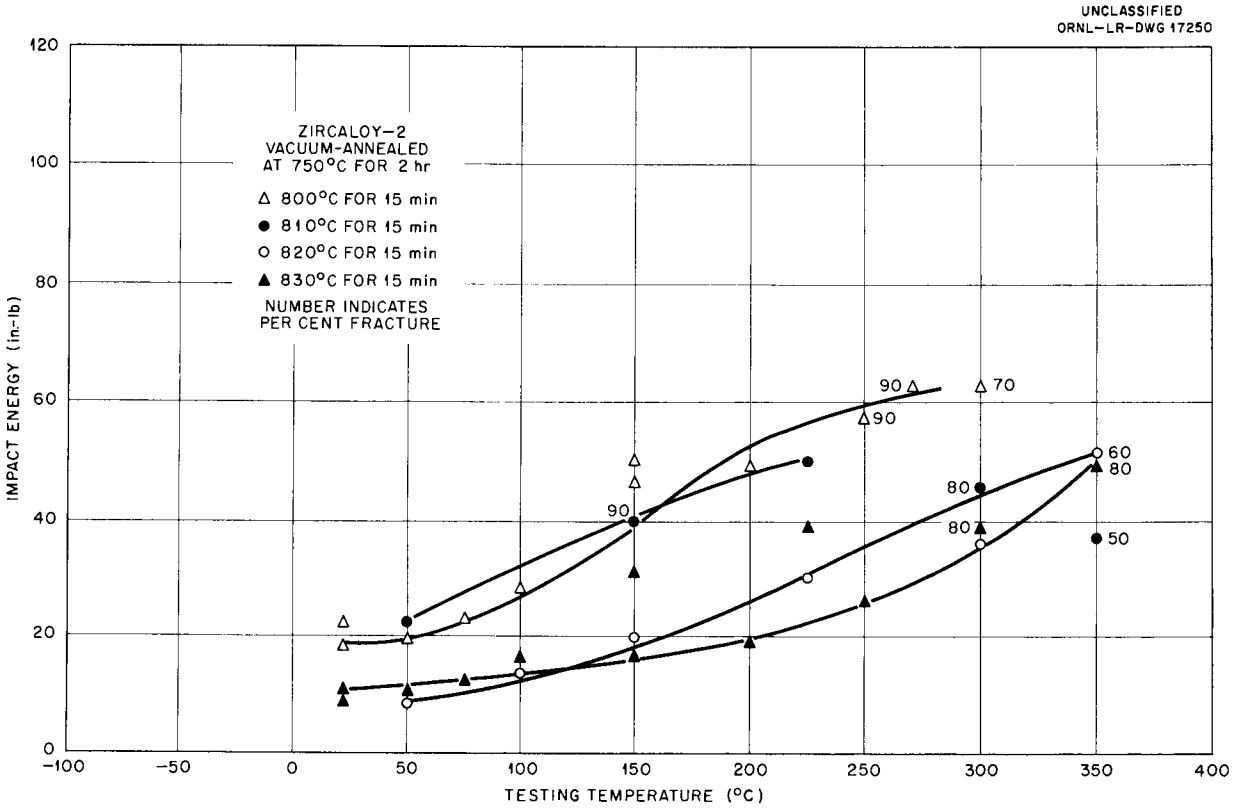

Fig. 14.4. Impact Transition Curve of Zircaloy-2 Heat-Treated in Low Alpha Plus Beta Field.

830°C show more scatter and are not plotted, but they do lie in the region between the two sets of curves. This would be expected from the metallographic work, since the amount of second phase in the boundaries does increase with time. The impact curve for the 830°C, 15-min specimens is an almost exact duplicate of the impact curve for the specimens of in-pile loop GG.[2]

This work indicates that at some time during their history the impact specimens in loop GG underwent a damaging heat treatment. The change in the impact curve was caused by this thermal treatment and not by radiation damage as had been reported.

14.1.3 Oxidation of Zirconium Alloys

The program of study of the growth and structure of oxide films on zirconium has been revived. Previous work on this program had led to the development of the zirconium-niobium alloys.[4] The zirconium-niobium alloys have been shown to develop a higher percentage of the densely packed phase in the oxide than any other zirconium-alloy system and also to possess a greater corrosion resistance. The purpose of the renewed effort is to increase further the percentage of densely packed oxide on the possibility that a corresponding increase in corrosion resistance will be found.

Fifty-three alloys were oxidized in air at 600 and 1100°C. The alloys were used in the form of filings and saw cuttings so that the oxides would be secured free of the metal and in a nondistorted structure. With the binary alloys, only those containing niobium showed appreciable amounts of a densely packed phase in the oxide. To obtain a completely densely packed phase (orthorhombic compound $6ZrO_2 \cdot Nb_2O_5$), it was necessary that the niobium content be 33 wt % and that the temperature of oxidation be high. The amount of compound increased with increasing niobium content.

It was thought that those elements which stabilized the beta phase in zirconium (body-centered

[4] G. M. Adamson *et al.*, *HRP Quar. Prog. Rep. Oct. 31, 1955*, ORNL-2004, p 156–163.

cubic) would promote the formation of a densely packed oxide phase. However, strong beta-stabilizing elements such as palladium and molybdenum, although they yielded other phases, did not diminish appreciably the amount of monoclinic zirconia in the scale. Niobium is the only element that yielded a densely packed oxide scale and that would not produce a high cross section in the resulting alloy.

TABLE 14.1. IMPACT STRENGTHS OF ZIRCALOY-2 SPECIMENS HELD AT 800, 810, 820, AND 830°C AND AIR COOLED

Heat Treatment	Break Temperature (°C)	Impact Strength (in.-lb)	Fracture (%)
15 min at 800°C, air cooled	50	19.0	Complete
	75	22.5	Complete
	100	28.0	Complete
	200	49.0	Complete
	250	57.0	90
	270	62.0	90
15 min at 810°C, air cooled	50	22.0	Complete
	150	40.0	90
	225	50.0	99
	300	34.5	80
	300	45.0	80
	350	37.0	50
15 min at 820°C, air cooled	50	9.0	Complete
	100	13.5	Complete
	150	20.0	Complete
	225	30.0	Complete
	300	36.5	95
	350	51.0	60
5 min at 830°C, air cooled	50	26.0	Complete
	100	16.0	Complete
	150	31.0	Complete
	225	39.0	Complete
	300	44.0	85
	350	34.5	60
15 min at 830°C, air cooled	50	10.0	Complete
	75	12.5	Complete
	100	13.0	Complete
	200	18.0	Complete
	300	35.0	95
	350	50.0	80

The oxides formed at 600°C were not well crystallized, and in no case were any significant amounts of densely packed phase formed. Several studies were made on oxides formed in air at lower temperatures, and the poor degree of crystallinity was even more evident.

The addition of other metals to the zirconium-niobium system does yield higher percentages of compound than would be found with niobium alone. Elements which are not effective as binary additions do help as ternary additions. The same general relationships found with binary niobium alloys also apply to the ternary systems.

The first studies of adherent black oxide films in place on strips of alloys were not fruitful, because the intensity relationships in the patterns were highly distorted. It was impossible to determine in any quantitative fashion the relative amounts of phases present in adherent films. Removal of the film from the metal without changing the relative quantities of the various phases present was found to be necessary to permit evaluation of the phases present.

Work is going on in the evaluation of the phases in films produced by HRT uranyl sulfate solution. The thinner films will be examined by electron diffraction, and the thicker films (produced by 1000 hr of exposure) will be studied by x-ray diffraction. Thirty-three different alloys are under test, 16 of which are zirconium-niobium base. The influence of 17 different elements will be ascertained.

While the data are far from complete, it does not appear that there is sufficient compound in the film of the zirconium-niobium alloys oxidized at low temperatures to explain their increased corrosion resistance.

14.1.4 Development of Simulated Weld and Heat-Affected Structures in Zirconium and Titanium

A contract project is under way at Rensselaer Polytechnic Institute to determine the effect of weld heat on the heat-affected zone of the base metal as to corrosion resistance and mechanical properties. The time-temperature cycle for selected points in the heat-affected zone of the base metal can be duplicated over entire specimens large enough to permit mechanical-property evaluation, $\frac{1}{4} \times \frac{1}{4} \times 4$ in. in size. This will ultimately permit the evaluation of radiation effects on the properties of the weld and the heat-affected zone adjacent to the weld.

To date, 40 tensile specimens, 30 impact specimens, and 60 corrosion specimens have been prepared of A55 titanium. The peak temperatures used in the cycle were 2500, 2200, 1800, 1400, and 1000°F, which reproduce the structures of the heat-affected zone at progressively greater distances from the fusion line of the weld. Zircaloy-2 specimens will be prepared as soon as material is available.

14.2 MECHANICAL METALLURGY

14.2.1 Embrittlement of Alpha Titanium by Hydrogen

The purpose of this study is to determine the effect of aging at 300°C on the room-temperature impact strength of commercially pure titanium containing various concentrations of added hydrogen. A problem resulted from the failure of a titanium sample holder in a corrosion loop and from speculation that in alpha titanium alloys the permissible hydrogen concentration based on data from alpha/beta alloys may be excessive.

This work was started at the University of Florida and has been continued at the Laboratory. The impact samples were machined from A-55 titanium plate. They were of a round subsize Izod type similar to those used in the in-pile loops. The specimens were vacuum annealed and were charged with the desired amount of hydrogen at 800°C.

At present, data are available only on the control specimens, 30 ppm H_2, and the vacuum-annealed specimens, <10 ppm H_2. With these low hydrogen concentrations no appreciable changes were noted with aging times up to 1000 hr.

The data in Table 14.2 are those from only the first point on the proposed curves; however, they do show large changes in impact properties with small hydrogen additions and are in line with data obtained by manufacturers.

TABLE 14.2. ROOM-TEMPERATURE IMPACT STRENGTH OF A55 TITANIUM CONTAINING VARIOUS LEVELS OF HYDROGEN AFTER AGING AT 300°C FOR 24 hr

Hydrogen (ppm)	Room-Temperature Impact Strength (in.-lb)	Remarks
10	52.9	Vacuum annealed at 800°C (completely recrystallized)
30	45.3	As-received condition (cold worked to some extent)
61	27.5	Charged at 800°C
140	13.5	Charged at 800°C

14.2.2 Drop-Weight Testing

The drop-weight test has been developed[5] to determine the highest temperature at which a material will fail in a brittle manner. This test actually determines the highest temperature at which a crack will propagate through a sample undergoing limited deformation. The crack originates in a brittle material that has been deposited on the surface and then had a notch cut in it. A heavy weight is dropped on the sample, whose total deformation is limited to a few degrees. If the base metal is brittle, the crack forms in the starter material and progresses through the entire plate.

During this period, suitable crack-starter deposits have been developed for titanium and zirconium. A brittle deposit on Zircaloy-2 was obtained by using a standard Zircaloy-2 welding rod but moving the Heliarc torch fast enough to expose the molten pool to air. A few preliminary tests with subsize, $1 \times \frac{1}{4} \times 9$ in., plates have indicated a nil-ductility temperature in Zircaloy-2 of about 10°F.

With titanium, a suitable crack-starter deposit was formed by charging the welding rod with hydrogen and welding in the usual manner.

14.3 WELDING DEVELOPMENT

14.3.1 Stainless Steel Welding with Preplaced Inserts

A procedure for welding type 347 stainless steel by using the Electric Boat (EB) type of preplaced inserts was developed previously.[6,7] The advantages of this procedure are that it is easier to

[5] P. P. Puzak, M. E. Schuster, and W. S. Pellini, *Welding J.* 33, 481S (1954).

[6] W. J. Leonard, *HRP Quar. Prog. Rep. Jan. 31, 1956*, ORNL-2057, p 105.

[7] HRP Welding Specification No. 9 – Inert Gas Shielded Arc Welding of Chromium Nickel Stainless Steels Using Pre-placed Root Insert Rings.

qualify the welders and that satisfactory welds may be made with less experienced welders. Its disadvantage is the expense of the shaped inserts.

Preliminary work indicates that a preplaced insert of round or flat cross section can be used for making the root bead in type 347 pipe welds. With these methods, as with the EB method, the wire is fitted between the root faces of butting pipe ends and fused with the tungsten arc into the root of the joint.

Subsequent to the beginning of this work at ORNL, one type of flat insert became available commercially; and it was learned that one manufacturer had successfully used the round insert.

The round insert particularly, but also the flat insert, is more economical than the EB type. At present, the round insert is believed to be more desirable than the flat type, especially on pipe larger than 1 in. in diameter. The round ring can be formed easily from standard weld rod, and the diameter can be changed to facilitate accurate fitup; both are advantages in field work.

On three occasions tungsten-arc welders, unfamiliar with the EB or other insert techniques, made satisfactory root passes with 2 to 4 hr of instruction and practice.

14.4 METALLURGICAL DEVELOPMENT AND SERVICE

14.4.1 Failure of Titanium-Alloy Valve Trim

A metallurgical examination was made of the two titanium-alloy trims which failed in the dump-valve test loop.[8] Photographs of the failed parts and operating descriptions were presented in the previous report. Details of the examination have been reported in ORNL CF-56-8-214. A program to be carried out on subcontract is being formulated for investigating the conditions responsible for initiating the reaction and for determining the conditions required to sustain it.

On each valve poppet, characteristic craters were found, in addition to a more widespread attack which was similar in appearance to cavitation corrosion. Each failure resulted in the consumption of about 4 g of metal.

Spatter, suggestive of violent reactions, was found on the stainless steel valve bodies several inches from the area of the failures. Both the shape and the location of the residue on the poppet indicate that it was molten. In spite of the indications of the presence of molten material, an almost negligible heat-affected zone was found in the base metal under the cavity (Fig. 14.5), indicating rapid reactions.

The scales removed from the cavities on the valve-trim parts were largely $TiO_{1.25}$, whereas spatter that had been transferred from the poppet to the seat was TiO_2 and other oxygen-rich oxides. Ingredients of the stainless steel valve body were found in the residues removed from the valve trim in the case of one of the failures.

The evidence suggested that the craters may have resulted from an initial violent reaction involving pyrophoric material produced under the conditions of testing and that the more prevalent erosive-type cavitation resulted from a subsequent steady-state burning made possible by the dynamic flow of a vapor-liquid medium past the trim parts. It is believed that the failure resulted from special conditions present in this valve test system. While further work and caution are needed, it is not thought that such failures are likely in other titanium applications.

14.4.2 Roll-Cladding Titanium on Steel

Under an ORNL contract, the feasibility of roll-cladding titanium on steel has been demonstrated by Armour Research Institute on an experimental basis. However, at the present time, the total reductions being used are so large as to make them impractical, and sample sizes have been no larger than $3 \times 9\frac{1}{2}$ in. The nature and strength of the bond are now being evaluated.

To circumvent the formation of brittle intermetallic compounds possible in a titanium-to-iron bond, a diffusion barrier of vanadium was originally employed. Although the iron-vanadium phase diagram contains the iron-vanadium compound (sigma), its formation under the conditions of roll-cladding is thought to be sufficiently sluggish to preclude serious difficulty. Since, however, small amounts of a discontinuous phase begin to appear at the vanadium-iron interface, some work is being done with vanadium and copper combined as the diffusion barrier.

Rolling coupons have been largely of the milled-cavity design. Sheets of material are placed in a milled-out cavity of the low-carbon-steel coupon in

[8] D. S. Toomb, A. M. Billings, and H. D. Wills, *HRP Quar. Prog. Rep. July 31, 1956*, ORNL-2148, p 68–69.

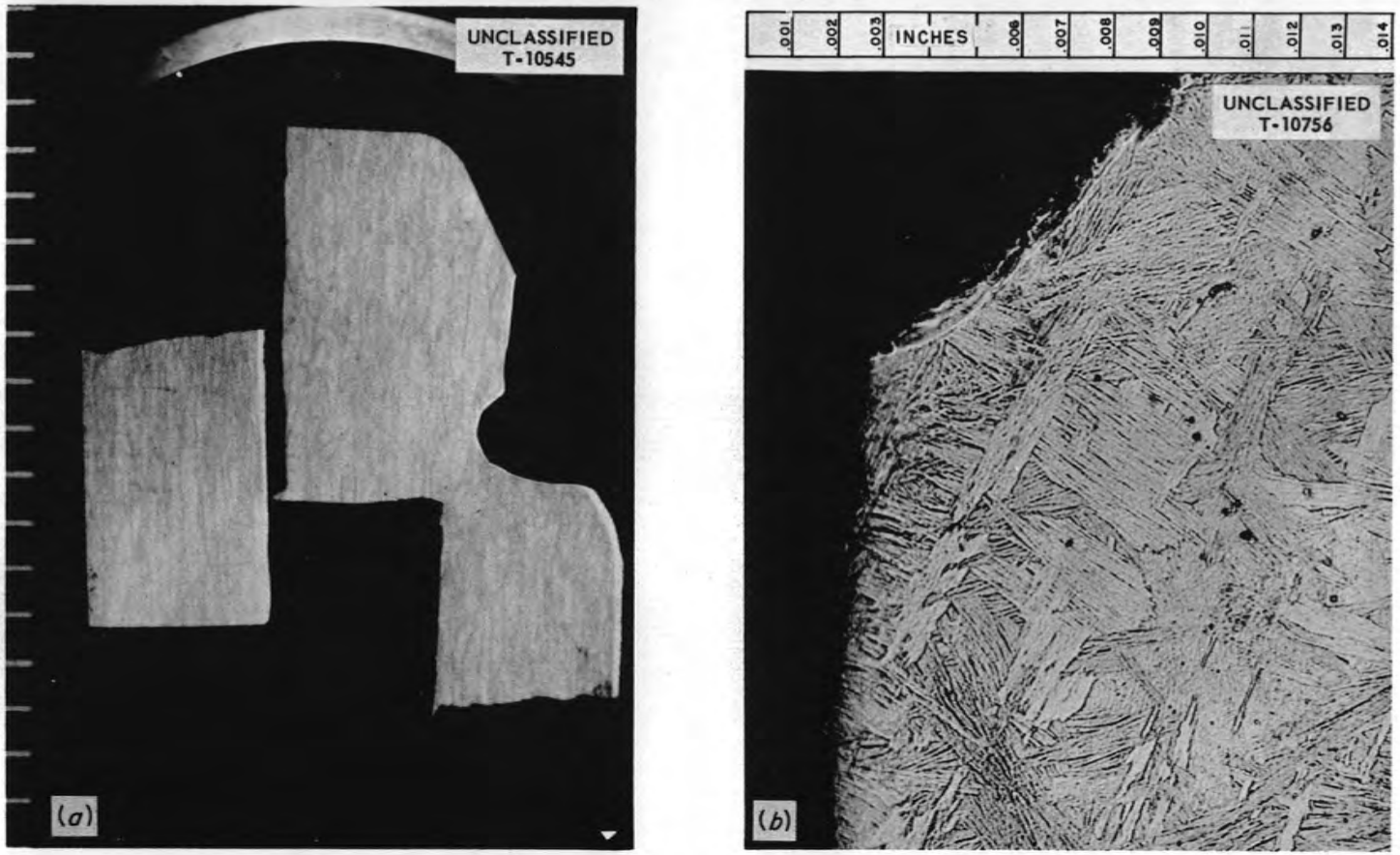

Fig. 14.5. Microstructure of Failed Titanium 6% Al–4% V Valve Poppet. (*a*) Longitudinal cross section of poppet showing extent of heat-affected zone (white-appearing rim) adjoining the cavity. 4X. (*b*) Microstructure (250X) on same cross section where cavity intersects the unaffected poppet surface; the scale at this point is less than 1 mil thick.

the order: 0.007 in. of Cu, when used, 0.025 in. of V, 0.125 in. of Ti, and steel cover plate. The thickness of the steel in the area of the cavity is 0.750 in., and the thickness of the cover plate is about 0.020 in. A steel-to-steel seam weld is made prior to rolling. Although some runs were made with evacuated coupons, this did not prove to be an essential step.

The better bonds to date have been made with about 85% total reductions at 1000°C with the use of reductions of 0.20 in. or, in the last month, 0.10 in. per pass. Samples have been bent slightly less than 180 deg without cracking with titanium in tension and 180 deg with titanium in compression. Cold reductions from 0.102 to 0.070 in. have been made without bond rupture.

It has been demonstrated by bend tests that the added copper barrier gives a definite improvement in the bond. Titanium-clad steel, with vanadium and copper combined as a diffusion barrier, showed no compound formation at any of the interfaces after annealing for 24 hr at 800°C.

Preliminary work was done on cladding titanium on type 304 stainless steel. With vanadium as the sole diffusion barrier, a discontinuous phase (believed to be sigma) is formed at the vanadium–stainless-steel interface as a result of roll-cladding. This phase apparently is eliminated by using copper with vanadium as the diffusion barrier.

The remaining work on this particular project will be confined to studies on the titanium-clad carbon-steel material with a vanadium-copper barrier and will determine the minimum total reduction required for an acceptable bond, the shear strength of the resulting bonds, and the effects of annealing and cyclic thermal treatments on the ductility and strength of the bond.

14.5 INSPECTION DEVELOPMENT

A reliable method for detecting flaws in tubular shapes has been worked out by the nondestructive test development group and has been used, in the HRP and other projects, on some 40,000 ft of tubing. The method employs a commercial pulse-echo ultrasonic instrument and its associated B-scan presentation unit (Fig. 14.6).

Tubing is rotated by a small lathe chuck at approximately 250 rpm; while a high-resolution transducer is translated along the tube at $\frac{1}{4}$ to $\frac{1}{2}$ in. per revolution (Fig. 14.7). The inspection is accomplished while the tubing is submerged in a tank of treated water to provide good ultrasonic coupling (Fig. 14.8). The method relies on the reflection of a 5-Mc pulsed ultrasonic beam by a flaw and the presentation of this reflection on an oscilloscope as a bright diagonal line. Figure 14.9 shows a crack, presented as a function of the tube rotation, 0.007 in. deep on the inside wall of the tubing; Fig. 14.10 shows the B-scan indication of the crack.

For instrument calibration an identifiable naturally occurring crack or, where feasible, a small milled notch is used. The calibration or reference defect must be on the inner surface of the tube.

The immersed ultrasonic method is best suited for the detection of cracklike defects oriented parallel to the length of the tube. It is the best inspection method for small, shallow cracks, and it is the only method that will reliably locate short defects that are less than 5% of the wall thickness. The ultrasonic method also detects scratches; hence, if detection of very small defects is desired, the tubing must be ground to eliminate long shallow scratches.

14.6 EFFECTS OF RADIATION ON STRUCTURAL METALS AND ALLOYS

14.6.1 Equipment and Facilities

Assembly of the elevated-temperature apparatus for use in the HB-3 facility of the MTR is progressing satisfactorily. Elevated temperatures in this experiment will be achieved by gamma heating. There are no auxiliary electric heaters, and therefore specimen temperatures will not be controlled but will be determined by the power level of the reactor and by the geometry of the specimen mounting system. The experiment will contain 187 impact test notches (52 multinotch specimens) and 79 tensile test specimens of 14 alloys. Representative specimen temperatures will be recorded, which will enable the calculation of all specimen temperatures. Designs of other irradiation experiments have been started. The mockup of an apparatus for irradiation of titanium- and zirconium-alloy specimens at 575°F in the MTR was operated, and it was found impractical to build reliable electric heaters for the particular arrangement considered. This part of the experiment is now being redesigned. Apparatus designs for irradiation of test specimens in the HRT, ORR, and ETR

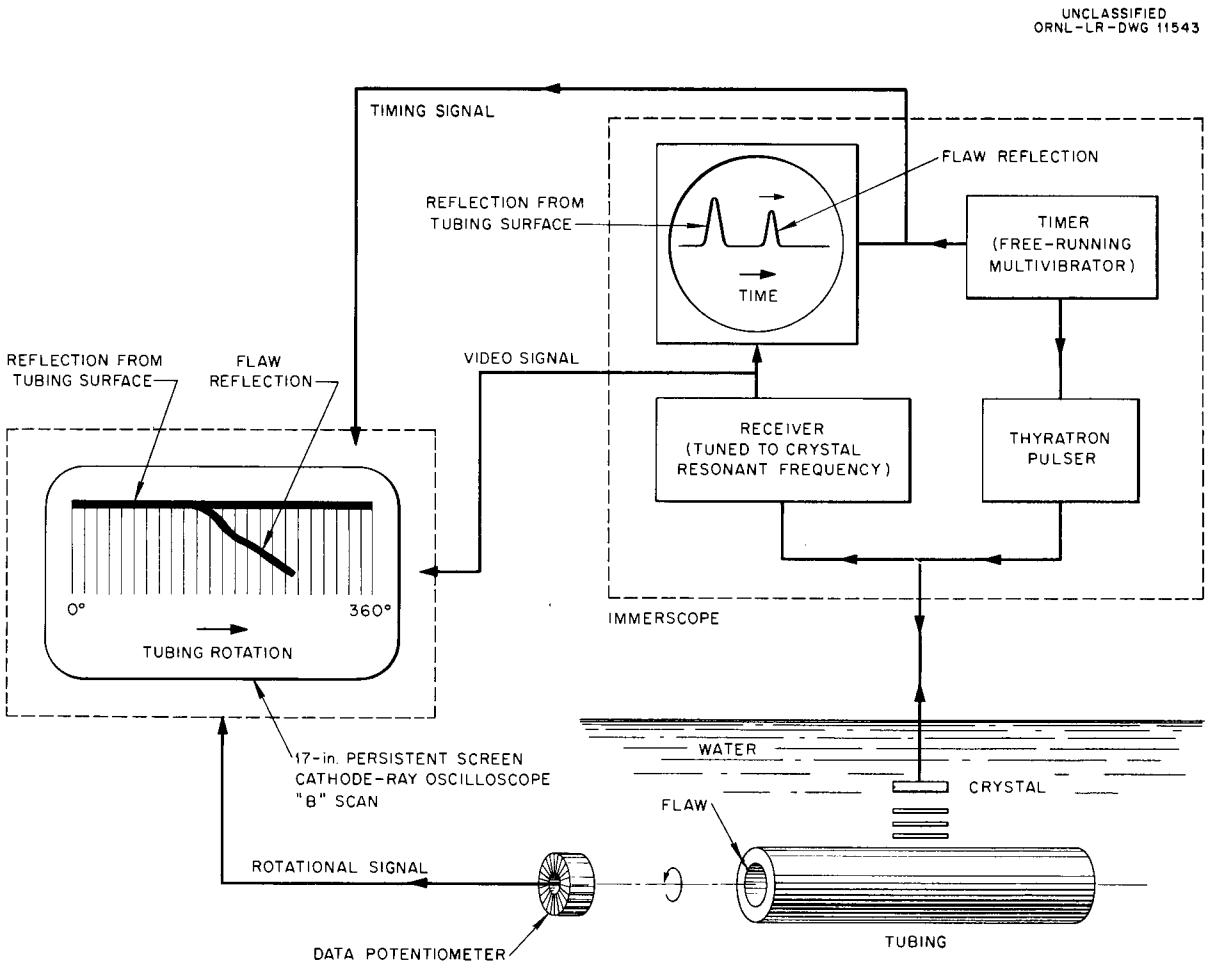

Fig. 14.6. Schematic Diagram of Immersed Ultrasonic Inspection Apparatus for Tubing Inspection.

were started. Assembly of an experiment containing 100 tensile specimens of stainless steel and titanium is almost completed and it will be shipped to the MTR soon for irradiation in an LB piece.

Modification of the Bell Laboratories model impact tester for remote operation is nearing completion, and it will be placed in hot-cell operation upon successful completion of trial tests. A full-size (220 ft-lb capacity), remotely operated, impact tester has been received and will be adapted for specimen temperature control.

14.6.2 Results of Irradiation Experiments

Changes in the properties of metals have been observed after exposure to radiations in nuclear reactors. Among these changes are elevation of the ductile-brittle transition temperature of carbon steels in the notched-bar impact test, increased yield and tensile strengths, decreased ductility in tension testing, and changes in behavior. A number of variables govern the magnitude and type of such irradiation-induced changes in metals. Irradiation variables such as temperature of irradiation, fast-neutron flux, and total neutron dose are parameters which must be studied. The study of variables such as grain size, chemistry, and heat treatment of the materials has shown that at least some of these are important. Furthermore, the effect of specimen size is being investigated because of the need for small specimens for irradiation-effects studies.

The results of irradiation studies that have been reported[9,10] indicate that, at 5×10^{18} *nvt* dose, irradiation at 600° F produces less change in most properties than does irradiation to the same dose at less than 200° F. The results of the one series of tests comparing coarse- and fine-grain ASTM A-106 steels indicate slightly less radiation sensitivity of mechanical properties for the fine-grain alloy than for the coarse-grain alloy. The radiation-induced changes in properties varied for different steels, indicating that the composition of the alloys was important. The chemical or metallurgical factors that caused this variation, however, are not known.

[9] *Papers Prepared for Radiation Effects Review Meeting, Congress Hotel, Chicago, July 31–Aug. 1, 1956*, TID-7515 (Part 2), p 50.

[10] R. G. Berggren and J. C. Wilson, *Recent Data on the Effects of Neutron Irradiation of Structural Metals and Welds*, ORNL CF-56-11-1 (to be issued).

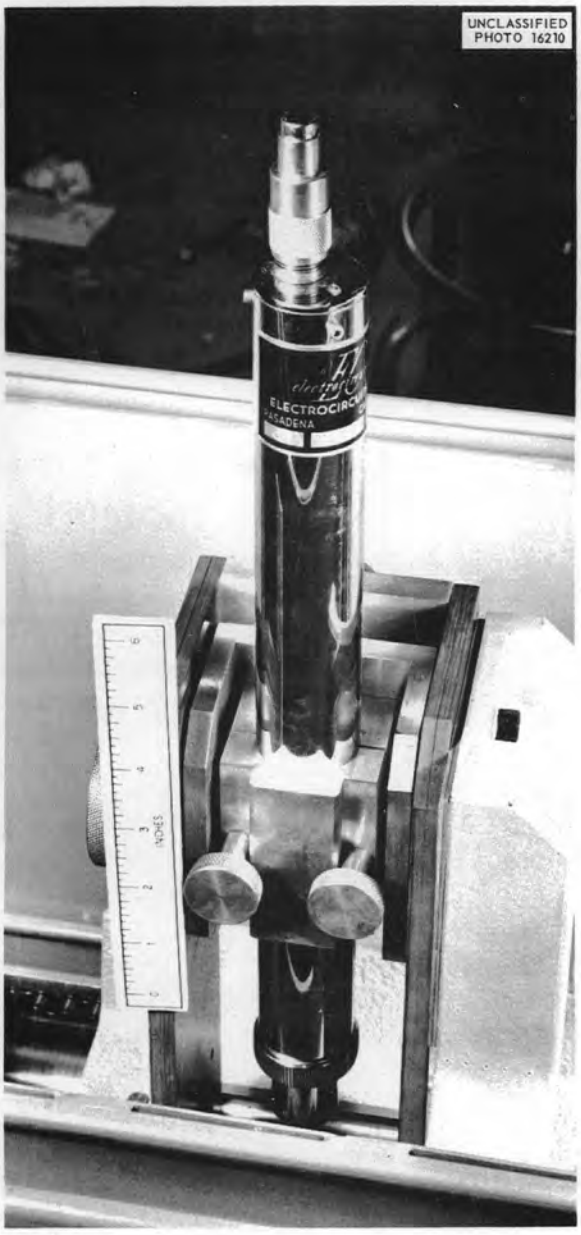

Fig. 14.7. Scanning Dolly and Search Tube Mounting for Immersed Ultrasonic Inspection.

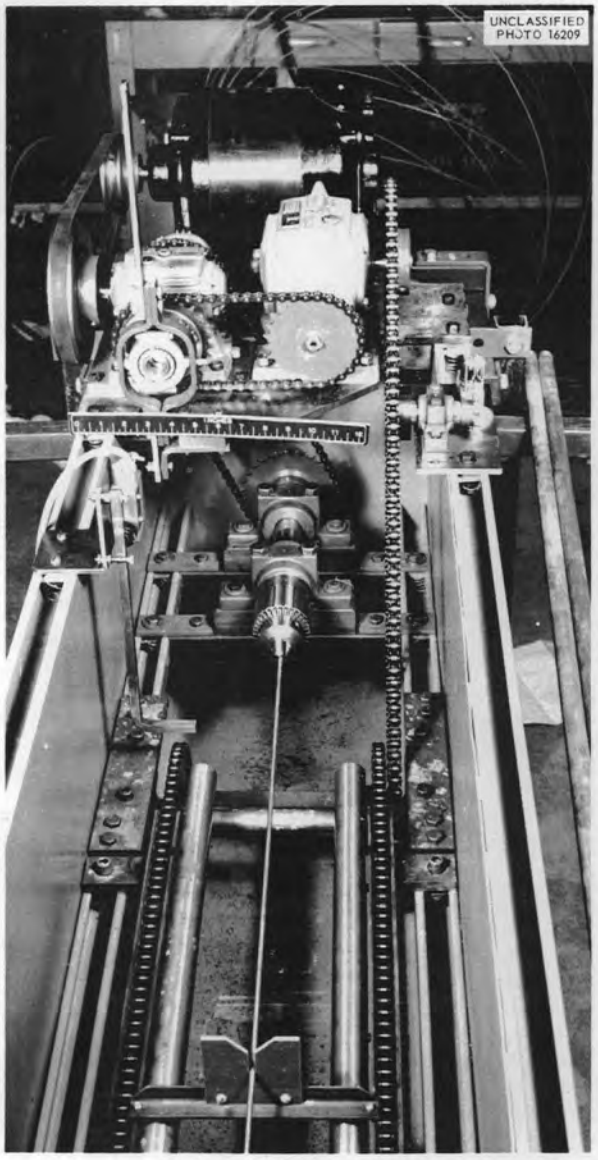

Fig. 14.8. Tank and Drive Mechanism for Immersed Ultrasonic Inspection.

Fig. 14.9. Crack Indication, Presented as a Function of Tube Rotation, of 0.007-in.-Deep Crack on Inside Wall of 0.035-in.-Wall Tubing.

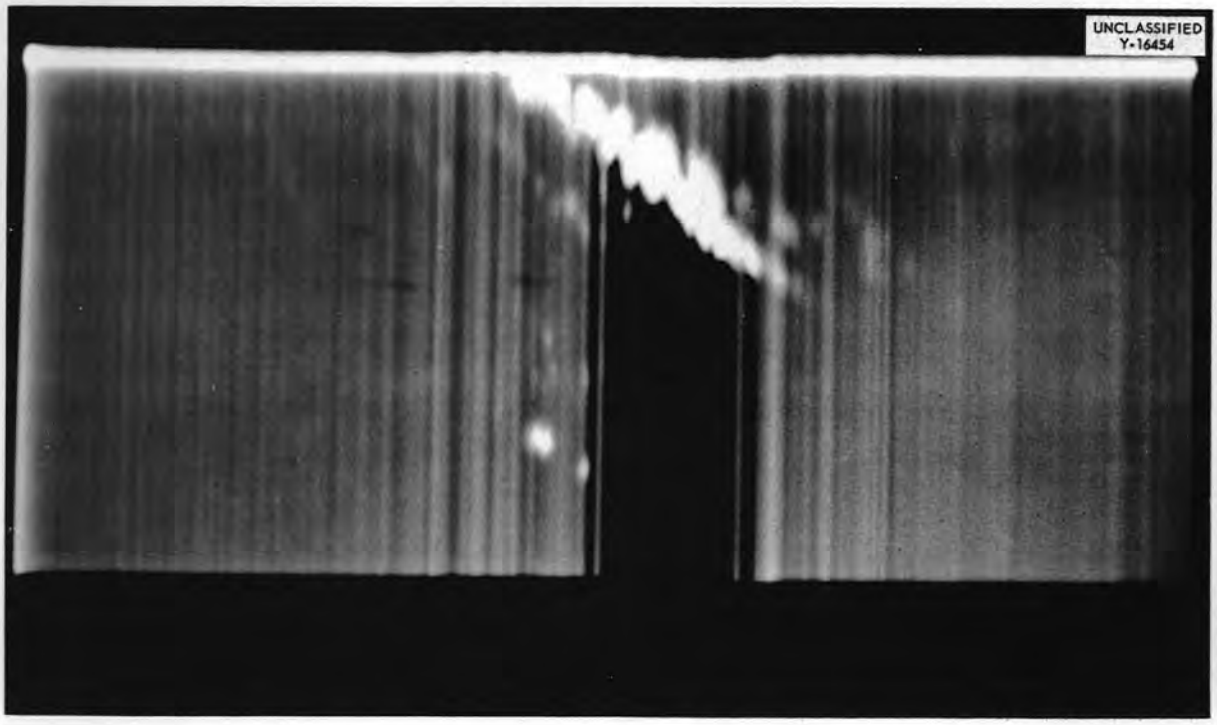

Fig. 14.10. B-Scan Indication of Tubing Crack Shown in Fig. 14.9.

Of particular significance to the HRP are the results of impact and tensile tests on specimens from an irradiated carbon-steel weldment. This weldment was similar to the girth closure of the HRT pressure vessel, although the base plate was possibly from a different heat of steel than the HRT pressure vessel. The carbon-steel base plate conformed to ASME Boiler Code specification SA 212, grade B, firebox quality, and was manufactured to SA 300, aluminum-killed, fine-grain, low-temperature practice. The stainless steel cladding was not included in this series of tests. The portion of the weld from which specimens were taken consisted of multiple passes with a low-hydrogen, carbon steel, coated electrode, E-7016. All specimens were cut from this plate, with longitudinal axes perpendicular to the weld and parallel to the plate face. Tensile and impact specimens referred to as "base plate" were from portions of the SA 212 plate sufficiently remote from the weld to be unaffected by the welding process. The test sections of impact and tensile specimens referred to as "weld" consisted entirely of deposited weld metal and were taken such that no dilution by the deposited iron passes had occurred. The impact specimens referred to as "heat-affected zone" were made such that the notch (and subsequent test fracture) was in the heat-affected zone of the base plate (within $\frac{1}{16}$ in. of the fusion line). Specimens were given no subsequent heat treatment. Chemical analyses and other information on this weldment will be available at a later date.

The results of impact tests on the base plate are shown in Fig. 14.11. Irradiation at 600°F to a dose of about 5×10^{18} *nvt* (>1 Mev) resulted in impact properties almost identical to those of the unirradiated steel. Irradiation at less than 200°F resulted in substantial changes in impact properties.

Results of impact tests on the weld metal and heat-affected zone near the weld are given in Fig. 14.12. The impact properties as measured by transition temperature and "ductile" energy of both the deposited weld and the heat-affected zone were superior to those of the base plate (Fig. 14.11) before irradiation. Both the irradiated weld metal and the heat-affected zone showed the greatest changes in impact behavior that have been observed in this study. However, comparison of Figs. 14.11 and 14.12 shows that the impact characteristics of the weld metal still appear to be better than those of either the base plate or the heat-affected zone at the highest neutron doses.

Tensile tests on irradiated specimens of the base plate and weld metal yielded the results shown in Table 14.3 and Figs. 14.13 and 14.14. The increases in yield and tensile strengths and the reductions in uniform and total elongations shown by the base plate were not unexpected. The load-elongation curves, Fig. 14.13, were conventional in that the steel retained some work-hardening capabilities even at the highest dose. The deposited weld metal, however, showed no observable work-hardening capability at 1.7×10^{19} *nvt* and higher, and local deformation (necking) occurred immediately after initial yielding, Fig. 14.14. The one tensile test of weld metal irradiated at an elevated temperature, Table 14.3, tentatively indicates a lessening of radiation effects due to the elevated temperature. This datum is not conclusive in that it is for a relatively low neutron dose. Data for higher neutron doses will be available at a later date.

It should be noted that the highest doses reported above exceed those to which the pressure vessel of the HRT will be exposed in a period of one year. The dose predicted for the HRT pressure vessel is 1×10^{19} *nvt* (>1 Mev) for one year of operation.[11] In addition, the property changes at an irradiation temperature of 575°F might be expected to be less than those reported for irradiations at less than 200°F.

[11] M. Tobias, *Fluxes at the Inside Surface of the Pressure Vessel as a Function of Lethargy for the HRT as Determined from the Univac Eyewash Code*, ORNL CF-55-5-66 (May 10, 1955).

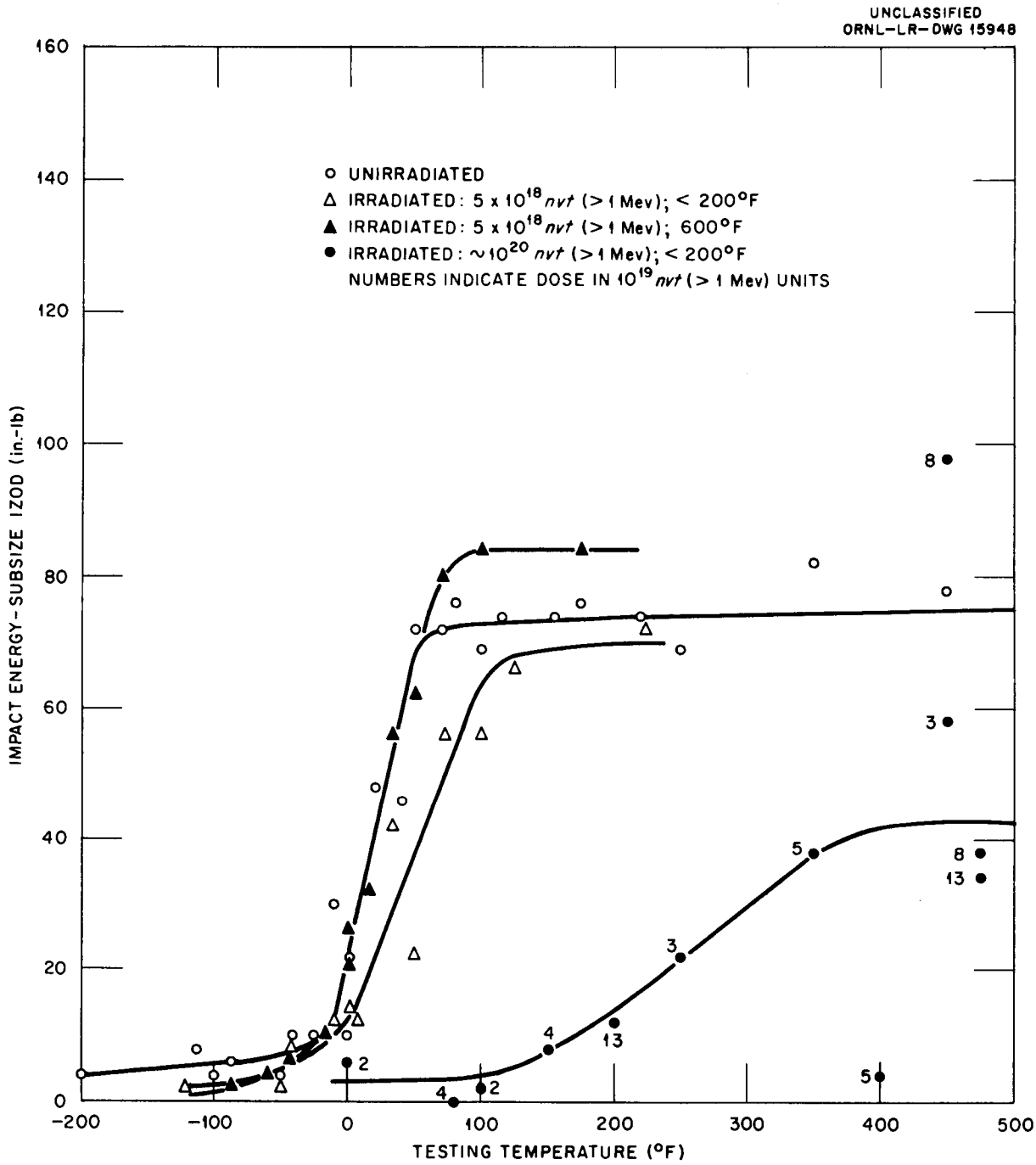

Fig. 14.11. Impact Strength of Irradiated Fine-Grain Carbon-Silicon Steel.

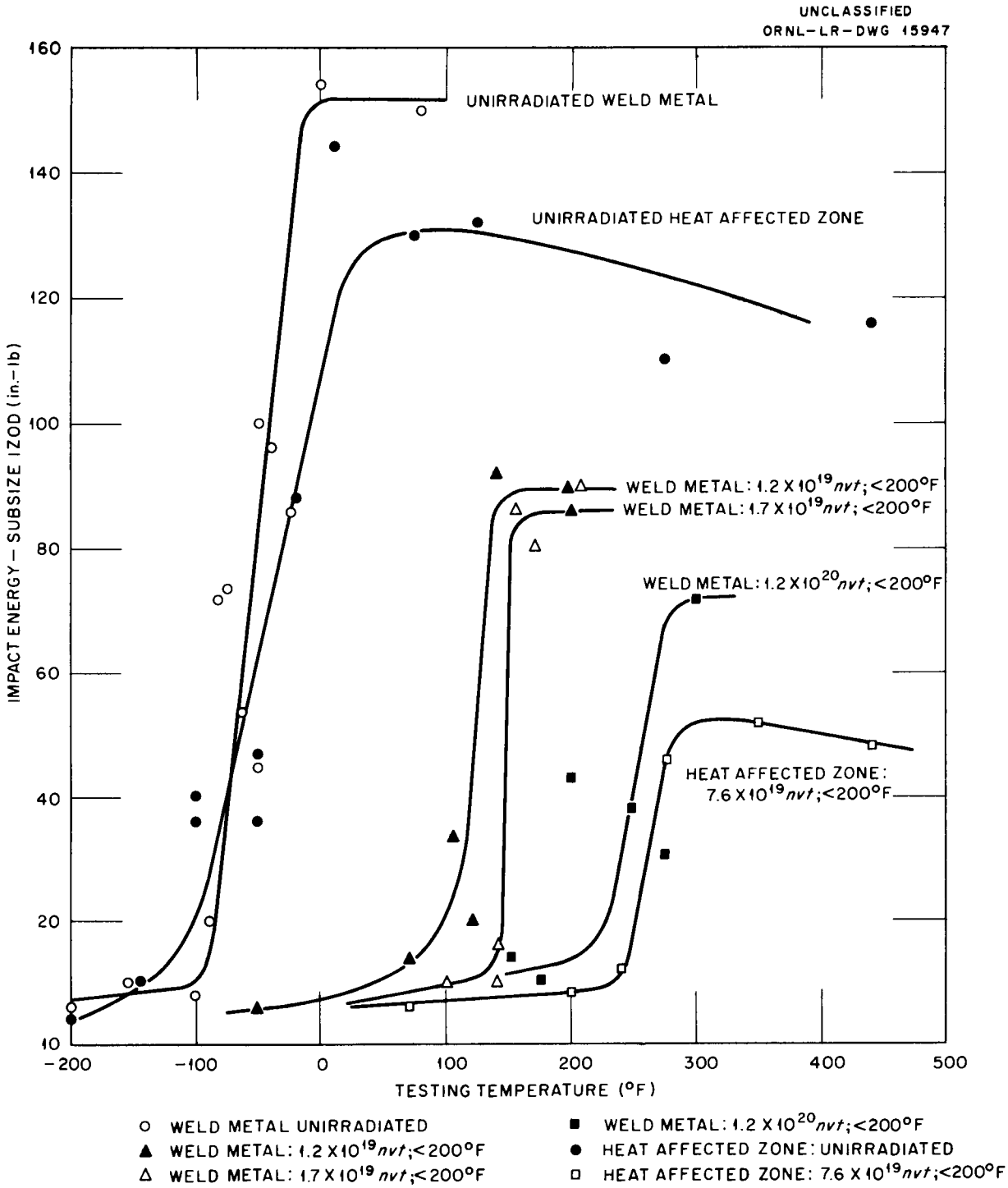

Fig. 14.12. Impact Strength of Irradiated E-7016 Carbon-Steel Weld Metal and Heat Affected Zone of Base Plate.

TABLE 14.3. TENSILE TESTS ON AN IRRADIATED CARBON-STEEL WELDMENT (ITEM 65)

Material	Neutron Dose (*nvt*)	Yield Strength (psi)	Tensile Strength (psi)	Total Elongation[a] (%)	Uniform Elongation[a] (%)
SA-212 base plate	0	41,300	75,400	36	27
	1.7×10^{19}	91,600	98,000	11.6	5.8
	1×10^{20}	108,500	115,800	7	4
E-7016 weld metal	0	57,900	73,200	25.5	15.5
	0	59,000	71,700	24	15
	0	66,500	74,000	20.5	12.5
	5×10^{18}	69,300	77,500	18.5	10.5
	5×10^{18}	61,000	76,700	25	16.5[b]
	1.7×10^{19}	108,700	c	8	0
	1.7×10^{19}	106,500	c	8.5	0
	1×10^{20}	115,000	c	7.5	0

[a]Total elongation in 8 diameters; uniform elongation is elongation before onset of necking; strain rate was 0.05 min^{-1}.

[b]Irradiation temperature, this specimen only, was 600°F. All other specimens were irradiated at less than 200°F.

[c]Load decreased continuously after initial yielding.

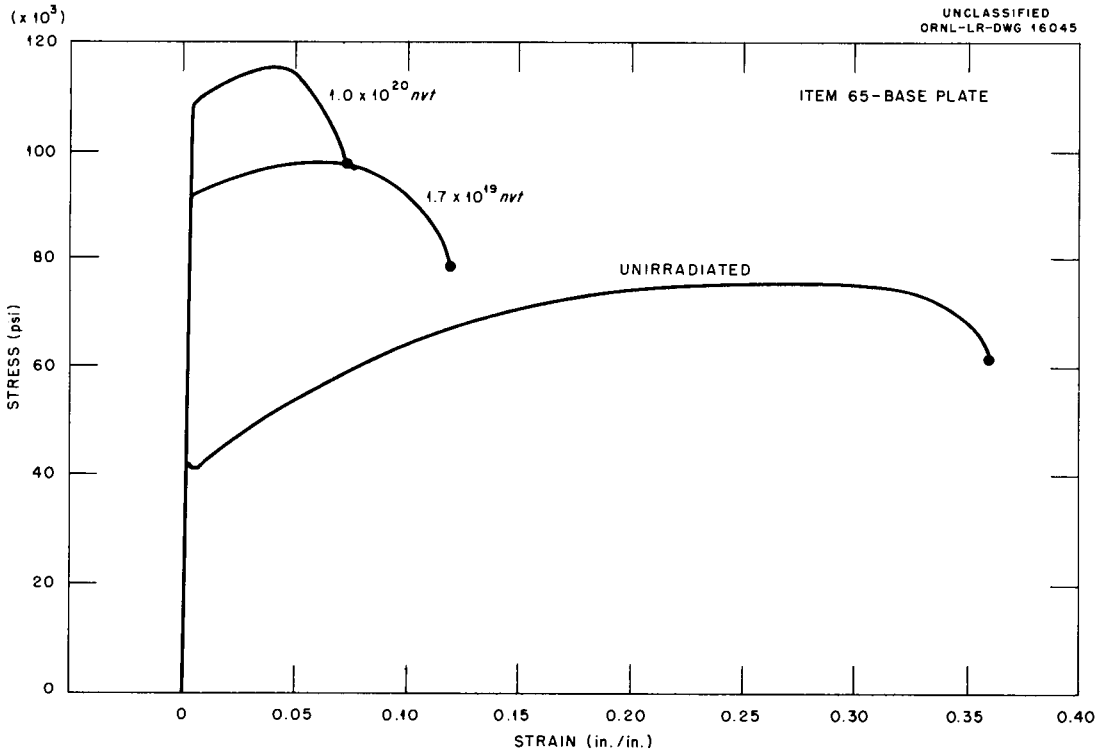

Fig. 14.13. Conventional Tension Stress-Strain Curves for Irradiated Fine-Grain Carbon-Silicon Steel.

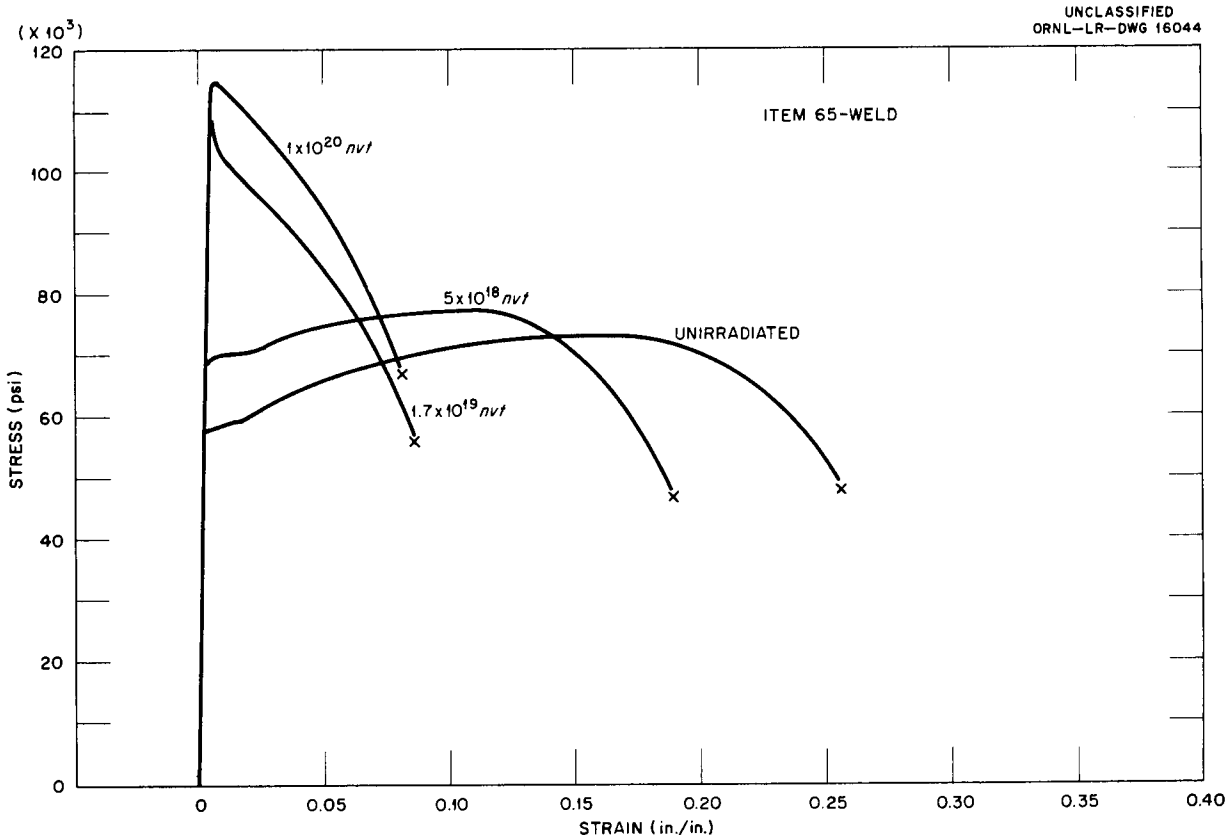

Fig. 14.14. Conventional Tension Stress-Strain Curves for Irradiated E-7016 Carbon-Steel Weld Metal.

Part V

CHEMICAL ENGINEERING DEVELOPMENT

F. R. Bruce

15. FUEL PROCESSING

D. E. Ferguson E. O. Nurmi
R. D. Baybarz N. A. Brown
S. D. Clinton R. A. McNees
S. Peterson

15.1 BEHAVIOR OF SOLIDS IN THE HRT MOCKUP

In further studies of the behavior of solids in circulating-loop systems, the ability of the hydroclone to concentrate solids in the underflow pot and to free the main loop stream of solid particles has been demonstrated with outstanding success. Solids concentrations in the underflow pot that were 1000 times greater than the concentration in the main loop stream have been attained, while the loop fluid has been freed of solids to such an extent that, under equilibrium operating conditions, solids concentrations in the neighborhood of 1 mg/liter have been routinely observed.

The experiments were carried out with preformed solids prepared by precipitating the hydroxides of iron, zirconium, chromium, and copper. The solids were washed with distilled water, autoclaved in 0.04 *m* UO_2SO_4 at 300°C for 16 hr, and suspended in 0.02 *m* UO_2SO_4; then mixed rare-earth sulfates with Nd^{147} tracer were added. While the hydroclone circuit of the mockup was in operation, 345 g of solids was injected into the loop in four daily aliquots. Nine hours after the last portion of solids was added, the hydroclone loop was shut off and the underflow pot drained. At this time the underflow pot contained 325 g of solids and the solids concentration in the loop was 0.560 g/liter. After an additional four days of hydroclone operation, 75 g of solids had been collected and the loop solids concentration was 0.170 g/liter. Continued operation of the hydroclone circuit gradually lowered the solids concentration in the loop to about 1 mg/liter. It should be noted that, although more solids were collected than were put into the system for this test, a heel of solids remained from previous tests, and these solids were partially brought into circulation by large fluctuations in temperature and operating conditions during this series of tests. Operation of the hydroclone circuit for a week with the loop containing about 1 mg of solids per liter and no solids added resulted in the collection of about 130 mg of solids per day. Corrosion of the 65 ft^2 of stainless steel in the system at a rate of 1.5 mpy should produce 6.8 g of corrosion-product oxides per day, but these did not appear in the circulating loop liquid.

Of the Nd^{147} activity added as tracer for the mixed rare-earth sulfates accompanying the mixed oxides added to the loop, 49% remained in the circulating loop stream. If all the activity was in solution (filtered samples could not be taken), the solubility of $Nd_2(SO_4)_3$ would be 45 mg per kilogram of H_2O. This compares favorably with a predicted value of 40 mg per kilogram of H_2O based on previous laboratory data. Of the remaining activity, 39% appeared in the underflow pot, while 12% was unaccounted for. Thus 75% of the precipitated $Nd_2(SO_4)_3$ was collected in the underflow pot, although experience with smaller loops had shown that only 15% was collected in the underflow pot, with 85% of the precipitated rare earths being collected in the heat exchanger.

The behavior of a dilute suspension of solids in the mockup loop was studied by injecting 9.18 g of preformed solids into the loop and sampling the loop system periodically. Two runs were made with the hydroclone circuit operating. In all three cases a plot of the logarithm of the solids concentration against time gave a straight line. The time required to reduce the solids concentration by a factor of 2 was 1.2 hr with the hydroclone circuit operating and 2.5 hr with the hydroclone circuit not operating.

15.2 REACTOR SOLIDS DISSOLUTION

Continuation of the development work on dissolving solids simulating those expected from chemical-plant operation in conjunction with the HRT has produced a more attractive method – alternate treatment with 10.8 and 4.0 *M* sulfuric acid solutions – than the methods reported previously.[1] This method eliminated the need for

[1] D. E. Ferguson *et al.*, *HRP Quar. Prog. Rep. July 31, 1956*, ORNL-2148, p 117.

mechanical agitation during digestion because at the lower acid concentration the solids already converted to the soluble sulfate form dissolved, and any unreacted solids remaining were exposed afresh to attack by 10.8 *M* sulfuric acid when the solution was reconcentrated. In laboratory experiments 10 g of solids was boiled with 50 ml of 10.8 M sulfuric acid for 4 hr, and then enough water was added to reduce the acidity to approximately 4 *M*. After a 1-hr reflux the water was distilled off until the acidity was again 10.8 *M*; then the digestion was continued for 4 hr. Again water was added and the dilute solution was refluxed for 1 hr, after which the amount of undissolved solids was determined. This dissolving method gave results fully as satisfactory as those obtained when mechanical stirring was used.

Two dissolvings on a unit-operations scale have been made. In the first test 5 ml of 10.8 *M* H_2SO_4 per gram of solids was used for about 360 g of solids. After three concentration-dilution cycles, ending with a 5.8 *M* H_2SO_4 solution, undissolved solids remained. Malfunction of experimental equipment with an unmeasured loss of water during heating resulted in an acid concentration greater than 15 *M* during some portion of the heating time. As a result, the solids remaining, although converted to the sulfate form, were only slowly dissolved in fresh 4 *M* H_2SO_4. In the second dissolving, 15 ml of 10.8 *M* H_2SO_4 was used for each gram of solids and the mixture was given three temperature-concentration cycles. Spectroscopic examination of the undissolved residue showed that only traces of the metals initially present in the solids remained in the residue. The undissolved residue was almost entirely silica as a result of the equipment used and an accidental inclusion of broken glass. Therefore it is not certain that three concentration cycles are required for a dissolving; further tests may show that only two cycles, as indicated by laboratory experiments, will be necessary in order to achieve satisfactory dissolution.

15.3 REPROCESSING OF UO_2SO_4

The precipitation of UO_4 from a solution of UO_2SO_4 containing soluble fission and corrosion products offers promise as a method for processing uranium withdrawn from a homogeneous reactor prior to its return to the fuel system of the reactor. In the HRT chemical plant the solids accumulated in the underflow pot will be dissolved, only in order to get analytical data necessary to evaluate reactor and chemical-plant operation. However, in processing the fuel taken from a large-scale reactor, the objective will be to return the uranium to the reactor system as rapidly as possible, and, if possible, it will be done in a D_2O system. High decontamination of the uranium is not necessary. One process envisioned would consist in taking the solids and liquid from the hydroclone underflow pot and lowering the temperature to less than 100°C and then separating the solids and washing them free of soluble uranium. The solution would contain soluble fission and corrosion products such as nickel, rare earths, and cesium in addition to uranium. Addition of a peroxide compound would then precipitate UO_4 and provide separation from undesired elements. After separation and washing of the solid UO_4, dilute D_2SO_4 would be added and the peroxide in solution destroyed by heating.

In preliminary experiments in the laboratory 99.9% of the uranium in a solution initially 0.17 *m* UO_2SO_4, 0.35 *m* $NiSO_4$, and 0.1 *m* H_2SO_4 was precipitated, when the pH of the solution was properly controlled, by addition of a peroxide compound. Either Na_2O_2 or H_2O_2 was a satisfactory source of the peroxide, but when H_2O_2 was used, addition of NaOH was necessary to control the pH of the solution. The solubility of UO_4 was strongly dependent on pH (Fig. 15.1). In the experiments using H_2O_2 and an NaOH solution to adjust the pH, better results were obtained by adjusting the pH of the solution after addition of the peroxide rather than before.

With either method a satisfactory separation of uranium from nickel and neodymium was obtained. With the H_2O_2 method the respective decontamination factors were 50 and 16; for the Na_2O_2 method the factors were 12 and 7, respectively. The smaller decontamination factors with the Na_2O_2 method probably result from the higher pH necessary for complete uranium precipitation.

15.4 IODINE CHEMISTRY

The effect of gamma irradiation on the oxidation state of iodine in homogeneous reactor fuel solution at 100°C has been found to depend on the irradiation intensity and on the composition of the gas phase in contact with the solution.

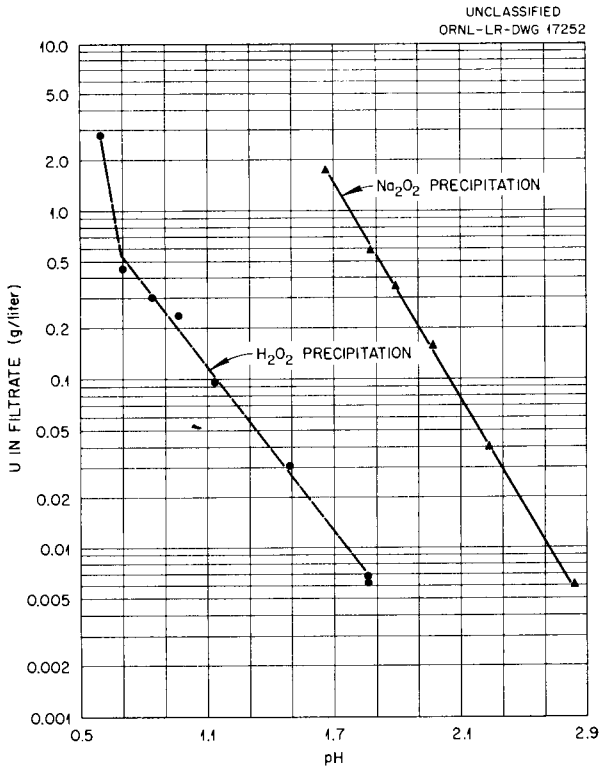

Fig. 15.1. Effect of pH on Precipitation of Uranium Peroxide from Simulated Uranyl Sulfate Fuel Solution.

When simulated fuel solution (0.02 *m* UO_2SO_4, 0.005 *m* H_2SO_4, 0.005 *m* $CuSO_4$, and 1.0×10^{-5} *m* KI) was kept overnight at 100°C in a stainless steel bomb, 15 to 50% of the iodine was present as elemental iodine; the remainder was iodide ion. The variation in this proportion appears to have been unrelated to the atmosphere in the bomb. When the bomb was closed with atmospheric air at room temperature, exposure (at 100°C) to radiation of 8×10^{17} ev/min per gram of H_2O (2 w/liter) from Co^{60} resulted in oxidation until a steady state was reached after about 3 hr; 1 to 2% of the iodine remained in the elemental state and the balance was iodate. At an intensity of 2×10^{17} ev/min per gram of H_2O, a similar but slower oxidation took place, until only 0.1 to 0.5% of the iodine was elemental after about 10 hr. The remainder was nearly all iodate, but it appeared to contain a small quantity of iodide, diminishing as the radiation was prolonged. When, after this exposure at lowered intensity, the solution was exposed at the higher intensity, the elemental-iodine content increased in less than 1 hr to the same steady state found in experiments started at that intensity. This dependence of steady state on intensity suggests that, at the high level expected in the HRT dump tank, iodine will be largely elemental.

When a hydrogen-oxygen mixture, instead of air, was sealed in the bomb with the solution, the oxidation was less rapid and less complete. Increasing the H_2/O_2 ratio decreased the rate of oxidation (Fig. 15.2). At an H_2/O_2 ratio of 3/1, the oxidation appeared to stop after reaching about 90% I_2, 5% I^-, 5% IO_3^-. In another experiment with different initial conditions (77% I_2, 15% IO_3^-, 8% I^-) and an H_2/O_2 ratio of 2/1, iodine in the solution was reduced to 96% iodide in 1.5 hr, and then oxidized to 70% I_2–30% IO_3^- in another 6 hr.

15.5 VOLATILITY OF IODINE UNDER REACTOR CONDITIONS[2]

In two different dynamic loop runs in which the rate of stripping of iodine from simulated reactor fuel was measured, the iodine concentration was reduced to one-half its original concentration in 13 min. Based on the previously reported[3] distribution coefficient of 7 for elemental iodine between vapor and liquid and the different flow rates used in the two runs, the calculated half-time would have been 15 and 17 min (assuming first-order kinetics). Conversely, using the stripping-rate data, the iodine distribution coefficient was calculated to be 7.6 and 8.4 for these two runs. In a third run a stripping rate about twice as fast as the rates obtained in the other two runs was observed, but the flow-rate measurements involved were of doubtful accuracy.

All three runs were made at 230°C and 1000 psi. The ejector loop was operated with a liquid flow rate of 1.4 to 1.8 gpm and a stripping-gas flow rate of 0.33 to 0.43 g-mole/min. The gas/liquid volume ratio ranged from 0.033/1 to 0.051/1. The ejector loop used[4] had previously given nonreproducible results, but prior to this work it was modified by replacing the liquid-vapor scrubber system with an absorber of silvered Alundum pellets.

---

[2]Vitro Laboratories, *HRP Quarterly Progress Report: July 1–September 30, 1956*, KLX-10045.

[3]H. F. Reichard *et al.*, *Homogeneous Reactor Fuel Reprocessing Quarterly Progress Report: July 1–September 30, 1955*, KLX-10012; summarized in *HRP Quar. Prog. Rep. Oct. 31, 1955*, ORNL-2004, p 196.

[4]H. F. Reichard *et al.*, *Homogeneous Reactor Fuel Reprocessing Quarterly Progress Report: October 1–December 31, 1955*, KLX-10020.

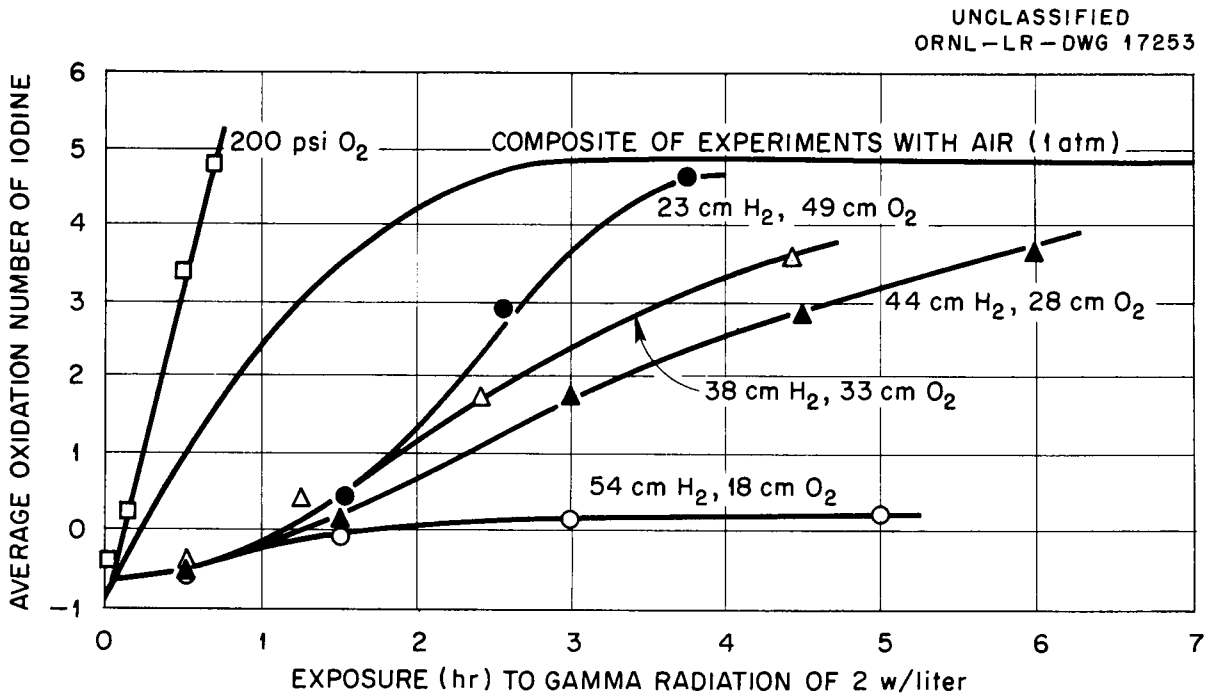

Fig. 15.2. Effect of Atmosphere on the Behavior of Iodine in Fuel Solution Under Gamma Irradiation at 100°C.

In a second series, consisting of two runs, the specific rate constants for conversion of iodate to iodine at 220°C in simulated homogeneous reactor fuel were 5.8 and 6.6 min^{-1}. Assuming that the conversion rate was first order with respect to iodate concentration, the time for 50% conversion of iodate to iodine was approximately 0.1 min. For these experiments, feed containing 7.89×10^{-4} mole of iodate per liter was pumped into the loop at a rate of 4.7 ml/min in the first run and 5.5 ml/min in the second run. Liquid was withdrawn from the loop at a rate of 5.0 ml/min in both runs. At steady state the iodate concentrations in the two runs were 6.4×10^{-7} and 6.6×10^{-7} mole/liter, and the respective iodine concentrations were 4.8×10^{-5} and 4.2×10^{-5} mole/liter. These data correspond to an iodine/iodate mole ratio of 75/1 and 64/1.

Vapor-liquid iodine equilibrium studies were continued in an Othmer still operating at atmospheric pressure and 100°C to simulate conditions in the HRT dump tanks and recombiner condensate system. The K values for water solutions at pH 4.18 and 4.12, containing 1 ppm of iodine, were 0.007 and 0.003, respectively (K = mole fraction of I^0 in the vapor phase/mole fraction of I^0 in the liquid phase). In the still bottoms, 95 to 98% of the iodine was in the elemental form. The K values compare well with the values of 0.010 reported[2] for water solutions containing 13 ppm of iodine. With clean simulated feed solution a K value of 0.314 was obtained, as compared with a previously reported[5] K value of 0.37. The addition of ferric iron (0.36 g/liter), ruthenium (0.05 g/liter), and type 347 stainless steel turnings (0.55 g/liter) to fuel solution gave apparent K values of 1.8, 0.62, and 0.20, respectively. The possibility of these contaminants interfering with the analytical methods used to determine iodine valence states is being investigated.

The iodine saturation capacity of the platinized Alundum pellets to be used in the HRT recombiner was found to be 5.53 mg/kg at 350°C and 7.6×10^{-3} mm pressure of iodine and 15.6 mg/kg at 500°C and 6.7×10^{-3} mm. Since the HRT gas recombiner contains 36 lb of such pellets, the iodine holdup in the recombiner is 0.275 day's production at 350°C, or 0.77 day's production at

[5]Vitro Laboratories, *HRP Quarterly Progress Report: April 1–June 30, 1956*, KLX-10034; summarized in *HRP Quar. Prog. Rep. July 31, 1956*, ORNL-2148, p 117.

500°C with the reactor operating at a power of 5 Mw. For these experiments a stream of oxygen, water vapor, and iodine was passed through a bed of pellets until the pellets were saturated with iodine, after which the iodine content of the pellets was determined by standard methods.

The stability of AgI on silver-coated Alundum pellets in an oxygen–water-vapor atmosphere was determined as a function of temperature. At 350°C silver iodide was stable, but decomposition was noted at higher temperatures. At 550 and 700°C approximately 78 and 85%, respectively, of the AgI was decomposed in 30 min. Thus a decomposition half time of 14 or 11 min is indicated. Similar tests will be made with pellets iodized at 350 to 500°C by passing iodine vapor over the pellets instead of precipitating AgI on the pellets at room temperature and then heating to the desired temperature.

Preliminary investigations were made on the feasibility of using copper oxide as an absorber for iodine at elevated temperatures. At temperatures up to 242°C copper oxide removed iodine from an oxygen–water-vapor–iodine gas phase; at temperatures between 240 and 295°C the reverse reaction was observed and iodine was liberated to the gas phase. The usefulness of the copper system thus seems to be limited to systems operating at temperatures below 240°C for the absorption cycle.

16. PLUTONIUM-PRODUCER BLANKET PROCESSING

D. E. Ferguson E. O. Nurmi W. E. Unger
R. D. Baybarz P. A. Haas
J. M. Chilton R. E. Leuze
S. D. Clinton W. F. Schaffer

The study of plutonium-producer blanket chemistry included investigation of plutonium behavior in uranyl sulfate at 250°C contained in pyrex, titanium, and type 347 stainless steel and the dissolution of corrosion-product oxides.

Processing of the plutonium-producer blanket, to remove precipitated plutonium and fission and corrosion products, will be studied on a large scale in loop P-1. Fabrication of this loop (Figs. 16.1 and 16.2) is complete, and installation of the loop and accessory equipment in Building 4501 is under way. The proposed program includes degreasing and testing, followed by operation with H_2O and UO_2SO_4 solution before plutonium is added. A prototype of the pressurizer was operated with an H_2O-H_2-O_2 system with no equipment failures.

16.1 HYDROLYSIS OF ZIRCONIUM SULFATE IN 0.17 *m* UO_2SO_4

When a solution of zirconium sulfate (containing 5 g of zirconium per kilogram of H_2O in 1.6 *m* UO_2SO_4) was slowly heated to 250°C, the concentration of zirconium in the solution began to decrease at 122°C and decreased sharply as the temperature

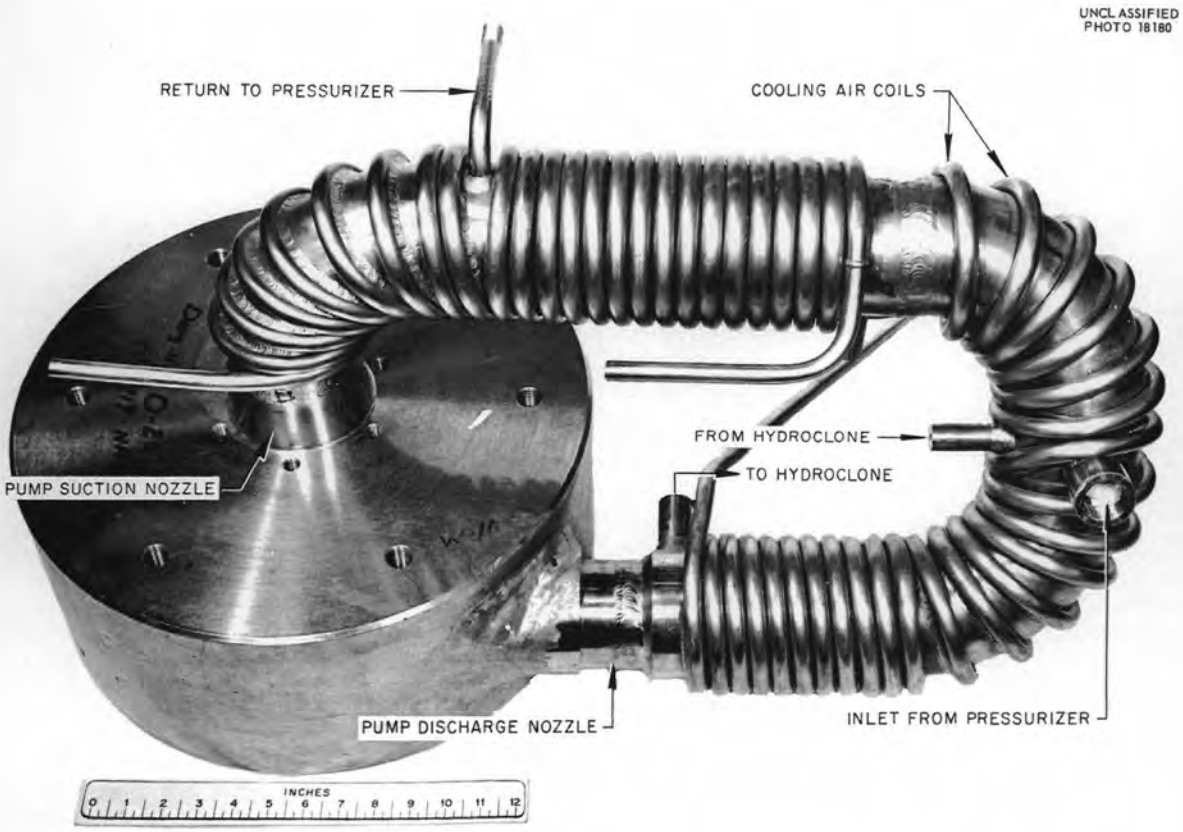

Fig. 16.1. Pump Scroll and Main Flow Circuit of Loop P-1.

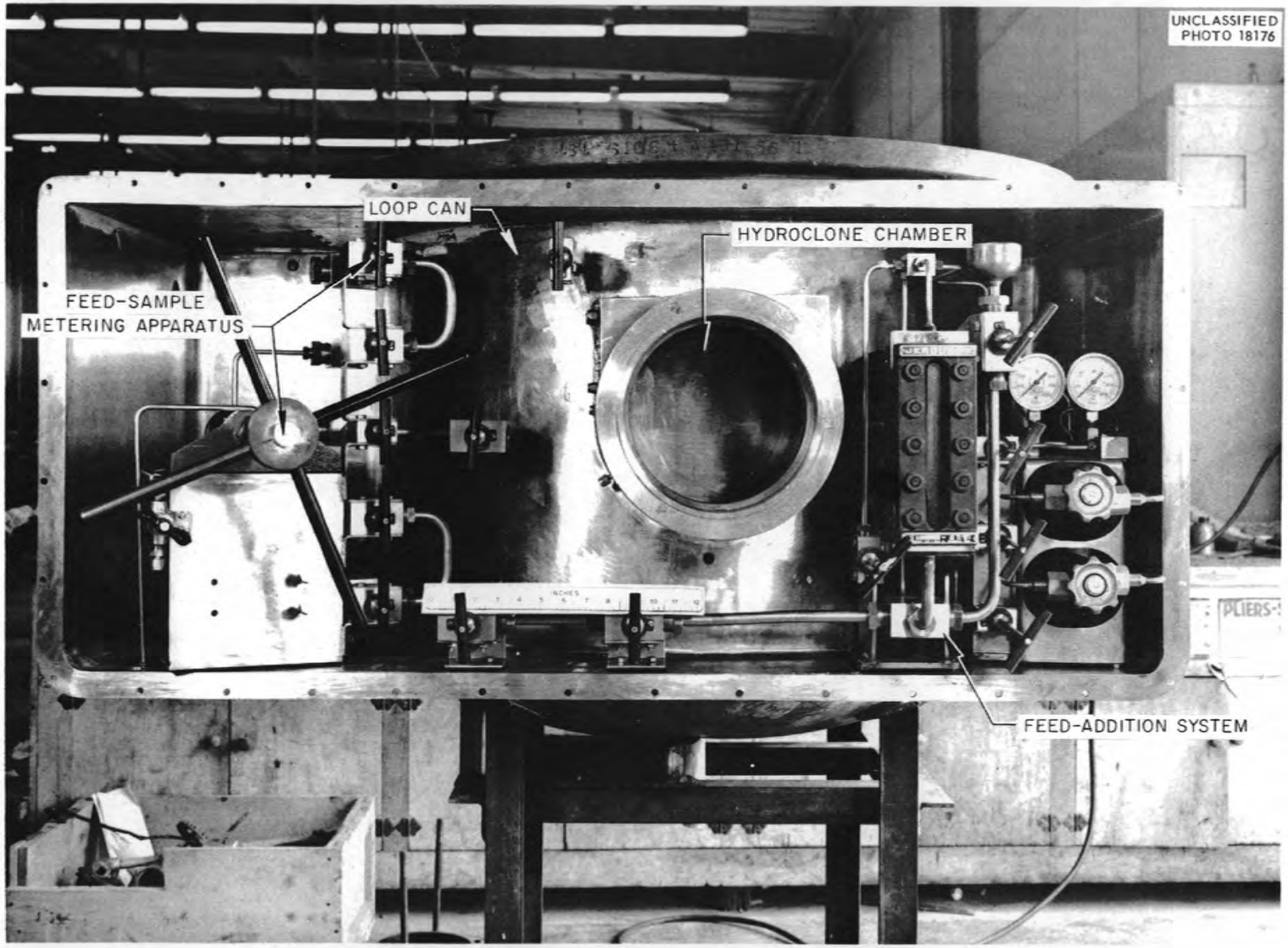

Fig. 16.2. Can Half of Loop P-1 Glove Box with Accessory Equipment Partially Installed.

of the solution was raised (Fig. 16.3). Since this was only a scoping experiment, it is not certain that equilibrium conditions existed at the various temperatures noted; therefore the data do not necessarily represent equilibrium solubility.

16.2 PROTOTYPE-PRESSURIZER TESTS

In tests with an H_2O-H_2-O_2 system in a prototype (Fig. 16.4) of the loop P-1 pressurizer, five rapid reactions, as indicated by a pressure recorder chart, were observed. Two of these, with about 20 and 27% stoichiometric H_2-O_2 mixtures, occurred as sudden pressure decreases during operation with a platinum resistance coil. The other three were initiated by heating a nickel coil in mixtures which were 35% or more stoichiometric H_2-O_2. These resulted in an audible rumble and almost instantaneous pressure-recorder jumps of 750 to 1000 psi above the initial pressure, followed by decreases to 150 to 300 psi below the initial pressures. No

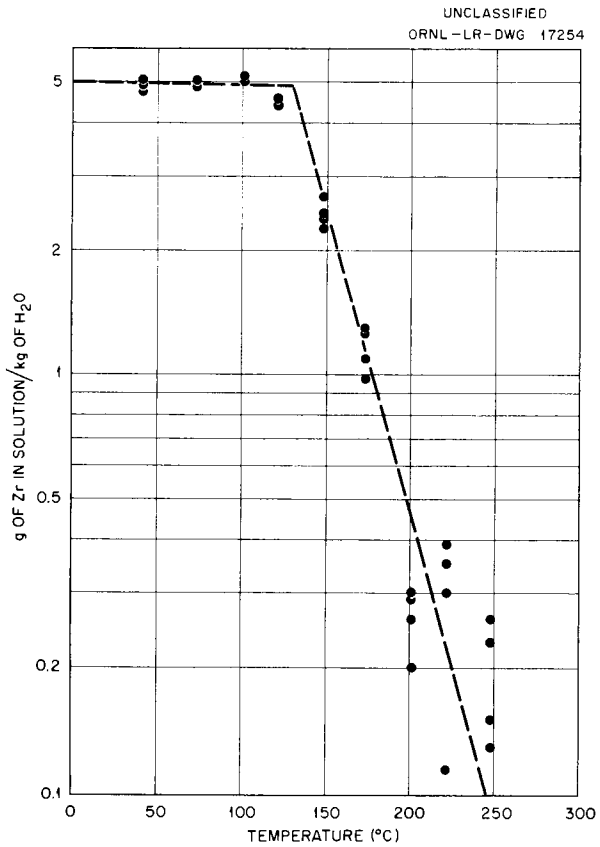

Fig. 16.3. Hydrolysis of $Zr(SO_4)_2$ in UO_2SO_4 Solution; 390 g of Uranium per Kilogram of H_2O.

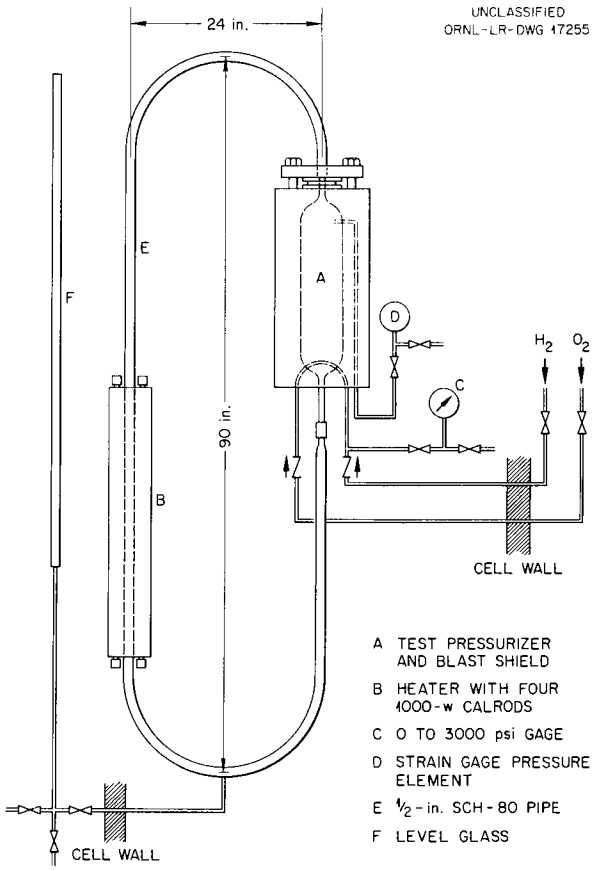

Fig. 16.4. Pressurizer Test Loop.

rapid reactions occurred for periods of up to 36 hr with 30 to 45% stoichiometric H_2-O_2 when a platinum coil or a heated nickel coil was not present. No equipment failures were observed as a result of the five rapid reactions observed.

The loop was started with H_2O only. After the desired temperature, usually 260°C, was reached, one gas was added. If the loop held this gas without leakage, the second gas was added to give the desired percentage of stoichiometric H_2-O_2, with the steam and excess gas considered as diluents. A spark plug was used for the leads to a resistance coil, which was heated electrically to ignite any combustible mixtures.

16.3 PLUTONIUM BEHAVIOR IN UO_2SO_4 SOLUTION AT 250°C

16.3.1 Pyrex Containers

No PuO_2 was formed by heating 1.4 *m* UO_2SO_4 at 250°C in a pyrex-lined autoclave under 100 psi O_2 and 200 psi H_2 when the plutonium concentration

was gradually increased to 26 mg per kilogram of H_2O. After the next addition, which increased the plutonium concentration to 28 mg per kilogram of H_2O, partial precipitation occurred, leaving 22 mg per kilogram of H_2O in solution. No further precipitation was noted while the plutonium concentration was being increased to 27.8 mg. Two more additions increased the plutonium concentration to 30.8 mg per kilogram of H_2O, at which time the experiment was terminated. During this experiment the plutonium was added as Pu(IV) sulfate, and most of the plutonium in solution after heating was present as Pu(IV). These results are in agreement with those previously reported,[1] in which no precipitation or only partial precipitation occurred when the initial plutonium concentration was less than 30 mg per kilogram of H_2O.

Once each day the pyrex-lined autoclave was cooled to room temperature and opened so that a sample could be removed and more plutonium could be added to the 1.4 *m* UO_2SO_4. The amount of plutonium added each day was approximately 2 mg per kilogram of H_2O.

Zirconium oxide did not act as an effective carrier for PuO_2 precipitation from 1.4 *m* UO_2SO_4 at 250°C. About 100 mg of zirconium per kilogram of H_2O was added to each of six 1.4 *m* UO_2SO_4 solutions containing 7.8, 13.8, 15.0, 23.1, 28.5, and 46.4 mg of plutonium per kilogram of H_2O. These solutions were heated in pyrex-lined autoclaves at 250°C under 100 psi O_2 and 200 psi H_2. Zirconium hydrolyzed and precipitated in all cases, and the plutonium remaining in solution was 6.3, 10.9, 9.0, 18.9, 19.4, and 39.0 mg per kilogram of H_2O, respectively. These results are similar to those obtained in the absence of zirconium hydrolysis and precipitation.

16.3.2 Titanium Containers

Plutonium behavior in 1.4 *m* UO_2SO_4 at 250°C contained in titanium was similar to that in pyrex. No PuO_2 was formed by heating 1.4 *m* UO_2SO_4 at 250°C in a titanium-lined autoclave under 100 psi O_2 and 200 psi H_2 when the plutonium concentration was increased to 21.3 mg per kilogram of H_2O by additions of plutonium in four batches. After the next addition, which increased the plutonium concentration to 25.8 mg per kilogram of H_2O, partial precipitation occurred, leaving 22.8 mg of plutonium per kilogram of H_2O in solution. Plutonium adsorption on titanium during the first 100 hr of this run, when no PuO_2 was formed, was 0.08 $\mu g/cm^2$.

16.3.3 Type 347 Stainless Steel Containers

Batch addition of plutonium to 1.4 *m* UO_2SO_4 contained in type 347 stainless steel was studied in an experiment similar to the ones described above. During the first six additions, which increased the plutonium concentration to 33.4 mg per kilogram of H_2O, there was no PuO_2 precipitation. After the next addition, which increased the plutonium concentration to 37.2 mg, precipitation of PuO_2 occurred, leaving only 7.5 mg per kilogram of H_2O in solution. Further plutonium additions also caused precipitation, leaving from 6 to 9 mg of plutonium per kilogram of H_2O in solution. Essentially all the plutonium remaining in solution was Pu(VI), even though the additions were made as Pu(IV). Plutonium adsorption on stainless steel during the first part of the run, when no PuO_2 was formed, was about 0.001 $\mu g/cm^2/hr$.

Conversion of Pu(IV) to Pu(VI) when heated in stainless steel equipment is probably due to chromium in the uranyl sulfate solutions. In scouting tests made in pyrex containers, plutonium in 1.4 *m* UO_2SO_4 containing chromium [added either as Cr(III) or Cr(VI)] was oxidized to Pu(VI) upon heating at 250°C under 100 psi O_2 and 200 psi H_2.

16.4 EFFECT OF TEMPERATURE ON PLUTONIUM VALENCE[2]

In all the plutonium-producer blanket-processing studies, analyses have been made on solutions at room temperature immediately after cooling from 250°C rather than at 250°C. Previous investigators[3] have reported that Pu(IV) disproportionates in various acids to Pu(III) and Pu(VI):

$$3Pu^{4+} + 2H_2O \rightleftharpoons 2Pu^{3+} + PuO_2^{2+} + 4H^+$$

Equilibrium values in hydrochloric acid at 25 and

[1] D. E. Ferguson *et al.*, *HRP Quar. Prog. Rep. July 31, 1956*, ORNL-2148, p 121–122.

[2] Analytical work by R. E. Biggers, Analytical Chemistry Division.

[3] R. E. Connick, p 221, esp 238–241, in *The Actinide Elements*, NNES, vol IV-14A, McGraw-Hill, New York, 1954.

70°C (Table 16.1) show that increasing the temperature increases the disproportionation. The smaller amount of disproportionation (Table 16.1) in uranyl sulfate is probably caused by the strong Pu(IV)-sulfate complex. It can be seen that Pu(IV) is stable at 25°C but, as the solution is heated to 90°C, that almost 30% of the Pu(IV) is converted to Pu(III) and Pu(VI). From these results it appears unlikely that any significant amount of Pu(IV) can exist in 1.4 *m* UO_2SO_4 at 250°C in the absence of strong oxidizing or reducing agents. This means that plutonium determined as Pu(IV) after cooling to room temperature probably existed as Pu(III) and Pu(VI) and perhaps as Pu(V) at 250°C. The amount of disproportionation of Pu(IV) in 1.4 *m* UO_2SO_4 was determined by spectrophotometric examination.

TABLE 16.1. EFFECT OF TEMPERATURE ON Pu(IV) DISPROPORTIONATION

Temperature (°C)	Distribution (%)		
	Pu(III)	Pu(IV)	Pu(VI)
	In 0.474 *M* HCl*		
25	29	56.5	14.5
70	60	10	30
	In 1.4 *m* UO_2SO_4		
25	0	100	0
70	1	98.5	0.5
80	4	94	2
90	19	71.5	9.5

*Data taken from ref 3.

16.5 BLANKET SOLIDS DISSOLUTION

In order to obtain a representative sample of the solids expected to be removed by the hydroclone during operation of the HRT chemical plant, it is necessary to dissolve them completely. Simulated blanket solids containing 70% Fe_2O_3, 18% Cr_2O_3, 9% NiO, 1.2% ZrO_2, 1% UO_3, and 0.8% PuO_2, prepared by hydrolysis at 250°C, were completely dissolved in anhydrous H_3PO_4 at 230°C. Complete solution was also obtained by heating the solids in 10.8 *M* H_2SO_4 at 156°C followed by dilution to 4.5 *M* H_2SO_4 and refluxing.

When simulated reactor solids were added to 85% H_3PO_4 (5 ml of solution per gram of solids) and heated to 230°C, they dissolved immediately, giving a clear solution. Diluting with a 4.5 *M* $NH_4H_2PO_4$ solution to 40% H_3PO_4 stabilized the zirconium, preventing hydrolysis and enabling the solution to be refluxed at 105°C for a two-week period without zirconium hydrolysis and precipitation. Baking the solids at the dissolving temperature for 30 min made dissolution easier.

Solids containing more than 60% ZrO_2 present some difficulty in dissolving because of the limited solubility of zirconium in H_3PO_4, making necessary a larger volume of phosphoric acid per gram of solids. Simulated HRT fuel-solution solids containing 50 to 60% ZrO_2 were dissolved with 20 ml of 85% H_3PO_4 per gram of solids at 230°C. When the solution was diluted with $NH_4H_2PO_4$ solution, the zirconium was stable in 40% H_3PO_4.

The simulated blanket solids were also dissolved with 10.8 *M* H_2SO_4 when heated at 156°C for 3 hr and then diluted to 4.5 *M* H_2SO_4 and refluxed for 12 hr. A clear stable solution, with the plutonium in solution, was produced.

17. THORIUM OXIDE SLURRY DEVELOPMENT

D. E. Ferguson
V. D. Allred
E. V. Jones
N. A. Krohn
J. P. McBride
L. E. Morse
C. E. Schilling
W. M. Woods

17.1 SLURRY IRRADIATION STUDIES

17.1.1 Slurry Irradiations in the LITR

Four slurry irradiation experiments were carried out in the LITR – two with slurries of pure thorium oxide and two with slurries of a mixed thorium-uranium oxide containing 0.5 mole % of 93% enriched uranium. The slurries contained 750 g of thorium per kilogram of H_2O and were irradiated at 300°C and a flux of 2.7×10^{13} neutrons/cm^2·sec in the dash-pot irradiation bomb. The slurries were stirred successfully in-pile with no change in apparent viscosity occurring as a result of the irradiation (Table 17.1).

One of the pure oxide slurries contained oxide prepared by the precipitation of thorium oxalate at 10°C followed by a multistage calcination ending at 900°C (TO-10-900-24).[1] The other was an aliquot of a pure oxide slurry (200A-6) which had been pumped for 100 hr at 200°C in loop 200A. The oxide in this slurry was in the form of spherical aggregates, with an average particle size of 10 to 15 μ (see Sec. 17.3). The in-pile stirring times for these slurries were 241 and 385 hr, respectively, with 198 and 344 hr at full reactor power.

The mixed oxide used in the two slurries was prepared by coprecipitating thorium and uranous oxalate and decomposing the mixed oxalates by a multistage calcination ending at 800°C. Prior to irradiation MoO_3 equivalent to 0.15 *m* concentration was added to each slurry. One of these slurries was stirred for 367 hr in-pile, 314 hr at full reactor power. In the other experiment stirring of the slurry ceased after 44 hr of irradiation as a result of improper temperature control during reactor shutdown. The calculated power density in these slurries under irradiation is 5 kw/liter; however, with the molybdenum oxide present no

[1] V. D. Allred, E. V. Jones, and J. P. McBride, *HRP Quar. Prog. Rep. Jan. 31, 1956*, ORNL-2057, p 115.

TABLE 17.1. IN-PILE BEHAVIOR OF THORIUM OXIDE SLURRIES

Slurry thorium concentration: 750 g per kilogram of H_2O
Temperature: 300°C
Flux: 2.7×10^{13} neutrons/cm^2·sec

Slurry	Time of Stirring In-Pile (hr)	Irradiation Time (hr)	Approximate Power Density (w/g of ThO_2)	Viscosity (centistokes)	
				Without Irradiation	During Irradiation
TO-10-900-24; oxalate precipitated at 100°C, calcined at 900°C	241	198	0.05	16.0	16.0
200A-6 oxide prepared by calcining at 800°C pumped 100 hr at 200°C in 200A loop	385	344	0.05	12.3	12.6
ThO_2–0.5 mole % uranium oxide; coprecipitated oxalates calcined at 800°C	48	44*	7	13.1	13.0
	367	314**	7	12.5	12.9

*Stirring failed as a result of improper temperature control.

**Ceased stirring temporarily for 27 hr in the middle of the experiment for unknown reason.

gas pressure in excess of steam pressure was observed in either experiment.

17.1.2 Viscosity Measurements in the Irradiation Bomb

A general description of the method of using the dash-pot irradiation bomb for viscosity measurement was reported previously.[2,3] For the data in this section the solenoid current was fixed and the frequency and/or load division adjusted so that the upper solenoid was cut off as soon as the stirrer reached its maximum height, as determined by the oscilloscope trace (Fig. 17.1). The load division divided by the frequency then gives the "rise time" of the stirrer. The apparent viscosity is then obtained by comparing the stirrer rise time with a calibration curve of rise time vs viscosity obtained with silicone oils of known viscosity.

The apparent viscosities of several pure thorium oxide slurries (TO-10-900-24, 200A-6) and of a slurry of a mixed thorium and uranium oxide (0.5 wt % uranium) were measured as a function of slurry concentration and temperature. In addition, the effect of sulfate additions on the viscosities of slurries of the 200A-6 oxide and of the mixed oxide was determined. In the absence of sulfate the viscosities of the slurries investigated increased slightly with increasing slurry thorium concentration from 250 to 1000 g per kilogram of H_2O but showed no particular temperature dependence between 25 and 300°C (Table 17.2).

The viscosity of a slurry of the 200A-6 oxide, 750 g of thorium per kilogram of H_2O, increased with increasing sulfate addition to 3000 ppm (based on ThO_2) but decreased with increasing slurry temperature at sulfate concentrations of 500 and 1000 ppm (Table 17.3). At higher sulfate concentrations little or no temperature dependence was observed. The addition of sulfate (0 to 3000 ppm) to a slurry of the mixed oxide, 500 g of thorium per kilogram of H_2O, had comparatively little effect on slurry viscosity (Table 17.3). After each addition of sulfate the slurries were heated at 300°C for 4 hr before the viscosity measurements were made.

17.1.3 Corrosion-Erosion Data Obtained in Out-of-Pile Tests with the Dash-Pot Irradiation Bomb

To obtain a base line for the interpretation of corrosion-product data obtained with irradiated slurries, the pickup of corrosion products during out-of-pile operation with the dash-pot irradiation bomb was obtained for water and a variety of slurries (Table 17.4). A pronounced increase in corrosion-product pickup was noted in the presence

[2] A. R. Jones *et al.*, *HRP Quar. Prog. Rep. Jan. 31, 1956*, ORNL-2057, p 109–113.

[3] N. A. Krohn, J. P. McBride, and W. M. Woods, *HRP Quar. Prog. Rep. April 30, 1956*, ORNL-2096, p 109–111.

TABLE 17.2. VISCOSITY OF THORIUM OXIDE SLURRIES OBTAINED IN DASH-POT BOMB

Oxide	Average Viscosity (centistokes) at 25 to 300°C			
	Concentration of Thorium (g per kg of H_2O)			
	250	500	750	1000
TO-10-900-24; oxalate precipitated at 100°C, calcined at 900°C	9.0	11.4	16.0	30
200A-6; oxide prepared by calcining at 800°C; pumped for 100 hr at 200°C in 200A loop	9.6	8.3	9.0	12.5
Above after being stirred for 24 hr in dash-pot bomb	12.6	12.0	12.3	16.8
ThO_2–0.4 wt % UO_3; coprecipitated Th-U(IV) oxalates calcined at 800°C	8.3	10.7	14.7	

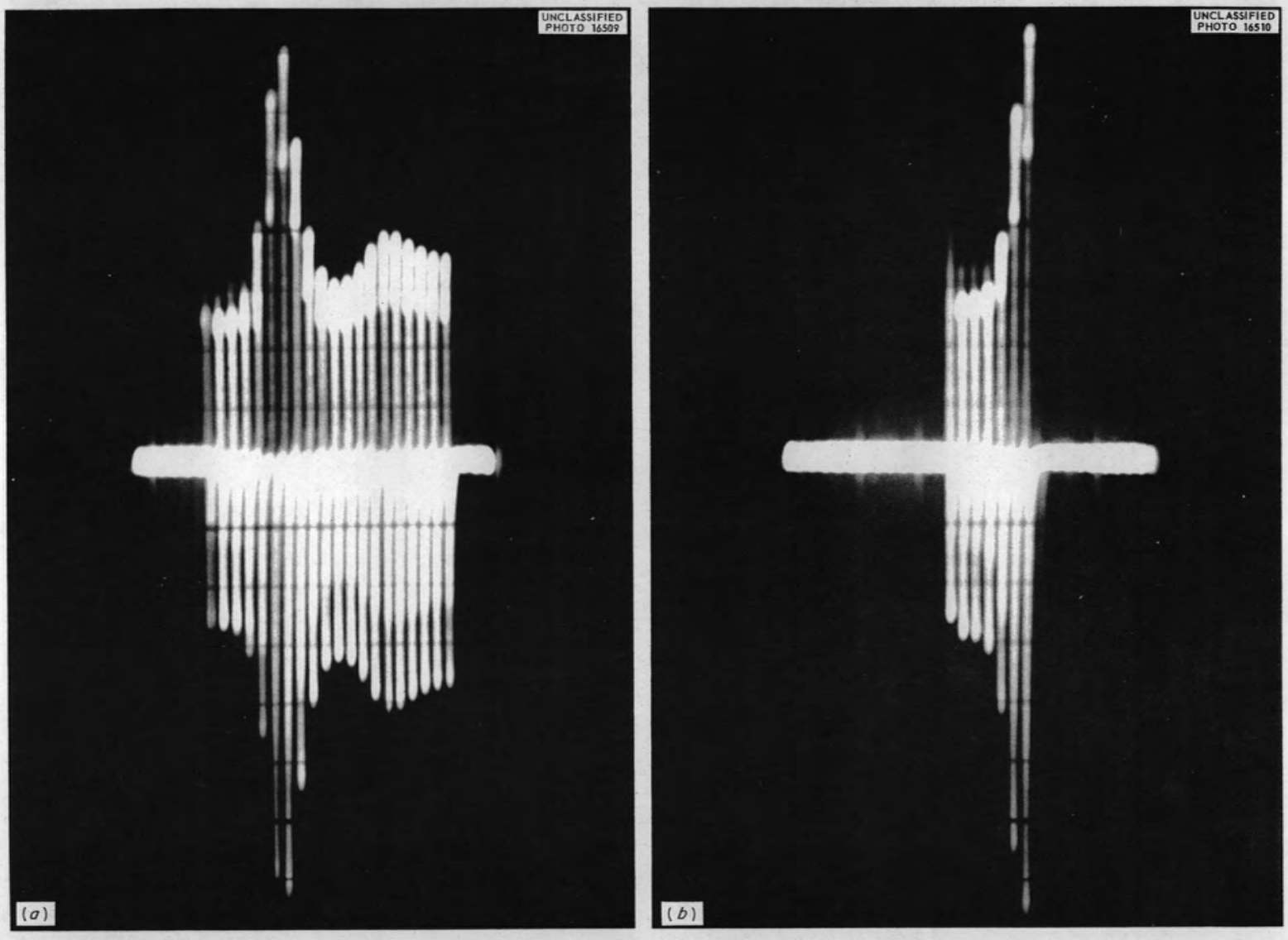

Fig. 17.1. Oscilloscope Trace (*a*) Unadjusted for Viscosity Measurements and (*b*) Adjusted for Viscosity Measurements.

TABLE 17.3. EFFECT OF SULFATE ON THE VISCOSITY OF THORIUM OXIDE SLURRIES

Sulfate added as $Th(SO_4)_2$

Slurry	Sulfate Concentration (ppm)*	Viscosity (centistokes)			
		60 to 70°C	110 to 120°C	200 to 220°C	300°C
200A-6; 800°C-calcined pilot-plant oxide, pumped for 100 hr at 200°C; 750 g of Th per kg of H_2O	0	12.8	12.6	12.2	
	500	13.4	12.2	9.5	8.4
	1000	16.5	14.6	13.6	12.7
	1500	15.6	15.9	14.2	13.6
	2000	18.3	16.8	15.1	15.7
	3000	19.6	18.7	18.2	19.1
ThO_2–0.4 wt % UO_3; coprecipitated Th-U(IV) oxalates, calcined at 800°C; 500 g of Th per kg of H_2O	0		9.6	10.0	12.9
	500		9.4	9.5	12.6
	1000		11.0	10.3	10.5
	1500		11.2	13.5	13.7
	2000		10.4	14.1	13.4
	3000		10.1	13.5	13.9

*Based on ThO_2.

TABLE 17.4. CORROSION-EROSION PRODUCT PICKUP IN DASH-POT BOMB

Temperature: 300°C

Slurry thorium concentration: 750 g per kilogram of H_2O

Material	Additive	Stirring Time (hr)	Total Iron (mg)	Iron (ppm)[a]
H_2O	None	0[b]	0.2	
	None	50	0.4	
	None	100	9.6	
	300 psi O_2, room temperature	0[b]	0.05	
	300 psi O_2, room temperature	100	0.2	
ThO_2 calcined at 900°C	None	0[c]	0.6	184
	None	45	8.4	2,400
ThO_2–0.4 wt % UO_3; coprecipitated oxalates calcined at 900°C	20,000 ppm MoO_3	121	47.2	13,500
ThO_2–0.5 wt % UO_3; coprecipitated oxalates calcined at 800°C	None	334	64.7	18,500
	20,000 ppm MoO_3			
	3000 ppm SO_4	340	33.2	9,500
	300 psi O_2, room temperature			
200A-6; 800°C-calcined ThO_2, pumped 100 hr at 200°C	None	385	16.1	4,600

[a]Based on ThO_2.

[b]Heated for 75 hr at 300°C.

[c]Heated for 120 hr at 300°C.

of a slurry when compared with water alone. An oxygen overpressure appeared to inhibit the attack rate.

17.1.4 Diagonal-Tube Irradiation Facility in the LITR

The diagonal-tube slurry irradiation facility should be completed by the middle of November. Fabrication of components is complete, with the exception of the bending and welding of the coaxial aluminum tubes, material for which has just been received. All items needed for completion are on hand, with a few small noncritical exceptions. Instrumentation and related installations are over 50% complete.

17.1.5 Bomb Dismantling Facility

The installation and checkout of the bomb opening facility in cell 7 of Building 3019 are essentially complete. The equipment operates satisfactorily according to the design intent.

17.2 GAS-RECOMBINATION STUDIES

Investigation of the catalytic recombination of hydrogen and oxygen by thorium oxide–uranium oxide slurries containing 0.05 *m* molybdenum oxide was continued. Studies were made on the effect on the catalytic activity of the molybdenum oxide preparation method, of a mixed oxide prepared by thermal decomposition of the coprecipitated thorium-uranium(IV) oxalates, and of the addition of iron oxide to the slurry containing molybdenum oxide, to simulate contamination by corrosion products. The Mo(VI) oxides prepared by several different methods showed comparable activities and gave hydrogen-oxygen combination rates more than sufficient to maintain a slurry blanket at 2000 psi total pressure under TBR conditions after the slurry had been activated by heating at 280°C with a hydrogen overpressure (1000 psi at room temperature). Reducing the dry Mo(VI) oxide to a lower oxidation state by treatment with hydrogen prior to its addition to the slurry did not produce an effective catalyst. The use of the mixed oxide prepared from coprecipitated oxalates, instead of mixed oxide prepared by the addition of UO_3 to ThO_2, did not impair the activity of the molybdenum oxide catalyst. The addition of 1000 to 1500 ppm of iron oxide to the slurry resulted in a marked decrease in combination activity.

The experiments were carried out by adding stoichiometric mixtures of hydrogen and oxygen to the slurries contained in small stainless steel autoclaves and brought to temperature while being vigorously agitated. The specific reaction-rate constant, k_{π}, and the rate of hydrogen consumption were obtained from the rate of total pressure decrease with time, assuming a first-order dependence on the hydrogen partial pressure and the applicability of the perfect-gas law.[4,5]

17.2.1 Effect of Molybdenum Oxide Preparation Method

Molybdenum oxide (MoO_3) for use in the recombination studies was prepared by three different methods: by heating ammonium paramolybdate at 480°C for 16 hr, by decomposing by heating at 400°C an oxalic-molybdic acid prepared by dissolving MoO_3 in oxalic acid and evaporating to dryness, and by calcining at 400°C molybdic acid precipitated from an ammonium paramolybdate solution by the addition of nitric acid (pH 3.0 to 3.5). The dry molybdenum oxides were mixed with 900°C-calcined thorium oxide and uranium oxide ($UO_3 \cdot H_2O$) and then suspended in water to give slurries 0.05 *m* in molybdenum oxide and containing 1000 g of thorium and 5 g of uranium per kilogram of H_2O. Prior to their use in combination experiments, the slurries were heated at 280°C for 3 hr under an oxygen overpressure (500 psi at room temperature). As prepared, none of the molybdenum oxide preparations tested showed the desired catalytic activity (>10 moles of hydrogen recombined per hour per liter of slurry). After the slurries were activated by heating for 1 hr at 280°C with a hydrogen overpressure (1000 psi at room temperature), all preparations gave combination rates equal to or greater than 28 moles of hydrogen per hour per liter of slurry at 150 to 180°C (Table 17.5). Reheating the activated slurries for 3 hr at 280°C under oxygen did not markedly decrease their catalytic activities.

Molybdenum dioxide prepared by decomposing the ammonium paramolybdate at 400°C in a hydrogen atmosphere showed a lower catalytic activity than

[4] D. E. Ferguson *et al.*, *HRP Quar. Prog. Rep. Oct. 31, 1954*, ORNL-1813, p 143–144.

[5] H. F. McDuffie *et al.*, *Reactor Sci. Technol.* 4(2), 23 (1954) (TID-2013).

TABLE 17.5. HYDROGEN-OXYGEN COMBINATION RATES IN THORIUM-URANIUM OXIDE SLURRIES CONTAINING MOLYBDENUM OXIDE CATALYSTS

Slurry composition: 1000 g of Th and 5 g of U per kilogram of H_2O, 0.05 *m* molybdenum oxide
Pretreatment: heated under O_2 (500 psi at 25°C) for 3 hr at 280°C

Molybdenum Oxide Preparation Method	H_2 Combination Rate, P_{H_2} = 500 psi (moles/hr/liter)		
	Slurry as Prepared	After Treatment with Hydrogen*	After Treatment of the Hydrogenated Slurry with Oxygen**
MoO_3, 480°C calcination of ammonium paramolybdate	2.8 (250°C)	29 (150°C)	29 (150°C)
MoO_3, 400°C calcination of oxalic-molybdic acid crystallized from oxalic acid solution	4.6 (270°C)	28 (172°C)	24 (167°C)
MoO_3, 400°C calcination of molybdic acid precipitated from ammonium paramolybdate	3.6 (270°C)	29 (180°C)	25 (164°C)
MoO_2, 400°C calcination of ammonium paramolybdate under hydrogen	1.9 (270°C)		

*Heated with H_2 (1000 psi at 25°C) for 1 hr at 280°C.
**Heated with O_2 (500 psi at 25°C) for 3 hr at 280°C.

did the molybdenum(VI) oxides. The slurries containing the molybdenum dioxide were originally blue-gray in color but changed to a light-tan color characteristic of the slurries containing the other molybdenum oxide preparations after being used in the gas-combination experiment. This indicates that this form of the oxide was neither stable under the experimental conditions nor was it the catalytically active species obtained by heating the slurries with a hydrogen overpressure.

17.2.2 Studies with Slurries Containing Thorium-Uranium Oxide Prepared from the Coprecipitated Oxalates

The catalytic activity of a slurry of thorium-uranium oxide, 1000 g of thorium per kilogram of H_2O, prepared by the 900°C calcination of thorium-uranous oxalate was studied both before and after the addition of the molybdenum oxide catalyst. Prior to its use in combination studies the thorium-uranium oxide slurry (without the catalyst) was heated at 280°C for 3 hr under oxygen. As prepared, the slurry exhibited only slight catalytic activity. Treatment with hydrogen at 280°C resulted in a temporary increase in catalytic activity, and a combination rate of 7 moles of hydrogen per hour per liter of slurry was obtained at 137°C. In successive experiments the combination rate progressively decreased, leveling off at 0.4 mole of hydrogen per hour per liter of slurry at 282°C.

The addition of 0.05 *m* MoO_3 to the slurry and subsequent activation by heating at 280°C under a hydrogen overpressure resulted in a very active slurry, showing a combination rate of 33 moles of hydrogen per hour per liter of slurry at 223°C (Table 17.6). Subsequent treatment of the slurry with oxygen at elevated temperatures failed to impair its catalytic activity.

17.2.3 Effect of Corrosion Products

The effect of corrosion-product pickup on catalytic activity was simulated by the addition of aliquots of an iron oxide sol to a mixed oxide slurry 0.05 *m* in MoO_3 and containing 1000 g of thorium and 5 g of uranium per kilogram of H_2O. Prior to the addition of the iron oxide and after activation with hydrogen, the slurry gave combination rates comparable to those given in Sec. 17.2.1 for similar slurries. The addition of 500

TABLE 17.6. HYDROGEN-OXYGEN COMBINATION RATES IN SLURRIES CONTAINING THORIUM-URANIUM OXIDE PREPARED FROM THE COPRECIPITATED OXALATES

Slurry composition: 1000 g of Th and 3.7 g of U per kilogram of H_2O
Pretreatment: heated under O_2 (500 psi at 25°C) for 3 hr at 280°C

Description and Treatment of Slurry	Reaction Temperature (°C)	H_2 Combination Rate, P_{H_2} = 500 psi (moles/hr/liter)
As prepared	281	0.04
Heated for 1 hr with H_2[a] at 280°C		
First experiment	137	7.1
Fifth experiment	282	0.4
Added 0.05 *m* MoO_3; heated for 1 hr with O_2[b] at 280°C	253	0.7
Reheated for 1 hr with H_2[a] at 280°C	223	33
Reheated for 3 hr with O_2[c] at 280°C	225	38

[a]1000 psi at 25°C.
[b]200 psi at 25°C.
[c]500 psi at 25°C.

and 1000 ppm of iron (based on thorium) depressed the catalytic activity of the slurry, but satisfactory combination rates were still obtained at temperatures less than 200°C. With the addition of 1500 ppm of iron, combination rates of equal to or less than 3.5 moles of hydrogen per hour per liter of slurry were obtained at 180 to 256°C (Table 17.7).

The catalytic activity of the slurry containing the 1500 ppm of iron was restored by heating the slurry with hydrogen at elevated temperatures, but, unlike the slurries containing no iron, the renewed activity was markedly reduced by subsequent oxygen treatment. This suggests that some lower oxide of iron was the catalytically active species produced by the hydrogen treatment of this slurry. It has been found,[6] for example, that Fe_3O_4 is a better catalyst than Fe_2O_3 for hydrogen-oxygen combination.

The Fe_2O_3 used was a sol, a commercial preparation made by dissolving $Fe(OH)_3$ which had been precipitated from $FeCl_3$ solution by NH_4OH. Each aliquot of sol was equivalent to the addition of 500 ppm of Fe and 48 ppm of Cl (based on thorium) to the slurry. After each addition of the sol the slurry was heated at 278°C for 1 hr in the presence of oxygen. After a series of three experiments with the stoichiometric gas mixture, the supernatant liquid was colorless and the slurry solids acquired the characteristic red color of iron oxide.

17.3 LABORATORY EVALUATION OF THE "STANDARD" SLURRY

A quantity of pumped thorium oxide slurry was prepared[7] for use as a standard or reference slurry in laboratory and engineering work. The material was prepared by pumping a slurry, containing 500 g of thorium per kilogram of H_2O, of 800°C-calcined pilot-plant oxide (LO-12) at 200°C in loop 200A at Y-12. Characteristic properties of the oxide before and after pumping were determined (Tables 17.8 and 17.9), and the sedimentation characteristics of the slurry were evaluated at room and elevated temperatures.

The most characteristic physical property of the standard slurry was the extremely rapid settling to a very dense but easily resuspended bed. This was in marked contrast to the comparatively slow settling rate and bulky sediment observed with the

[6] *Chemistry and Engineering Division Progress Report, October–December 1953*, PR-CE-20, p 31 (classified).

[7] R. B. Gallaher and A. S. Kitzes, *Preparation of Standard Oxide*, ORNL CF-56-10-8 (Oct. 3, 1956).

TABLE 17.7. HYDROGEN-OXYGEN COMBINATION RATES IN THORIUM-URANIUM OXIDE SLURRIES CONTAINING FERRIC OXIDE

Slurry composition: 1000 g of Th and 5 g of U per kilogram of H_2O, 0.05 *m* molybdenum oxide
Pretreatment: heated under O_2 (500 psi at 250°C) for 1 hr at 280°C

Experimental Conditions	Reaction Temperature (°C)	H_2 Combination Rate, P_{H_2} = 500 psi (moles/hr/liter)
As prepared	254	2.7
Heated for 1 hr with H_2* at 280°C	154	31
Added 500 ppm of ferric oxide**	152	26
	159	26
Added 500 ppm of ferric oxide**	157	11
(total ferric oxide 1000 ppm)	184	17
Added 500 ppm of ferric oxide**	182	2.7
(total ferric oxide 1500 ppm)	203	3.5
	225	2.7
	225	1.6
	256	1.8
Heated slurry for 1 hr with H_2* at 280°C	168	19.0
	182	31
Heated slurry with O_2		
1 hr at 206°C (O_2, 100 psi at 25°C)	181	6.8
	210	9.9
3 hr at 280°C (O_2, 1000 psi at 25°C)	208	2.4
	224	1.7

*1000 psi at 25°C.
**After each 500 ppm iron oxide addition, slurry was heated under O_2 (500 psi at 25°C) for 1 hr at 280°C.

S-90 pumped oxide prepared from a similar source material (LO-11) and pumped under similar concentration and temperature conditions but in loop 100A (S loop). Microscopic examination of the standard slurry showed it to be composed of rather large microspheres, 15 μ in size (Fig. 17.2), which account for the peculiar sedimentation characteristics of this slurry.

Sedimentation particle-size distribution curves (Fig. 17.3) show marked differences between the standard slurry, the source material, and the S-90 slurry, particularly in the high percentage of agglomerates >6 μ found in the standard slurry. Previous experience, as with the S-90 material, has shown degradation of the oxide on pumping to less than 1 μ.

No differences were observed in the chemical and physical characteristics of the standard material, when compared with other pumped oxides, which could give an insight into the mechanism by which the microspheres were formed. For example, analysis showed no unusual chemical constituents in the standard slurry, and no crystallite growth from pumping was observed in either the standard or the S-90 slurries. Furthermore, the oxides from both failed to show crystallite growth when they were fired at 900°C for 24 hr. Failure of the crystallites to grow on refiring indicates that degradation of the initial particles to crystallite dimensions had occurred.[1] Further evidence of degradation to crystallite dimensions of the oxide particles, prior to ball formation in the case of the standard slurry, is seen in the

TABLE 17.8. CHEMICAL ANALYSIS OF STANDARD SLURRY AND RELATED MATERIALS

Analysis	LO-12[a]	Standard Slurry	S-90[b]
Thorium content (wt %)[c]	87.5	86.8	87.2
Loss on ignition (wt %)[c]	0.2	0.4	0.4
Ionic analysis (ppm)			
CO_3	2800	1700	2000
NO_3	8	18	10
SO_4	5	35	40
PO_4	38	6	<10
Si	9	<10	<10
F	<10	25	13
Cl	<5	40	4
Al		(75)	(160)
Fe	<10	370	685
Cr	<10	40	75
Ni	<10	65	98

[a]Original oxide, i.e., 800°C-calcined pilot-plant product.

[b]Included for comparison since a similar oxide was used in this study; S-90 was pumped under the same conditions of temperature and pressure in loop 100A (S loop).

[c]Weight per cent after drying at 200°C.

TABLE 17.9. CHARACTERISTIC PROPERTIES OF THE STANDARD OXIDE AND RELATED MATERIALS

Property	LO-12*	Standard Slurry	S-90**
Average sedimentation particle size (μ)	4.5	~15	1
Specific surface area (m^2/g)	16.6	29.0	30.0
Crystallite size (Å)			
As received	225	225	215
After refiring 24 hr at 900°C	570	280	255

*Original oxide, i.e., 800°C-calcined pilot-plant product.

**Included for comparison since a similar oxide was used in this study; S-90 was pumped under the same conditions of temperature and pressure in loop 100A (S loop).

fact that the specific surface has been increased to a value which would be predicted from the crystallite size.[8]

Sulfuric acid titration curves (pH vs sulfate-equivalents-to-surface-area ratio) of the standard slurry and of the original oxide (LO-12) are shown in Fig. 17.4. These data indicate that the specific surface activity of the pumped slurry is comparable to that of the original oxide despite the almost twofold increase in surface area.

Stability of the microspheres varied greatly. For example, stirring under atmospheric conditions at

[8]V. D. Allred and S. R. Buxton, *HRP Quar. Prog. Rep. July 31, 1955*, ORNL-1943, p 181–188.

Fig. 17.2. Photograph of Spherical Agglomerates Found in the Standard Slurry.

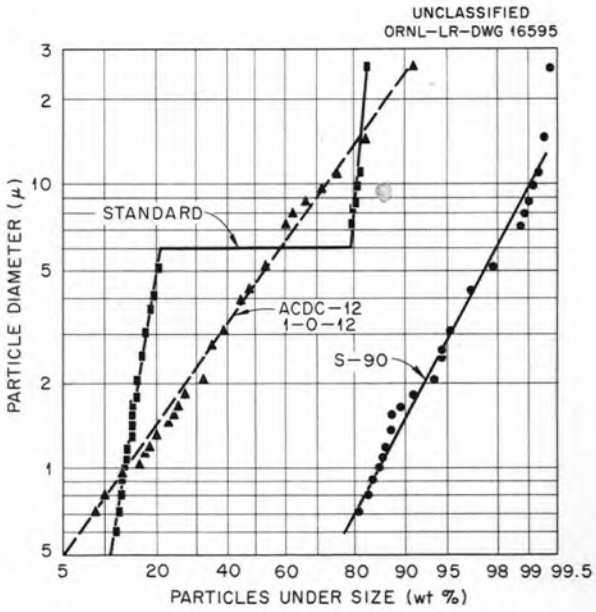

Fig. 17.3. Particle-Size Distribution of the Standard Slurry and Related Materials.

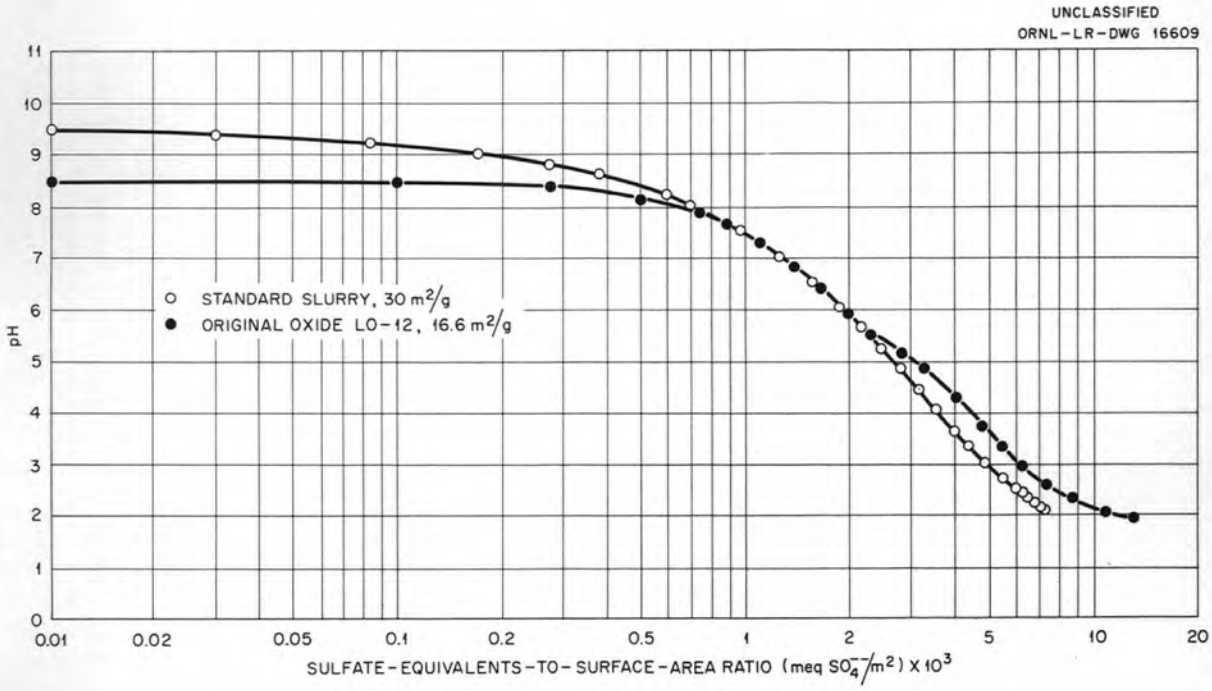

Fig. 17.4. Sulfuric Acid Titration Curves for Standard Slurry and Original Oxide – 2.275 g of ThO_2 Titrated with 0.0988 *N* Acid.

98°C in laboratory glassware caused pronounced degradation and ultimate dispersion, whereas vigorous shaking in a stainless steel autoclave at temperatures to 300°C seemed to greatly enhance the stability and in some cases induce further particle growth, as evidenced by an increase in the settling rate with successive experiments at constant temperature.

Sedimentation data typical of the behavior of the standard slurry in laboratory glassware under mild stirring are shown in Figs. 17.5 and 17.6. The time dependence of the subsidence rate indicates the rate of degradation of the spheres. Conductivity data (Fig. 17.7) show that the enhanced dispersion occasioned by stirring at 98°C is accompanied by a marked increase in conductance. This could indicate that an impurity in the atmosphere such as CO_2 may be responsible, since the dispersion effect was not observed in the sealed stainless steel autoclaves.

The effect of thorium sulfate additions on the high-temperature sedimentation properties is shown in Fig. 17.8. The abnormal increase in the hindered-settling rate in the temperature region 150 to 200°C upon the addition of between 500 and 1000 ppm sulfate and again at about 5000 ppm sulfate appears to be characteristic of 800°C-fired pumped oxide (surface area $\sim 29\ m^2/g$).[9] The region of 2000 to 3000 ppm ($\sim 2 \times 10^{-3}$ meq SO_4/m^2 surface) appears to be one of a relatively settling rate and good temperature stability.

Also appearing in Fig. 17.8 is the sulfuric acid titration curve (pH vs sulfate/surface ratio) obtained with the standard slurry. It should be noted that the sulfate-concentration regions of temperature instability bracket the break in the pH curve and that the region of temperature stability occurs between pH 6 and 7. Room-temperature bulk-density data in sulfate systems have shown[10] a minimum in the bulk density to occur at about pH 7. It appears from the data that a simple titration of a slurry with sulfuric acid indicates the sulfate concentration required for temperature stability.

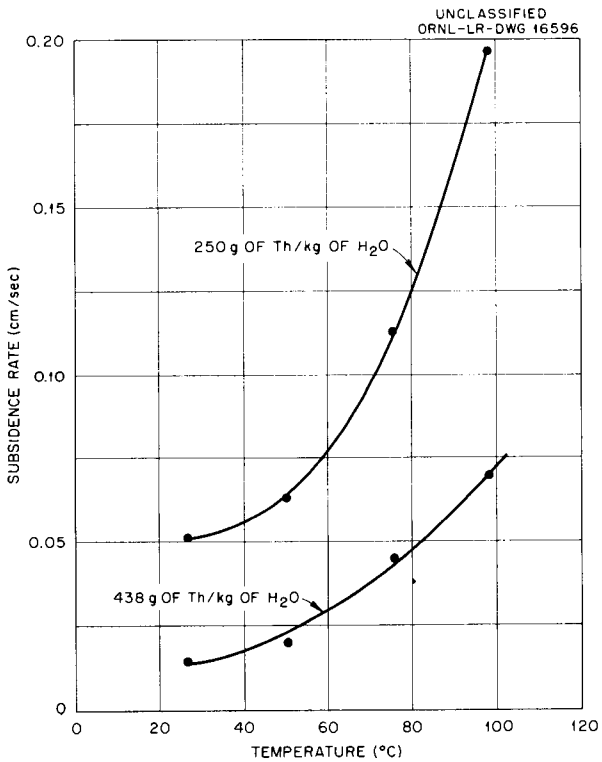

Fig. 17.5. Effect of Temperature on Sedimentation Rate for Standard Slurry.

[9] V. D. Allred, E. V. Jones, and J. P. McBride, *HRP Quar. Prog. Rep. July 31, 1956*, ORNL-2148, p 130.

[10] D. E. Ferguson *et al.*, *HRP Quar. Prog. Rep. July 31, 1955*, ORNL-1943, p 195.

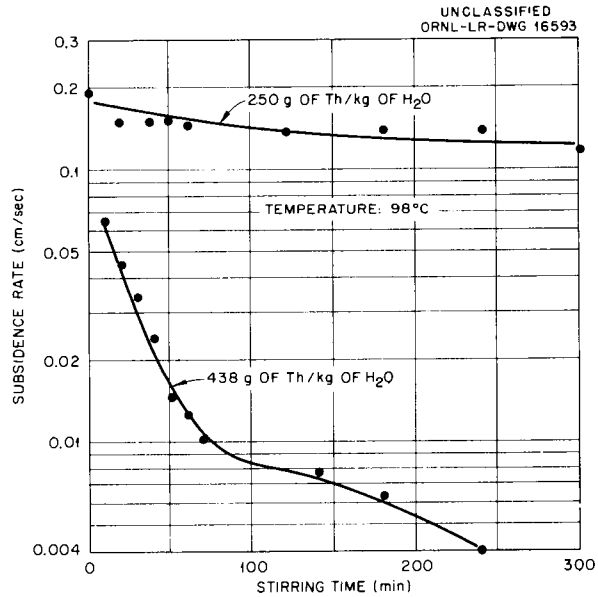

Fig. 17.6. Effect of Stirring Time on Sedimentation Rate of Standard Slurry at 98°C.

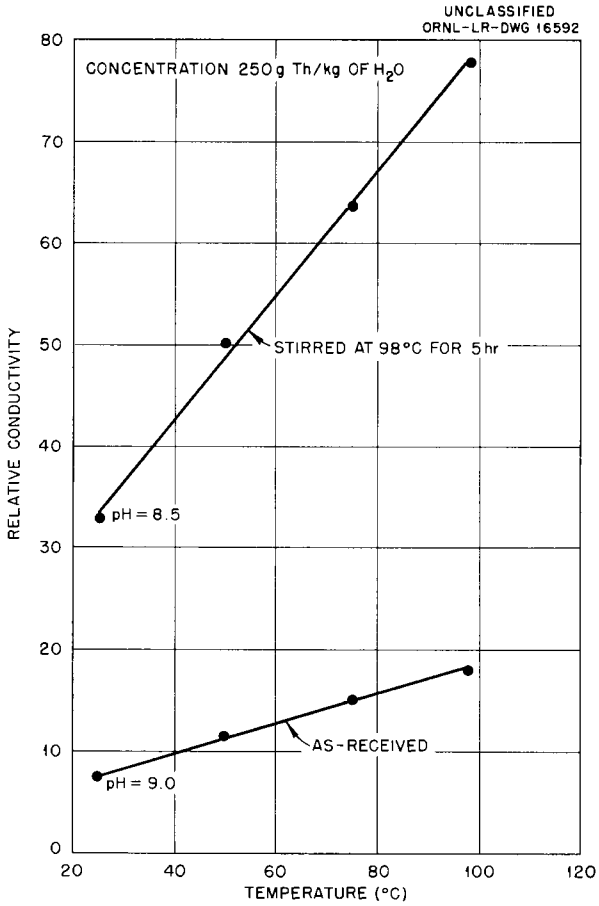

Fig. 17.7. Effect of Temperature and Stirring on Conductivity of Standard Slurry.

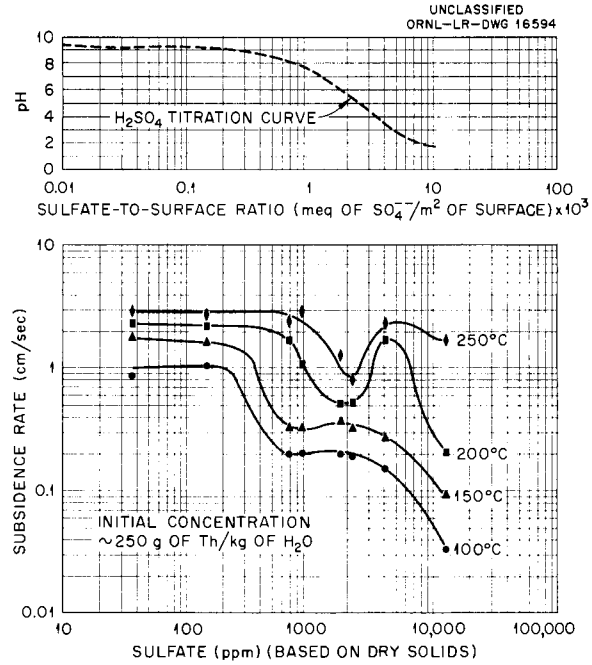

Fig. 17.8. Effect of Thorium Sulfate Addition on the Sedimentation of Standard Slurry.

The effect of slurry concentration on the sedimentation rates of a pumped slurry of oxide prepared from 900°C calcination of 10°C-precipitated oxalate (TO-10-900-24) and of the standard slurry is shown in Figs. 17.9 and 17.10. The data indicate that the slurry settling rate is an exponential function of concentration and has the form

$$\ln \frac{U_0}{U_s} = aC \quad , \tag{1}$$

where U_0 is the measured sedimentation rate, U_s is the settling rate at infinite dilution where Stokes' law should govern the particulate settling, C is the slurry concentration, and a is the slope of the logarithmic settling-rate–slurry-concentration curve. As indicated in Fig. 17.9, the shapes of the concentration curves are at variance with those predicted from the concentration term $(1 - \epsilon)/\epsilon^3$ in DallaValle's equation.[11]

Equation 1 can be used to calculate an effective agglomerate size provided that the density term required for the Stokes' equation can be evaluated. Assuming an agglomerate density of 5.0 g/cc, Stokes' law particle diameters have been calculated for the standard slurry from the data of Fig. 17.10 (Table 17.10).

The calculated diameters are much larger than those obtained by particle-size analysis. It is interesting to note that the calculated diameters remain constant over a wide temperature range. This implies that a fundamental relation is involved, that is, the logarithmic dependence of settling rate on slurry concentration, although its exact significance is not recognized at this time.

17.4 PREPARATION AND CHARACTERIZATION OF AQUEOUS THORIA SOLS AND SUSPENSIONS[12]

Ultrafiltration of 0.25 *M* (pH 4) thorium nitrate sols through cellophane membranes (50 Å pore

[11] J. M. DallaValle, private communication (cited also in *HRP Quar. Prog. Rep. Jan. 31, 1956*, ORNL-2057, p 120).

[12] Work done by Houdry Process Corporation.

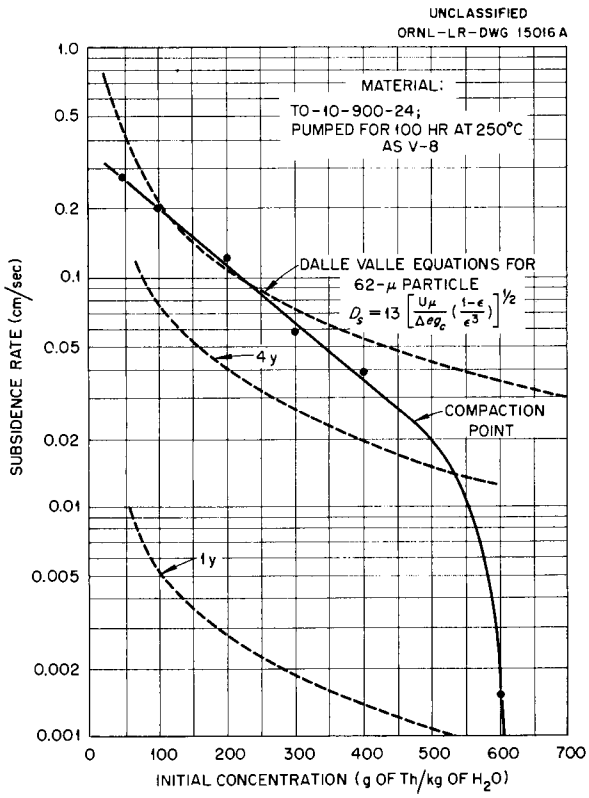

Fig. 17.9. Effect of Slurry Concentration on the Room Temperature Settling Rate of a Pumped Thorium Oxide Slurry.

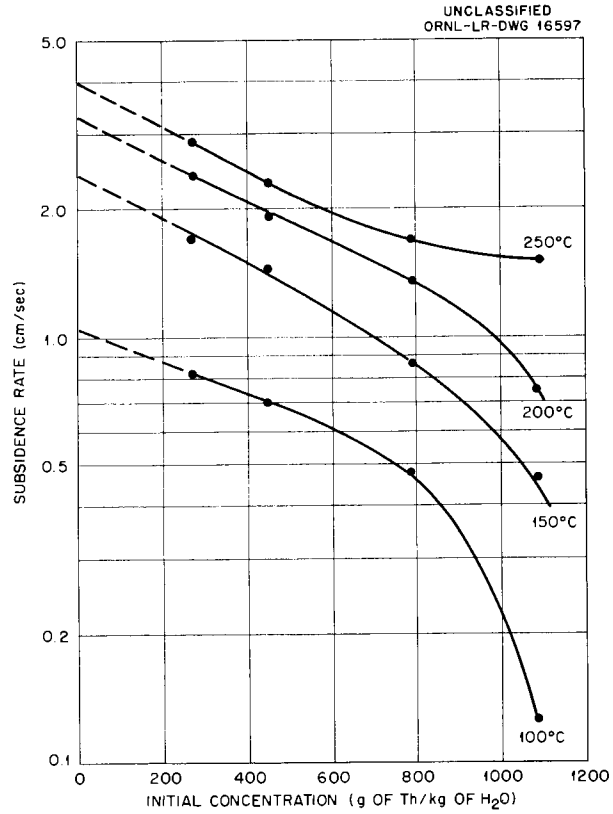

Fig. 17.10. Effect of Initial Concentration on Sedimentation Rate of Standard Slurry.

diameter) has given sols of 7.5:1 weight ratio of thoria to nitrate in a single pass, with 80% recovery of the thoria. These sols contain thoria micels with an average diameter of 140 Å, indicated by x-ray small-angle scattering, and 25 Å crystallite diameter, from x-ray diffraction line broadening. Further work is planned to determine whether additional nitrate can be removed by repeated treatment and the effect of heating upon crystallite growth and aggregate size.

A small quantity of beads of thorium phosphate gel has been prepared for evaluation as ion-exchange material and for hydrothermal stability tests.

Preliminary work has been completed on the preparation of thorium oxide gels. It was found that both hexamethylenetetramine and ammonium acetate buffers can be used to coagulate thoria sols into good gels. Work is continuing on this system, with the object of preparing thoria beads or microspheres suitable for use in reactor blanket systems.

TABLE 17.10. CALCULATED STOKES' LAW AGGLOMERATE DIAMETERS FOR STANDARD SLURRY

Assumed density: 5.0 g/cc

Temperature (°C)	U_s (cm/sec)	Diameter (μ)
250	4.0	44
200	3.3	45
150	2.4	45
100	1.2	40

Design work on the ultrasonic interface follower is proceeding satisfactorily at Sperry Products, Inc.

The development of electrophoretic techniques for studying thoria sols and slurries is continuing. Experiments with a simple cell have shown that pure thoria slurries contain positively charged particles.

18. EQUIPMENT DECONTAMINATION

D. E. Ferguson

R. D. Baybarz R. E. Leuze

18.1 ELECTROLYTIC PREPARATION OF CHROMOUS SULFATE FOR USE IN DECONTAMINATION

It was previously reported[1] that chromous sulfate–dilute sulfuric acid solutions were successful in defilming type 347 stainless steel exposed to uranyl sulfate solutions at 250 to 300°C. It has been necessary to develop a method to prepare large volumes of $CrSO_4$ solution on relatively short notice for possible reactor decontamination. Previously, solutions of chromous sulfate were prepared by reaction with zinc in a Jones type column. However, this method is slow and the efficiency decreases as a result of the buoyant action of hydrogen on the zinc particles.

Electrolytic reduction of Cr(III) to Cr(II) was successful. A solution was prepared by dissolving 0.4 mole of $KCr(SO_4)_2$ per liter of 1 *M* H_2SO_4. Reduction was carried out at a current density of 0.1 amp/cm^2 applied for 1 hr across amalgamated lead electrodes in anode and cathode compartments separated by an anion-exchange membrane. Since CrO_3 is a less expensive source of chromium, reduction of Cr(VI) to Cr(II) in dilute sulfuric acid was attempted. A solution was prepared by dissolving 3.2 moles of CrO_3 per liter of 3.5 *M* H_2SO_4. The Cr(VI) was reduced to Cr(III) in 9 hr with a current density of 0.19 amp/cm^2 with lead electrodes. The solution was then diluted to 1.0 *M* Cr(III) and reduced in a two-compartment anion-exchange membrane cell with a current density of 0.10 amp/cm^2.

The electrolytic method of preparing chromous sulfate is attractive. However, several drawbacks need to be worked out, such as $PbCrO_4$ precipitation at high current densities from the CrO_3 solution.

18.2 DESCALING WITH H_3PO_3-NaH_2PO_2

It was previously reported[1] that a 2% H_3PO_3–2% NaH_2PO_2 solution at 175°C would defilm, in 20 hr, stainless steel that had been exposed to UO_2SO_4 solutions at 250°C. The solution effected a very limited amount of descaling in one of the Y-12 corrosion loops. The results indicate that in the laboratory tests the oxide film was less adherent than it was in the loop; the solution is therefore not recommended for defilming of loops that have been exposed to UO_2SO_4.

[1] D. E. Ferguson *et al.*, *HRP Quar. Prog. Rep. July 31, 1956*, ORNL-2148, p 132–133.

Part VI

SUPPORTING CHEMICAL RESEARCH

E. H. Taylor

19. AQUEOUS SYSTEMS AT ELEVATED TEMPERATURES

C. H. Secoy

F. E. Clark J. S. Gill

R. Slusher

19.1 AN EXPLORATION OF THE SYSTEM $CuO-UO_3-SO_3-H_2O$ AT 304°C

A study of the heterogeneous equilibria in the base-saturated region of the four-component system $CuO-UO_3-SO_3-H_2O$ at 100°C has been reported previously.[1] Although there are two small areas in the 100°C isotherm that require further study, an investigation of the 300°C isotherm has been initiated.

Since such a system may contain several solid and/or liquid phases simultaneously and the techniques for the isolation of individual phases at high temperature are not well developed, the problem is being approached by making qualitative observations in sealed quartz tubes. In this manner the composition regions in which a particular type of phase phenomena occurs can be defined approximately. With this information at hand, it should be possible to select an experimental method appropriate for each specific region to yield quantitative information about some of the phases or all of them.

The results of the first set of exploratory experiments are shown in Fig. 19.1. In this set all solutions were stoichiometric in UO_2SO_4 and $CuSO_4$, and the compositions indicated by the points on the graph were those at 25°C. All tubes were filled approximately half full at room temperature and were not deaerated. The actual temperature of observation was 304 ± 1.0°C. As can be seen from the figure, the composition map is divided into three principal regions. In general, the copper-rich solutions yield one or more solid phases, while uranium-rich solutions yield a second liquid phase and no solid. In between is a rather large region in which one or more solids, two liquids, and a vapor phase all coexist.

The next set of experiments, now in progress, involves a repetition of the work at the same temperature but with solutions to which an amount of excess H_2SO_4 proportional to the combined amount of $CuSO_4$ and UO_2SO_4 is added. By repeating such observations at several different acidities, the entire isothermal liquidus surface and the composition of the solid phases can be determined by methods of analytical geometry. However, this method neglects the vapor phase entirely and is therefore not very accurate. Very dilute solutions, less than 0.60% $CuSO_4$ and 1.5% UO_2SO_4, are not being included, since they are the subject of a separate study reported in the following section.

19.2 DILUTE SOLUTIONS IN THE SYSTEM $UO_2SO_4-CuSO_4-NiSO_4-H_2SO_4-H_2O$

A previous report[2] presented data for the maximum temperature at which solutions of specified compositions could be held without the appearance of a solid or a second liquid phase. The lack of reliability in these data was pointed out in the earlier report. There were two principal uncertainties:

1. Was the very short equilibration time (not more than 15 min) adequate?
2. Did corrosion of the quartz tubes influence the observations?

The answers to these questions were believed to depend largely on the nature of the phase change occurring and on the composition of the solution. In the region where a second liquid phase was encountered, the establishment of equilibrium is very rapid and the temperatures observed in the quartz tubes are believed to be reasonably accurate. In the region where a green solid phase appeared, there was no evidence of corrosion but the question concerning rate remained. In the region in which white, yellow, or orange solids appeared, both uncertainties are present. A repetition of some of this work or all of it employing a technique designed to answer or eliminate these questions seemed in order. As a matter of secondary interest it was hoped that more would be learned about the solid phases.

[1] F. E. Clark, R. Slusher, and C. H. Secoy, *HRP Quar. Prog. Rep. July 31, 1955*, ORNL-1943, p 236.

[2] C. H. Secoy *et. al.*, *HRP Quar. Prog. Rep. April 30, 1956*, ORNL-2096, p 130.

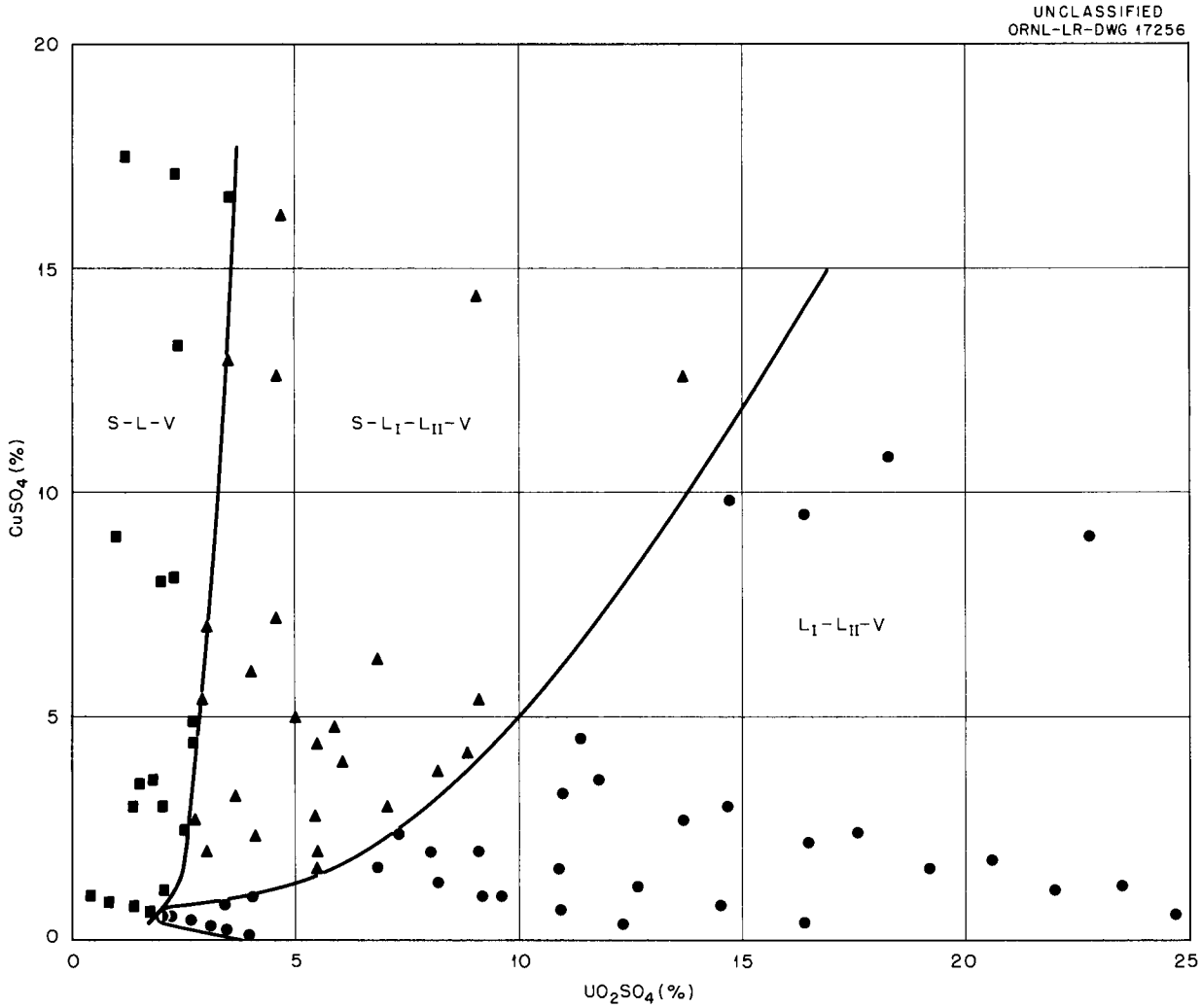

Fig. 19.1. Coexisting Phases in $CuSO_4$-UO_2SO_4 Solutions at 304°C.

The method selected involved establishing equilibrium in titanium capsules equipped with capillary tubes and valves so that samples of the liquid phase could be removed. In order to make rate studies, it was necessary that a number of successive liquid samples be removed from the same bomb without the volume of liquid in the bomb being changed to a serious extent. Since Cu^{++}, Ni^{++}, and UO_2^{++} are all colored ions and readily form colored complexes, the spectrophotometer offered promise as a rapid means of checking concentration changes with very small samples (50-μl samples are adequate for copper and nickel; 500-μl samples are required for uranium).

The solutions explored to date all lie in the region in which a green precipitate was observed in the quartz-tube experiments. Crystals of this solid have been removed at the conclusion of each bomb experiment and subjected to x-ray diffraction study. In all cases the principal constituent is the basic copper sulfate, $3CuO{\cdot}SO_3{\cdot}2H_2O$. However, also in all cases, a set of unidentified lines was present. Indirect analytical evidence indicates that this unknown solid does not contain either nickel or uranium; so it is probably another basic copper sulfate.

The results of a typical rate study in the titanium bombs are shown in Fig. 19.2, in which the optical densities for the principal nickel and

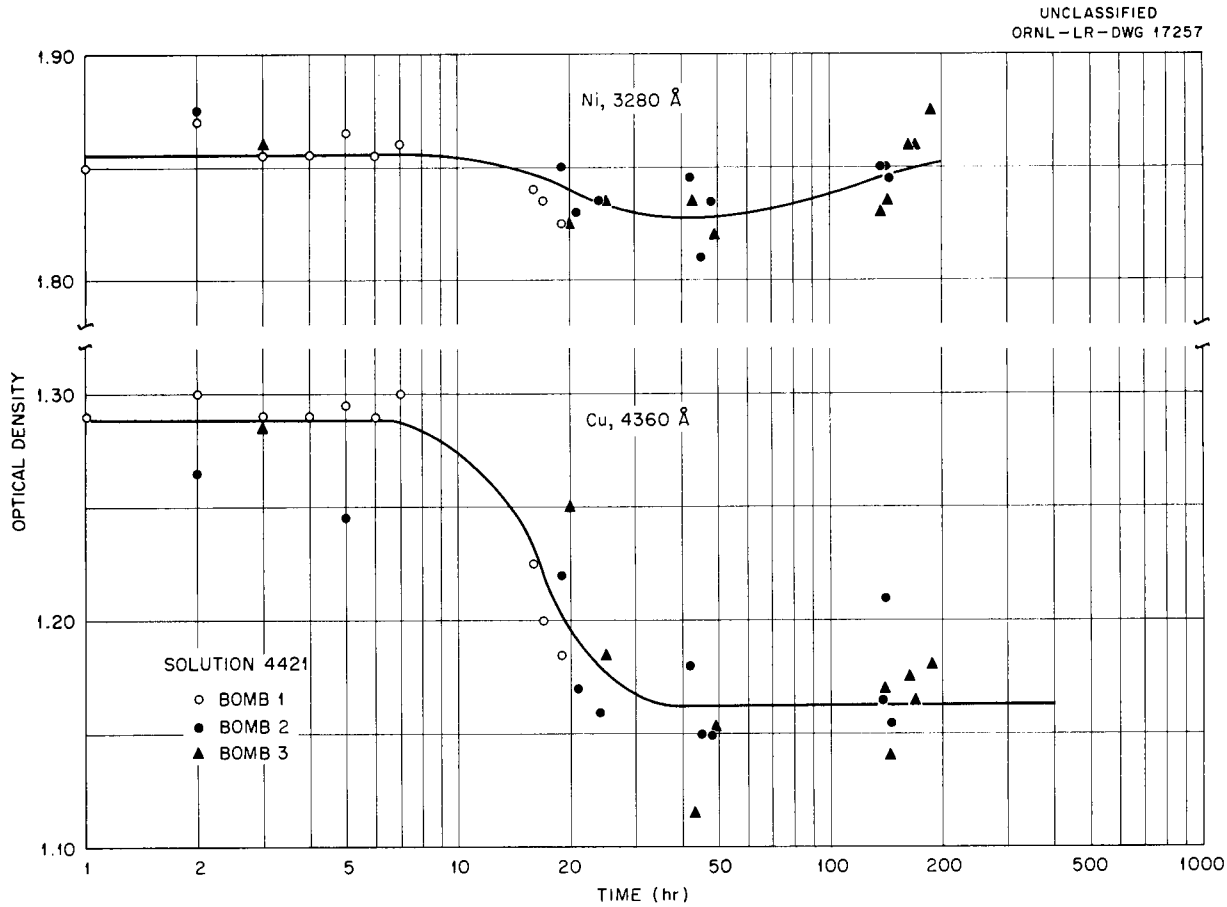

Fig. 19.2. Typical Rate of Equilibration Study.

copper lines are plotted against time on a logarithmic scale for solution No. 4421 (0.04 *m* UO_2SO_4, 0.04 *m* $CuSO_4$, 0.02 *m* $NiSO_4$, and 0.01 *m* H_2SO_4) at 190°C. The copper points indicate, even though there is some scatter, that nothing much happens for the first several hours. This period is followed by the precipitation process, which requires perhaps 20 hr for its completion. Although the scatter in the nickel points may be entirely due to random error, there is some indication of a slight drop in nickel concentration occurring simultaneously with the copper-salt precipitation and followed by a slow increase back to its original value. This may be a manifestation of occlusion of nickel ion by the precipitate during its formation, the nickel being released to the solution by prolonged digestion.

As a result of the rate studies, an equilibration period of 48 hr was selected as adequate. Figure 19.3 illustrates the data obtained in establishing the temperature of initial precipitation. All points on Fig. 19.3 were obtained from successive 50-μl samples from a single bomb taken at approximately 10°C intervals and with at least 48 hr allowed for equilibration at each temperature. The temperature of initial precipitation is clearly indicated by the break in the optical-density line for copper. The uranium was not determined in these experiments, because previous tests showed that, like the nickel, it was essentially unaffected and because its determination would have required larger samples.

TABLE 19.1. TEMPERATURES OF THE APPEARANCE OF NONHOMOGENEITY

Solution No.	Solution Composition (m)				Temperature (°C)	
	UO_2SO_4	H_2SO_4	$CuSO_4$	$NiSO_4$	Quartz Tube	Titanium Bomb
4231	0.04	0.01	0.02	0.03	255	214
4311	0.04	0.01	0.03	0.01	255	216
4321	0.04	0.01	0.03	0.02	238	203
4331	0.04	0.01	0.03	0.03	220	197
4401	0.04	0.01	0.04	None	256	199
4411	0.04	0.01	0.04	0.01	226	189
4421	0.04	0.01	0.04	0.02	215	186
4431	0.04	0.01	0.04	0.03	208	185

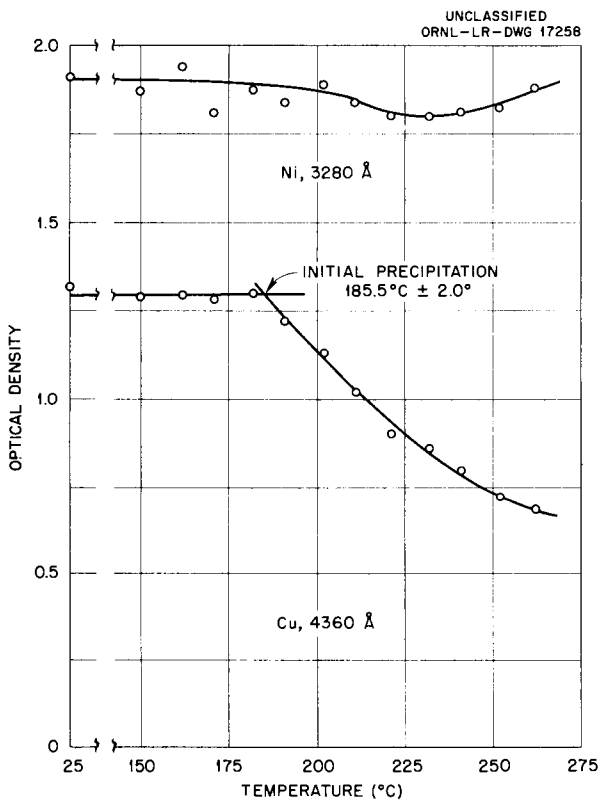

Fig. 19.3. Temperature of Precipitation, Solution 4421.

Table 19.1 summarizes the temperatures of initial precipitation observed by this technique to date, along with values previously reported from the quartz-tube work. In all cases the quartz-tube values are 20 to 50°C too high, as would be expected from the results of the rate studies. These lower values show that the solubility surface in this region is very steep with temperature, especially above 200°C. In other words the amount of $CuSO_4$ that can be retained in solution at 200°C is not much greater than that at 300°C.

20. EFFECT OF URANYL ION ON FERROUS OXIDATION

J. W. Boyle H. A. Mahlman

The yield of ferric ions from the oxidation of ferrous ions in air-saturated 0.8 *N* H_2SO_4 has been determined for Co^{60} gamma rays in the presence of uranyl ion up to 0.4 *M*. The data are given in Fig. 20.1 and confirm and extend the results of Ehrenburg and Saeland.[1] The reduction in ferric yield is attributed to reaction of the uranyl ion with hydrogen atoms before they react with dissolved oxygen in the solution. The reduced uranium is then reoxidized by either hydrogen peroxide, ferric ion, or oxidizing radicals, and therefore no net change is observed in the uranyl concentration. This mechanism is in agreement with the fact that the ferric yield at a given uranyl concentration was found to be independent of initial ferrous concentration but dependent on the oxygen concentration. In a 0.04 *M* uranyl solution the ferric yield was 3% greater in an oxygen-saturated solution than in an air-saturated solution.

Preliminary work on the reduction of ceric ion in 0.8 *N* H_2SO_4 by gamma rays in the presence of uranyl ion indicated that the ceric reduction is enhanced by uranyl ion. This is in disagreement with the results of Dyne,[2] who reported a linear decrease in the yield of ceric sulfate reduction with uranyl concentration.

It has previously been shown that uranyl solutions lower the hydrogen yield for all types of radiation.[3] All these data – the reduction of ferric yield, the enhancement of ceric reduction, and the lowering of the hydrogen yield – are consistent with the assumption that the uranyl ion reacts with hydrogen atoms.

[1] L. Ehrenburg and E. Saeland, *Chemical Dosimetry of Radiation Giving Different Ion Densities. An Experimental Determination of G Values for Fe^{+2} Oxidation*, JENER Publication No. 8, p 15, Kjeller per Lillestrom, Norway (1954).

[2] P. J. Dyne, *Progress Report July 1 to September 30, 1955, Chemistry and Metallurgy Branch*, PR-CM-3, p 6.

[3] J. W. Boyle *et al.*, *Proceedings of the International Conference on the Peaceful Uses of Atomic Energy*, vol 7, p 576–582, United Nations, New York, 1956.

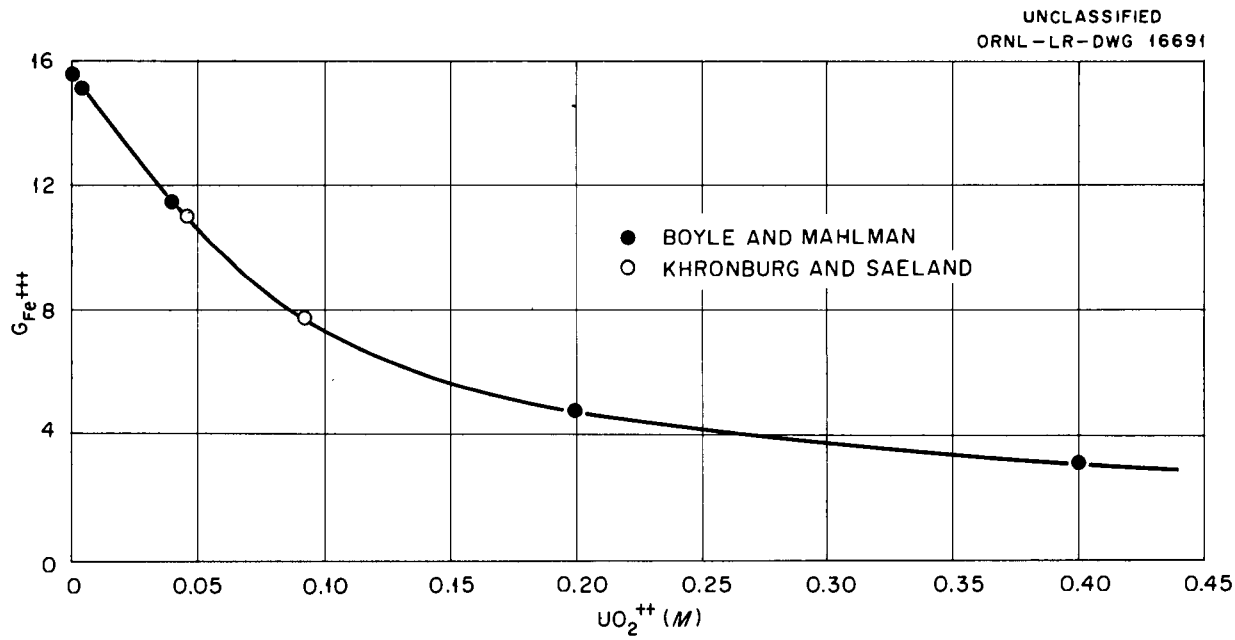

Fig. 20.1. Effect of Uranyl Ion Concentration on the Oxidation of $FeSO_4$ in Air-Saturated 0.8 *N* H_2SO_4 by Co^{60} Gamma Rays.

OFFICIAL USE ONLY

OAK RIDGE NATIONAL LABORATORY
HOMOGENEOUS REACTOR PROJECT

NOVEMBER 1, 1956

PROJECT DIRECTOR
R. B. BRIGGS D

ASSOCIATE PROJECT DIRECTOR
C. E. WINTERS** D
A. L. GUNNELS, SEC. D

PROJECT EDITOR
W. O. REEL I&R

DESIGN AND ENGINEERING
J. A. LANE, DIRECTOR
R. N. LYON, ASSISTANT DIRECTOR
REACTOR EXPERIMENTAL ENGINEERING DIVISION
T. S. CARLSMITH, SEC. REE

DESIGN
W. R. GALL, SECTION CHIEF REE
M. I. LUNDIN, ASSISTANT SECTION CHIEF REE

MECHANICAL DESIGN
F. C. ZAPP, GROUP LEADER REE
C. A. BURCHSTED REE
C. J. CLAFFEY REE
R. C. MOREN WESTINGHOUSE

LONG RANGE STUDIES
C. L. SEGASER, ACTING GROUP LEADER REE
E. GIFT REE

PLANT LAYOUT AND DRAFTING
T. H. THOMAS, GROUP LEADER REE
W. ROBINSON REE
W. TERRY REE
R. W. BORGERS REE
H. H. BRADFORD REE
R. L. CAUBLE REE
C. W. DAY REE
J. P. DILORENZO REE
R. L. HALE REE
A. S. LUDLOW REE
C. A. ROBERTS REE
R. D. SATTERFIELD REE
R. H. SIGLER REE
W. T. STERLING REE

PROCESS DESIGN
R. C. ROBERTSON, GROUP LEADER REE
R. F. HUGHES KAIGHIN AND HUGHES
H. A. MCLAIN REE

STRESS ANALYSIS
R. D. CHEVERTON, GROUP LEADER REE
J. N. ROBINSON REE

REACTOR ANALYSIS
P. R. KASTEN, SECTION CHIEF REE

REACTOR PHYSICS
C. W. NESTOR, JR. REE
M. W. ROSENTHAL REE
M. P. LIETZKE REE

LONG RANGE STUDIES
H. C. CLAIBORNE REE
S. JAYE REE
M. TOBIAS REE
T. B. FOWLER REE

ENGINEERING DEVELOPMENT
I. SPIEWAK, SECTION CHIEF REE

CENTRIFUGAL PUMPS AND HEAT EXCHANGERS
W. L. ROSS, GROUP LEADER REE
J. M. BAKER REE
P. P. HOLZ REE
J. C. MOYERS REE
I. K. NAMBA REE

FEED PUMPS, TITANIUM PROGRAM, MISCELLANEOUS EQUIPMENT
C. H. GABBARD, GROUP LEADER REE
R. BLUMBERG REE
S. D. DRAPER TVA
E. C. HISE REE

HRT MOCKUP, RECOMBINERS
P. H. HARLEY, GROUP LEADER REE
B. A. HANNAFORD REE
H. C. ROLLER REE
D. E. WILLIS REE

TECHNICIAN POOL
T. L. CASTILE REE
T. W. CATE REE
A. B. DAFFRON REE
R. GOODMAN REE
J. P. HURST REE
C. C. HURTT REE
W. B. KRICK REE
R. J. LOCKETT REE
W. M. PARKS REE
L. E. PENTON REE
S. R. WEST REE
T. R. WILSON REE

INSTRUMENTATION AND CONTROLS
D. S. TOOMB, SECTION CHIEF REE

HRT
J. C. GUNDLACH** I&C
J. D. GRIMES TVA
R. L. MOORE* I&C
P. E. SMITH I&C

HRP SUPPORTING FACILITIES
D. G. DAVIS I&C
G. W. GREENE I&C
P. G. HERNDON I&C
J. A. RUSSELL I&C
H. D. WILLS REE

VALVES AND ACTUATORS
A. M. BILLINGS I&C
P. F. MURAY I&C
A. J. SHARENBERGER I&C

INSTRUMENT DEVELOPMENT
R. L. MOORE* I&C

ENGINEERING RESEARCH
R. B. KORSMEYER, SECTION CHIEF REE

COMPONENT DEVELOPMENT
A. S. KITZES, GROUP LEADER REE
R. B. GALLAHER REE
M. RICHARDSON REE
C. F. VANDEN BULCK UCNC
R. P. WICHNER REE

SLURRY SYSTEM DEVELOPMENT
L. F. PARSLY, GROUP LEADER REE
I. M. MILLER REE
H. L. FALKENBERRY TVA

SLURRY PROPERTIES
D. G. THOMAS, GROUP LEADER REE
R. H. NIMMO REE
C. S. MORGAN REE

TECHNICIAN POOL
A. N. SMITH REE
T. L. BOSWELL REE
R. E. CARNES REE
J. T. DICKIE REE
C. M. FITZPATRICK REE
C. A. GIFFORD REE
P. H. HAYES REE
C. A. MCLAUGHLIN REE
H. G. MOORE REE
R. E. POTTER REE
R. M. SUMMERS REE
B. J. SUTTON REE
D. H. WALLACE REE

REACTOR MATERIALS RESEARCH
E. G. BOHLMANN, ASSISTANT DIRECTOR
REACTOR EXPERIMENTAL ENGINEERING DIVISION
T. F. KELLY, SEC. REE
R. E. WACKER, RECORDS REE

SOLUTIONS
J. C. GRIESS,** ASSISTANT SECTION CHIEF C

LOOPS
R. S. GREELEY REE
S. R. BUXTON REE
W. H. HINOS REE
J. E. EVE REE

LABORATORY STUDIES
J. L. ENGLISH,** GROUP LEADER REE
E. F. HOUSE** REE
L. L. FAIRCHILD,** LEADER REE
H. L. BARKER** REE
H. R. TINCHER* REE
J. L. UNDERWOOD** REE

SLURRIES
E. L. COMPERE, ASSISTANT SECTION CHIEF C

LOOPS
S. A. REED REE

TOROIDS
G. E. MOORE C
R. F. BENSON REE
F. E. MCDANIEL REE

HRT LIAISON
D. M. RICHARDSON C

ENGINEERING
H. C. SAVAGE, ASSISTANT SECTION CHIEF REE

SOLUTIONS
W. C. ULRICH REE
L. F. WINESETTE, LEADER REE
L. L. ALLEN REE
C. R. BENSON REE
C. M. BURCHELL REE
C. L. FRANCIS REE
J. B. FRENCH REE
J. W. GOOCH REE
J. E. JACKSON REE
G. A. MOORE REE
L. G. PHELPS REE
A. E. PUGH REE
T. F. RAYBURN REE
W. H. WAGNER REE

SLURRIES
R. M. WARNER REE
B. W. SCOTT REE

RADIATION
S. E. BOLT REE
T. H. MAHNEY REE
R. M. PIERCE TVA
D. B. WEAVER TVA
J. D. BARNES REE
C. H. BURBAGE REE
J. R. HART REE
H. F. HENDERSON REE

RADIATION
G. H. JENKS, SECTION CHIEF C
D. T. JONES, ENGRG. COORDINATOR C
V. R. BULLINGTON REE

IN-PILE LOOPS
J. R. MCWHERTER, GROUP LEADER REE
J. E. BAKER REE
R. A. LORENZ REE
F. J. WALTER* REE
S. H. WHEELER REE
J. W. BROWN, LEADER REE
K. G. CHANDLER REE
J. P. GORDON REE
E. H. GUINN REE
R. A. JONES REE
J. W. MOSIER REE
J. W. MYERS REE
C. E. ROBERTS REE
R. G. ROSS REE
O. M. SMITH REE
A. L. SUTTON REE
W. P. TEICHERT REE
R. M. WALLER REE

IN-PILE BOMBS
R. J. DAVIS, GROUP LEADER C
V. A. DECARLO REE
F. J. WALTER* REE
K. S. WARREN C
L. F. WOO C
J. L. RUTHERFORD REE

SUPPORTING RESEARCH
A. L. BACARELLA C
M. D. SILVERMAN C
W. C. YEE C

REMOTE EVALUATION
A. R. OLSEN REE
B. W. MCCOLLUM, SHIFT LEADER REE
R. L. PLEMONS REE
W. J. SCHILL REE
W. H. SMITH, JR. REE
J. C. THOMPSON REE

METALLURGY
G. M. ADAMSON, SECTION CHIEF M
J. P. HAMMOND M
W. J. LEONARD M
M. L. PICKLESIMER M
J. J. PRISLINGER M
R. L. STEPHENSON M
J. K. WHITE M
C. H. WODTKE M
P. J. JONES M
C. M. SMITH M
M. A. WHEELER M
J. J. WOODHOUSE M

METALLOGRAPHY
R. S. CROUSE** M
T. M. KEGLEY, JR. M
E. R. BOYD M
B. F. DAY** M
B. J. REESE** M
L. G. SHRADER** M

RADIATION DAMAGE
R. G. BERGGREN SS
A. E. RICHT SS
D. O. THOMPSON SS
J. C. WILSON** SS

SUBCONTRACTS

ARMOUR RESEARCH FOUNDATION
BABCOCK & WILCOX COMPANY
FOSTER WHEELER CORPORATION
HOUDRY CORPORATION
RENSSELAER POLYTECHNIC INSTITUTE
SYRACUSE UNIVERSITY
TULANE UNIVESITY
UNIVERSITY OF FLORIDA
VITRO CORPORATION

AC	ANALYTICAL CHEMISTRY DIVISION
C	CHEMISTRY DIVISION
CT	CHEMICAL TECHNOLOGY DIVISION
D	DIRECTOR'S DIVISION
E&M	ENGINEERING AND MECHANICAL DIVISION
I&C	INSTRUMENTATION AND CONTROLS DIVISION
I&R	INFORMATION AND REPORTS DIVISION
M	METALLURGY DIVISION
REE	REACTOR EXPERIMENTAL ENGINEERING DIVISION
SS	SOLID STATE DIVISION
TVA	TENNESSEE VALLEY AUTHORITY
UCNC	UNION CARBIDE NUCLEAR COMPANY, NEW YORK
*	DUAL CAPACITY
**	PART TIME

PERSONNEL SUMMARY

	FULL TIME	PART TIME	INDUSTRIAL PARTICIPANTS
ADMINISTRATION	6	5	
ANALYTICAL CHEMISTRY	42		
DESIGN AND ENGINEERING	98	1	6
CHEMICAL RESEARCH	9	10	
CHEMICAL TECHNOLOGY	57	4	1
HOMOGENEOUS REACTOR TEST	38		6
REACTOR MATERIALS RESEARCH	87	12	2
TOTAL	337	32	15

CHEMICAL TECHNOLOGY
F. R. BRUCE,** ASSOCIATE DIRECTOR
CHEMICAL TECHNOLOGY DIVISION
J. HOPPE, SEC. CT

CHEMICAL DEVELOPMENT
D. E. FERGUSON,** ASST. SECTION CHIEF CT

BLANKET PROCESSING
R. E. LEUZE, PROBLEM LEADER CT
R. D. BAYBARZ** CT
J. M. CHILTON CT
S. S. KIRSLIS CT
J. M. DELOZIER CT
R. L. HICKEY CT
O. K. TALLENT CT

CORE PROCESSING
R. A. MCNEES, PROBLEM LEADER CT
M. H. LLOYD CT
S. PETERSON CT
W. B. HOWERTON CT

BLANKET PROCESSING
J. P. MCBRIDE, PROBLEM LEADER CT
V. D. ALLRED CT
E. V. JONES C
N. A. KROHN CT
L. E. MORSE CT
R. L. PEARSON CT
C. E. SCHILLING CT
W. M. WOODS CT
C. W. GREENE CT
W. L. PATTISON CT
H. F. SCARO CT

DESIGN
W. E. UNGER,** ASSISTANT SECTION CHIEF CT

PROCESS DESIGN
H. O. WEEREN CT
B. F. BOTTENFIELD CT

PROJECT DESIGN
A. M. ROM, PROBLEM LEADER CT
G. B. BERRY E&M
F. C. MCCULLOUGH CT
R. H. WINGET CT
E. E. BRIDGES (CATALYTIC CONST. CO.) CT
J. D. CUPP (CATALYTIC CONST. CO.) CT
H. W. FALLON (CATALYTIC CONST. CO.) E&M
R. L. KNIPPING (CATALYTIC CONST. CO.) CT
J. H. MANNEY E&M
F. L. PEISHEL E&M
J. PHILLIPS (CATALYTIC CONST. CO.) CT
L. G. SIMMONS (CATALYTIC CONST. CO.) CT
K. F. STOOKSBURY E&M
J. N. WHEELER E&M

LOOP DESIGN
T. A. AREHART CT
W. J. CLOSSEY (CATALYTIC CONST. CO.) CT
W. F. SCHAFFER CT

INSTRUMENTATION
R. K. ADAMS I&C
C. S. LISSER I&C

UNIT OPERATIONS
E. O. NURMI, GROUP LEADER CT

LOOP STUDIES
R. W. HORTON CT
R. D. ARTHUR CT
F. N. MCLAIN CT
G. E. WOODALL CT

BLANKET PROCESSING
P. A. HAAS CT
S. D. CLINTON CT
R. C. EARLY CT
J. BEAMS CT
D. A. MCWHIRTER CT

EQUIPMENT EVALUATION
C. C. HAWS, JR. CT
N. A. BROWN TVA
V. L. FOWLER CT

PILOT PLANT
R. B. LINDAUER,** SECTION CHIEF CT

SLURRY PREPARATION
E. M. SHANK, PROBLEM LEADER CT
J. R. PARROTT CT

CHEMICAL RESEARCH
E. H. TAYLOR,** DIRECTOR
CHEMISTRY DIVISION
E. SCHAPPEL, SEC. C

FUEL SOLUTION CHEMISTRY
C. H. SECOY, GROUP LEADER C
F. E. CLARK C
J. S. GILL C
G. M. HEBERT C
D. W. SHERWOOD C
R. SLUSHER C
H. H. STONE C
F. H. SWEETON C
H. F. MCDUFFIE C

RADIATION CHEMISTRY
C. J. HOCHANADEL,** GROUP LEADER C
J. W. BOYLE** C
H. A. MAHLMANN** C

HEAVY ELEMENT CHEMISTRY
R. W. STOUGHTON,** GROUP LEADER C
J. HALPERIN** C
M. H. LIETZKE** C
W. C. WAGGENER** C

INORGANIC SOLUTION CHEMISTRY
K. A. KRAUS,** GROUP LEADER C
T. A. CARLSON** C
H. D. PHILLIPS** C

ANALYTICAL CHEMISTRY
MYRON T. KELLEY,** DIRECTOR
C. D. SUSANO,** ASSOCIATE DIRECTOR
K. ODOM, SEC. AC

CORROSION ANALYTICAL LABORATORY
O. MENIS,* SUPERVISOR AC
H. P. HOUSE, ASSISTANT SUPERVISOR AC

RESEARCH
O. MENIS,* GROUP LEADER AC
R. G. BALL AC
C. M. BOYD AC
G. GOLDSTEIN AC
D. L. MANNING AC
R. H. POWELL AC
I. B. RUBIN AC

SERVICES
C. K. TALBOT, GROUP LEADER AC
H. M. FERGUSON AC
F. L. LAYTON AC
T. C. RAINS AC
T. P. BACON AC
W. D. CLAPP, JR. AC
C. A. CLARK AC
C. G. FUSON AC
P. S. GOODWIN AC
T. G. MILLER AC
V. S. NORMAN AC
E. ONSK AC

HRT AND IN-PILE LOOP ANALYSES
U. KOSKELA, SUPERVISOR AC
L. G. FARRAR, ASSISTANT SUPERVISOR AC
J. E. ATTRILL AC
R. E. CORCORAN AC
S. R. DINSMORE AC
P. V. HOFFMAN AC
J. L. MOTTERN AC
C. P. BAKER AC
G. M. CAMPBELL AC
G. I. GAULT AC
B. D. HICKS AC
M. F. MCCORQUODALE AC
J. SLESSINGER, JR. AC
W. R. WARREN AC
H. L. WEBB AC
H. L. WHITTINGTON AC

HRT DEVELOPMENT
P. F. THOMASON, GROUP LEADER AC
R. E. BIGGERS AC
F. J. MILLER AC
S. A. REYNOLDS, GROUP LEADER AC
T. H. HANDLEY AC

HIGH RADIATION LABORATORY
C. L. BURROS AC

HOMOGENEOUS REACTOR TEST
S. E. BEALL,* PROJECT ENGINEER REE
B. EUBANK, SEC. REE

OPERATIONS
S. E. BEALL,* ACTING CHIEF REE
G. H. JOHNSTONE REE
R. SMITH, JR. REE
J. S. CULVER, SUPERVISOR REE
R. E. BROOKSBANK CT
N. W. CURTIS PA. POWER AND LIGHT CO.
D. F. FRECH REE
W. T. BOSTIC CT
H. D. CURTIS REE
R. J. SHANNON CT
J. E. WOLFE REE
J. W. HILL, SUPERVISOR REE
J. R. ENGEL CT
J. D. FLYNN REE
H. K. SEARCH PA. POWER AND LIGHT CO.
E. W. BROWN CT
A. L. JOHNSON REE
T. G. HILL REE
C. E. WADDELL CT
S. I. KAPLAN, SUPERVISOR REE
T. H. GLADNEY TVA
J. O. KOLB REE
G. W. RIVENBARK REE
D. T. GODWIN REE
R. J. HUNTER REE
J. L. STEPP REE
J. A. WATTS REE

REMOTE MAINTENANCE
R. W. JURGENSEN AM. GAS AND ELEC. CO.
T. E. HAYNES REE

CHEMICAL PLANT COORDINATION
W. D. BURCH CT
N. C. BRADLEY CT
R. H. WINGET CT
W. A. SHANNON CT

REACTOR ANALYSIS
P. H. HAUBENREICH REE
D. M. JOHNSON GLENN L. MARTIN CO.
J. D. JONES REE

TRAINING
H. M. MCLEOD CT
H. F. BAUMAN CT
J. R. BUCHANAN CT
R. H. GUYMON CT
R. R. WIETHALIP CT
L. J. SHERSKY CT

REACTOR COORDINATION
R. VAN WINKLE REE
B. H. HAMLING UCNC